**From the Fraunhofer Research Institution for Marine Biotechnology**

**Department of Medical Cell Technology**

**of the University of Lübeck**

**Director: Prof. Dr. Charli Kruse**

# "Genetic engineering of mesenchymal stem cells for improved homing"

Dissertation

for Fulfillment of

Requirements

for the Doctoral Degree

of the University of Lübeck

from the Department of Natural Sciences

Submitted by

Franziska Nitzsche

born in Gotha, Germany

Lübeck 2016

First referee: Prof. Dr. Johannes Boltze

Second referee: Prof. Dr. Volker Tronnier

Date of oral examination: 10.04.2017

Approved for printing. Lübeck, 12.05.2017

## Abstract

Stem cell therapy using mesenchymal stem cells (MSC) has emerged as a potential strategy for the treatment of cerebrovascular disorders such as stroke. Migration and homing towards the injured tissue play a crucial role for the therapeutic success. Since the desire for a minimally invasive transplantation strategy favors systematic administration of MSC after cerebral ischemia, homing also requires egress from the blood vessel. This impairs the already limited homing of MSC even more and drives the need to enhance their migration capabilities. To this end, the genetic engineering provides to opportunity for modification of the MSC receptor configuration enhancing their susceptibility for navigation signals towards cerebral ischemia.

In the first parts of this study, the genetic engineering with integrin alpha 4 (ITGA4), as a key molecule for extravasation, was applied on the basis of mRNA transfection or lentiviral modification. Transfection of *in vitro* synthetized mRNA (IVT mRNA) led to transient ITGA4 protein expression peaking 12-24h after delivery. Furthermore, extent of protein expression was dependent from the 5'cap of mRNA. Posttranscriptional, physiological capping was very efficient what is probably related to facilitated recognition by the translation machinery. The overexpressed ITGA4-protein was processed physiologically and matured to a fully functional VLA4 receptor. In addition, MSC characteristics and viability were not disturbed after IVT mRNA lipofection, what makes this a valuable method for clinical grade genetic modification.

Lentiviral vectors are common tools to drive protein overexpression on MSC what is related to their wide host range and their ability to infect non-dividing and hard-to-transfect cells. In this study, they have been shown to induce a long-term expression of ITGA4. By that, it was possible to generate modified MSC for proof-of-principle-studies where protein expression is not affected by time. Also, the optimization of ITGA4 protein expression by promoter substitution (UbC, EF1α, CMV, or TRE) was in focus of this study. The promoter strength influenced crucially efficiency and extent of ITGA4-expression, endurance of protein expression, as well as cell fitness. Stronger promoters drove ITGA4 efficient but the expense of cell fitness.

The last part of this study concerned the homing capabilities of MSC towards cerebral ischemia after overexpression of the adhesion molecule ITGA4 or the chemokine receptor CCR2. Migration capabilities were initially tested *in vitro*, where enhanced (trans)migration was observed from MSC overexpressing ITGA4. This was associated with enhanced endothelial interaction. In contrast, CCR2 overexpression affected probably the physiological behavior of MSc crucially and, thus, impaired the basal *in vitro* transmigration. Homing of control and modified MSC was evaluated in an experimental model of stroke. Biodistribution was traced by SPECT-imaging after intra-arterial transplantation. Modalities of transplantation, however, led to a misallocation into facial soft tissue than towards the brain. Thus, the potentially improved homing of modified MSC toward cerebral ischemia remains an open question. Nevertheless, a relocation towards internal organs was observed as a potential mechanism of clearance from transplanted cells. Of note, immunohistology of a few selected animals could identify MSC within the brain tissue. This was evidence that MSC basically left the blood vessel and entered the brain parenchyma, but also triggered probably an immune response. The question, if overexpression of ITGA4 or CCR2 enhanced in vivo homing to cerebral ischemia could not be answered and remains to be elucidated in the future.

## Zusammenfassung

Zell-basierte Therapien mit mesenchymalen Stammzellen (MSC) gelten als vielversprechend für die Behandlung zerebrovaskulärer Krankheiten wie z.B. dem Schlaganfall. Maßgeblich für den therapeutischen Erfolg ist die Einwanderung (Migration) und Akkumulierung der MSC im geschädigtem Gewebe (Homing). Diese Migration ist prinzipiell von der Expression bestimmter Oberflächenrezeptoren abhängig, kann aber auch, zumindest teilweise, durch die Transplantationsroute beeinflusst werden. Üblicherweise wird eine nichtinvasive, systemische Verabreichung der MSC favorisiert, allerdings wird die therapeutische Effizienz hierdurch limitiert. Dies ist darauf zurück zu führen, dass der Austritt der Zellen aus dem Blutgefäß (Extravasation) notwendig wird, die Rezeptorausstattung der MSC aber hierfür nicht optimal ist. Gentechnische Methoden bieten eine Möglichkeit zur Modifikation der Oberflächenrezeptoren und können daher die Homing-Eigenschaften von MSC verbessern.

Die ersten Ziele dieser Arbeit betrafen die mRNA-basierte Modifizierung von MSC mit Integrin alpha 4 (ITGA4), welches ein Schlüsselmolekül der Extravasation darstellt. Die Transfektion von synthetisch hergestellter mRNA führte zu einer vorübergehenden ITGA4-Proteinexpression, welche nach 12-24h ihren Höchststand erreichte. Das Ausmaß der Proteinexpression war dabei abhängig von der Art des Caps am 5‘-Ende der mRNA. Posttranskriptionales, physiologisches Capping war hierbei äußerst effizient, was auf verbesserte Erkennung durch die Translationsmaschinerie zurückgeführt wurde. Weiterhin wurde das überexprimierte ITGA4 physiologisch prozessiert und reifte zu einem funktionalen VLA4 -Rezeptor heran. Es ist besonders herauszuheben, dass die Eigenschaften und Viabilität der MSC nicht durch die mRNA-Lipofektion beeinträchtigt wurden. Dies macht die mRNA-Transfektion zu einer wertvollen Methode der gentechnischen Modifizierung von MSC mit klinischer Reife.

Lentivirale Vektoren werden weitverbreitet eingesetzt um relevante Proteine in MSC über zu exprimieren. Dies ist vor allem darauf zurückzuführen, dass sie ein weitreichendes Wirtsspektrum besitzen und weiterhin dazu befähigt sind Zellen zu infizieren, die sich nicht im Teilungsstadium befinden oder schwer zu transfizieren sind. In dieser Studie wurde gezeigt, dass lentivirale Vektoren eine lang andauernde ITGA4-Expression erzielen können. Dies erlaubt die Herstellung modifizierter MSC für Machbarkeitsstudien, ohne einer zeitkritischen Proteinexpression unterworfen zu sein. Darüber hinaus war auch die Optimierung der ITGA4-Expression durch einen Promoteraustausch (UbC, EF1α, CMV oder TRE) ein Studienschwerpunkt. Hierbei war die Promoterstärke auschlaggebend für Effizienz und Ausmaß der Proteinexpression, für die Dauer der Proteinexpression und für die Fitness der Zellen.

Im letzten Teil der Studie stand das MSC-Homingvermögen hin zur zerebralen Ischämie nach Überexpression des Adhäsionsmoleküls ITGA4 oder des Chemokinrezeptors CCR2 im Mittelpunkt. Initial wurden die Migrationseigenschaften mittels *In vitro*-Studien untersucht. Hier zeigte sich eine verstärkte Transmigration nach Überexpression von ITGA4. Dies wurde auf eine verstärkte Interaktion mit dem Endothel zurückgeführt. Die Überexpression von CCR2 interferierte im Gegenzug wohl grundlegend mit dem physiologischen Verhalten der MSC und verursachte dadurch eine Beeinträchtigung des basalen Transmigrationsvermögens. Das Homing von Kontroll- und modifizierten MSC wurde weiterhin in einem experimentalen Schlaganfallmodell untersucht. Die biologische Verteilung wurde nach intra-arterieller Transplantation mittels SPECT/CT-Bildgebung

verfolgt. Es stellte sich heraus, dass die Modalitäten der Transplantation zur einer Fehlleitung der MSC hin zum Gesichtsgewebe anstelle zum Gehirn führten. Der Einfluss der gentechnischen Modifizierung auf das Homingverhalten der MSC konnte daher nicht geklärt werden. Unabhängig davon wurde jedoch eine Umverteilung zu den inneren Organen beobachtet, was als potentielle Abwehr der MSC gedeutet wurde. Es ist allerdings herauszustellen, dass im Zuge der immunhistologischen Untersuchung ausgewählter Tiere MSC im Gehirn nachgewiesen wurden. Dies weist darauf hin, dass diese Zellen das Blutgefäß verlassen haben und ins Hirnparenchym eingewandert sind. Allerdings lag auch hier der Schluss nahe, dass eine immunologische Reaktion ausgelöst wurde. Die Frage, ob die Überexpression von ITGA4 oder CCR2 das zerebrale Homing der MSC verbessert hat, konnte im Zuge dieser Studie nicht beantwortet werden und ist Gegenstand zukünftiger Untersuchungen.

## Table of contents

Abstract ..... I
Zusammenfassung ..... III
List of tables ..... XI
List of figures ..... XIII
List of abbreviations ..... XV

1 Introduction ..... 1
1.1 Adult stem cells ..... 1
1.2 Mesenchymal stem cells ..... 2
1.3 Therapeutic potential of MSC ..... 4
1.4 MSC therapy for stroke ..... 6
1.5 State-of-the-art: systemic homing of MSC towards injury and transendothelial migration ..... 8
1.6 Current frontiers for MSC based therapy ..... 9
1.7 Cell engineering for improved homing ..... 10
1.8 Aims and objectives ..... 13

2 Materials ..... 15
2.1 Cell lines ..... 15
2.2 Laboratory equipment ..... 15
2.3 Disposables ..... 16
2.4 Chemicals and reagents ..... 16
2.5 Kits ..... 17
2.6 TaqMan®Gene expression Assays ..... 17
2.7 Media and buffers ..... 18
2.8 Oligonucleotides ..... 19
2.9 Plasmids ..... 19
2.10 Enzymes ..... 20
2.11 Antibodies ..... 20
2.12 Software ..... 21

3 Methods ..... 22
3.1 Cell Culture ..... 22

3.1.1 General subcultivation of adherent cells ... 22
3.1.2 Freezing and thawing ... 22
3.1.3 Culture of HEK 293T ... 23
3.1.4 Culture of GPNT ... 23
3.1.5 Cultivation of MSC ... 23
3.1.6 Differentiation of MSC ... 23
3.2 Proliferation, viability and toxicity ... 24
3.2.1 Growth curves and determination of population doubling time ... 24
3.2.2 MTT-Assay ... 24
3.2.3 LDH-Assay ... 25
3.3 Cloning ... 25
3.3.1 Transformation of competent bacteria ... 25
3.3.2 Plasmid amplification and isolation ... 26
3.3.3 Restriction digestion of plasmid DNA ... 26
3.3.4 DNA gel electrophoresis and gel extraction of DNA fragments ... 26
3.3.5 Ligation ... 27
3.3.6 Cloning of pFN19, pFN-3M and pFN-7M expression vectors ... 27
3.3.7 Cloning of pFN-4L1, pFN-4R, pFN-4S, and pFN-4T expression vectors ... 27
3.4 *In vitro* synthesis of mRNA ... 28
3.4.1 Generation of a DNA-Template for *in vitro* transcription ... 28
3.4.2 Generation of pre-IVT-mRNA, capping and polyadenylation ... 29
3.4.3 Purification of mRNA ... 30
3.4.4 RNA gel electrophoresis ... 31
3.5 Genetic engineering ... 31
3.5.1 mRNA transfection ... 31
3.5.2 Lentiviral infection ... 32
3.5.2.1 Production of lentiviral particles ... 32
3.5.2.2 Harvesting of lentiviral particles and transduction of target cells ... 32
3.6 Flow cytometry ... 33
3.6.1 Sorting ... 33
3.6.2 Cell staining for flow cytometry ... 33
3.6.3 LDV-FITC binding ... 34
3.6.4 Quantification by flow cytometry ... 34
3.7 Molecular biology ... 34
3.7.1 Isolation of total RNA from cultured cells ... 34
3.7.2 Reverse transcription ... 35

3.7.3 Isolation of genomic DNA ... 35
3.7.4 Quantitative RT-PCR ... 35
3.8 Protein biochemistry ... 36
3.8.1 Whole cell lysates ... 36
3.8.2 Determination of protein concentration ... 36
3.8.3 Discontinuous SDS-PAGE ... 37
3.8.4 Western Blot ... 37
3.8.5 Immunological detection and chemiluminescent reaction ... 38
3.8.6 Immunocytochemistry ... 38
3.9 Migration ... 39
3.9.1 Vital staining of cells ... 39
3.9.1.1 PHK26-labelling ... 39
3.9.1.2 CFSE-labelling ... 39
3.9.2 Transwell migration ... 40
3.9.3 Quantification of FluoroBlok transwell migration ... 40
3.9.4 Analysis of migration using confocal microscopy ... 41
3.10 *In vivo* experiments ... 41
3.10.1 Experimental groups and timeline ... 42
3.10.2 Animals ... 42
3.10.3 Transient MCAO ... 43
3.10.4 MRI ... 43
3.10.5 Cell preparation and $^{111}$In labelling ... 43
3.10.6 Cell transplantation ... 44
3.10.7 SPECT/CT imaging ... 44
3.10.8 Gamma counting ... 44
3.10.9 Imunohistochemistry ... 44
3.11 Statistical analyses ... 45

4 Results ... 46
4.1 mRNA-driven overexpression of ITGA4 on MSC ... 46
4.1.1 IVT and mRNA-transfection of MSC ... 46
4.1.2 Vitality and toxicity following mRNA transfection ... 47
4.1.3 Maintenance of multilineage differentiation potential following mRNA transfection ... 49
4.1.4 Protein expression after mRNA transfection of MSC ... 49
4.1.4.1 Evaluation of ITGA4 expression ... 49

4.1.4.2 Western Blot ... 52
4.1.4.3 LDV-FITC binding ... 53
4.1.5 GFP expression after mRNA-transfection ... 55
4.2 Optimizing lentiviral modification of MSC with ITGA4 ... 57
4.2.1 Transgene expression ... 57
4.2.1.1 mRNA expression of ITGA4 after promoter substitution ... 57
4.2.1.2 Evaluation of ITGA4 protein expression after promoter substitution ... 58
4.2.2 Copy numbers ... 60
4.2.3 Characterization of MSC overexpressing ITGA4-GFP under control of various promoters ... 61
4.2.3.1 Growth curves and population doubling time ... 61
4.2.3.2 Cell viability ... 62
4.2.4 *In vitro* migration of EF1α-ITGA4-MSC ... 63
4.3 Enhancing homing of MSC towards cerebral ischemia ... 64
4.3.1 Transgene expression after lentiviral infection ... 64
4.3.2 Growth profiling after stable modification of MSC with ITGA4 or CCR2 ... 67
4.3.3 Maintenance of trilineage differentiation potential ... 68
4.3.4 *In vitro* characterization of transmigration ... 69
4.3.4.1 Transmigratory activity across endothelial barrier ... 69
4.3.4.2 Classification of migrating MSC ... 71
4.3.5 *In vivo* homing of modified MSC ... 74
4.3.5.1 Mortality and evaluation of cerebral lesion ... 74
4.3.5.2 SPECT/CT-Imaging ... 74
4.3.5.3 Evaluation of MSC-distribution after intra-arterial transplantation ... 77
4.3.5.4 Immunohistochemical tracking of transplanted MSC ... 78

5 Discussion ... 81
5.1 mRNA as a tool for genetic engineering of MSC ... 82
5.1.1 ITGA4 mRNA lipofection of MSC ... 82
5.1.2 Structural characteristics and stability of cellular mRNA ... 83
5.1.3 Efficiency of ITGA4-IVT-mRNA translation ... 85
5.1.4 Processing of ITGA4 after mRNA-transfection and implications for its biological function ... 87
5.1.5 Concluding remarks for mRNA-based modification of MSC ... 88
5.2 Lentiviral-based modification of MSC and its optimization by promoter substitution ... 89
5.2.1 Lentiviral modification: a matter of promoter choice? ... 90

5.2.2 Promoter-dependent silencing ... 92
5.2.3 Promoter-dependent transgene expression: impact on cell viability ... 92
5.2.4 Concluding remarks for promoter-dependent lentiviral modifications ... 93
5.3 Overexpression of surface receptors for improved homing towards cerebral ischemia ... 94
5.3.1 The relevance of CCR2 and ITGA4 for MSC-migration towards cerebral ischemia ... 94
5.3.2 Lentiviral modification of MSC for improved homing ... 95
5.3.3 Characterization of modified MSC ... 96
5.3.4 (Trans)migration activity of modified MSC *in vitro* ... 97
5.3.5 Interaction of MSC with endothelium *in vitro* ... 100
5.3.6 Delivery and homing of MSC towards cerebral ischemia after intra-arterial transplantation ... 103
5.3.7 MSC after intra-arterial transplantation: are they really gone? ... 106
5.3.8 Concluding remarks for improved homing after ITGA4- and CCR2 overexpression ... 107
6 Conclusions and outlook ... 109
7 References ... 112
8 Supplements ... 135

Acknowledgements ... 143
Statement of authorship ... 145
Selbständigkeitserklärung ... 145
Curriculum vitae ... 147
List of publications ... 149

## List of tables

Tab. 1 Thermal cycling condition for DNA-template PCR ..... 29
Tab. 2 Components of IVT cocktail ..... 29
Tab. 3 Components of capping cocktail for Cap0 or Cap1 generation ..... 30
Tab. 4 Components of polyadenylation cocktail ..... 30
Tab. 5 Thermal cycling conditions for TaqMan™ quantitative RT-PCR ..... 36
Tab. 6 Distribution of transplanted MSC in SHAM and MCAO animals. ..... 75
Tab. 7 Comparison of lentiviral and mRNA based modification of MSC ..... 110

## List of figures

Fig. 1 Model of stem cell differentiation..... 2
Fig. 2 Mulitlineage differentiation potential of MSC..... 4
Fig. 3 Assumed repair mechanisms of stroke upon transplantation of MSC. ..... 7
Fig. 4 Multistep model of leukocyte extravasation..... 9
Fig. 5 Assembly of components for tank blot procedure.. ..... 38
Fig. 6 Scheme of a modified Boyden chamber setup..... 40
Fig. 7 Scheme of MSC localization to endothelium for category allocation..... 41
Fig. 8 Experimental design for evaluation of MSC homing towards cerebral ischemia. ..... 42
Fig. 9 In vitro transcription (IVT) and transfection using various transfection reagents. ..... 46
Fig. 10 mRNA level for ITGA4 ..... 47
Fig. 11 Viability of CTRL and transfected MSC.. ..... 48
Fig. 12 Toxicity of controls and transfected MSC. ..... 48
Fig. 13 Differentiation into adipogenic, osteogenic and chondrogenic lineage after mRNA transfection.. ..... 49
Fig. 14 Transfection of MSC with post-transcriptionally or co-transcriptionally capped ITGA4-mRNA and analysis via flow cytometry. ..... 50
Fig. 15 ITGA4 expression after mRNA transfection of MSC. ..... 51
Fig. 16 Evaluation of ITGA4-GFP translation following mRNA-transfection. ..... 52
Fig. 17 Flow cytometric assessment of LDV-FITC binding after MSC transfection with ARCA-, Cap0-, or Cap1-ITGA4 mRNA. ..... 54
Fig. 18 Fluorescence microscopy after LDV-FITC binding. (A). ..... 55
Fig. 19 Flow cytometry of controls and MSC transfected with ARCA-GFP, Cap0-GFP, and Cap1-GFP..... 56
Fig. 20 mRNA expression of ITGA4 under control UbC-, EF1α-, CMV-, and TRE-promoter.. ..... 57
Fig. 21 Evaluation of transgene expression of MSC infected with UbC-, EF1α-, CMV-, or TRE-ITGA4 tagged with GFP. ..... 59
Fig. 22 Western Blot analysis of MSC after infection with ITGA4-GFP..... 60
Fig. 23 Copy number determination at day 8 and day 20 after lentiviral infection of MSC. ..... 61
Fig. 24 Growth characteristics of MSC overexpressing ITGA4 under the control UbC-, EF1α-, CMV-, or TRE-promoter and controls. ..... 62

Fig. 25 Viability of CTRL and lentivirally infected MSC. ..... 62
Fig. 26 Transmigratory activity of EF1α-ITGA4-MSC and CRL-MSC. ..... 63
Fig. 27 Lentiviral modification of MSC with ITGA4 +tdTomato(ITGA4-MSC), CCR2 + tdTomato (CCR2-MSC), and tdTomato alone (CTRL-MSC).). ..... 64
Fig. 28 mRNA expression of CCR2 (A), ITGA4 (B) and ITGB1 (C) after lentiviral infection and sorting of MSC. ..... 65
Fig. 29 Overexpression of ITGA4 on MSC.)..... 66
Fig. 30 Phenotypic characterization of MSC after lentiviral modification ..... 67
Fig. 31 Growth characteristics of ITGA4-MSC, CCR2-MSC and CTRL-MSC. ..... 68
Fig. 32 Differentiation of MSC.. ..... 69
Fig. 33 Transmigratory activity of MSC in the FluoroBlok Boyden chamber. ..... 70
Fig. 34 Classification of migrating MSC. ..... 72
Fig. 35 Categorization of transmigration of CTRLs and modified MSC. ..... 73
Fig. 36 Representative MR images. ..... 74
Fig. 37 SPECT-CT-based analysis of MSC biodistribution following MCAO and intra-arterial transplantation. ..... 76
Fig. 38 Radioactive counts represented as percent of injected dose per tissue sample weight (%ID/g) ..... 77
Fig. 39 Detection of MSC based on their expression of a fluorescence reporter protein ..... 78
Fig. 40 Double immunofluorescence staining against MSC reporter protein (GFP, tdTomato) and lectin..... 79
Fig. 41 Double immunofluorescence staining against MSC reporter protein (GFP, tdTomato) and IBA1.. ..... 80
Fig. 42 mRNA capping. ..... 84
Fig. 43 Interplay between chemokine signaling and Integrin activation. ..... 99
Fig. 44 MSC transmigration over an endothelial monolayer. ..... 101
Fig. 45 Vascular anatomy of the rat. ..... 105
Fig. 46 Plasmid maps ..... 141
Fig. 47 SPECT-CT images and analysis of selected animals with cerebral influx of transplanted cells. ..... 142

## List of abbreviations

| | |
|---|---|
| % | Percent |
| %ID/g | Percent of injected dose per gram |
| °C | Degree Celsius |
| µg | Microgram |
| µL | Microliter |
| µm | Micrometer |
| 5mC | 5-methylcytidine |
| A.dest | Latin for aqua destillata, destilled water |
| APS | Ammonium persulfate |
| ARCA | Anti-reverse cap analogon |
| ASC | Adult stem cell |
| ATP | Adenosine triphosphate |
| AU | Arbitrary Unit |
| BBB | Blood brain barrier |
| BCA | Bichinon acid |
| BDNF | Brain-cell derived neurotrophic factor |
| bFGF | Basic fiboblast growth factor |
| BMP2 | Bone morphogenetic protein 2 |
| bp | Base pair |
| C/EBPβ | CCAAT/enhancer binding protein beta |
| CBF | Cerebral blood flow |
| CCR | C-C- motif chemokine receptor |
| CD | Cluster of differentiation |
| cDNA | Complementary deoxyribonucleic acid |
| cm | Centimeter |
| CMV | Cytomegalovirus |
| CNS | Central nervous system |
| cPPT | Central polypurine tract |

| | |
|---|---|
| CRIPR/Cas9 | Clustered regularly spaced short palindromic repeat associated protein 9 |
| CT | Computed tomography |
| Ct | Cycle threshold |
| CXCR | C-X-C motif chemokine receptor |
| DAPI | 4',6-diamidino-2-phenylindole |
| DEPC | Diethylpyrocarbonate |
| DMSO | Dimethyl sulfoxide |
| DNA | Deoxyribonucleic acid |
| DTT | Dithiothreitol |
| ECA | External carotid artery |
| EDTA | Ethylene-diamine-tetra-acetic acid |
| EF1α | Elongation factor 1 alpha |
| EGF | Epidermal growth factor |
| eGFP | Enhanced green fluorescent protein |
| eIF4E | Eukaryotic initiation factor 4E |
| ERK | Extracellular signal regulated kinase |
| ESC | Embryonic stem cell |
| et al. | Et alia |
| FCS | Fetal cow serum |
| FGF2 | Fibroblast growth factor 2 |
| FOV | Field of view |
| g | Gravitational force |
| GAPDH | Glyceraldehyde 3-phosphate dehydrogenase |
| GDNF | Glial-cell derived neurotrophic factor |
| GEF | Guanine exchange factors |
| GFP | Green fluorescent protein |
| GMP | Guanosine-monophosphate |
| GPCR | G-protein coupled receptor |
| GRO1 | Growth regulated oncogene 1 |
| GTP | Guanosine triphosphate |
| h | Hour |

| | |
|---|---|
| HGF1 | Hepatocyte growth factor 1 |
| HIV | Human immunodeficiency virus |
| HRP | Horse radish peroxidase |
| IBMX | Isobutylmethylxanthine |
| ICC | Immunocytochemistry |
| IFNs | Type I interferons |
| IGF1 | Insulin-like growth factor 1 |
| IL6 | Interleukin 6 |
| iPSC | Induced pluripotent stem cells |
| IRES | Internal ribosomal entry site |
| ISCT | International Society for Cell Therapy |
| ITGA4 | Integrin alpha 4 |
| ITGB1 | Integrin beta 1 |
| IVT | *In vitro* transcription |
| Kas | Equilibrium association constant |
| kb | Kilo base pair |
| kDa | Kilo Dalton |
| kVp | Peak kiloVoltage |
| LB | Luria broth |
| LDH | Lactate dehydrogenase |
| Log | Logarithm |
| M | Molar mass |
| mA | Milli Ampere |
| MAPK | Mitogen-activated protein kinase |
| MBq | Mega Becquerel |
| MCA | Middle cerebral artery |
| MCAO | Middle cerebral artery occlusion |
| MCP1 | Monocyte chemotactic protein 1 |
| MFI | Mean fluorescence intensity |
| min | Minute |
| mL | Milliliter |

| | |
|---|---|
| mm | Millimeter |
| mM | Millimolar |
| mmol | Millimole |
| MOI | Multilicity of infection |
| MRI | Magnetic resonance imaging |
| mRIPA | Modified radioimmunoprecipitation assay |
| mRNA | Messenger ribonucleic acid |
| MSC | Mesenchymal stem cell |
| MTT | 3-(4,5-dimethylthiazol-2-y-yl)-2,5-diphenyltetrazolium |
| $NAD^+$ | Nicotinamid adenine dinucleotide, oxidized |
| NADH | Nicotinamid adenine dinucleotide, reduced |
| ng | Nanogram |
| nm | Nanometer |
| NMDA | N-Methyl-D-aspartate |
| NTP | Nucleotide triphosphate |
| OD | Optical density |
| ORF | Open reading frame |
| PBS | Phosphate buffered saline |
| PC5A | Pre-protein convertase 5A |
| PCR | Polymerase chain reaction |
| PD | Population doubling |
| pDNA | Plasmid deoxyribonucleic acid |
| PDT | Population doubling time |
| PEI | Polyethyleneimine |
| PFA | Paraformaldehyde |
| pH | Potential hydrogen |
| PLC | Phospholipase C |
| PPARγ | Peroxisome proliferator-activated receptor gamma |
| PRR | Pattern recognition receptors |
| RMS | Rostral migratory stream |
| rpm | Rounds per minute |

| | |
|---|---|
| RRE | Rev responsive element |
| rtTA | Reverse tetracycline-controlled transactivator |
| Runx2 | Runt-related transcription factor 2 |
| s | Second |
| S.O.C. medium | Super optimal broth medium with catabolite repression |
| SDF1 | Stromal derived factor 1 |
| SDS | Sodium dodecyl sulfate |
| SDS-PAGE | Sodium dodecyl sulfate polyacrylamide gel electrophoresis |
| SPECT | Single photon emission computed tomography |
| SRP | Signal recognition pathway |
| SV40 | Simian vacuolating virus 40 |
| SVZ | Subventricular zone |
| T | Tesla |
| TAE buffer | Tris-acetate-EDTA buffer |
| tdTomato | Tandem tomato protein |
| TEMED | Tetramethylethylenediamine |
| TGFβ | Transforming growth factor beta |
| TLN1 | Talin 1 |
| TNFα | Tumor necrosis factor alpha |
| TRE | Tetracycline response element |
| U | Unit |
| UTR | Untranslated region |
| UV | Ultra violet |
| V | Volt |
| VCAM1 | Vascular cell adhesion molecule 1 |
| VEGF | Vascular endothelial growth factor |
| VLA4 | Very late antigen 4 |
| VSV-G | Glycoprotein G of the vesicular stomatitis virus |
| WPRE | Woodchuck hepatitis virus posttranscriptional regulatory element E |
| ψ | Pseudouridine |

# 1 Introduction

## 1.1 Adult stem cells

Stem cells have been in the focus of biomedical research over the last decades. Their potential for self-renewal and differentiation raised the hope to employ stem cells for regenerative purposes and tissue-repair strategies in a wide range of disorders.

In general, stem cells can be distinguished in two classes: embryonic and adult stem cells. Embryonic stem cells (ESC) are pluripotent cell types and, thus, show the capability of indefinite proliferation and differentiation into almost every cell type of the body (Paul et al. 2002). However, their particular risk for carcinoma formation after transplantation is considered as fraught with problems. In addition, immense ethical and moral concerns are caused by their isolation from embryos. Hence, a strong demand is raised for an alternative attention towards adult stem cells (ASC) (Pessina and Gribaldo 2006).

Pluripotent ESC differentiate into cells of ectodermal, mesodermal, or endodermal lineage during embryogenesis (Wagers and Weissman 2004). Progressing differentiation gives rise to tissue-specific progenitors that mature into ASC, also called somatic or non-embryonic stem cells (Fig. 1) (Paul et al. 2002). Throughout the entire lifetime, ASC can be found as self-renewing cells within specialized tissues and organs including brain, skeletal muscle, heart, gut, liver, blood vessels or bone marrow (Poulsom et al. 2002). There, ASC quiescently reside within the so-called stem cell niche, a specific microenvironment that support maintenance of stem cell characteristics (Lin 2002; Spradling et al. 2001). Usually, only sparse in numbers during the non-dividing state, ASC start proliferation upon injury, disease or in need for tissue maintenance. Progeny of distinct organ-specific cell types are based on their multipotency. However, since ASC have undergone some specialization, their differentiation potential is limited to the committed lineage. Hematopoetic stem cells, for example, are adult stem cells that give rise to all cell types in blood, but only few beyond. The terminal differentiation is induced by certain environmental cues. The cell passes through several maturation stages on its way to specialization. This is combined with a steady decrease of proliferation capacity and increased expression of cell type-specific markers (Fig. 1) (Baksh et al. 2004).

Against initial skepticism, it was shown that ASC are capable of a phenomenon named transdifferentiation. This process is the differentiation into cell lineages that are not restricted to tissue in which the stem cell resides (Korbling et al. 2003; Phinney and Prockop 2007). A neuron-like morphology, for example was derived from mesenchymal stem cells (MSC) (Manochantr et al. 2010), that typically give rise to lineages of the connective tissue. The fact that differentiation of ASC is not exclusive to their designated cell lineage has amplified the biomedical research interest.

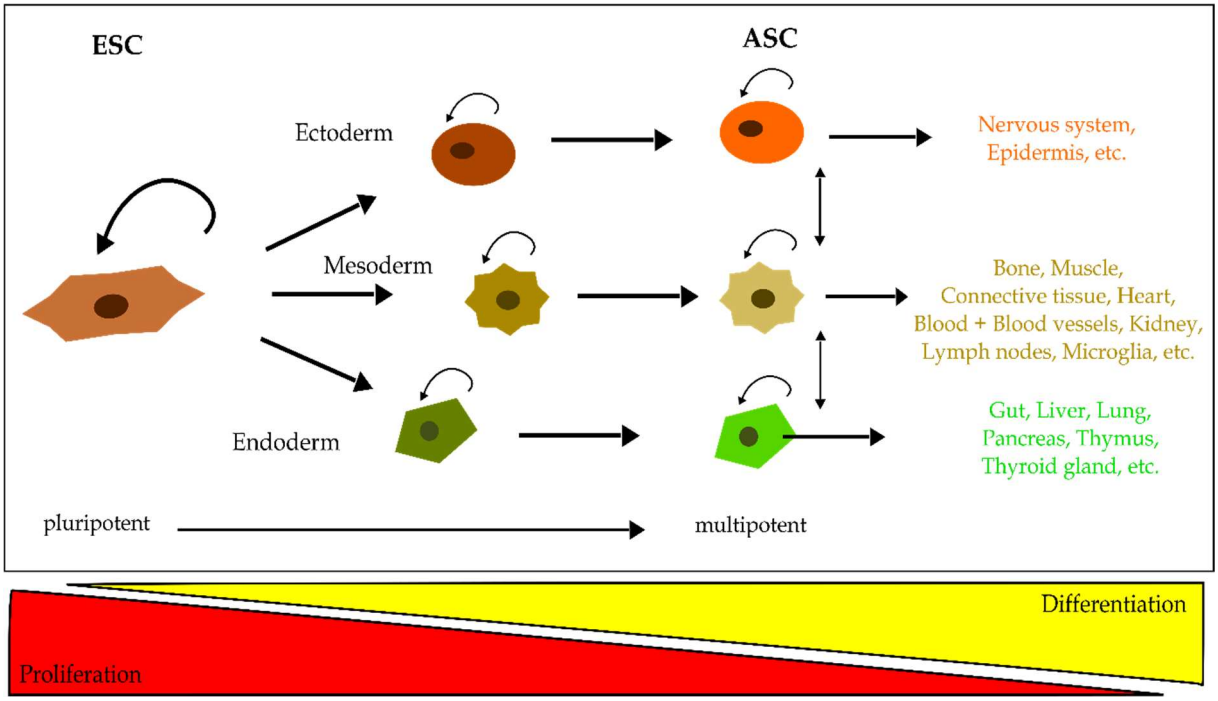


***Fig. 1 Model of stem cell differentiation.*** *Embryonic stem cells (ESC) give rise to cells of ectodermal, mesodermal, and endodermal lineage. Lineage committed cells mature and their offspring specialize to progenitors and adult stem cells (ASC). Importantly, stem cells show self-renewal and proliferation. Symmetrical or asymmetrical cell division yield at least one daughter cell identical to the mother cell. However, their proliferative capacity decreases with specialization and differentiation. (Picture modified after Baksh et al. 2004).*

## 1.2 Mesenchymal stem cells

Among ASC, MSC have gained an increase in prosperity over the last years. First identified and isolated by Friedenstein et al., MSC comprises heterologous cell populations with fibroblastiod morphology and colony-forming capabilities on plastic surfaces (Friedenstein et al. 1976). MSC replicate themselves and maintain their naïve phenotype, but also differentiate into specialized mesenchymal tissue such as bone, cartilage, muscle, tendon, ligament, fat, and other connective tissues (Pittenger et al. 1999; Caplan 1994; Borlongan et al. 2011). Moreover, MSC occur in almost every organ including bone marrow, skin, or fat, and are, therefore, easy to isolate (Caplan and Bruder 2001). Besides isolation from adult tissues, MSC were also identified in various fetal sources such as umbilical cord blood (Laitinen et al. 2016), placenta (Mathews et al. 2015), amniotic fluid, fetal tissues or Wharton´s jelly (Carvalho et al. 2011).

Initial MSC preparations were derived from bone marrow (Haynesworth et al. 1992), which is the most frequently used source so far. Aspirates are usually taken from the iliac crest in humans and larger animals or from the tibia or femur in rodents (Barry and Murphy 2004). After enrichment of MSC-containing fraction by density gradient centrifugation, plastic adherence enables purification of MSC and simultaneous removal of non-adherent hematopoietic cells *in vitro*. *Ex vivo* expansion capacity is extremely high (Bruder et al. 1997) and allows production of a large quantity of usable cells (Caplan and Bruder 2001).

The MSC population can be characterized by distinct surface markers. Albeit they are not expressing a single specific surface marker, their identification is possible by collective assessment of CD105 (endoglin), CD90, and CD73 (Pittenger et al. 1999). In addition to that, MSC lack hematopoietic markers as CD45, CD14, CD11b, CD133, or CD34 and express further surface molecules such as chemokine and cytokine receptors, adhesion proteins and extracellular matrix proteins (Conget and Minguell 1999; Pittenger et al. 1999). Since the MSC frequency within the bone marrow is very low, only limited data are available about freshly isolated and non-expanded MSC (Boiret et al. 2005). Therefore, the fact has to be stressed that findings regarding specific surface markers rely on *in vitro* yielded MSC, what is relevant since culture conditions and endurance of cultivation might alter surface molecule expression (Bobis et al. 2006).

*In vitro* trilineage differentiation into osteoblasts, adipocytes and chondrocytes is crucial for MSC characterization (Augello et al. 2010). Beyond that, MSC differentiation into distinct cell types of connective and musculoskeletal tissue indicates their multipotent phenotype (Fig. 2). The paradigm, that MSC give only origin to cells of the mesenchymal cell line has changed, and differentiation into hepatocytes (Sawitza et al. 2015), neurons (Takeda and Xu 2015), myelin-forming cells (Qiu et al. 2015), or glial cells (Leite et al. 2014) has also been successful.

In order to meet the stem cell definition, MSC should show unlimited self-renewal. Usually it is possible to observe a significant proliferation after isolation, but it is also highly variable during serial *in vitro* propagation (Bruder et al. 1997). Population doublings are ranging between 20-50 while retaining cell cycle distributions and stemness (Devine 2002; Majore et al. 2011). The MSC proliferation rate decreases over time until complete inhibition of cell division, what also depends on initial cell density and cultivation duration (Majore et al. 2011).

Notwithstanding, varying culture protocols led to incongruent data regarding MSC characteristics. Culture medium, cell culture supplements, addition of growth factors, cell density, and incubation environment crucially affect MSC proliferation and have major impact on the final yield. Addition of growth factors such as EGF, FGF2 or TGFβ, as well as low seeding densities will increase number of population doublings (Baksh et al. 2004; Majore et al. 2011). Further variation derives from interdonor and interpopulation heterogeneity of MSC. Isolates from different donors, for example, can show disparities in growth kinetics or differentiation potential, a phenomenon referred to as intra-population heterogeneity. In addition, inter-population heterogeneity is related to inhomogeneity within the MSC population (Pevsner-Fischer et al. 2011). As already mentioned, long-term cultivation leads to change in expression profiles and partial differentiation leading to mixture of phenotypes. Also, de- and transdifferentiation within and between lineages results in occurrence of different subsets with similar morphology as well as switch from asymmetrical to symmetrical division during progression of precursors (Pevsner-Fischer et al. 2011; Baksh et al. 2004).

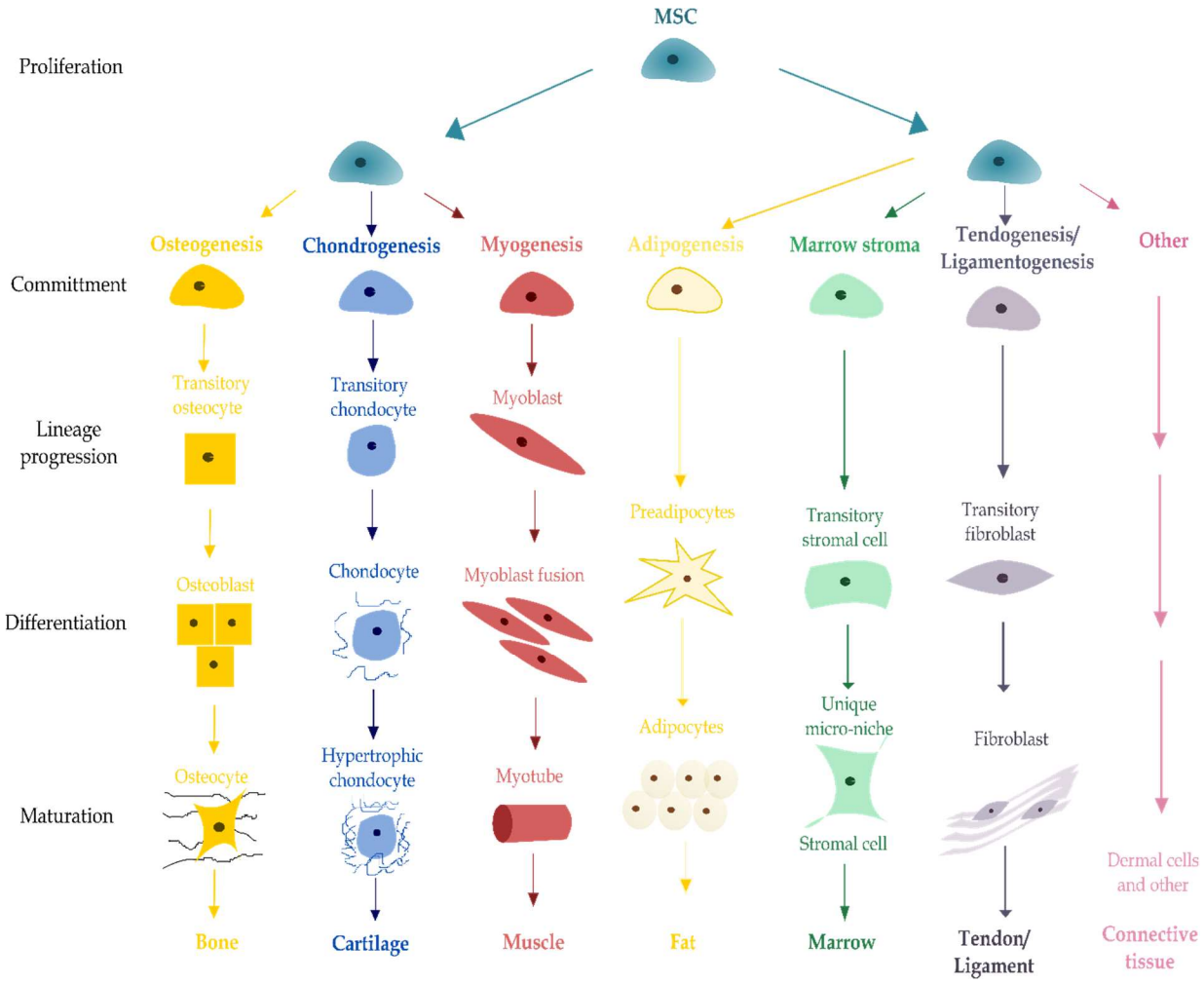


***Fig. 2 Mulitlineage differentiation potential of MSC.*** *After initial proliferation, MSC can give rise to cells of osteogenic, chondrogenic, myogenic, and adipogeic lineage. Differentiation into cell types of the connective tissue underpinn their multipotent character (Picture modified after Caplan and Bruder 2001).*

## 1.3 Therapeutic potential of MSC

Cell therapies are applied in order to replace or to regenerate injured tissue to ultimately establish normal tissue functionality. It is commonly assumed that stem cells migrate to site of injury after local or systemic administration. Under local environmental cues, cells are intended to differentiate and to integrate into host tissue. Furthermore, they can support regeneration by release of cytokine and growth factor cocktails (Caplan and Correa 2011; Kean et al. 2013) or by increasing self-healing capacity (Lee 2010). Feasibility of isolation from various tissues and non-immunogenic phenotype (Keating 2012) accompanied with only minimal ethical concerns related to their use put MSC in the focus of cell based therapies (Kumar et al. 2008). Moreover, autologous isolation of MSC allows a syngeneic therapeutic approach potentially paving the way for personalized cell therapy. MSC have already been studied successfully in several clinical fields and diseases such as in

hematology, graft vs. host disease, wound healing, orthopedics and skeletal diseases, cardiovascular diseases, neurodegenerative disorders, and immunological diseases.

In fact, the therapeutic potential of MSC is primarily characterized by their trophic activity. A plethora of growth factors, cytokines, and chemokines is secreted by MSC including HGF1, TGFβ, VEGF, TSG6 and prostaglandin E2 (Madrigal et al. 2014). Trophic factors support tissue regeneration by the stimulation of angiogenesis, cell survival, proliferation, as well as by reduction of radicals and reactive oxygen species production (Murphy et al. 2013). These effects can be mediated directly or indirectly inducing intracellular signaling or activate a cell in vicinity to secrete a bioactive molecule (Caplan and Dennis 2006).

One of the most significant MSC properties is the lack of immunogenicity. Neither transplantation of autologous nor allogenic MSC has been shown to induce a major immune response in the host tissue. This means that MSC are not rejected and can even support engraftment and survival of other transplants (Bartholomew et al. 2001; Grinnemo et al. 2004). Maturation of T-cells to their respective antigens is inhibited by secretion of soluble MSC factors or by direct cell-cell contact (Pittenger and Martin 2004). MSC further inhibit proliferation of T-cells, B-cells and NK cells and modulate their phenotype towards a more anti-inflammatory or tolerant direction (Aggarwal and Pittenger 2005). On top, the nonimmunogenic phenotype also suggests MSC as an ideal vehicle for gene therapy applications (Baksh et al. 2004). To this end, MSC can be modified to express a bioactive molecule or protein, which is secreted at the injury site (D'souza et al. 2015).

The antiapoptotic potential is another important feature of MSC (Murphy et al. 2013). It has been shown that direct interaction between MSC and ischemic cardiomyoblasts decreases the numbers of apoptotic cells (Cselenyak et al. 2010). The MSC-mediated prevention of apoptosis is not completely understood but it is assumed that secretion of IGF1 or IL6 plays a role through interference in Act signaling pathway (Mitsiades et al. 2002). Most likely MSC also produce molecules such as growth factors (VEGF or TGF1β) or address transcription factors reversing apoptosis (Jin et al. 2015; Qin et al. 2015). Furthermore, a gate keeper function blocks apoptotic signaling of axons and neuronal endings as well as the secretion of the pre-lysosomal degrading enzyme prosaposin (Li et al. 2010).

In order to facilitate recovery, MSC have to migrate to the site of injury, to engraft, to survive the hostile injured environment and finally to differentiate into required cell types (Maltman et al. 2011). Several studies have addressed these aspects and it has been shown that MSC are potentially able to migrate to and partly survive in the host tissue. However, active migration, subsequent engraftment and differentiation is more challenging than initially assumed. Major limitations arise from limited homing after (systemic) transplantation. Only a few cells reach the target tissue and engraft into the host tissue (Becker and van Riet 2016; Ezquer et al. 2016), what has been ascribed to the restricted expression of homing molecules (Becker and van Riet 2016). Furthermore, only a limited number of studies were able to proof *in vivo* differentiation of MSC after transplantation, although there have been numerous evidences of differentiation into organ-specific phenotypes *in vitro* (Li et al. 2002; Mezey and Chandross 2000).

## 1.4 MSC therapy for stroke

Ischemic stroke is caused by the disruption of the brain supply with glucose and oxygen due to an occlusion of one of the cerebral arteries (Endres et al. 2009). Since the brain is not capable of storing glucose and oxygen, the blood flow interruption results in collapse of ATP-production and membrane potential. The induction of the so called ischemic cascade causes edema, excitotoxicity, activation of catabolic enzymes, free radicals, apoptosis and, therefore, massive cytotoxicity (George and Steinberg 2015; Endres et al. 2009). Depending on localization and extent of cell and tissue damage, incising loss of function or even death are the consequences. The major problems after an ischemic insult are the highly limited brain repair capacities being unable to induce complete restoration of function. Although several therapeutic interventions are available to restore blood flow, their success depends on time-effective stroke management. Beyond a crucial time-window of 4.5h after onset, the treatment options are extremely limited and rely on long-term rehabilitation with only restricted success (Veerbeek et al. 2014). Therefore, the development of alternative cell based therapies to restore neurological function is highly attractive (Bliss et al. 2010).

MSC have already been found to improve functional outcome in a considerable number of experimental stroke studies by addressing mechanisms such as neuroprotection, axonal sprouting, anti-apoptosis, angiogenesis, support of local progenitors, and regulation of immune reactions (Fig. 3) (Borlongan et al. 2011; Gutierrez-Fernandez et al. 2013; Yang et al. 2015b). Infarct sizes were reduced and the functional outcome improved after MSC transplantation in rodent models of cerebral ischemia (Honmou et al. 2012). The molecular mechanism by which MSC mediate stroke recovery are not fully understood. It is assumed that tissue recovery is supported by replacement of lost cells and secretion of bioactive factors (Tolar et al. 2010). Both mechanisms are not exclusive, but it is believed that MSC beneficially affect tissue regeneration, inflammation, and vascularization most likely by the release of trophic mediators (Phinney and Prockop 2007), growth factors and other chemokines (Phinney and Prockop 2007).

Since an ischemic insult leads to significant cell death in the brain, the rescue of dying neurons is important to limit cell loss. MSC are able to mediate neuroprotective effects by several factors. For example, their secretion of GDNF and BDNF is associated with enhanced neuronal survival *in vitro* (Wilkins et al. 2009; Tate et al. 2010) and *in vivo* (Liang et al. 2014) ischemia models. Furthermore, there is evidence for release of soluble factors that protect neurons from N-Methyl-D-aspartate (NMDA) induced calcium influx and subsequent glutamate excitotoxicity (Voulgari-Kokota et al. 2012). Superoxide radicals are scavenged by the antioxidant enzyme superoxide dismutase 3 and its secretion by MSC was found to mitigate neurotoxic effects (Kemp et al. 2010). In addition, neurotrophic, neuroprotective, and pro-oligodendrogeneic factors are released after indirect stimulation by MSC-borne prosurvival and antiapoptotic molecules (Eckert et al. 2013). The neuroprotective molecules bFGF and SDF1, for example, were secreted by engrafted MSC after transient ischemia in rats. Improved functional recovery and smaller infarct sizes were achieved by their impact (Toyoshima et al. 2015).

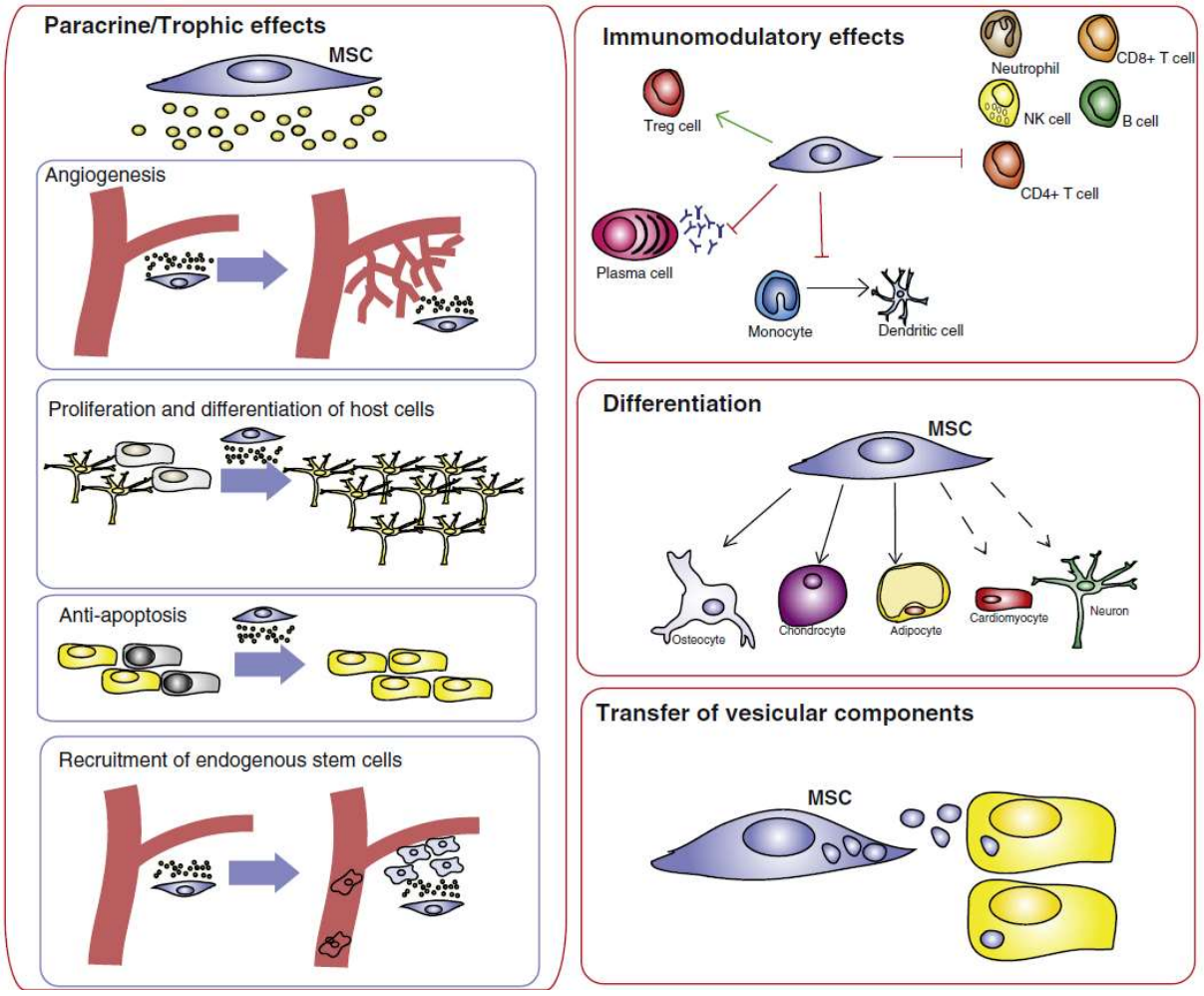


***Fig. 3 Assumed repair mechanisms of stroke upon transplantation of MSC.*** *MSC support brain repair mechanisms by the release of trophic factors. Angiogenesis, support of local progenitors, anti-apoptotic effects, and immunomodulatory effects are enhanced after MSC transplantation. Picture derived from (Bronckaers et al. 2014).*

The interplay of matrix metalloproteinases, growth factors, chemokines, adhesion molecules, and angiogenic inhibitors is fundamental during postischemic angiogenesis (Bronckaers et al. 2014; Carmeliet and Jain 2011). This process is particularly enhanced after MSC transplantation due to their release of angiogenic factors such as VEGF and angiopoietin 1 and 2 (ang1, ang2). Notably, ang1 contributes to angiogenesis, as well as maturation, stabilization and remodeling of blood vessels (Honmou et al. 2012). VEGF, in turn, is essential for proliferation and differentiation of endothelial progenitors (Chen et al. 2003b; Zacharek et al. 2007). Of note, improved functional recovery has also been associated with enhanced neovascularization and vascular density (Yan et al. 2014).

Following stroke, the generation of neural progenitor cells is physiologically enhanced in the subventricular zone (SVZ). The newborn neurons either harbor in the well-adjusted niche or migrate along the rostral migratory stream (RMS) (Jin et al. 2001) as well as towards the injured brain area (Ding et al. 2013; Guzman et al. 2008). This process is stimulated by molecular compounds including bFGF, EGF, BNDF, and IGF1 (Chopp et al. 2007). It has been

shown that this effect is even more increased after transplantation of MSC (Chen et al. 2003a; Park et al. 2015a; van Velthoven et al. 2013).

## 1.5 State-of-the-art: systemic homing of MSC towards injury and transendothelial migration

Homing towards injury is crucially affecting the therapeutic success of MSC, but details addressing its initiation and mechanism are lacking (Matsushita et al. 2011; Karp and Teo, 2009). Nevertheless, the body of literature on this topic is growing, driven by the need to understand and improve homing mechanism of MSC. The following section is intended to give an overview on current understanding of MSC homing after systemic transplantation.

Based on a leukocyte model of extravasation (Fig. 4), common mechanisms were deduced for MSC (Henschler et al. 2008; Ley et al. 2007). These models assume a similar orchestration of migratory cues including chemokines, cytokines and growth factors released from the injury site. It is known from leukocytes, that selectin receptors are necessary to capture the flowing cell from the blood stream and to initialize subsequent tethering and rolling on the activated endothelium (Muller 2011). During rolling, the leukocyte slows down and chemokine activated integrins establish a firm adhesion (Muller 2009). A particular role for adhesion is attributed to interaction between VLA4, expressed on flowing cells, with VCAM1, upregulated on the inflamed endothelium (Ley et al. 2007). Subsequently, the leukocyte flattens, polarizes, and starts to crawl in order search for the right spot of transmigration. At optimal localization, leukocyte overcomes the endothelial barrier and migrates through the interstitium towards the inflammation.

The recruitment of MSC towards sites of injury is based on a chemotactic gradient established by the release of soluble molecules. In response to this gradient, the MSC is attracted and migrates towards the releasing point (Marquez-Curtis and Janowska-Wieczorek 2013; Herzmann et al. 2016). The MSC itself expresses a variety of receptors enabling it to "sense" chemokines and cytokines (Sohni and Verfaillie 2013). One of the best studied receptors in MSC homing is the C-X-C motif chemokine receptor (CXCR) 4 and its ligand stromal derived factor-1 (SDF1) (Marquez-Curtis and Janowska-Wieczorek 2013). Blocking experiments revealed that the SDF1 facilitated migration is impaired when treating MSC with the CXCR4 antagonist AMD3100 (Cao et al. 2013). However, several chemokine receptors are expressed on MSC that might also play a role for homing, including CCR1 (Sordi 2009), CCR2 (Chamberlain et al. 2007), and CXCR7 (Marquez-Curtis and Janowska-Wieczorek 2013).

Adhesion receptors such as integrins, CD44, or CD24 (Chamberlain et al. 2007) mediate the attachment to extracellular matrix components and to other cells. Therefore, they play a crucial role for the homing process. Exit from the circulation, for example, requires integrin-dependent establishment of contact between MSC and the endothelium. MSC have been found to express a variety of integrins from the β and α subunits, assembling to a heterodimer receptor (Semon et al. 2010; Ip et al. 2007).

Following intravascular administration, MSC are distributed through the body. Close to the injury site, they are intended to leave the vascular system and to migrate towards the damaged tissue, a process referred to as pathotropism (Bing et al. 2016). Therefore, active or passive arrest is required within the vasculature followed by transmigration across the

endothelium (Karp and Teo 2009). During inflammation, the endothelium reacts with the upregulation of certain adhesion receptors and consequently provide an anchorage point for MSC.

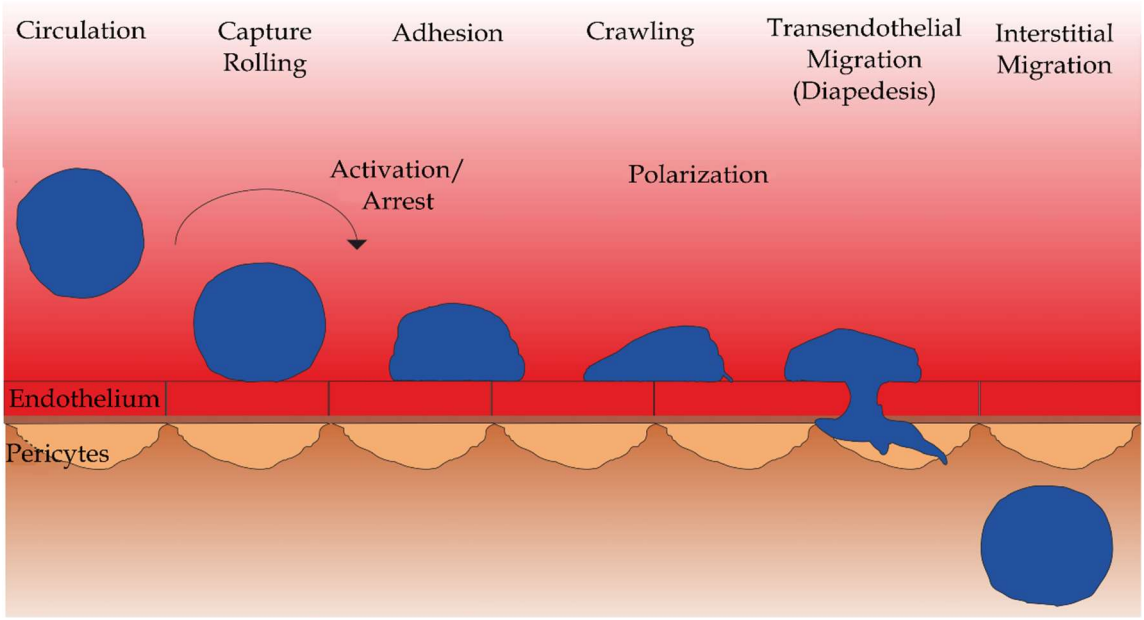


***Fig. 4 Multistep model of leukocyte extravasation.*** *The model comprises several subsequent steps outlined as selectin-mediated capturing and rolling, arrest on inflamed endothelium, integrin (VLA4)-mediated firm adhesion, crawling, and transendothelial migration to leave the blood vessel.*

MSC can undergo rolling and integrin-mediated adhesion similar to leukocytes. Notwithstanding, significant differences have been identified between MSC and leukocytes. Duration of -MSC transmigration is considerably longer as compared to leukocytes (Teo et al. 2012; Schmidt et al. 2006a). There is also evidence that selectin-dependent rolling is not necessarily required for MSC and their transmigration is rather driven by integrin-mediated adhesion (Ip et al. 2007). Furthermore, it has been shown that MSC show little lateral migration on the endothelium. Formation of filo-and pseudopodia as well as nonapoptotic membrane blebs have been observed (Teo et al. 2012). It has further hypothesized, that MSC form transmigratory cups and establish a cooperation with endothelial cells (Teo et al. 2012).

## 1.6 Current frontiers for MSC based therapy

So far, success of cell therapy is restricted and limitations arise from shortcomings in homing, survival, and engraftment (Hodgkinson et al. 2010). Of note, homing of MSC can be at least partly influenced by their administration route. The available modes of administration are distinguished between systemic or local transplantation. Systemic administration comprises intravenous, intra-arterial, or intraperitoneal injection whereas local administration is realized by intralesional transplantation (e.g. intracranial, intracerebral, subcutaneous) (Zhang et al. 2015).

Systemic delivery has several advantages and circumvents potential problems related to site-specific transplantation (Steingen et al. 2008; Chamberlain et al. 2011). It circumvents the

immediate hostile influence of ischemia, inflammation, and fibrosis (Mastri et al. 2014). Furthermore, intra-arterial or intravenous infusion of MSC is less invasive than direct transplantation into injured tissue and allows repetitive administrations (Lundberg et al. 2012). However, MSC migration and engraftment after systemic delivery is not very effective (Khaldoyanidi 2008), making it difficult to concentrate sufficient cell numbers at the site of injury (Khaldoyanidi 2008; Kumar and Ponnazhagan 2007). As one of the most common observations, cell entrapment in the filter organs reflects the inability to home to injured tissue (Khabbal et al. 2014; Kerkela et al. 2013; Vasconcelos-dos-Santos et al. 2012; Fischer et al. 2009). A major risk is given when entrapment results in a secondary infarction of filter organs due to MSC induced supply block (Everaert et al. 2012).

Therapeutic MSC application stagnated due to their assumptive incapacity to home to site of tissue injury in sufficient numbers (Salem and Thiemermann 2010). Typically, less than 5% of injected MSC are rediscovered at injury site (Kurtz 2008). A critical step in recruitment of MSC to sites of injury and inflammation is extravasation (Teo et al. 2012). The processes of blood flow egress and crossing the endothelial cell barrier are not fully understood for MSC. It is unclear, for example, whether transplanted MSC are actively adhering to the endothelium or simply get stuck within the vasculature (Walczak et al. 2008). As elucidated in the foregoing chapter, the well-described leukocyte transendothelial migration process could serve as a reasonable role model (Steingen et al. 2008) for identification of migratory cues and to explain MSC homing behavior. Culture conditions are believed to affect the MSC expression profile of chemokine receptors and adhesion molecules (Aldridge et al. 2012) and, therefore, influence adhesion capabilities (Karp and Teo 2009; Becker et al. 2007). Also, passage number and isolation methods are critical for homing efficiency (Maijenburg et al. 2012).

Beyond that, it has been reported that transplanted cells disappear within a short time frame after transplantation without any evidence for extended survival (Shen et al. 2007). Despite the question whether or not transplanted cells are crucially needed for a longer time range and if engraftment is indeed necessary, it is clear that residence in vital and functional condition is favorable for therapeutic effects. Conditions during isolation and *in vitro* expansion (Wei et al. 2010) as wells as a toxic environment at the injury site after transplantation (Francois et al. 2013; Lin et al. 2013) can increase stress and cell mortality (Amiri et al. 2015). As advised by Amiri et al., consideration of guidelines for MSC pretreatment might prevent premature cell death (Amiri et al. 2015), but require a stricter definition and characterization of MSC (Keating 2012).

## 1.7 Cell engineering for improved homing

Since insufficient homing of MSC might contribute to limited therapeutic success, numerous approaches have been developed to enhance homing capabilities. Recruiting, adhesion, and survival can be improved by a number of techniques that manipulate pre-existing adhesive mechanisms and cell membrane properties (Kavanagh et al. 2014). Enzymatic manipulation of endogenously expressed surface proteins can be used (Ansboro et al. 2012) besides optimizing culture conditions by addition of growth factors and cytokines (Segers, Vincent F M et al. 2006) or by creating a hypoxic atmosphere (Kang et al. 2012). Notably, adjustment

and manipulation of stem cells are mainly realized by genetic engineering including the use of integrating viral vectors as well as delivery of plasmid DNA or mRNA (Nowakowski et al. 2013). These techniques should be addressed in this section.

History of delivery of foreign nucleic acids started in 1990, when naked plasmid DNA (pDNA) was taken up by muscle cells (Wolff et al. 1990). Since then, several methods have been developed to introduce pDNA into cells for transgene expression. Following transfection, the DNA has to enter the nucleus, where it is transcribed into mRNA. Then, the mRNA has to return to the cytoplasm for protein translation (Nowakowski et al. 2013). Considering these processes, the occasionally low efficiency of pDNA transfection is hardly surprising. Low efficiencies have also been observed for MSC (Park et al. 2015b) so pDNA delivery is not believed to be a reasonable option.

The key mechanisms of integrating viral vectors is to incorporate their genetic information into a host genome. The transferred genes are expressed and also inherited to following generations. Retroviruses and lentiviruses, baculovirus, but also adeno-associated viruses have been applied for MSC modification (Park et al. 2015b). Since particularly lentiviruses are able to infect cells with high efficiency, they are applied to deliver therapeutic genes to MSC without impacting proliferation or differentiation (McGinley et al. 2011). Overexpression the CXCR4 gene by lentiviral transduction, for example, successfully enhances *in vitro* migration and homing of MSC towards bone marrow of irradiated mice (Chen et al. 2013). Generation of lentiviral particles with minimalized risk of self-replication in target cells was achieved by relocation of structural viral genes to additional helper plasmids and by placing the respective transgene onto a viral backbone plasmid (Nowakowski et al. 2013). After transfection of these plasmids to a helper cell line, viral particles are assembled and can be used to infect the target cells. While this generally results in a long-term transgene expression, it also harbors risks for insertional mutagenesis and activation of oncogenes (Knight et al. 2013). Nevertheless, despite the proven efficiency of lentiviral vectors for MSC engineering, several structural components can influence the transgene expression. The choice of the promoter that drives the transgene influences the expression level, but is frequently based on technical convenience (Qin et al. 2010). To facilitate a more rational decision and vector tailoring for a particular experiment, systematic comparison of promoters is demanded.

Another option for introduction of therapeutically relevant proteins is the delivery of synthetic mRNA (Tavernier et al. 2011; Sahin et al. 2014). Advances addressing inherent properties of mRNA such as stability or immune-stimulatory activity (Kariko et al. 2005) pave the way for numerous applications. A major advantage of mRNA is the bypass of the nuclear transport providing direct access to translation machinery. This allows rapid protein expression (Tavernier et al. 2011). mRNA based modifications are a valid option for non-dividing cells due to their independence from the cell-cycle (Van Tendeloo, Viggo F I et al. 2007). The risk of genome insertion or mutagenesis is completely eliminated. Moreover, the clinical safety profile is strengthened by the only transient protein expression and the complete degradation by physiological pathways. IVT mRNA can be potentially used as a tool to equip MSC with homing receptors for improved navigation towards cerebral ischemia. Adhesion molecules as VCAM1 and chemokines are upregulated shortly after an ischemic insult and their expression is maintained within a temporary time window. Since

the expression of key homing regulators is restricted, the transient expression of their counterparts seems to be sufficient. Effective modification of MSC with homing receptors has already been shown by Ryser et al., who used a synthetic mRNA to overexpress CXCR4 for increased chemotaxis (Ryser et al. 2008). Taken together, it is easy to envisage that IVT mRNA-based cell engineering will increasingly have a broader impact on regenerative medicine applications.

## 1.8 Aims and objectives

In order to develop a valid cell based therapy, MSC need to be effectively targeted to the injury site. In spatial proximity, MSC can efficiently support repair mechanisms by release of trophic factors. To date, the homing process of MSC towards injury is not completely elucidated and, thus, development of MSC based therapies was proven to be challenging.

An important point regarding efficient homing is the sufficient expression of respective surface receptors. Those receptors, identified from leukocyte homing mechanisms, enable cells to migrate, adhere and detach, as well as to navigate towards the lesion. In comparison with leukocytes, the expression of surface receptors on MSC is slightly different and some of the key receptors are only present on a small subset of cells. To that, variety of isolation and cultivation protocols (Wagner and Ho 2007), as well as extend cultivation periods have been shown to influence the surface receptor expression and resulted in downregulation of relevant receptor molecules. Particularly chemokine receptors such as CXCR4, CCR1 or CCR2 as well as adhesion receptors including integrins are affected.

The overexpression of relevant key receptors is intended to equip MSC for more efficient recruitment and migration towards a lesion site. Stem cell homing is guided by SDF1, MCP1, MCP3, growth regulated oncogene 1 (GRO1) or IGF1 (Penn and Mangi 2008), being released from damaged area. Recently, overexpression of CXCR4 enhanced migration towards its ligand SDF1 (Marquez-Curtis et al. 2013). Also MCP1 counts as a potent recruiter, but the expression of its receptor CCR2 has been found to be low on MSC (Ringe et al. 2007; Baek et al. 2011). CCR2 overexpression was shown to lead to enhanced homing in a mouse model of myocardial infarction. With a different setup, it was possible to increase homing by upregulation of integrins thus improving adhesion on inflamed endothelium and transmigration (Kumar and Ponnazhagan 2007). Since MSC do express the integrin subunit β1, but not α4, the adhesion receptor VLA4 cannot be formed. Consequently, MSC adhesion on inflamed endothelium is impaired

A broad variety of engineering techniques is available which allow the manipulation of protein expression, but require optimization and tailoring for the respective cell type. While delivery of plasmid DNA to MSC was proven to be inefficient, mRNA-based and viral infection seems to be a suitable alternative. Recent advances in mRNA research led to overcome of stability obstacle and paved the way for transient mRNA-based modification of MSC. It has been reported that especially features located at 5´end and the 3´end have stabilizing effects, prevent degradation and, of note, regulate protein translation. Particularly the 5´cap provides a platform for translation initiation. The first aim deals with evaluation of MSC engineering utilizing mRNA and focusses on its qualification for modification of MSC with respect to homing receptors.

Objective (I) MSC engineering using mRNA transfection of ITGA4

With this approach, transient modification using synthetic mRNA coding for ITGA4 had to be generated and introduced to MSC. Those modified MSC should be analyzed regarding mRNA transfer efficiency into the cell and subsequent protein expression. Furthermore, structural modification of mRNA capping (Cap0, Cap1, and ARCA) should be analyzed in

terms of influence on protein expression. Potential impact on cell properties should also be addressed.

Lentiviral vectors can induce the long-term expression of a desired transgene. Furthermore, extended transgene expression provides the possibility of cell preparation without time-limited transgene expression. However, efficiency and extent of transgene expression strongly depends on the used promoter. The second aim addressed lentiviral overexpression of ITGA4 and repercussions of promoter choice.

Objective (II) Optimization of lentiviral transduction for genetic engineering of MSC with ITGA4

Long-term overexpression of ITGA4 shall be evaluated after lentiviral modification. Several constitutive active promoters (Ubiqitin C (UbC) promoter, Cytomegalovirus (CMV) promoter, Elongation factor 1 alpha (EF1α) promoter) or a doxycycline-inducible TRE promoter had to be cloned in front of the transgene-encoding region. Promoter dependent transgene expression should be analyzed on mRNA and protein level. Tolerance of lentiviral modification and promoter-dependent protein expression should be addressed as well.

MSC are a promising source for the development of cell-based therapies for neurological diseases including stroke. The efficient and minimally invasive delivery of MSC to the brain is still restricted and requires the development of alternative methods. Intra-arterial transplantation of MSC is a promising strategy when targeting the brain. The MSC-homing towards cerebral ischemia is not sufficient and requires extravasation. Thus, the last aim of the present work was to increase homing efficiency of MSC towards cerebral ischemia by functional overexpression of CCR2 or ITGA4.

Objective (III) Evaluation of *in vitro* migration and *in vivo* homing of MSC overexpressing CCR2

Enhancing susceptibility for the inflammatory chemokine MCP1 should improve navigation and migration towards increasing chemokine concentrations. Therefore, MSC were genetically manipulated by infection with a CCR2 carrying lentivirus to assess whether or not the overexpression of CCR2 improves migration *in vitro* and *in vivo*.

Objective (IV) Evaluation of *in vitro* migration and *in vivo* homing towards ischemic brain tissue of ITGA4-overexpressing MSC

Using this approach, it should be tested whether enhancing adhesion to and interaction with endothelium by ITGA4 overexpression can lead to improved transendothelial migration *in vitro* and *in vivo*.

# 2 Materials

## 2.1 Cell lines

| Name | Description | Origin |
|---|---|---|
| HEK 293 T | Human embryonic kidney cells | ATCC |
| GPNT | Brain vascular cell line from Lewis rats | Purchased from Sigma-Aldrich/ECACC |
| MSC | Bone-marrow derived mesenchymal stem cells from Wistar rats | Purchased from Cyagen |

## 2.2 Laboratory equipment

| Device | Specification | Company |
|---|---|---|
| Biosafety cabinet | HERAsafe® KS18 | Thermo Fisher Scientific |
| Cell culture incubator | Heracell 240i | Thermo Fisher Scientific, |
| Centrifuge | Megafuge® 40R | Thermo Fisher Scientific |
| Centrifuge | 5415 R | Eppendorf |
| Chemiluminescence detection system | Advanced Fluorescence/ECL imager | INTAS Science Imaging Instruments |
| Counting chamber | Neubauer improved | Marienfeld |
| Electrophoresis power supply | PowerPac™ 300 | Bio-Rad |
| Electrophoresis system | PerfectBlue™ Gel System Mini M | Peqlab |
| Flow Cytometer | FACS Canto II | Beckton Dickinson |
| Flow Cytometer | FACS Aria | Beckton Dickinson |
| Fluorescence Microscope | Nikon ECLIPSE Ti, Inverted research microscope | Nikon |
| Freezer, -20°C | GUw 1213 | Liebherr |
| Freezer, -80°C | Forma® 900 Series | Thermo Fisher Scientific |
| Freezing container | Nalgene® Mr. Frosty | Thermo Fisher Scientific |
| Gel imaging system | MultiImage Light Cabinet | Alpha Innotech |
| Incubator | Heracell 240i | Thermo Fisher Scientific |
| Microcentrifuge | Rotilabo®-mini-centrifuge | Carl Roth |
| Microscope, inverted | DM IL | Leica |
| Microwave oven | HMT755F | Bosch |
| Photometer | Infinite 200 Magellan | Tecan Group Ltd |
| Pipette controller | accu-jet® pro | Brand |
| Pipettes | Reference® | Eppendorf |
| Pipettes | Reference®, Research Plus ® | Eppendorf |
| Real Time cycler | 7900HT Fast Real Time cycler | Applied Biosystems® by Life Technologies |
| Refrigerator, 4 °C | FKU 1800 | Liebherr |
| Spectrophotometer | NanoDrop 2000 | Thermo Fisher Scientific |
| Tank Blot chamber | 2-Gel Tetra and Blotting Module | Bio Rad Laboratories |
| Thermocycler | TProfessional Thermocycler Standard | Biometra |
| UV illuminator | AlphaImager® Mini system | ProteinSimple |
| Vortex shaker | Vortex Genius 3 | IKA |
| Water bath | 1083 | GFL |
| Water purification system | Milli-Q® Synthesis A10 | Merck Millipore |

## 2.3 Disposables

| Component | Company |
|---|---|
| Amersham Protean 0.2 Nitrocellulose membrane | GE Healthcare Europe |
| Blunt-end cannula, 18G | B. Braun |
| Cell culture dishes T75, T25, 6-Well Plates, 24-Well plates, 35mm dishes, 60mm dishes, 10cm dishes | Greiner Bio One |
| Cell scraper, 240mm | Greiner Bio One |
| Conical Tubes, 50mL, 15mL | Greiner Bio One |
| Cryogenic vials, 2mL | Corning |
| Eppendorf® tubes 0.2mL, 0.5mL, 1.5mL, 2mL | Eppendorf AG |
| FluoroBlok transwell inserts (24-Well), 8µm pore size + Companion plate | Corning |
| Glas Cover slides, 12mm | Glaswarenfabrik Karl Hecht |
| Glass slides, Superfrost® Plus | Menzel-Gläser |
| Lenti-X-GoStix™ | Clontech Laboratories |
| MicroAmp® Fast Optical 96-Well Reaction Plate | Life Technologies G |
| MicroAmp® Optical Adhesive Film | Life Technologies |
| Parafilm® M sealing film | Bemis |
| Pipet tips 0.5-20µL, 10-200µL, 100-1000µL | Greiner Bio One |
| Round bottom tube, 12mL | Greiner Bio One |
| Serological pipettes 5mL, 10mL, 25mL, 50mL | Greiner Bio One |
| Syringe filter, 0.2µm, 0.45µm | Corning |
| Syringe, 10mL | B. Braun |
| ThickBlot filter paper, 7.5 x 10cm | BioRad Laboratories |

## 2.4 Chemicals and reagents

| Chemical/Reagent | Company |
|---|---|
| 10 x Trypsin/EDTA (0.5%/0.2%) | Biochrome |
| 3-(N-Morpholino)-propane sulfone acid (MOPS), ≥99.5% | Carl Roth |
| 6 x DNA Loading Dye solution | Fermentas by Thermo Fisher Scientific |
| Acetic acid | Carl Roth |
| Agar-Agar | Carl Roth |
| Agarose | Sigma-Aldrich |
| Ampicillin (100mg/mL) | Sigma-Aldrich |
| Collagen from calf skin (1mg) | Sigma-Aldrich |
| DEPC | Carl Roth |
| DMEM | Gibco® by Life Technologies |
| DMSO | Carl Roth |
| Doxycycline | Clontech Laboratories |
| DTT | Promega |
| Ethidium bromide 1% (10mg/mL) | Carl Roth |
| Fetal Bovine Serum (FCS) | PAN-Biotech |
| Formaldehyde 37% ROTIPURAN® | Carl Roth |
| Gelatine | Sigma Aldrich |
| GlutaMax™ (100x) | Gibco® by Life Technologies |
| Glycerol anhydrous | Sigma-Aldrich |
| Hams F-10 Nutrient Mix | Gibco® by Life Technologies |
| HEPES | Carl Roth |
| Hydrogen peroxide 35% | Carl Roth |
| Kanamycin | Sigma Aldrich |

| Chemical/Reagent | Company |
|---|---|
| KnockOut™ DMEM/F12 (1x) | Gibco® by Life Technologies |
| LB broth powder | Carl Roth |
| Lenti-X-Concentrator | Clontech Laboratories |
| Lipofectamine ® 2000 | Invitrogen |
| Magnesium chloride | Carl Roth |
| Normal Goat serum (NGS) | PAA Laboratories |
| Oligo(dT) 15 primer | Promega |
| Opti-MEM® | Gibco® by Life Technologies |
| PCR-nucleotide mix, 10mM | Promega |
| Penicillin/Streptomycin (100x) | PAA Cell Culture Company |
| Phosphate buffered saline (10x) | Sigma-Aldrich |
| Polybrene® | Santa Cruz Biotechnology |
| RNasin® | Promega |
| Rotiphorese® | Carl Roth |
| SDS (20% solution) | Carl Roth |
| Sodium acetate ≥98.5% | Carl Roth |
| Sodium chloride (NaCl) | Carl Roth |
| Sodium Desoxycholate | Carl Roth |
| Tris(hydroxymethyl)-aminomethane (TRIS) | Carl Roth |
| Triton-X-100 | Carl Roth |
| Trizol® | Ambion by Thermo Fisher Scientific |
| Tryptone/Peptone ex Casein | Carl Roth |
| Tween 20 | Carl Roth |
| Yeast extract | Carl Roth |
| α-MEM | Gibco® by Life Technologies |

## 2.5 Kits

| Kit | Company |
|---|---|
| CellTrace™ CFSE Cell Proliferation Kit | Thermo Fisher Scientific |
| Direct-zol™ RNA MiniPrep Kit | Zymo Research Corp., |
| DNA Clean&Concentrator | Zymo Research Corp. |
| Gibson Assembly™ Cloning Kit | New England Biolabs |
| mMessage mMachine T7 Ultra Kit | Ambion by Thermo Fisher Scientific |
| Pierce BCA Protein Assay Kit | Thermo Fisher Scientific |
| PKH26 Red Fluorescent Cell Linker Kit | Sigma-Aldrich |
| Q5® Hot Start High-Fidelity 2x Master Mix | New England Biolabs |
| Quick Ligation™ Kit | New England Biolabs |
| Rat Mesenchymal Stem Cell Identification Kit | R&D |
| Stemfect™ RNA Transfection Kit | Stemgent |
| T7 mScript Standard Production system | Cellscript |
| Taqman® Fast Advanced Master Mix | Applied Biosystems® by Life Technologies |
| Zymoclean™ Gel DNA Recovery Kit | Zymo Research Corp. |
| Zyppy™ Plasmid Midiprep Kit | Zymo Research Corp. |
| Zyppy™ Plasmid Miniprep Kit | Zymo Research Corp. |

## 2.6 TaqMan®Gene expression Assays

| Gene | Accession number | ID | Company |
|---|---|---|---|
| ACTB | NM_031144.3 | Rn00667869_m1 | Life Technologies |
| CCR2 | NM_021866.1 | Rn01637698_s1 | Life Technologies |
| GAPDH | NM_017008.4 | Rn01775763_g1 | Life Technologies |

| Gene | Accession number | ID | Company |
|---|---|---|---|
| ITGA4 | NM_001107737.1 | Rn01512798_m1 | Life Technologies |
| ITGA4 | NM_001107737.1 | Rn01512802_g1 | Life Technologies |

## 2.7 Media and buffers

| Media | Composition |
|---|---|
| 1 x Mops buffer | 100mL 5x MOPS buffer, 400mL DEPC- $H_2O$ |
| 1 x TAE buffer | 980 mL A.dest, 20mL 50xTAE buffer |
| 2x RNA loading dye | 720µL formamid, 320µL 5x MOPS buffer, 260µL formaldehyde, 150µL DEPC-$H_2O$, 50µL ethidiumbromide (10mg/mL), 80µL glycerol/bromphenol blue/xylencyanol |
| 4x Lower buffer | 91g Tris, 10mL 20% SDS solution, A. dest to 0.5L, pH=8.8 |
| 4x Upper buffer | 15.25g Tris, 5ml 20% SDS solution, A.dest to 250mL, pH=6.8 |
| 5 x MOPS buffer | 1L DEPC- $H_2O$, 41,84g MOPS, 4,11g sodium acetate, 20mL 0.5M EDTA, pH=7 |
| 50xTAE buffer | 242g Tris base, 57.1 mL acetic acid, 37,2g EDTA, A.dest to 1000mL |
| Adipogenic differentiation medim | α-MEM basal medium, 1% adipogenic supplement |
| Bacterial growth medium I | 25 g LB broth powder, A.dest to 1L |
| Bacterial growth medium II | 16g Tryptone/Peptone, 10g Yeast extract, 5g NaCl, A.dest to 1L, pH=7 |
| Chondrogenic differentiation medium | DMEM/F12, 1% ITS supplement, 1% Pen/strep, 0.5% chondrogenic supplement |
| FACS antibody buffer | 1%NGS, 0.1%Saponin in PBS |
| FACS permeabilization buffer | 1 % FCS, 0.1 % Saponin in PBS |
| FACS washing buffer | 1% FCS in PBS |
| Freezing solution | FCS, 10% DMSO |
| GPNT growth medium | Hams F-10 Nutrient Mix, 10% FCS, 1% Pen/Strep |
| HEK 293T growth medium | DMEM-High Glucose, 10% FCS, 1% Pen/Strep |
| ICC blocking buffer | 10% normal goat serum, 0.1% Triton-X-100, in PBS |
| ICC permeabilization buffer | 0.05g Sodiumacide, 0.1% Triton-X-100 in PBS |
| LDH substrate buffer | 50 mM potassium phosphate buffer, 0.4 mM NADH, 1.7 mM sodium-pyruvate |
| LDV-FITC staining buffer | 2 mM $MgCl_2$, 2 mM $CaCl_2$, 100 nM LDV-FITC in 1M HEPES |
| mRIPA lysis buffer | 1% Igepal, 1% Na-Desoxycholat, 0.1% SDS, 50mM HEPES, 150mM NaCl, 10% glycerol, 1.5mM $MgCl_2$, A. dest to 50mL |
| MSC growth medium | KO-DMEM/F12, 7.5% FCS, 1% GlutaMax, 1% Pen/Strep |
| MTT | 5mg/mL in PBS |
| MTT lysis buffer | 100mL DMSO, 0.6mL acetic acid, 10g SDS |
| Osteogenic differentiation medium | α-MEM basal medium, 5% osteogenic supplement |
| Ponceau S staining solution | 0.5g Ponceau S, 1mL glacial acetic acid, A.dest to 100mL |
| Running buffer | 3g Tris, 14.4 g glycine, 7.5mL 20% SDS solution, A.dest to 1L, pH=8.3-8.6 |
| S.O.C. medium | Gibco® by Life Technologies |
| Sorting medium | Opti-MEM® + 10% FCS |
| TBS-T | 2.42g Tris, 8g NaCl, A.dest to 1L, 0.1% Tween 20, pH=7.6 |
| TE buffer | 10mM Tris-HCl, 0.1mM EDTA, pH=8.5 |
| Transfer buffer | 6g Tris, 28.827g glycine, 400mL methanol, 2mL 20% SDS solution, A.dest to 2L |
| Urea lysis buffer | 1.5M Tris-HCl (pH 6.8), 8M Urea, 1mL Glycerol, 20% SDS, 1M DTT, 1M PMSF |
| α-MEM basal medium | α-MEM, 10% FCS, 1% Pen/Strep |

## 2.8 Oligonucleotides

| Name | Purpose | Sequence |
|---|---|---|
| att-ITGA4 | Generation pDest47-ITGA4 | Fwd: 5`-GGGACAAGTTTGTACAAAAAAGCAGGCTATGGCTGCGGAAGCGATGT<br>Rev: 5`-GGGGACCACTTTGTACAAGAAAGCTGGGTATCAGTCATCATTGCTTTTGCT |
| Dest47 | DNA template for IVT | Fwd: 5`-AGAGAACCCACTGCTTAC<br>Rev: 5`-TAGAAGGCACAGTCGAGG |
| DscGFP-Eco | Construction of pFN-4L1 | Fwd: 5`-CCATCCACGCTGTTTTGAC<br>Rev: 5`-TATTGAATTCTTACACATTGATCCTAGCAGAAG |
| ITGA4-SOKM | | Fwd: 5`-GGGCTGCAGGTCGACTCCACCATGGCTGCGGAAG<br>Rev: 5`-GCTGGATCGGTCGAATTCTGGGTAGTCATCATTGCTTTTGCTG |
| CMV | Construction of pFN-4S | Fwd: 5`-TCCAGCAGGTCGCGTTGACATTGATTATTG<br>Rev: 5`-GCAGCCCAAGCTGCTTATATAGACCTCCC |
| S-BB | | Rev: 5`-TGTCAACGCGACCTGCTGGAATCTCG |
| EF1alpha | Construction of pFN-4R | Fwd: 5`-TCCAGCAGGTCCACGCTGTTTTGACCTCC<br>Rev: 5`-GCAGCCCAAGCGTAGGCGCCGGTCAC |
| R-BB | | Rev: 5`-AACAGCGTGGACCTGCTGGAATCTCG |
| TRE | Construction of pFN-4T | Fwd: 5`-TCCAGCAGGTTCGGGTTTATTACAGGGACAG<br>Rev: 5`-GCAGCCCAAGCGGAGGCTGGATCGGT |
| T-BB | | Rev: 5`-ATAAACCCGAACCTGCTGGAATCTCG |
| RST-ITGA | Construction of pFN-4R, S, T | Rev: 5`CGGTCCAGTACGATGATCCCGGGGCCCCCATCACAA |
| tdTomato-Eco | Construction pFN-3M, pFN-7M | Fwd(3M): 5`-GATGACTGAGATCCCGCCCCTCTCCCT<br>Fwd(7M): 5`-GTTGTAATACGATCCCGCCCCTCTCCCT<br>Rev: 5`-GTTATTAGGTCCCTCGACGCGTTCACTTGTACAGCTCGTCC |
| 3M-ITGA | Construction of pFN-3M | Fwd: 5`-CTGCAGGTCGACTCTAGAGCCACCATGGCTGCGGAAG<br>Rev: 5`-GCGGGATCTCAGTCATCATTGCTTTTGCTGTTG |
| 7M-CCR2 | Construction of pFN-7M | Fwd: 5´-CTGCAGGTCGACTCTAGAGGCTCCACCATGGAAGACAG<br>Rev: 5`-GCGGGATCGTATTACAACCCAACTGAGACTTC |

## 2.9 Plasmids

This list provides an overview of used plasmids. Detailed plasmid maps can be found in the supplements (Fig. 46).

| Plasmid | Description | Source |
|---|---|---|
| pMD2.G | Envelope plasmid for production of lentiviral particles, encodes vesicular stomatitis virus G (VSV-G) glycoprotein | Addgene |
| psPAX2 | Packaging plasmid for production of lentiviral particels, encodes gag, pol, rev, and tat | Addgene |
| FUW-SOKM | Polycistronic lentiviral transfer vector of mouse Oct4, Sox2, Klf4 and c-Myc cDNA, isolation of backbone | Addgene |
| pDest47 | Gateway expression vector with LR-attachment sites, coding for ccdB and eGFP | Invitrogen |
| pENTR221 | Gateway entry vector with BP-attachment sites | Invitrogen |
| pLVX-IRES-tdTomato | Lentiviral expression vector containing tdTomato sequence with and upstream located IRES | Clontech Laboratories |
| pFN-3M | Lentiviral transfer vector coding for ITGA4 and tdTomato | This study |
| pFN7M | Lentiviral transfer vector coding for CCR2 and tdTomato | This study |
| pFN18 | Lentiviral transfer vector coding for copGFP | This study |

| Plasmid | Description | Source |
|---|---|---|
| pFN19 | Lentiviral transfer vector coding for tdTomato | This study |
| pFN-4L1 | Lentiviral transfer vector coding for ITGA4-GFP fusion construct with UbC-promoter | This study |
| pFN-4R | Lentiviral transfer vector coding for ITGA4-GFP fusion construct with EF1α-promoter | This study |
| pFN-4S | Lentiviral transfer vector coding for ITGA4-GFP fusion construct with CMV-promoter | This study |
| pFN-4T | Lentiviral transfer vector coding for ITGA4-GFP fusion construct with TRE-promoter | This study |
| pDest47-ITGA4 | Gateway expression vector coding rat ITGA4 | This study |
| pDest47-GFP | Gateway expression vector coding destabilized copGFP | This study |
| FUW-M2rtTA | Lentiviral transfer vector coding for reverse tetracycline transactivator | Addgene |
| pGreenFire-Pax6 (TR031A) | Lentiviral transfer vector serving as PAX6 transcription reporter by destabilized CopGFP and Luciferase | Sys Bio |

## 2.10 Enzymes

| Enzyme | Company |
|---|---|
| BP clonase II enzyme mix | Life Technologies |
| EcoNI | New England Biolabs |
| LR clonase II enzyme mix | Life Technologies |
| Q5 Polymerase | New England Biolabs |
| SmaI | New England Biolabs |
| Superscript III Reverse Transcriptase | Invitrogen by Thermo Fisher Scientific |
| XbaI | New England Biolabs |

## 2.11 Antibodies

| Antibody | Host | Clonality | Dilution | Company |
|---|---|---|---|---|
| *Primary antibodies* | | | | |
| Aggrecan | Goat | Polyclonal | 1:100 | R&D |
| CCR2 | Rabbit | Polyclonal | ICC: 1:100<br>WB: 1:500 | Novus Bio |
| FABP4 | Goat | Polyclonal | 1:100 | R&D |
| GAPDH (14C10) | Rabbit | Monoclonal | 1:1000 | Cell Signaling by New England Biolabs |
| IBA1 | Rabbit | Polyclonal | 1:200 | WAKO |
| Integrin alpha 4 (D2E1) | Rabbit | | ICC: 1:250<br>WB: 1:1000 | Cell Signaling by New England Biolabs |
| Lectin-biotinylated | Potato | - | 1:300 | Vector Laboratories |
| Osteocalcin | Mouse | Monoclonal | 1:100 | R&D |
| Turbo-GFP | Rabbit | Polyclonal | 1:1000 | Evrogen |
| *Secondary antibodies* | | | | |
| IgG anti rabbit, Alexa Flour® 546 | goat | Polyclonal | 1:500 | Life technologies by Thermo Fisher Scientific |
| IgG anti rabbit, Alexa Flour® 488 | goat | polyclonal | 1:500 | Life technologies by Thermo Fisher Scientific |
| IgG anti rabbit IgG-HRP | goat | Polyclonal | 1:5000 | Dianova |
| IgG anti mouse IgG-HRP | sheep | Polyclonal | 1:5000 | Dianova |
| IgG anti goat Alexa Flour®488 | Donkey | Polyclonal | 1:250 | Life technologies by Thermo Fisher Scientific |

| Antibody | Host | Clonality | Dilution | Company |
|---|---|---|---|---|
| IgG anti goat Alexa Flour®546 | Donkey | Polyclonal | 1:250 | Life technologies by Thermo Fisher Scientific |
| Streptavidin Alexa 647 | - | - | 1:500 | Dianova |

## 2.12 Software

| Name | Company |
|---|---|
| AlphaImager® 1220 v5.1 | Alpha Innotech |
| Citavi 5 | Swiss Academic Software |
| FACSDiva™ | Becton Dickinson |
| Flow Jo | Flow Jo Software |
| GraphPad Prism 6 | GraphPad Software, Inc. |
| HiSPECT | SciVis |
| Image J 1.50 | National Institute of Health |
| Inkscape 0.91 | Free Software Foundation |
| InVivoScope | Bioscan |
| LinReg PCR | University of Amsterdam |
| Microsoft Office 2016 | Microsoft |
| NanoDrop 2000 | Thermo Fisher Scientific |
| NIS Elements AR 4.11.00 | Nikon GmbH |
| Oligo 7 Primer Analysis Software | Molecular Biology Insights, Inc. |
| Quantity One® | BioRad Laboratories |
| Sequence Detection Systems (SDS) 2.4 | Life Technologies |
| Snap Gene | GSL Biotech LLC |
| ZEN-blue edition/black edition | Carl Zeiss, Jena |

# 3 Methods

## 3.1 Cell Culture

All procedures and experiments were conducted under aseptic conditions using a sterile laminar hood. All media and buffers used for cell culture were also kept sterile and were warmed to 37°C before utilization.

### 3.1.1 General subcultivation of adherent cells

Subcultivation was conducted when cells were near the end of exponential growth and monolayer reached subconfluent state. Initially, growth medium was poured off and monolayer was washed with PBS by carefully swaying the culture vessel to remove remains of serum and cations. Following removal of PBS, the cell monolayer was incubated with 0.05% trypsin until dissociation (~5min). An appropriate volume of growth medium was subsequently added to stop dissociation and inhibit trypsin digestion. Thereafter, the cell suspension was transferred to a conical tube. Following centrifugation, the supernatant was carefully aspirated without disturbing cell pellet. The pellet was resuspended in the respective growth medium. A sample of 10µL was removed for determination of cell number using a Neubauer improved counting chamber. Finally, a volume containing calculated number of cells was transferred to a fresh cell culture vessel and placed into an incubator with an adjusted atmosphere.

### 3.1.2 Freezing and thawing

Cell lines and modified MSC were frozen and stored before use. Therefore, adherent subconfluent cells were trypsinized and centrifuged as described above. After quantification, cell suspension was centrifuged again and cell pellet was resuspended in FCS containing 10% DMSO as cryoprotectant. Volumes of 1mL were transferred to cryogenic vials. In the following, vials were placed into a precooled frosting container filled with isopropanol. After storage at -80°C for at least 24h, vials were transferred to liquid nitrogen for long-term storage.

For recovery of frozen cells, cryogenic vials were removed from liquid nitrogen and prewarmed in a water bath at 37°C until ice was almost completely melted. Thereafter, cells were transferred to a conical tube containing 5mL prewarmed culture medium. Additional 10mL of growth medium were added. Following centrifugation, supernatant was removed and cell pellet was resuspended in 1mL growth medium. After quantification, cells were seeded at appropriate density into cell culture dishes and incubated as indicated. Medium was replaced after 24h to remove dead cell, debris and traces of freezing solution.

### 3.1.3 Culture of HEK 293T

HEK 293T were used for production of lentiviral vectors. This human embryonic kidney derived cell line expresses Simian Vacuolating virus (SV) 40 large T antigen necessary for effective replication of viruses.

HEK 293T cells were cultured using HEK growth medium under normoxic conditions. Cells were subcultured by splitting them in a 1:10 or 1:20 ratio twice a week.

### 3.1.4 Culture of GPNT

In this study, brain vascular endothelial cell line from Lewis rats were used for *in vitro* migration experiments. GPNT cell line was derived from immortalized GP8 line by transfer of the puromycin resistance gene. In contrast to freshly isolated endothelial cells, it was possible to culture GPNT cells over several passages without affecting their phenotype or senescence.

Therefore, cell culture dishes were coated using bovine collagen (0.1mg/mL) at 37°C for 2-4h. Culture vessel was air-dried for 1h after removal of coating solution. GPNT cells were seeded with a density of 10,000 – 20,000 cells/$cm^2$ and incubated at humified atmosphere at 37°C, normoxia, and 5% $CO_2$. Medium was replaced every 2-3 days.

### 3.1.5 Cultivation of MSC

MSC were isolated from Wistar rat bone marrow and tested for expression of CD90, CD44, and CD29 as well as absence of CD34, CD45, and Cd11b/c by manufacturer.

MSC were maintained in KO-DMEM/F12 based growth medium to ensure their stemness properties. Furthermore, MSC were cultured under hypoxic conditions (5% $O_2$). Subcultivation was performed as described above by ensuring a seeding density of 3,000-6,000 cells/$cm^2$. Throughout the cultivation period, MSC were regularly evaluated by light microscopy for their cell shape and appearance. MSC were maintained in culture and used for experiments before reaching passage 9.

### 3.1.6 Differentiation of MSC

Trilineage differentiation into adipogenic, osteogenic and chondrogenic cells is a characteristic property of MSC. In order to test MSC differentiation potential of used MSC, rat mesenchymal stem cell kit was used.

Prior to adipogenic and osteogenic differentiation, a 24-well plate equipped with cover slides was coated with 0.1% gelatine for at least 1h. Thereafter, MSC were trypsinized and resuspended in α-MEM basal medium. Cells were seeded with a density of 37,000 cells/well for adipogenesis and with 7,400 cells/well for osteogenesis. After 24h of incubation, α-MEM basal medium was replaced by either adipogenic or osteogenic differentiation medium and changed every 3-4 days. Within a period of 14d, adipogenic cells showed lipid vacuoles,

while osteogenic cells were starting to express osteocalcin. Following this, cells were fixed using 4% PFA.

MSC undergoing chondrogenesis were trypsined, resuspended in chondrogenic differentiation medium before 0.25 x $10^6$ cells were transferred to a 15mL conical tube. Cells were kept in pellet formation after centrifugation and cultivated within the conical tube at 37°C. Medium was replaced every third day and micromasses were fixed with 4% PFA after 21 days. Afterwards, immunocytochemistry was performed to proof the expression of FABP4, osteocalcin or aggrecan indicating differentiation into respective lineage.

## 3.2 Proliferation, viability and toxicity

### 3.2.1 Growth curves and determination of population doubling time

Growth characteristics of native and modified MSC were evaluated by generation of growth curves. Therefore, MSC were trypsinized and replated onto 6-well culture vessels in 6 replicates. Cell numbers of one replicate were determined every second day over 12 days. MSC were trypsinized and counted using a Neubauer improved counting chamber. Results were plotted onto a log linear scale and population doubling time (PDT) was calculated as follows:

$$PDT = \frac{duration * \log(2)}{\log(final\ cell\ number) - \log(initial\ cell\ number)}$$

### 3.2.2 MTT-Assay

The MTT assay is a method to assess metabolic activity and viability of cells. It is based on a colorimetric reaction initialized by reduction of 3-(4,5-dimethylthiazol-2-y-yl)-2,5-diphenyltetrazolium (MTT) to purple colored, insoluble formazan.

MSC were seeded in 24 well plates and transfected (see chapter 3.5.1 for details). At indicated time points, supernatants of transfected MSC and controls were replaced by MSC growth medium containing 0.5 mg/mL MTT. During a 4h incubation period at 37°C, cells were allowed to reduce MTT to formazan. Subsequent addition of 200µL MTT lysis buffer led to cell lysis and resolution of formazan complexes. Finally, absorbance was measured at 570nm against a reference wavelength at 630nm using a microplate reader. Background absorbance from culture media was determined by blank measurement without cells and subtracted from measured data.

### 3.2.3 LDH-Assay

Analysis of transfection effects on cell death has been conducted utilizing lactate dehydrogenase (LDH) assay (Smith et al. 2011). LDH is an enzyme released from the cytosol of damaged and dying cells and catalyzes reduction of $NAD^+$ to NADH.

In this study, supernatants of transfected and control cells were collected at respective investigation time points in a reaction tube and processed immediately. Fifty microliters of each sample were added to 200 µL of pre-warmed LDH substrate buffer loaded into a low-absorbance 96-well plate. The plate was transferred to a tempered photometer and NADH absorbance was measured at 340nm over a time course of 10min. Data were acquired every 30s and resulting slope was used to calculate LDH activity according to the Lambert-Beer-law using following formula:

$$A\left[\frac{U}{I}\right] = \frac{\Delta E}{\Delta t[min]} * \frac{Vtest[mL]}{Vsample[mL]} * \{\frac{1000}{\varepsilon\left[\frac{l}{mmol} * cm\right] d[cm]}\}$$

*A= LDH activity;*

*E= extinction;*

*ε= extinction coefficient NADH (6200L/mol*cm);*

*d= thickness of plate (0.964 cm)*

## 3.3 Cloning

### 3.3.1 Transformation of competent bacteria

Transformation was performed to replicate circular plasmid DNA using chemically competent Escherischia coli (E. coli) strains as Subcloning Efficiency DH5alpha or OneShot®TOP10.

Bacteria, stored in aliquots at -80°C, were removed from the freezer and thawed on wet ice. Following this, 10ng of plasmid DNA were gently added and the suspension was incubated on ice for 30min. Afterwards, a heat shock was conducted using 42°C water bath for 20-30s and the bacterial suspension was placed on ice for 2min. Pre-warmed S.O.C. medium (950µL) was added to the bacteria suspension and placed in a bacterial incubator under continuous shaking (225rpm) for 1h before spreading 200µL on pre-warmed LB-agar-plates supplemented with antibiotic agent (ampicillin or kanamycin) for selection. Subsequently, plates were placed in a bacterial incubator at 37°C overnight.

### 3.3.2 Plasmid amplification and isolation

Individual colonies from transformed bacteria were picked from LB-agar plates with a pipet tip. Colonies were then stirred into bacteria growth medium I or II in round-bottom tubes or Erlenmeyer flask for small- or mid-scale plasmid preparation. Respective antibiotics (100µg/mL ampicillin or 50µg/mL kanamycin) were added and tubes were incubated in a bacterial round-shaker at 37°C, 225rpm overnight.

The next day, plasmid DNA was isolated from liquid culture utilizing Zyppy™ Plasmid MiniPrep or ZyppyTM Plasmid MidiPrep Kit following manufacturer´s instructions. For this, a modified alkaline lysis buffer was added directly to the bacterial suspension in a 1:6 ratio. After neutralizing and centrifugation, the supernatant was loaded onto DNA-binding spin columns and centrifuged. Several washing steps were conducted to remove genomic DNA, salts and endotoxins, and, finally, plasmid DNA was eluted in TE buffer. Concentration was determined spectrophotometrically and plasmids were stored at -20°C.

### 3.3.3 Restriction digestion of plasmid DNA

Enzymatic restriction digestion was conducted to cleave particular DNA fragments at specific sites or for analysis of plasmids.

In order to perform a restriction digestion, a reaction mix was assembled with 1µg DNA, 2µL of 10x enzyme-specific reaction buffer, nuclease-free water and 1µL (1U/µL) of a nucleotide sequence-specific restriction endonuclease. The mixture was incubated at 37°C for 1h. Restricted DNA was then analyzed by agarose DNA gel electrophoresis.

### 3.3.4 DNA gel electrophoresis and gel extraction of DNA fragments

Upon plasmid preparation, restriction digestion or PCR, a gel electrophoresis was performed to assess quality and size of the DNA.

For this purpose, a 1% gel was prepared by dissolving agarose in 1x TAE buffer under calefaction for 2min in a microwave. Upon cooling down, ethidium bromide was added in a final concentration of 0.1µg/mL to the solution and filled into a gel electrophoresis chamber. The chamber was filled with 1x TAE buffer until the gel was covered after polymerization.

DNA samples were mixed with an appropriate volume of 6x DNA loading dye and transferred into the gel wells using a pipet. To allow assessment of fragment size, a marker with DNA fragments of known molecular weights was loaded onto the same gel. Gel was run at 90-120V until sufficient separation of DNA fragments (~1h). Ethidium bromide within the gel incalated into the DNA fragments generating a fluorescence signal upon UV light exposure and DNA bands were visualized using an UV illuminator.

If an extraction of a particular DNA fragment was needed, the band was carefully cut out of the gel using a scalpel. The DNA was extracted from the gel piece using Zymoclean™ Gel DNA recovery Kit. By following the manufacturer´s instructions, the gel piece was melted in agarose dissolving buffer. Then, the solution was transferred to a spin column and

centrifuged. Upon washing, the DNA was eluted using 10µl TE buffer and concentration was determined using a spectrophotometer.

### 3.3.5 Ligation

In order to combine two DNA fragments, the Qick Ligation™ Kit was used. According to manufacturer´s instructions, 50ng of vector were mixed with a 3-fold molar excess of insert and the mix was adjusted to 10µL with nuclease-free water. Then, 10µL of 2x Quick Ligation buffer and 1µL of Quick T4 DNA Ligase were added. The mixture was incubated at room temperature for 5min. The reaction was stopped by chilling the sample on ice and the resulting product was transformed to chemically competent bacteria.

### 3.3.6 Cloning of pFN19, pFN-3M and pFN-7M expression vectors

In order to stably modify MSC with ITGA4 or CCR2, the lentiviral vectors pFN-3M and pFN-7M were subcloned into a FUW-SOKM backbone. The transgene sequence was linked to a tdTomato coding sequence by an internal ribosomal entry site (IRES) to allow coupled reporter gene expression. A vector coding for a fluorescent protein (tdTomato, GFP) solely served as control (pFN18 and pFN19).

In the beginning, IRES- tdTomato sequence was prepared from pLVX-IRES-tdTomato vector by PCR using tdTomato-EcoRI primer pair. The PCR product was further digested with EcoRI to generate fitting 5’ overhangs. The FUW-SOKM vector was digested by EcoRI and treated with alkaline phosphatase to avoid relegation. The vector pFN19 emerged after joining both fragments by DNA ligation. In the following, ITGA4 or CCR2 coding inserts were isolated from pDest47 expression vector by PCR and the pFN19 vector was reopened by EcoRI restriction digestion.

A two fragment Gibson-assembly was performed based on ligation of DNA fragments using oligonucleotides with overlapping sequences. The fragments were assembled in a single tube and incubated at 50°C for 1h after addition of 2x Gibson Assembly MasterMix. During the incubation, a 5’ exnuclease catalyzed the generation of overhangs, gap filling and annealing of single stranded regions was performed by polymerase and a ligase sealed nicks within the assembled DNA. Following this, samples were transformed into competent E. coli. Plasmids were amplified and isolated. Verification of correct assembly and DNA sequence was done by restriction digestion and DNA sequencing (Seqlab).

### 3.3.7 Cloning of pFN-4L1, pFN-4R, pFN-4S, and pFN-4T expression vectors

For comparison of promoter-dependent transgene expression, lentiviral vectors were prepared from a FUW-SOKM backbone coding for ITGA4-GFP fusion transgene under control of UbC-1(pFN-4L1), EF1α-(pFN-4R), CMV (pFN-4S) or TRE (pFN-4T) promoter.

Initially, pFN-4L1 vectors were prepared. Therefore, a dscGFP fragment was derived by PCR from TRO31A plasmid using dscGFP-EcoRI primer pair and subsequent restriction digestion

with EcoRI. The obtained fragment was cloned into an EcoRI opened FUW-SOKM vector by DNA ligation. The resulting vector was reopened by XbaI and DNA inserts coding for gene of interest were prepared from pDest47-ITGA4 by PCR. A two fragment Gibson-assembly was conducted as described in the previous section being followed by plasmid transformation, amplification, and isolation.

Originated from pFN4-L1 vectors, pFN-4R, pFN-4S and pFN-4T vectors were cloned. For this purpose, the pFN-4L1 vector was double digested (EcoNI/SmaI) and separated by gel electrophoresis. The respective DNA bands (8kb) were extracted from the gel and purified. PCR-generated DNA fragments coding for promoter, transgene, or a part of the vector backbone (cPPPT/CTS, RRE) were assembled with gel excised fragment by conducting a four fragment Gibson-assembly. Plasmids were amplified and isolated after transformation into chemically competent bacteria. Subsequent DNA sequencing and restriction digestion were performed to verify correct assembly.

## 3.4 *In vitro* synthesis of mRNA

### 3.4.1 Generation of a DNA-Template for *in vitro* transcription

*In vitro* transcription (IVT) of mRNA required a suitable DNA template. In order generate a DNA template that allowed transcription of mRNA complementary sense RNA (5´→3´ orientation) a plasmid containing cDNA sequence of rat *itga4* and a T7 promoter was cloned.

The *itga4* cDNA sequence was recloned with or without a stop codon utilizing the gateway cloning system. Therefore, a polymerase chain reaction was performed to generate a DNA fragment containing *itga4* sequence with *attB*-sites. A BP-recombination reaction was conducted to transfer this fragment into the entry vector pENTR221 followed by LR recombination reaction to clone the cDNA fragment into the destination vector pcDNA-Dest47. Each recombination reaction required assembly of respective enzyme mix (BP clonase® II or LR clonase® II) with target plasmids (100ng) and incubation at 25°C for 1h. The recombination was terminated by addition of 2µg Proteinase K solution and plasmids were isolated after transformation. Restriction digestion and sequencing confirmed successful recombination. Final linear DNA-templates for *in vitro* transcription were acquired from resulting pcDNA-Dest47 vector with PCR using Q5® Hot Start HF 2 x Master Mix and Dest47 fwd and Dest47 rev primer using the following PCR conditions:

**Tab. 1 Thermal cycling condition for DNA-template PCR**

| Step | Temperature | Time | Cycle |
|---|---|---|---|
| Initial denaturation | 98°C | 30s | 1 |
| Denaturation | 98°C | 10s | |
| Annealing | 56.5°C | 1min | 2-40 |
| Elongation | 72°C | 3min | |
| Final extension | 72°C | 4min | 41 |
| Hold | 4°C | ∞ | 42 |

PCR products were qualified by agarose gel-electrophoresis and purified with DNA Clean&Concentrator according to manufacturer's instructions. Briefly, 5 volumina of DNA binding buffer were added to the PCR product and loaded onto a spin column. After centrifugation (16,000g; 30s) and repeated washing steps, DNA was eluted with 12µL DNA elution buffer.

Control transcripts, only containing the open reading frame for GFP, were prepared from pDest47 vector using the same protocol.

### 3.4.2 Generation of pre-IVT-mRNA, capping and polyadenylation

The T7 mScript Standard Production system or mMessage mMachine T7 Ultra kit were used according to manufacturer's instructions for synthesis of *in vitro* mRNA.

Firstly, the transcription of DNA to mRNA was performed. Therefore, the reaction cocktail was assembled with respective kit components as listed in table 2, and incubated as indicated. To terminate the transcription, 1µL of DNase was added to digest the DNA template.

**Tab. 2 Components of IVT cocktail**

| Component | T7 mScript | mMessage mMachine |
|---|---|---|
| DNA template | 1µg | 1µg |
| 10x reaction buffer | 2µL | 2µL |
| NTP solution | 7.2µL | 10µL of 2x NTP/ARCA mix |
| 100mM DTT | 2µl | included in reaction buffer |
| RNase inhibitor | 0.5µl | included in enzyme mix |
| enzyme Mix (with RNA polymerase) | 2µl | 2µl |
| nuclease-free water | To 20µL | to 20µL |
| Incubation | 37°C, 30min | 37°C, 2h |

In this study, 5' capping and 3' polyadenylation were included to yield a durable mRNA. Furthermore, capping may also influence translation efficiency and was performed either co-

transcriptionally or post transcription. Co-transcriptional capping was performed by simply using a nucleotide solution supplemented with anti-reverse cap analogue (ARCA) directly during transcription. In contrast, post-transcriptional capping required an additional synthesis step. Therefore, purified pre-mRNA was heat-denaturated at 65°C for 10min. Subsequently, it was added to a capping cocktail (table 3) allowing generating of either Cap0 or Cap1 structure. Capping reaction was incubated at 37°C for 30min.

**Tab. 3 Components of capping cocktail for Cap0 or Cap1 generation**

| Component | Cap0 | Cap1 |
|---|---|---|
| pre-mRNA | 55µg (in 72µL $H_2O$) | 55µg (in 72µL $H_2O$) |
| 10x ScriptCap Capping buffer | 10µL | 10µL |
| 10mM GTP | 5µL | 5µL |
| 20mM SAM | 2.5µL | 2.5µl |
| Script Guard RNase inhibitor | 2.5µL | 2.5µL |
| nuclease-free water | 4µL | - |
| Script-2`O methyltransferase | - | 4µL |
| Script Cap capping enzyme (10U/µL) | 4µL | 4µL |

Additional stabilization of mRNA transcripts was achieved by synthesis of 3´poly-A-tail with a length of ~120bp. Therefore, a polyadenylation cocktail was assembled as given in table 4. Poly-A-polymerase was attaching multiple adenine nucleobases to the 3´end of mRNA during incubation at 37°C for 30min.

**Tab. 4 Components of polyadenylation cocktail**

| Component | Volume |
|---|---|
| Capped pre-mRNA | 100µL |
| Script Guard RNase inhibitor | 0.5µL |
| 10x a-plus tailing buffer | 12µL |
| 20mM ATP | 6µL |
| A-plus Poly-A-polymerase (4U/mL) | 5µL |

### 3.4.3 Purification of mRNA

Traces of buffers, not incorporated nucleotides and enzymes from previous reaction were possible interference factors for subsequent procedures. Therefore, the mRNA was purified prior to and after posttranscriptional capping and poly-A-tailing with the following procedure.

At first, the reaction volume was filled up with RNase-free water to 200µL and rigorously mixed with an equal volume of phenol/chloroform/isoamylalcohol. Ensuing phase

separation was enhanced by centrifugation at 10,000g for 5min. The resulting upper, watery phase was carefully aspirated and transferred into a fresh reaction tube. The lower phenolic phase as well as protein interface were discarded. 5M ammonium acetate was added in a 1:1 ratio to the watery phase. A 15min incubation on ice was followed by addition of 1mL isopropanol and precipitation at -20°C for at least 1h. mRNA was pelleted by 15min centrifugation, washed with 70% ethanol and air dried until pellet turned transparent. Finally, the pellet was dissolved in an appropriate volume RNase-free water and concentration was determined utilizing Nanodrop spectrophotometer. If needed, mRNA was adjusted to 1µg/mL and stored in aliquots at -80°C.

### 3.4.4 RNA gel electrophoresis

Quality control of IVT mRNA was conducted by RNA gel electrophoresis. Separation of RNA molecules by size allowed verification of transcript length, successful polyadenylation and detection of potential degradation.

The electrophoresis chamber was cleaned with DEPC- $H_2O$ to reduce carryover of RNases prior to gel preparation. A 1% denaturating agarose-formaldehyde gel was prepared by dissolving 0.5g agarose in 35mL DEPC- $H_2O$ during a short calefaction in a microwave oven. Quickly after, 10mL 5xMOPS buffer and 5mL 37% formaldehyde were added. The mixture was poured into the electrophoresis chamber. After cooling down and stiffening, the chamber was filled with a sufficient volume of 1xMOPS buffer to cover the gel and put into a pre-run without samples for 45min.

Samples of IVT mRNA were taken prior and after polyadenylation and diluted in with 2x RNA loading dye containing ethidium bromide. Samples were denatured at 65°C for 10min and stored on ice until loading. Then, RNA samples were transferred into gel wells.

Gel was run at 75V for approximately 90min. Visualization under UV light (365nm) was possible by intercalation of ethidium bromide with nucleic acid. Parallel separation of a RNA molecular weight marker allowed length identification of RNA fragments.

## 3.5 Genetic engineering

In this study, overexpression of desired target protein was performed either by IVT mRNA transfection or by infection of target cells with an appropriate lentiviral vector.

### 3.5.1 mRNA transfection

In preparation of mRNA based modification, MSC in passage 5 were replated 3 days before transfection. A confluency of 70-80% was reached on the day of transfection. mRNA transfection was conducted utilizing Stemfect™ RNA transfection kit according to manufacturer´s recommendations. In brief, MSC were rinsed with RNase-free PBS and incubated in KO-DMEM/F12 for 45min. Hereafter, the transfection solution was prepared by composing transfection buffer, transfection reagent and mRNA in a 50:4:1 ratio. Initially, an

adequate volume of transfection buffer was transferred to each of two reaction tubes. Transfection reagent was added to the first tube, while mRNA (1µg/µL) was added to the second tube and carefully resuspended. Both solutions were combined and formation of mRNA transfection complexes took place during a 12min incubation.

Complexes were subsequently added to the cell monolayer in a dropwise manner and equally distributed by gently rocking the culture vessel. Thereafter, cells were returned to the incubator, and the supernatant was replaced with MSC growth medium after 4h incubation. Transfected and control MSC were harvested for analysis at 0h, 4.5h, 12h, 24h, 48h, 72h, and 96h.

### 3.5.2 Lentiviral infection

For long-term overexpression of desired transgene, a lentiviral infection protocol was established. It was composed of progressive lentiviral production and repeated infection (transduction) of target cells by lentiviral particles. Lentiviral particles were used as a vector to transfer the gene of interest into the genome of the target cells.

#### 3.5.2.1 Production of lentiviral particles

Lentiviral particles were produced by the helper cell line HEK 293T after transfection with a second generation system. This system consists of 3 components including a lentiviral transfer plasmid encoding for the gene of interest, a packaging plasmid (psPax2), and an envelope plasmid (pMD2G).

HEK 293T cells were plated with a concentration of 0.9-1 x $10^6$ cells/6 well cavity one day prior to transfection. The following day, HEK growth medium was replaced by 1.5mL supplement-free Opti-MEM. Transient transfection was carried out utilizing Lipofectamine® 2000. Therefore, the three plasmids were combined in a 1:1:1 molar ratio (4µg total DNA) and diluted in 250µL Opti-MEM®. In a second tube, 12µL Lipofectamine® 2000 were mixed with 250µL Opti-MEM® and, then, after 5min of incubation, merged with diluted plasmids. A 20min incubation allowed the formation of cationic liposomes complexes carrying the DNA. Afterwards, 500µL were dropwisely added to HEK 293T cells. The transfection medium was exchanged with fresh HEK growth medium after 6h. The lentiviral particles were released into supernatant upon cell lysis.

#### 3.5.2.2 Harvesting of lentiviral particles and transduction of target cells

Lentiviral particles were harvested using the Lenti-X-concentrator 24h and 48h after transfection of HEK 293T cells. For this, supernatant from 1-2 wells was aspirated using a blunt-end cannula and a syringe, filtered through a 0.45µm syringe filter and collected in a 50mL conical tube. Then, a 20µL sample was taken and analyzed with a Lenti-X gostix according to manufactures instructions. Only if at least 5x$10^5$ infectious units/mL were achieved, the viral supernatants were further processed. These supernatants were combined with one third volume Lenti-X-concentrator. The mixture was incubated at4°C for 1h and

subsequently centrifuged at 1,500g, 4°C for 45min. Supernatant was removed and the pellet resuspended in 1mL MSC growth medium before being transferred to target cells grown in a 6-well cavity. To this, Polybrene® with a final concentration of 8µg/mL was added to improve transduction efficiency. After incubation at 37°C for 4-6h, infection medium was replaced with MSC medium. MSC only treated with Polybrene® were carried along as control. Of note, MSC receiving pFN-4T derived particles were co-infected with M2rtTA particles in a 1:1 ratio. Transgene expression was induced by supplementing growth medium constantly with 2 µg/mL doxycycline.

## 3.6 Flow cytometry

### 3.6.1 Sorting

Sorting of MSC stably modified with pFN-3M, pFN-7M and respective controls was carried out in cooperation with the FACS core unit at University of Leipzig. Transgene expression was coupled to expression of a red fluorescent protein (tdTomato), which allowed the positive identification of successfully modified MSC.

MSC were expanded over 1-2 passages after lentiviral transduction. Prior to the sorting procedure, cells were trypsinized and resuspended in 300µL sorting medium. To remove cell clumps, the cell suspension was filtered over a mesh (pore size 70µm) into a flow cytometry tube. The sorting itself was carried out with a BD FACS-ARIA machine after determining autofluorescence and the fluorescent threshold level using unmodified control cells. Therefore, the tube containing the cell suspension was connected to the nozzle and a collection tube with 200µL sorting medium was placed in the tube holder. After the fluidic stream left the nozzle, drops are formed (containing a single cell), and the drop delay was adjusted to efficiently collect positive cells. When a positive cell was detected, a charge was applied to the stream leading to redirection into the collection tube.

After sorting, MSC were seeded with an appropriate density and expanded over 1-2 additional passages before they were directly used or stored in liquid nitrogen for experiments.

### 3.6.2 Cell staining for flow cytometry

Intracellular staining was performed in order to assess protein translation of ITGA4 after mRNA transfection. In brief, MSCs were harvested, washed with and fixed with 4 % paraformaldehyde. This was followed by permeabilization to allow entrance of antibody later on. After additional washing, cells were incubated with rabbit-anti-ITGA4 antibody at 4°C for 25 min. Unbound antibody was removed by repeated washings before the cell suspension was incubated with Alexa Fluor® 546-labeled donkey-anti-rabbit IgG antibody. Finally, cells were resuspended in washing buffer and measured by flow cytometry.

### 3.6.3 LDV-FITC binding

Assembly and membrane localization of VLA4 after ITGA4-IVT-mRNA transfection was verified by LDV-FITC assay. LDV-FITC is a fluorochrome-labelled small peptide that binds specific to VLA4.

For LDV-FITC binding, transfected and control MSCs were trypsinized, washed, and centrifuged. The resulting cell pellets were resuspended in LDV-FITC staining buffer and returned to the incubator. After incubation for 30min, cells were washed and measured immediately by flow cytometry. Autofluorescent controls were prepared for each cell population without addition of LDV-FITC.

### 3.6.4 Quantification by flow cytometry

Quantification of cells after lentiviral or mRNA-based modification was performed by flow cytometry. Preparation of cells included a trypsinization and in cases, where no reporter protein was expressed, subsequent cell staining. Cell suspension was prepared in sorting medium. Approximately 6,000-20,000 single and viable cells were measured per analysis using FACS Canto or Aria with FACS Diva software.

Post-acquisition data processing was conducted using FlowJo software. Quantity and mean fluorescence intensity (MFI) of modified cells were determined by correlation to the autofluorescence of unlabeled controls and in comparison with adequately processed control cells.

## 3.7 Molecular biology

### 3.7.1 Isolation of total RNA from cultured cells

To analyze mRNA levels after MSC modification, cells were homogenized and total RNA was extracted using Direct-zol™ RNA MiniPrep kit.

Cells of interest were directly lysed in the culture vessel using an appropriate amount of TRIzol® reagent (1mL per 60mm dish). The reagent was eually distributed by rocking of the culture dish. Resuspension of the suspension was performed for complete lysis. Homogenizate was transferred to a 2mL tube and stored at -80°C until RNA isolation.

For RNA isolation, homogenizates were thawed at room temperature and an equal volume of 100% ethanol was added to the sample. Then, the mix was loaded onto a spin column and centrifuged at 12,000g for 30s. The flow-through was discarded and the column was washed with Direct-zol™ RNA PreWash and RNA wash buffer. Finally, RNA was eluted in 30µL nuclease-free water. RNA was stored at -80°C after determination of concentration using the Nanodrop spectrophotometer.

### 3.7.2 Reverse transcription

Generation of complementary DNA (cDNA) from RNA is a crucial step prior to quantitative RT-PCR and was conducted using reverse transcription.

Therefore, 2µg of isolated RNA (chapter 3.8.1.) were diluted with nuclease-free water to a total volume of 11µL. Subsequently, 1µL Oligo(dT) 15 primer (250ng/µL) and 1µL of a 10nM PCR nucleotide mix were added and incubated at 65°C for 5min. This step was crucial for denaturation of RNA secondary structures that are possible inhibitors of the transcription. The reaction tube was chilled on wet ice to allow hybridization of Oligo(dT) 15 primer to the poly(A) tails of mRNAs. To every sample, 4µL of 5-fold first strand buffer, 1µL of 0.1M DTT, 1µL of RNAsin® RNase inhibitor and 1µL of Superscript III reverse transcriptase (200U/µL) were added and subjected to a 3 step incubation process. Initially, the reaction was incubated at room temperature for 5min, and, then at 50°C for 1h. Finally, the reaction was terminated at 70°C for 15min. The resulting cDNA was diluted to a final concentration of 80ng/µL using molecular grade water and stored at -20°C.

### 3.7.3 Isolation of genomic DNA

Genomic DNA (gDNA) was isolated using Quick-gDNA™ MiniPrep for evaluation of successful integration after lentiviral transduction of MSC.

Growth medium was aspirated from cells of interest and 1mL genomic lysis buffer was added to the culture vessel (T25 flask). The vessel was placed on a rotating plate shaker for 10min. The lysate was loaded onto a spin column and centrifuged at 10,000g for 1min. The spin column was washed repeatedly. Twenty microliters of DNA elution buffer were added to the center of the spin column, and after 5min of incubation, the gDNA was eluted by centrifugation. After spectrophotometric determination of the concentration, the gDNA was stored at -20°C until use.

### 3.7.4 Quantitative RT-PCR

Quantitative real time PCR (qPCR) was performed using TaqMan™ Fast Advanced MasterMix and TaqMan™ gene expression assays. The TaqMan™ gene expression assay was composed of a pair of PCR primers and a sequence-specific TaqMan™ probe carrying a 5` fluorescent reporter dye and a 3' nonfluoresceent quencher. The probe anneals to the target sequence between the primer sites. Once the PCR was running, the probe was cleaved by 5`exonuclease activity of the TaqMan™ polymerase, what separates the quencher from the dye, leading to an increasing reporter dye signal. Therefore, 400ng of the cDNA sample was mixed with 2x TaqMan™ Fast Advanced MasterMix, 1µL of TaqMan™ gene expression assay and filled with nuclease-free water to a final volume of 20µL. The qPCR was conducted using the following thermal conditions and 7900HT Fast Real-Time system:

**Tab. 5 Thermal cycling conditions for TaqMan™ quantitative RT-PCR**

| Step | Temperature | Time | Cycle |
|---|---|---|---|
| Initial polymerase activation | 95°C | 20s | 1 |
| Denaturation | 95°C | 1s | 2-41 |
| Annealing/Extension | 60°C | 20s | |

Relative quantitation was conducted using the standard curve method after Ct calculation from raw data using LinRegPCR software. For each probe, standard curves of at least 3 samples were acquired by a serial dilution. After performing qPCR, Ct-values were determined, plotted against input and from that, linear equation was calculated. In the following, it was possible to assess quantity of target within the experimental samples by reference to standard curve. Expression levels were determined after normalization of target quantity to respective housekeeping genes.

## 3.8 Protein biochemistry

### 3.8.1 Whole cell lysates

Preparation of whole cell lysates is a crucial step prior to SDS-PAGE and Western blotting. Lysates were acquired by using modified radio-immunoprecipitation buffer (mRIPA) or Urea lysis buffer. Chemokine receptors, such as CCR2, tend to form oligo- or multimers (Armando et al. 2014), what complicated the detection and evaluation of correct protein size and necessitate the use of the more rigid urea lysis buffer.

In order to prepare whole cell lysates, cells were grown on 10cm dishes under standard conditions. When reaching subconfluence, the cell monolayer was detached using a cell scraper and transferred to a 15mL conical tube. Cells were pelleted by centrifugation (300g, 4°C, 5min) and washed with PBS. Thereafter, the cell pellet was lysed by addition of 100-200µL mRIPA or urea lysis buffer. To enhance cell lysis and resolution of multimers, a 10min sonication was performed using an ultrasound water bath. Further cell lysis was conducted during incubation by vigorous shaking at 4°C for 30min. Unsolvable fragments and debris were pelleted by centrifugation at 10000g, 4°C for 10min. Then, the supernatant containing proteins was transferred to a fresh tube and stored at -80°C.

### 3.8.2 Determination of protein concentration

A bicinchoninacid (BCA) microplate test was conducted for determination of protein concentration. Initially, the BCA working reagent was prepared by mixing 50 parts of reagent A with one part of reagent B. From that, 200µL/sample were transferred to a 96 well microplate and mixed with 10µL of the experimental sample. The plate was covered and kept at 37°C for 30min. During this incubation step, divalent copper-ions were reduced to $Cu^{+}$ by peptide bonds. Then, the monovalent copper ion was chelated with two molecules of

bicinchoninacid indicated by purple color. After cooling down to room temperature, the absorbance at 562nm was measured using a photometric plate reader.

For each measurement, doubled BSA standards were conducted in parallel covering concentration range from 0 to 2mg/mL. A standard curve was prepared by plotting absorbance against protein concentration. Protein concentration of experimental samples was calculated with aid of resulting linear equation.

### 3.8.3 Discontinuous SDS-PAGE

Separation of protein according to their molecular weights was conducted with sodium dodecyl sulfate polyacrylamide gel electrophoresis (SDS-PAGE).

Prior to gel electrophoresis, a polyacryamid gel was prepared, which was composed of a separating gel with 8-10% polyacrylamide content and a stacking gel with 3% acrylamide. Each part was composed of an appropriate volume of 30% Rotiphorese®, a 4 x upper or lower buffer, and A. dest. As soon as TEMED and 40% ammonium persulfate (APS) were added, the mixture was poured between two glass plates in a gel caster for polymerization. A comb was added to create sample wells while stacking gel was still liquid.

For SDS-Page gel electrophoresis, 15µg of whole cell lysates were used for each sample. Lysates were diluted with a 6 fold SDS loading buffer and in case of mRIPA lysate denatured at 95°C for 5min and, afterwards, kept on wet ice until loading. Urea lysates were incubated at room temperature for 30min to ensure sufficient protein denaturation and resolution of complex protein structures.

In the following, the electrophoresis chamber was prepared by inserting the gel and filling with 1 x running buffer. The comb was removed from the gel and samples were loaded into the sample wells. A suitable protein marker with a range of 4.6-300kDa was also loaded for determination of molecular weights from protein of interest. Then, an electrical current with 25-35mA and 300V was applied, what lead to initial accumulation within the stacking gel and to the size-dependent migration of negatively charged proteins through the separating gel. SDS-Page gel electrophoresis was terminated when proteins reached lower gel margin.

### 3.8.4 Western Blot

Transfer of electrophoretically separated proteins on a nitrocellulose membrane was carried out using a tank blot procedure. The stacking gel was carefully removed from the separating gel, which was then arranged together with the nitrocellulose membrane, filter papers, and fiber pads into a sandwich cassette (Fig. 6).

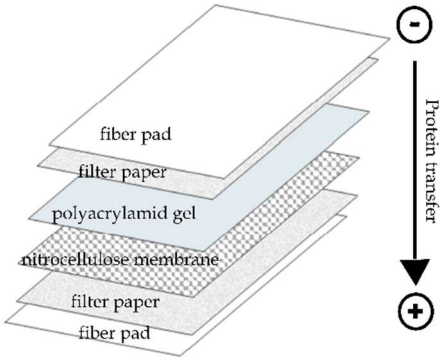


***Fig. 5 Assembly of components for tank blot procedure.*** *Proteins were transferred from SDS-polyacrylamide gel onto a nitrocellulose membrane. Negatively charged proteins are migrating with applied current towards direction of the anode.*

The cassette was placed into a tank blot chamber and covered with transfer buffer. Proteins were blotted onto the membrane by applying an electrical current of 1V for 50-70min. Afterwards, the setup was disassembled and protein transfer was verified by Ponceau S staining of the nitrocellulose membrane. Therefore, the membrane was placed into Ponceau S staining solution for 5min. Pink-colored protein bands became visible by subsequent rinsing of the membrane. The membrane was washed with A.dest until Ponceau S staining was completely vanished and was then subjected to immunological detection.

### 3.8.5 Immunological detection and chemiluminescent reaction

Nitrocellulose membranes carrying blotted proteins were incubated in TBS-T supplemented with 1% non-fat dry milk to block unspecific binding sites under continuous shaking for 1-2h. Thereafter, membranes were washed using TBS-T and stained with the primary antibody against the respective protein at 4°C overnight. The next morning, membranes were washed with TBS-T and incubated with a horse raddish peroxidase (HRP)-labelled secondary antibody directed against the Fc-part of the primary antibody at room temperature for 2h. Thereafter, membranes were repeatedly washed and protein bands of interest were visualized by a chemiluminescent reaction.

For this, the membrane was shortly incubated (~1min) in a freshly prepared luminol-cumar acid reaction solution. Luminol was oxidized by HRP under light emission. Light signals were recorded using a chemiluminescence chamber over a period of 10min.

Thereafter, analysis was conducted with Quantity One software. Band intensity was determined over the respective area. After subtraction of background, data from protein of interest were normalized against a housekeeping protein (GAPDH).

### 3.8.6 Immunocytochemistry

Immunocytochemical staining was performed for microscopic evaluation of expression of protein of interest.

MSC were grown on glass cover slides coated with 0.1% gelatin in a 24-well-plate. Cells were fixed with 4% PFA on ice for 20min. After repeated washing with PBS, cell membranes were

permeabilized by applying ICC permeabilization buffer for 3min. Traces of permeabilization buffer were removed by subsequent washing with PBS. Then, unspecific binding sites were blocked with ICC blocking solution at room temperature. During the 1h incubation step, the antibody solution was prepared by diluting the primary antibody in blocking buffer and drops of 30µL were pipetted on Parafilm. Thereafter, cover slides were placed with upside-down orientation onto the drops and incubated in a wet chamber at 4°C overnight. The following day, cover slides were removed from the Parafilm and returned to the well plate. Unbound antibody was removed by washing with PBS. A subsequent incubation with a suitable secondary antibody and DAPI was conducted under light protection at room temperature for 1.5h. Cover slides were mounted onto microscopic slides with fluorescent mounting medium after repeated washings. Visualization was conducted using a fluorescence microscope.

## 3.9 Migration

### 3.9.1 Vital staining of cells

GPNT and MSC were vitally stained for improved visualization during imaging. In general, confluent GPNT cells were directly labelled within the transwell migration chamber. MSC were labelled in suspension following trypsinization.

#### 3.9.1.1 PHK26-labelling

PKH26-labelling was performed according to manufacturer´s instructions. Therefore, a 1x staining solution was prepared by diluting 2µL PKH26 per mL diluent C. In the following, growth medium was removed from cells and replaced by the staining solution. After a 5min incubation in the dark, the labelling reaction was terminated by adding growth medium. A subsequent incubation of 1min allowed binding of excessive dye. Finally, the cells were finally washed twice with growth medium.

#### 3.9.1.2 CFSE-labelling

In arrangement of CFSE-labelling, the CellTrace™ reagent solution was prepared according to manufacturer´s recommendations. To this end, 18µL of DMSO (component B) were transferred to one vial of CellTrace™ reagent (component A) and further diluted in PBS to a final dye concentration of 12µM. Thereafter, growth medium was removed from cells and CellTrace™ reagent solution was added. The reagent covalently bound to intracellular amines during a light-protected 30min period. The binding process was interrupted by addition of 5 volumes of supplement-free medium. CellTrace™ reagent underwent acetate hydrolysis during a subsequent incubation of 30-45min repeatedly interrupted by gentle agitation of cells. After substitution of reagent solution with migration medium, cells were attributed to *in vitro* migration experiments.

### 3.9.2 Transwell migration

Evaluation of migratory capacity of modified MSC and respective controls were performed using a modified Boyden chamber setup (Fig. 5) with either FluoroBlok transwell inserts or standard transwell system. Transwell systems were chosen with a pore size of 8µm and migration was conducted over an endothelial monolayer.

GPNT endothelial cells were seeded two days prior to migration in the upper chamber of the collagen-coated standard transwell inserts with a density of 0.1 million cells/insert. Within 24h, the endothelial cells became adherent and formed a confluent monolayer. Upon reaching confluence, GPNT cells were stimulated with TNFα (100ng/ml, supplemented to the growth medium) over night. The following day, the GPNT monolayer was labelled with either PKH26 or CFSE. MSC were labelled using the complementary dye and seeded into the insert with a concentration of 25,000 cells. To assess the migratory capacity towards MCP1 (CCL2), the chemokine was added into the bottom well with a final concentration of 10ng, 50ng or 100ng. After overnight incubation at 37°C in a normoxic humified atmosphere, the inserts were fixed with 4% PFA for 20min and washed repeatedly with PBS. Transwell meshes were excised and mounted onto a microscope slide with DAPI mounting medium.

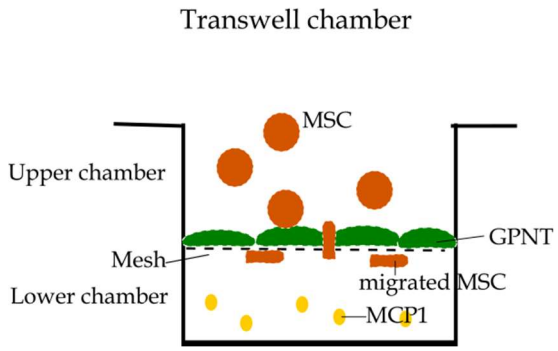


***Fig. 6 Scheme of a modified Boyden chamber setup.*** *Endothelial monolayer is grown on the mesh in the upper Transwell chamber. A MCP1 is added to the lower chamber and attracts MSC applied to the upper chamber. Pore size was 8µm.*

Transwell migration performed with FluoroBlok system were conducted in a similar manner, but leaving out GPNT labelling. MSC were stained using CFSE labelling method without exception.

### 3.9.3 Quantification of FluoroBlok transwell migration

The light-blocking properties of the FluoroBlok transwell migration allowed quantification of migrated MSC by fluorescence microscopy. Fluorescence signals from upper mesh side were shielded from signals of the bottom side. This allowed the specific detection of migrated MSC by using an inverted fluorescence microscope.

FlouroBlok plates were imaged using a Nikon inverted fluorescence microscope. Per transwell, pictures of 5 randomly chosen spots were recorded at 10x magnification. Quantification of migrated cells was based on an area analysis of pictures using Image J software.

### 3.9.4 Analysis of migration using confocal microscopy

MSC transmigration over GPNT-monolayer was evaluated by confocal imaging of mounted standard transwell systems using a LSM 710 with ZEN software. GPNT-confluence of 100% and occurrence of at least 5 MSC per frame were required and defined as criteria for imaging. From each transwell mesh, 5 spots were randomly chosen and controlled for imaging criteria. Thereafter, multi-layered pictures (z-stacks) were taken of target areas covering upper and lower part of the transwell mesh. Pictures were taken with analogous settings.

Confocal images were processed in order to generate 3-dimensional z-stack reconstructions. MSC were classified and counted with respect to their localization as follows: (i) spherical shaped MSC, first contact; (ii) flattened MSC on endothelium, (iii) flattened MSC under endothelium but above mesh, (iv) integrated in endothelial monolayer, (v) within the pore, and (vi) migrated MSC visible at bottom part of transwell mesh. MSC visible in the pore were further distinguished between (v)a cell body above transwell mesh, but processes within pore, (v)b cell completely in pore, and (v)c cell migrated and cell body below transwell mesh with processes within the pore (Fig. 7).

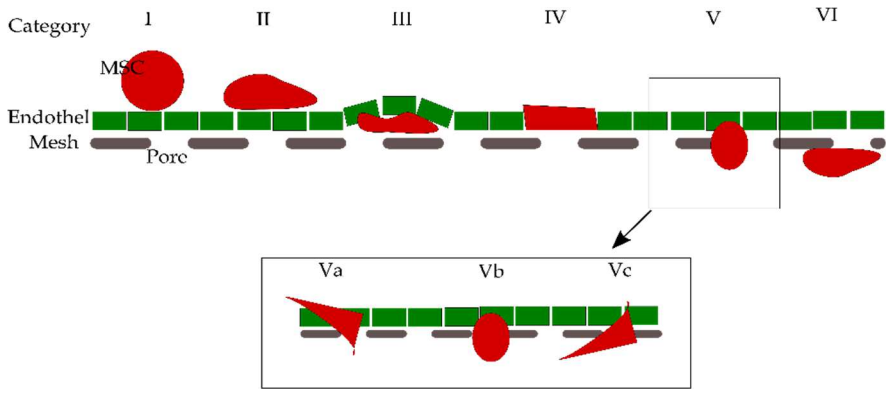


***Fig. 7 Scheme of MSC localization to endothelium for category allocation***

## 3.10 *In vivo* experiments

*In vivo* experiment were carried out in cooperation with Charles River Discovery Research Services in Kuopio, Finland under the governance of animal protocol CRL0615. All procedures involving animal handling and surgery, as well as cell labelling and imaging were conducted by Tuulia Huhtala (PhD), Jussi Rytkönen (PhD), and Laura Tolpanen (as described in chapters 3.10.2 till 3.10.8). Materials used in this part were provided by Charles River, except for MSC and MSC growth medium as well as supplies for immunohistochemistry. Study design and planning were realized by myself. Regularly reports and support was realized remotely. Experiments were carried out according to the regulations for the care and use of laboratory animals of the National Institute of Health (NIH). Approval was given by the National Animal Experimental Board of Finland.

### 3.10.1 Experimental groups and timeline

Homing capabilities of MSC were evaluated after lentiviral overexpression of CCR2 or ITGA4 receptors. Biodistribution and MSC migration towards ischemic brain tissue after middle cerebral artery occlusion (MCAO) and intra-arterial cell transplantation was studied in 20 rats.

Rats were subjected to MCAO in the right hemisphere. After 24h, magnetic resonance imaging (MRI) was conducted to verify the success of the MCAO. Animals were assigned to experimental groups, if the lesion was visible on at least 4 successive MRI pictures within two-thirds of the ipsilateral cortex and striatum. SHAM animals underwent the same procedure, but must not have developed a lesion.

1. SHAM rats receiving control MSC (Sham + CTRL-MSC), n=5
2. MCAO rats receiving control MSC (MCAO + CTRL-MSC), n=5
3. MCAO rats receiving ITGA4 overexpressing MSC (MCAO + ITGA4-MSC), n=5
4. MCAO rats receiving CCR2 overexpressing MSC (MCAO + CCR2-MSC), n=4

$^{111}$In-labelled MSC were infused intra-arterially without immunosuppression. SPECT/CT imaging was performed repeatedly starting directly after cell transplantation. Animals were terminated 72h after MCAO. In addition, the radioactivity of blood and internal organs was measured with a gamma counter. Thereafter, brains were stored for approximately 1 month until sufficient decay of the radioactive label and then analyzed by immunohistochemistry. An overview of the time schedule is given in Fig. 8.

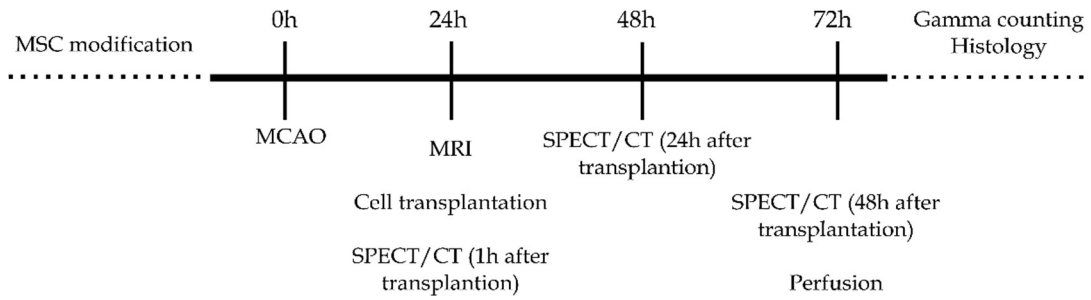


***Fig. 8 Experimental design for evaluation of MSC homing towards cerebral ischemia.***

### 3.10.2 Animals

Twenty male Wistar rats, weighing 179-259g, were purchased from Charles River (Sulzfeld, Germany). Animals were housed under standardized conditions with ad libitum access to food and water, 22±1°C and a controlled light-dark cycle (12h/12h).

### 3.10.3 Transient MCAO

Focal cerebral ischemia was induced by occlusion of middle cerebral artery (MCA) using the filament technique according to Koizumi with modifications (Koizumi 1986). Prior to the surgery, a monofilament nylon thread with 0.25mm diameter was prepared and its tip blunted. Anesthesia of rats was induced with 5% isoflurane (in 70 % $N_2O$, 30 % $O_2$; flow 300 mL/min) and reduced to 1-1.5% during the surgery. Throughout the surgery, the body temperature of the animal was kept at 37°C by a feedback-controlled heating pad connected to a rectal probe.

Right common artery and external carotid artery (ECA) were exposed by cutting throat skin, dissection of muscles, and careful removal of surrounding connective tissue. The ECA was ligated distal from the carotid bifurcation. Thereafter, the ECA was cut, a filament was inserted into the stump of the artery, and inserted into the internal carotid artery (~22-23mm). Filament was moved up to the origin of the MCA, where it disrupted the blood flow and induced ischemia. After 120min of ischemia, blood flow was restored by thread removal and the vessel was closed by cauterization. The animals were allowed to wake up in their home cages after the wound was carefully closed by a surgical suture. After recovery from anesthesia, animals were carefully monitored for complications. Supplementary saline (0.9%, 4mL) was administered intraperitoneally to prevent dehydration. Sham animals underwent the same surgical procedure without inserting a filament.

### 3.10.4 MRI

MRI was performed with a 7T horizontal scanner (Bruker) 1d after MCAO. Therefore, rats were anesthetized with isoflurane and positioned into the magnet bore in standard orientation. T2-weighted scans were acquired using a multi-slice multi-echo sequence with a relaxation time (TR) of 2.5s, field of view (FOV) of 30 x 30mm, matrix of 256 x 128, and 18 slices with a thickness of 1mm.

### 3.10.5 Cell preparation and $^{111}$In labelling

To analyze the biodistribution over 3 days, MSC were labeled with $^{111}$In-oxine. This tracer has a half-life period of 2.8 days. Within the cell $^{111}$In became firmly attached to cytoplasmic proteins and provides a stable label.

MSC-labelling with the radioactive tracer was carried out shortly before intra-arterial transplantation. Therefore, frozen cell suspensions were recovered using the standard thawing protocol (see chapter 3.1.2.). The recovered cells were directly subjected to the labelling procedure after determination of cell number and viability by trypan blue exclusion.

The cells were incubated with $^{111}$In-oxine (37MBq/mL, Nycomed Ammersham) in Tris–buffer for 30min at 37°C. Thereafter, the cells were washed to remove free tracer. Radioactive labelling of the cell suspension was controlled by a gamma counter Finally, MSC were resuspended in vehicle medium for intra-arterial transplantation. Viability was

determined once more after the labelling. The cell suspension was adjusted to $0.5x10^6$ MSC within 600-700µl prior to transplantation. The cell suspension was kept shortly in a water bath with 37°C until transplantation.

### 3.10.6 Cell transplantation

For cell transplantation, rats were kept anesthetized with 1-2% isoflurane. The stump of the ECA was carefully exposed similar as described for MCAO. A cannula connected to a tube was inserted into the stump. Thereafter, $^{111}$In-labelled MSC ($0.5x10^6$ cell/animal) were infused over a time span of less than <5min. Then, the stump was closed by coagulation and muscles were carefully placed back in position. The wound was closed by stitching up the skin.

### 3.10.7 SPECT/CT imaging

In order to visualize biodistribution of transplanted cells, a SPECT imaging was performed using a small animal SPECT/CT at 1h, 24h, and 48h after cell infusion.

Prior to imaging, rats were anesthetized using 1-2% isoflurane. In the following, 3D images of the animals, combined with CT, were acquired with an imaging protocol consisting of planar tomography images (55kVp, 500ms exposure time), which were used as a reference. After choosing the imaging area, helical SPECT imaging was performed from the same coordinates with 45s/frame. High resolution multi-pinhole apertures (NSP-105-R15-WB) were used to enhance resolution. After SPECT imaging helical CT was performed with 180 projections at 55kVp. SPECT image reconstruction was conducted using HiSPECT and image processing performed using InVivoScope. After the last imaging, animals were terminated with an isoflurane overdose. A blood sample was collected via cardiac puncture. Thereafter, animals were perfused with 4% PFA and rinsed with saline.

### 3.10.8 Gamma counting

After blood sample collection and animal perfusion, internal organs including heart, lung, liver, kidney, spleen and brain were collected. Radioactivity of the samples was measured using gamma counter after determination of organ weight. The organ weights were used to calculate the total radioactivity to the total activity of administered cells and applied against 1 g of organ (percentage of injected dose per gram of organ, %ID/g). Prior to calculation, decay correction to injection time was performed.

### 3.10.9 Imunohistochemistry

Perfused and PFA-fixed rat brains were cut in coronar sections with a slice thickness of 20µm using a cryotom. After mounting the slices on microscopic slides, they were stored at -20°C until staining. For immunohistochemical staining, slides were defrosted at room temperature for 15-20min. Thereafter, slides were repeatedly washed in PBS and brain slices were

surrounded by a wax line using a DAKO pen. A volume of 100µl blocking buffer was applied and slices were incubated in a wet chamber at room temperature for 1h. During blocking, antibodies were diluted in respective buffer. Then, blocking buffer was replaced with antibody solution and kept in a wet chamber at 4°C overnight. The following day, sliced were washed 3 times in PBS and incubated with a buffer containing the secondary antibody for 2h. Finally, slides were washed and covered using fluorescent mounting medium and a cover glass. Immunofluorescence stainings were visualized by confocal microscopy.

## 3.11 Statistical analyses

General raw data processing was performed using Microsoft Excel 2010. Statistical analyses were conducted with GraphPad Prism 6 using one-way analysis of variance (ANOVA) and two-way ANOVA for repeated measurements with Tukey´s post hoc test for multiple comparisons unless indicated otherwise. Data are represented as mean ± SD. P-values lower 0.05 were considered statistically significant.

# 4 Results

## 4.1 mRNA-driven overexpression of ITGA4 on MSC

mRNA transfection is a valuable tool with the potential for clinical application. This method was evaluated in terms of MSC modification with ITGA4 for enhanced homing.

### 4.1.1 IVT and mRNA-transfection of MSC

ITGA4-mRNA was prepared by IVT with co-transcriptionally (ARCA) or post-transcriptionally capping (Cap0, Cap1). IVT led to generation of mRNA with an appropriate size (3100bp for ITGA4, 4020bp for ITGA4-GFP) independently from capping. Furthermore, polyadenylation prolonged mRNA by ~150bp as indicated by higher molecular weight of denaturing RNA gel electrophoresis (Fig. 9A).

Initial mRNA transfection using the reagents PEI, TransIT or Lipofectamine 2000 to deliver GFP-mRNA resulted in high mortality of MSC accompanied with low efficiency. Cationic lipofection with Stemfect was well tolerated by cells and led to protein expression (Fig. 9B).

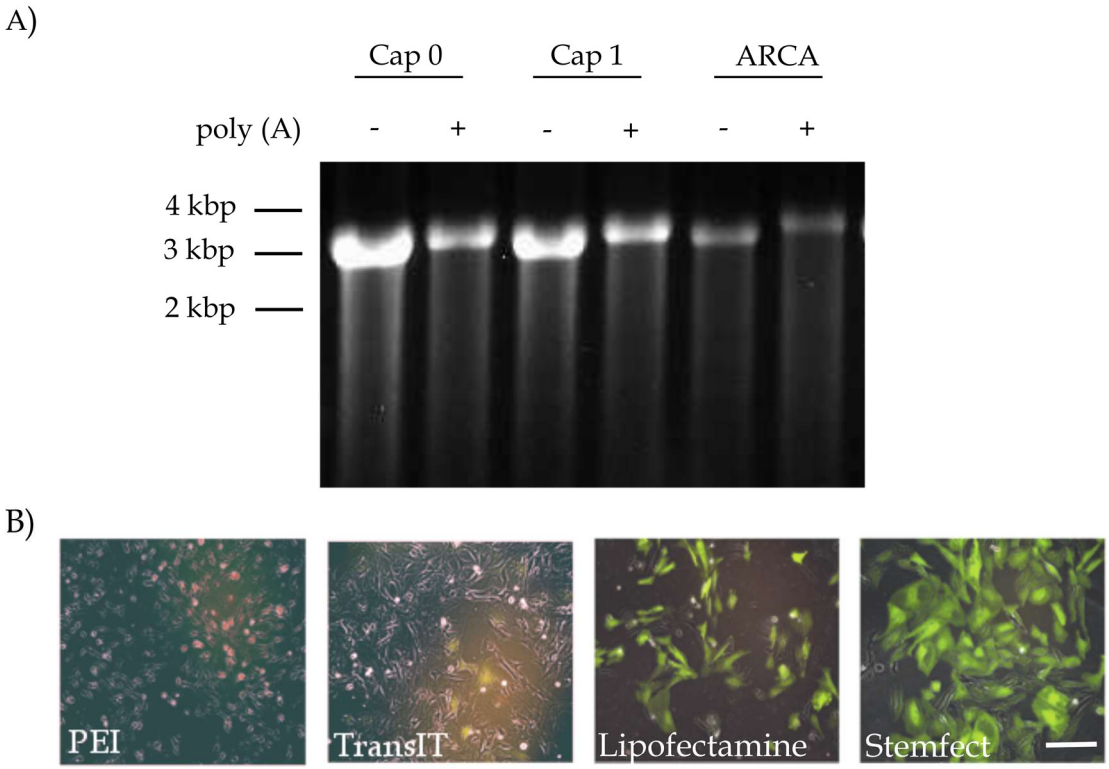


***Fig. 9 In vitro transcription (IVT) and transfection using various transfection reagents.*** *(A) RNA gel electrophoresis verified the correct transcript size of 3100bp for ITGA4, stabilized with either Cap0, Cap1, or ARCA. Polyadenylation increased transcript size to 3250bp. (B) Representative fluorescence images after transfection of MSC with GFP mRNA using PEI, TransIT, Lipofectamine 200, or Stemfect. Dying cells showed increased red auto-fluorescence, while GFP was detectable by green signals. Scale bar indicates 50µm.*

Evaluation of ITGA4-mRNA levels by RT-PCR revealed a significant increase in transfected MSC compared to untransfected controls (Fig. 10). Shortly after termination of lipofection (4.5h), significant differences to CTRL were observed (2915.65 AU for Cap1, 2228.95 AU for Cap0, 2098.09 AU for ARCA, 0.697 AU for CTRL). mRNA level declined thereafter, but did not return to control level during the 96h post-transfection period. This kinetic was observed for MSC transfected with Cap0-ITGA4, Cap1-ITGA4, or ARCA-ITGA4. A general mRNA half-life time of 4.5h was determined for both, co-transcriptionally and post-transcriptionally capped mRNA.

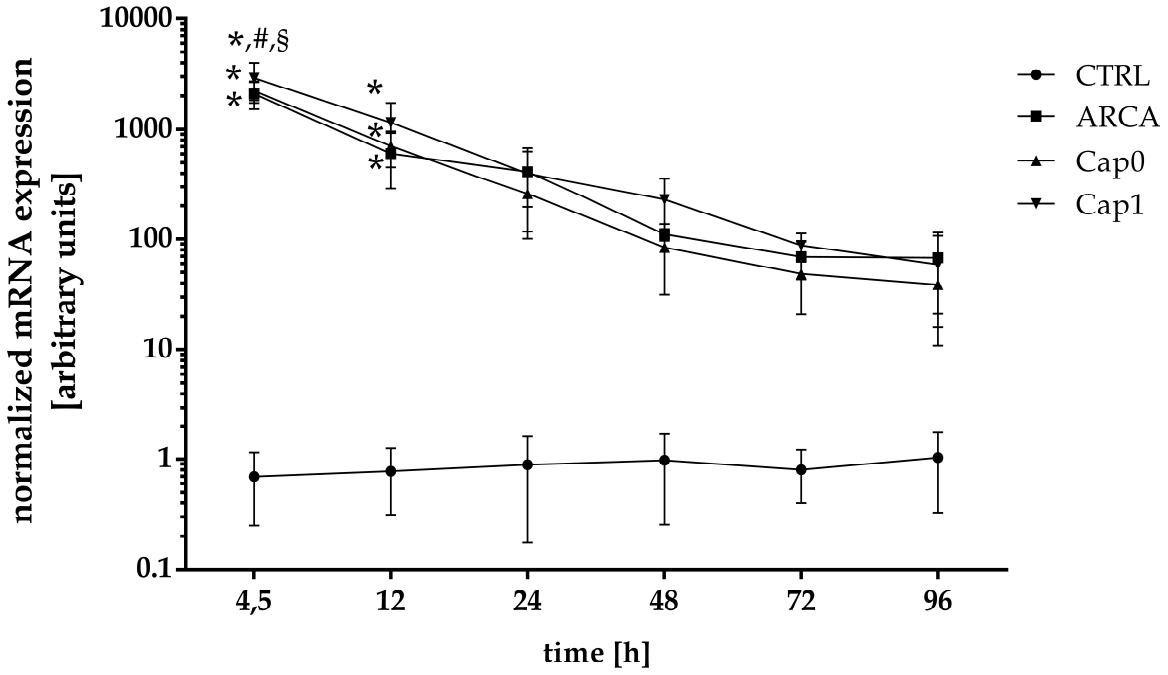


***Fig. 10 mRNA level for ITGA4*** *determined over a time course from 4.5h till 96h after transfection. Data are given as mean ± SD of 4 independent biological replicates (n=4). Statistical differences between MSC transfected with Cap0-, Cap1-, or ARCA-ITGA4 mRNA and CTRL were calculated with a two-way ANOVA with Tukey´s post hoc multiple comparisons (* $p < 0.05$ vs. CTRL, # $p < 0.05$ vs. Cap0-ITGA4; § $p < 0.05$ vs. ARCA-ITGA4).*

### 4.1.2 Vitality and toxicity following mRNA transfection

Impact of transfection on cell fitness was evaluated using MTT and LDH assay.

mRNA-transfection had an impact on cell viability as illustrated in Fig. 11. Although the OD values were decreased in comparison to untransfected control cells, no significant differences were determined. OD values of transfected MSC and controls increased over time. ARCA-ITGA4 transfected MSC showed reduced mean viability at 48h, 72h, and 96h after transfection, but there were no significant differences compared to controls (ARCA-ITGA4 vs CTRL p (48h) = 0.1; p (72h) = 0.052; p(96h) = 0.06).

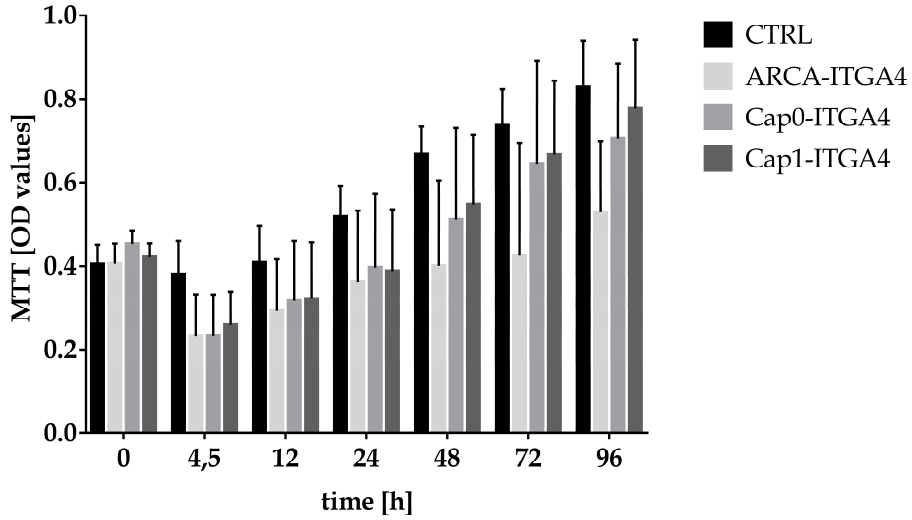


***Fig. 11 Viability of CTRL and transfected MSC.*** *Absorbance (optical density, OD) was determined after reduction of MTT. Data are represented as mean ± SD of 3 independent biological trials (n=3). Statistics were performed using two-way ANOVA with Tukey´s post hoc multiple comparison.*

Release of LDH was evaluated as an indicator of cell toxicity. Transfection caused minor toxicity in MSC as observed 4.5h and 12h after onset. (Fig. 12). LDH release from transfected MSC was further elevated 24h and 48h after transfection, while LDH concentration maintained the same as in controls. Thereafter, LDH determination was relinquished to avoid misjudgment after medium change. Except for Cap0-ITGA4 at 48h after transfection, no significant differences were observed between transfected cells and controls throughout the observation time.

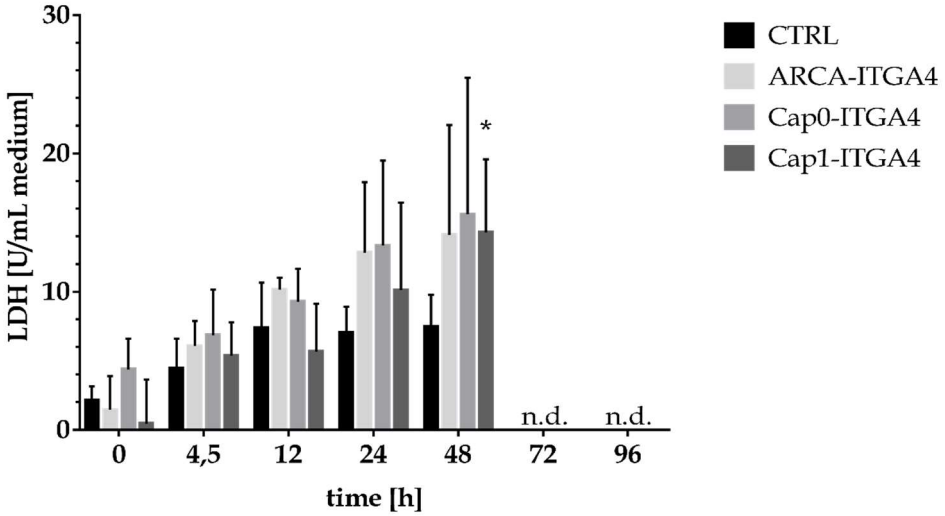


***Fig. 12 Toxicity of controls and transfected MSC.*** *LDH levels were determined in supernatants collected from respective cell populations by reduction of $NAD^+$ to NADH. Data were not collected at 72h and 96h due to possible falsification by change of growth medium (not determined, n.d.). Data are represented as mean ± SD from 3 independent biological trials (n=3). Statistics were performed using two-way ANOVA with Tukey´s post hoc multiple comparisons (* $p < 0.05$ vs. CTRL).*

### 4.1.3 Maintenance of multilineage differentiation potential following mRNA transfection

Multipotency after mRNA-transfection was evaluated by differentiation into adipocytes, osteocytes and chondrocytes. FABP4 indicated the differentiation into the adipogenic lineage (Fig. 13, top row). Furthermore, osteocalcin-immunoreactivity verified the osteogenic differentiation (Fig. 13, middle row). As apparent in the bottom row of Fig. 13, immunohistochemical staining of aggrecan indicated successful differentiation into chondrocytes. Trilineage differentiation potential was not affected by the transfection procedure or the delivery of mRNA. In addition, no differences were observed after transfection of co-transcriptionally or post-transcriptionally capped mRNA.

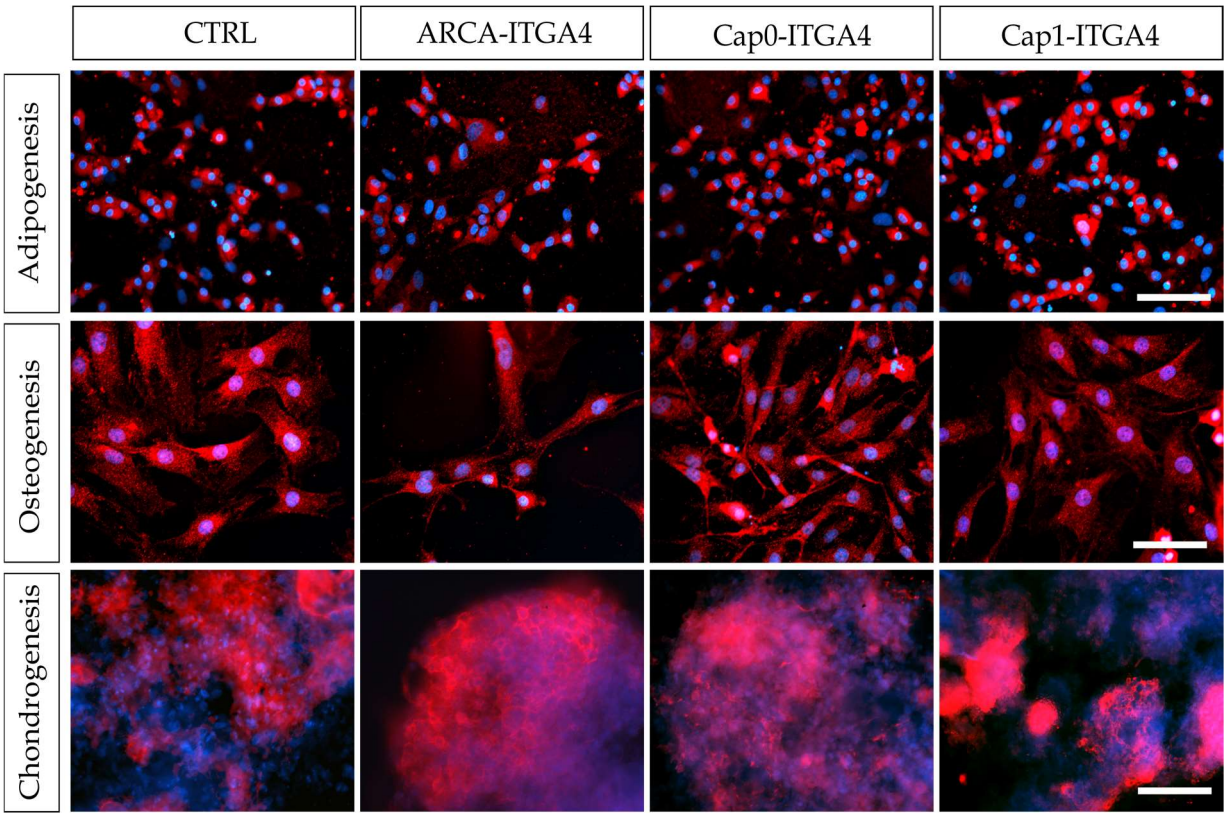


***Fig. 13 Differentiation into adipogenic, osteogenic and chondrogenic lineage after mRNA transfection.*** *MSC were subjected to differentiation 24h after transfection. Adipogenesis (upper row) was verified by detection of FABP4 (red channel) 14 d after switch to adipogenic medium. Osteogenesis (middle row) was associated with osteocalcin appearance (red channel) within 14d and formation of aggrecan (red channel, bottom row) proved chondrogenesis. The nuclei were visualized with DAPI stain (blue channel). Scale bars indicate 50µm.*

### 4.1.4 Protein expression after mRNA transfection of MSC

For evaluation of ITGA4 expression following mRNA expression, several detection methods as flow cytometry analysis, immunofluorescence staining, and Western Blot were performed.

#### 4.1.4.1 Evaluation of ITGA4 expression

Analysis of equally processed Cap0-, Cap1-, or ARCA-mRNA were conducted by flow cytometry and fluorescence microscopy.

As already observed by Western Blot analysis, ITGA4 levels increased shortly after termination of transfection (Fig. 14A, 4.5h). However, MSC transfected with ARCA-ITGA4-mRNA showed delayed increase in comparison to Cap0- or Cap1-ITGA4-mRNA. Furthermore, a maximum of 49% positive MSC were observed 12h after transfection of ARCA-transcripts and decreased thereafter. In contrast, transfection of post-transcriptionally capped mRNA led to 62% (Fig. 14A; Cap1-ITGA4, 12h) or 63% (Fig. 14A; Cap0-ITGA4, 24h) ITGA4-positive cells. A decline was noticed after 48h. Minor ITGA4 expression was observed in untransfected controls (9-18%).

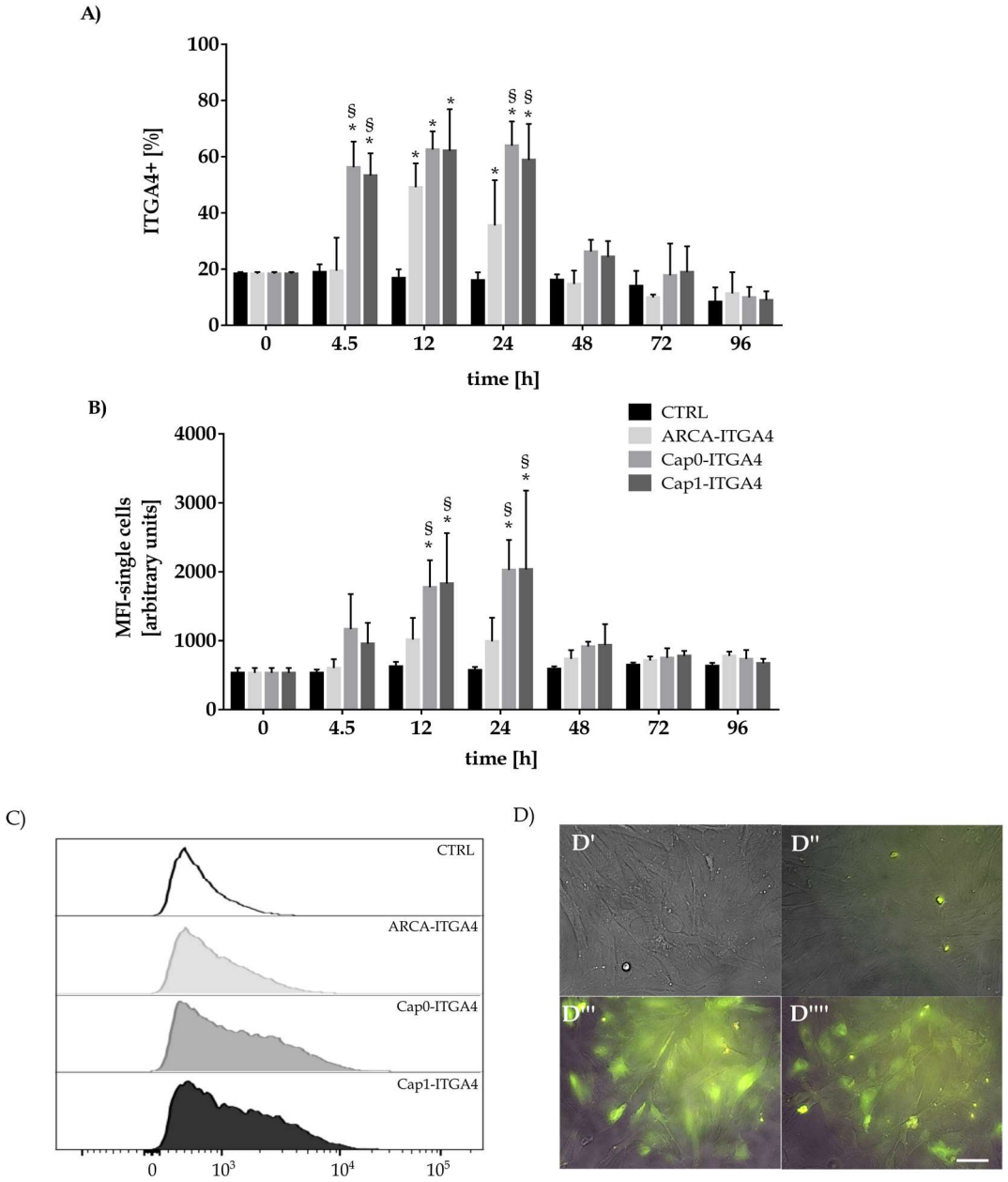


***Fig. 14 Transfection of MSC with post-transcriptionally or co-transcriptionally capped ITGA4-mRNA and analysis via flow cytometry****. Quantitation of ITGA4 positive cells (A) and MFI (B) revealed cap-associated differences. Data are represented as mean ± SD of 3 independent biological trials (n=3; * p < 0.05 vs. CTRL, § p < 0.05 vs. ARCA-ITGA4, in two-Way ANOVA with Tukey´s post hoc multiple comparison). Representative histograms of ITGA4 positive MSC (C) are given for CTRLs and MSC transfected with ARCA-, Cap0-, and Cap1-ITGA4 (Y-axis in normalized to mode range for PE). Representative photographs (D) are given for CTRL-MSC (D'), and 12h after transfection with ARCA-ITGA4-GFP (D''), Cap0-ITGA4-GFP (D'''), or Cap1-ITGA4-GFP (D''''). Positive cells are visible in green. Scale bar represents 10µm.*

Significant differences were also observed after analysis of single cell MFI. MSC transfected with post-transcriptionally capped transcripts showed a significant higher MFI than MSC transfected with ARCA-capped constructs or controls after 12-24h (Fig. 35B, Cap0-ITGA4 1780 AU, Cap1-ITGA4-1828 AU, ARCA-ITGA4 1014 AU, 12h). Although a slight MFI elevation was detected, no statistically significant differences were determined for ARCA-capped ITGA4 mRNA in comparison to controls.

To further evaluate transient overexpression after ITGA4-mRNA transfection, immunofluorescence staining was carried out after cell fixation. MSC demonstrated ITGA4 protein kinetics similar to that observed previously (Fig. 15). 4.5h after mRNA delivery, first ITGA4 was visualized in perinuclear regions from MSC received post-transcriptionally capped mRNA (Fig. 15, Cap0-ITGA4 and Cap1-ITGA4, 4.5h). With progressing time, ITGA4 signals increased and spread across the cell body. Moreover, ITGA4 was also clearly localized at cell borders and within processes (Fig. 15., 12h, white arrow heads). Then, ITGA4 signals attenuated and became more condensed probably due to beginning relocation towards central cell body (Fig. 15, 24h, ARCA-, Cap0-, and Cap1-ITGA4). After 48h, most of transfected cells were negative for ITGA4. Of note, all transfected MSC showed a similar spatial and temporal pattern of ITGA4 expression, but it was much less pronounced after transfection of ARCA-ITGA4 mRNA (compare to Fig. 14, A and B). Controls showed no or very reduced ITGA4 immunoreactivity.

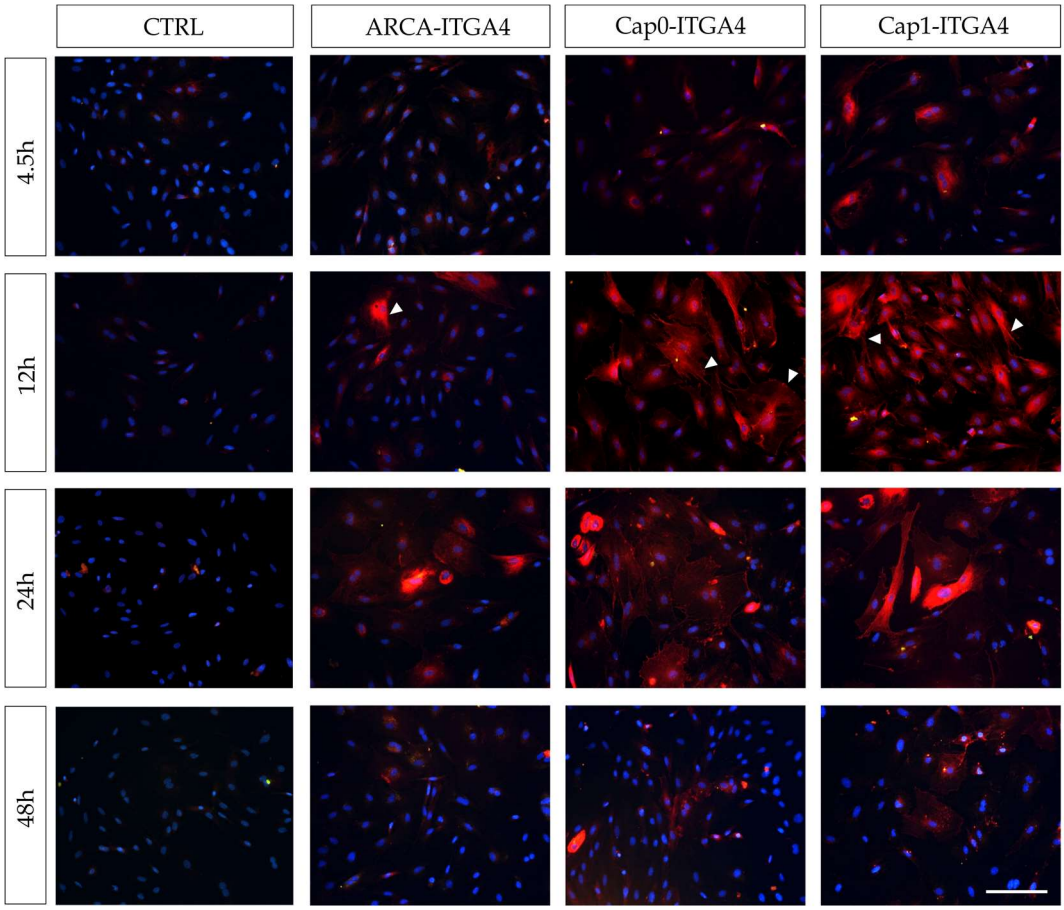


***Fig. 15 ITGA4 expression after mRNA transfection of MSC.*** *Representative immunofluorescence images of CTRLs and MSC transfected with ARCA-, Cap0-, or Cap1-ITGA4 after staining against ITGA4 (red channel). White arrowheads indicate ITGA4 localization at cell borders and processes. Nuclei are visualized with DAPI (blue channel). Scale bar indicates 100µm.*

### 4.1.4.2 Western Blot

Evaluation of ITGA4-GFP expression was carried out from MSC lysates after mRNA transfection.

First bands for ITGA4 were detected already 4.5h after transfection. As shown in Fig 37C, processing of ITGA4 resulted in the detection of two fragments with a molecular weight of 100kDa (C-terminal fragment of ITGA4 + GFP) and 170kDa (full length ITGA4 + GFP). Separate analysis of both bands revealed a predominant occurrence of full-length protein (compare Fig. 16, A and B; 4.5h). Thereafter, an increase of the cleaved C-terminus was observed up to 24h. ITGA4 protein expression declined 24h after mRNA transfection. However, basal ITGA4 expression was observed independently from time or experimental group (Fig. 16C).

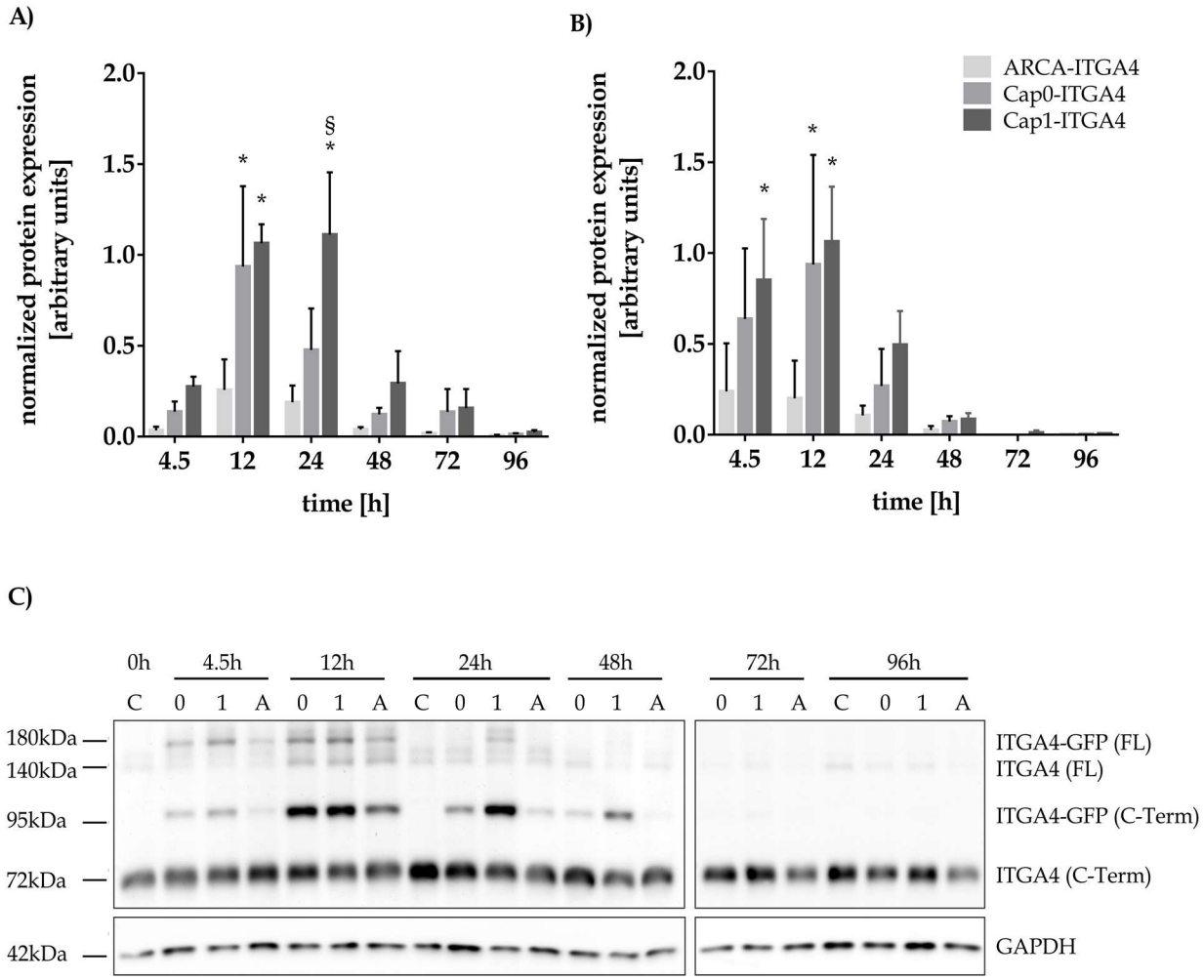


***Fig. 16 Evaluation of ITGA4-GFP translation following mRNA-transfection.*** *Determination of C-terminal (A) and full-length (B) ITGA4-GFP expression was normalized to the housekeeping protein GAPDH. Data are represented as mean ± SD of 3 independent biological trials (n=3). Statistical differences were calculated by two-way ANOVA with Tukey´s post hoc multiple comparison (* $p < 0.05$ vs. CTRL, # $p < 0.05$ vs. Cap0-ITGA4; § $p < 0.05$ vs. ARCA-ITGA4,). Representative Western Blot images are given from MSC lysates over a time window from 0h to 96h (C). Endogenous ITGA4 and overexpressed ITGA4-GFP were detected as C-terminal (70kDA + 30kDA, C-Term) and full-length protein (140kDa + 30kDa, FL) for MSC transfected with Cap0 (0), Cap1 (1)- or ARCA (A) mRNA. Untransfected MSC served as control (C). GAPDH (42kDA) was used as loading control.*

Translation kinetics were not affected by capping and followed the principle of translation onset, maintenance and termination. In terms of translation magnitude, distinct differences were observed between MSC transfected with Cap0-, Cap1-, or ARCA-ITGA4 mRNA. Full-length (Fig. 16 B, 4.5h and 12h) and C-terminal ITGA4 (Fig. 16 A; 12h and 24h) were significantly increased for Cap0- and Cap1 mRNA in comparison with ARCA-mRNA, where protein levels were much lower. However, protein expression was the most efficient and persistent after transfection with Cap1-ITGA4 mRNA.

#### 4.1.4.3 LDV-FITC binding

Further, flow cytometric analysis was conducted with MSC treated with VLA4-binding ligand LDV-FITC.

The LDV-FITC binding kinetic proceeded similar to that observed with ITGA4 stained MSC (compare Fig. 14). Basal binding was determined for untransfected controls showing 18-25% LDV-FITC positive cells. Following transfection with Cap0- or Cap1-ITGA4 mRNA, the amount of LDV-FITC positive cells increased up to 66-68% within 12h (Fig. 17A). Afterwards, a reduction of the positive fraction was observed. ARCA-capped ITGA4 mRNA increased LDV-FITC in about 45% of MSC 4.5h after transfection. This level was maintained at 24h and declined subsequently. Significant increase of LDV-FITC binding was found for all transfected MSC compared to untreated controls (Fig. 17A; 4.5h until 24h). Despite that, Cap0- and Cap1-ITGA4 elevated LDV-FITC binding significantly as compared to ARCA-ITGA4 mRNA.

Furthermore, MFI of LDV-FITC reassembled cap-dependent differences. However, significant MFI enhancement was only observed for MSC transfected with Cap0- or Cap1-ITGA4 mRNA (Fig. 17B).

Since LDV-FITC binds to the fully assembled VLA4 receptor and does not crosses the cell membrane, it was considered to be suitable for surface localization of ITGA4.

Fig. 18A shows that clearly weaker fluorescence signals for LDV-FITC were obtained from controls and ARCA-ITGA4 transfected MSC. As expected, increase and decrease of LDV-FITC binding followed the ITGA4 up- and downregulation, as illustrated for Cap0-ITGA4 transfected MSC in Fig. 18B. Fluorescence signals were strongest between at 12 and 24h after transfection. Minor LDV-FITC binding was observed for controls (Fig. 18, A and B).

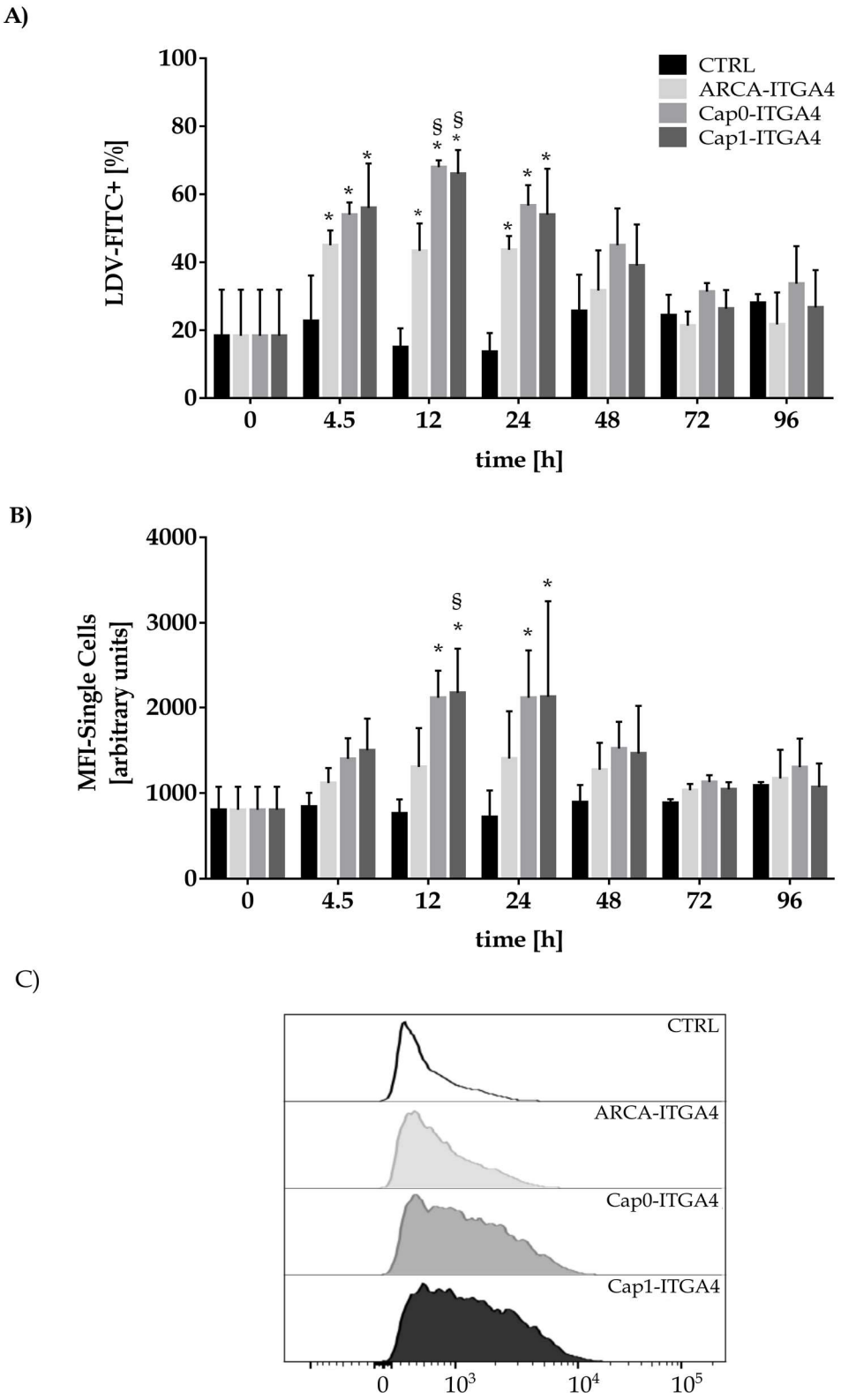


***Fig. 17 Flow cytometric assessment of LDV-FITC binding after MSC transfection with ARCA-, Cap0-, or Cap1-ITGA4 mRNA.*** *Quantitation of LDV-FITC positive cells (A) and determination of singlet MFI (B) revealed time- and cap-dependent differences. Data represent mean ± SD of 3 independent biological trials (n=3). Statistical differences were determined by two-way ANOVA with Tukey´s post hoc multiple comparison (* $p < 0.05$ vs. CTRL, § $p < 0.05$ vs. ARCA-ITGA4). Representative histograms (C) are displayed for transfected or control single cells (y-axis in normalized to mode range for FITC).*

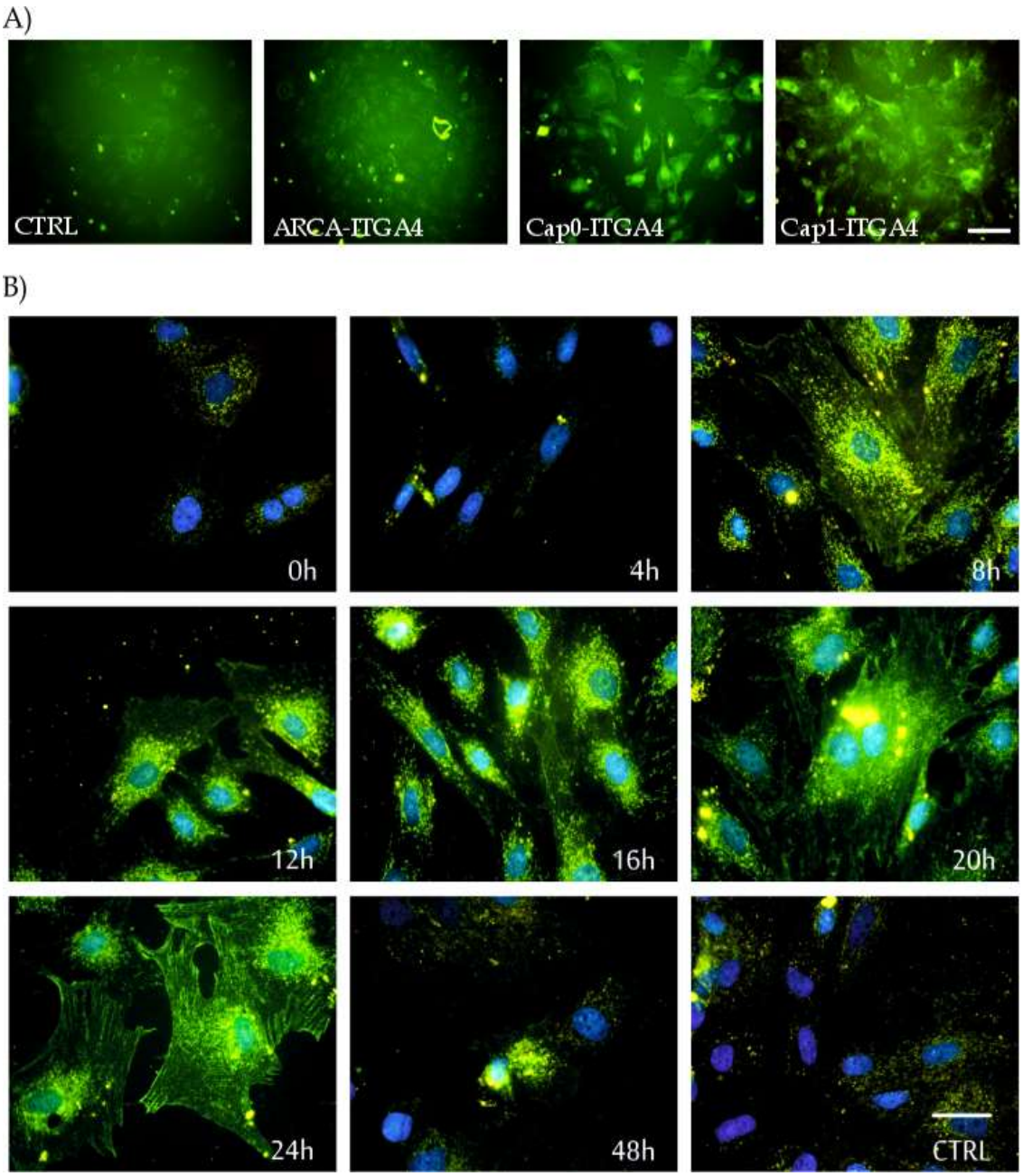


***Fig. 18 Fluorescence microscopy after LDV-FITC binding. (A)*** *Representative immunofluorescence images taken 12h after mRNA transfection with ARCA-, Cap0-, or Cap1-ITGA4, and untreated controls. MSC were incubated with LDV-FITC (green channel) and fixed using PFA. Scale bar indicates 50µm. (B) Time course of LDV-FITC binding shown for Cap0-ITGA mRNA transfected MSC. Nuclei were visualized with DAPI (blue channel). Scale bar indicates 10µm.*

### 4.1.5 GFP expression after mRNA-transfection

In parallel to mRNA-transfection of ITGA4, control experiments utilizing equally processed GFP-mRNA were performed. While ITGA4-mRNA induced desired protein expression in about 60% of the cells, it was possible to obtain 81-88% positive cells after transfection with GFP-mRNA (Fig. 19A). Of note, quantitation of positive cells revealed significant differences between MSC transfected with Cap0- or Cap1-GFP mRNA and ARCA-GFP mRNA.

Cap-dependent differences became even more distinctive after comparison of MFI between experimental groups. As displayed in Fig. 19B, MFI of ARCA-GFP transfected cells was elevated to 6937 AU in comparison to 32 AU for untransfected MSC, but did not reach significance. Post-transcriptionally capped GFP-mRNA, in contrast, led to significant increase of MFI compared to both, controls and ARCA-GFP transfected MSC. Nonetheless, MFI did not increase to similar extent after transfection of ITGA-mRNA and was much weaker as seen for GFP-mRNA transfection (compare Fig. 14B and Fig. 19B).

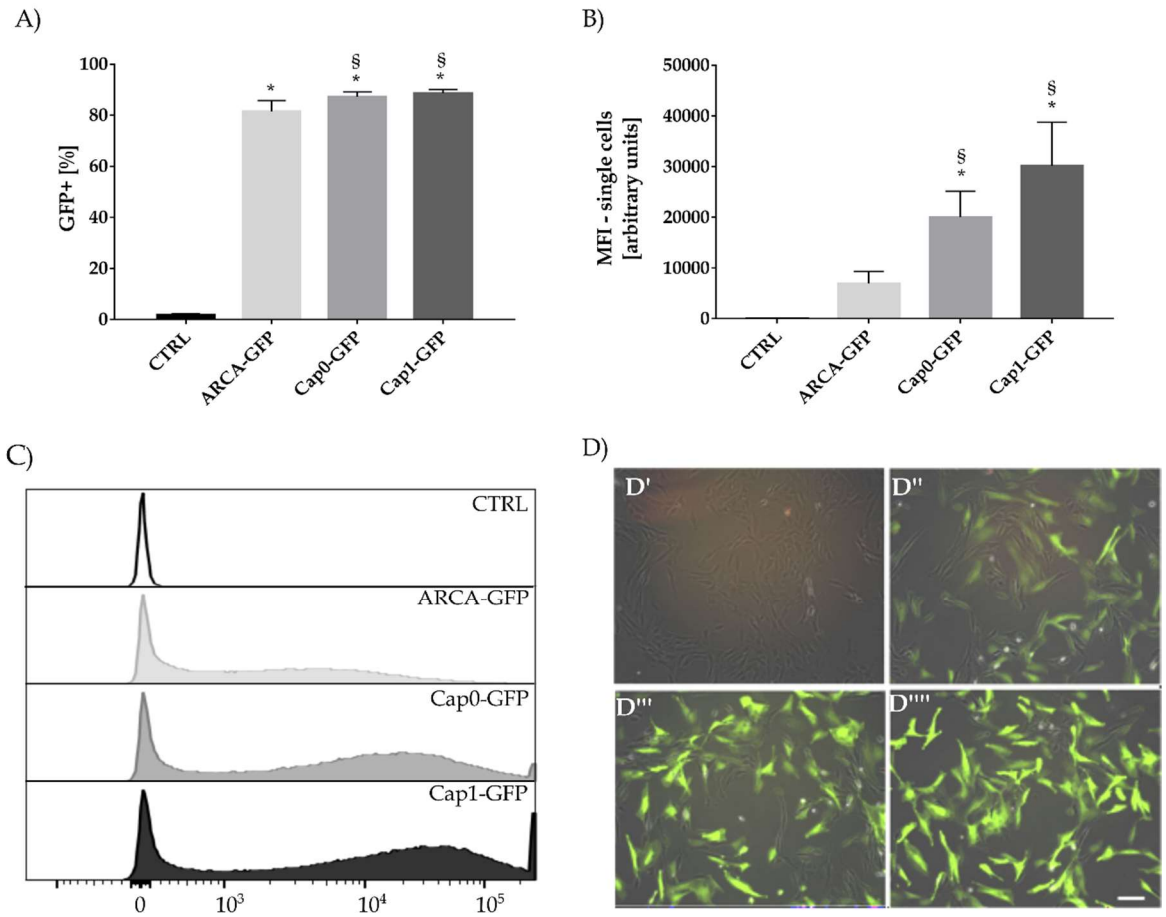


***Fig. 19 Flow cytometry of controls and MSC transfected with ARCA-GFP, Cap0-GFP, and Cap1-GFP.*** *Quantitation of GFP positive MSC (A) as well as MFI of single cell population (B) are shown 12h after transfection ARCA-, Cap0-, or Cap1-processed transcripts. Data are represented as mean ± SD of 4 independent biological trials (n=4) and statistics were conducted using one-way ANOVA with Tukey´s post hoc multiple comparison (* $p < 0.05$ vs. CTRL, § $p < 0.05$ vs. ARCA-GFP). Representative histograms (C) are displayed for transfected or control single cells (y-axis in normalized to mode range for FITC). Representative photographs(D) are given for CTRLs (a), and 12h after transfection with ARCA-GFP (b), Cap0-GFP (c), or Cap1-GFP (d). Positive cells are visible in green. Scale bar represents 20µm.*

## 4.2 Optimizing lentiviral modification of MSC with ITGA4

Lentiviral modifications allow the long-term expression of a desired transgene. The transgene expression depends on the lentiviral construct what requires tailoring. To evaluate the impact of the promoter, four common promoters were cloned in front of an ITGA4-GFP fusion insert. Lentiviral particles, prepared from those constructs, were used to transduce MSC. ITGA4-GFP transgene expression driven by various promoters was evaluated over a period of 20d after infection.

### 4.2.1 Transgene expression

Transgene protein expression was analyzed by qRT-PCR, flow cytometry and Western Blot.

#### 4.2.1.1 mRNA expression of ITGA4 after promoter substitution

Total RNA was isolated from MSC at days 4, 8, 12, and 20 after transduction with the lentiviral particles and translated into cDNA. The results obtained by subsequent qPCR are illustrated in Fig. 20.

A basal expression was observed for ITGA4 in native MSC (CTRL) and Polybrene®-treated MSC (PB-CTRL). Following infection with the lentiviral particles, upregulation of mRNA-level was detected for all constructs. ITGA4-mRNA levels driven by UbC-promoter, for example, were elevated by approximately a 2-fold magnitude compared to controls.

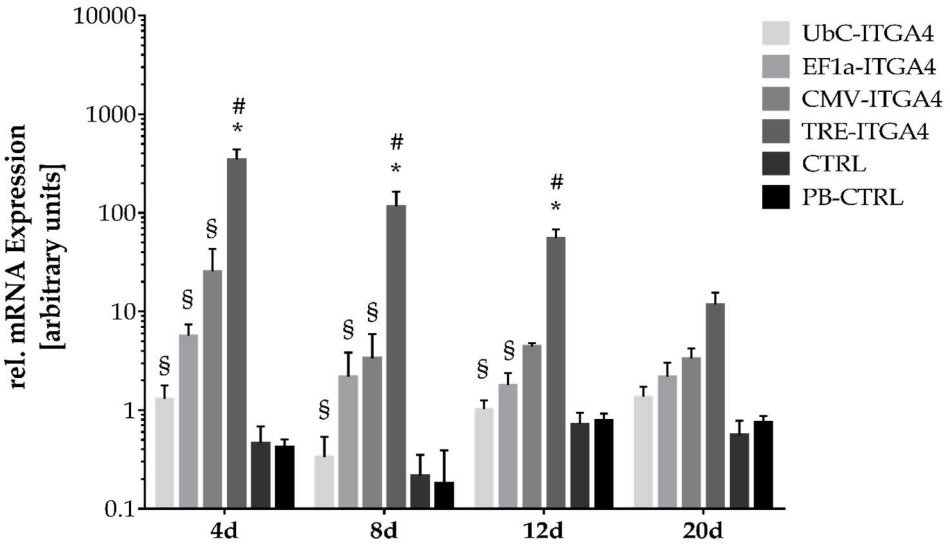


***Fig. 20 mRNA expression of ITGA4 under control UbC-, EF1a-, CMV-, and TRE-promoter.*** *Transcript levels showed a promoter-dependent magnitude after normalization to the expression of housekeeping control ACTB. Data are represented as mean ± SD of 3 independent biological replicates (n=3). Statistical significance was determined by two-way ANOVA with Tukey´s post hoc multiple comparison (p < 0.05, * vs. CTRL, # vs. PB-CTRL, § vs. TRE-ITGA4).*

Comparison of ITGA4-mRNA level as function of promoter strength showed that UbC-promotor led to only moderate increase of transcript quantity (Fig. 20). Higher mean mRNA-levels were observed under EF1α- or CMV driven expression, but their difference was not statistically significant (EF1α-ITGA4 vs. CTRL p (D4-D20) >0.9; CMV-ITGA4 vs CTRL p(D4) =0.7, p (D8-D20) >0.9). Significant elevation was detected under control of TRE-promoter at day 4, 8, and 12 after transduction. A profound downregulation was detected over time. Only for UbC-promoter, ITGA4-mRNA expression remained at the same level up to day 20.

#### 4.2.1.2 Evaluation of ITGA4 protein expression after promoter substitution

Lentiviral constructs used for promoter comparison were designed for the expression of a ITGA4-GFP fusion protein. This GFP-tag allowed the detection of the overexpressed transgene by fluorescence microscopy.

Fig. 21 depicts ITGA4-GFP expression at day 4, 8, 12, and 20 after lentiviral transduction. Only a few MSC expressed the fusion protein under control of the UbC-promoter at day 4. The amount of ITGA4-GFP-positive cells remained at the same level at day 20 post infection. EF1α- and CMV driven transgene expression appeared to be more effective, but a decrease of ITGA4-GFP-positive cells became evident over the observation period. ITGA4-GFP-signals were distributed across the cell body, but were dim in the majority of the MSC. TRE-driven transgene expression initially led to clear and bright ITGA4-GFP-signals (Fig. 21A, TRE-ITGA4, Day 4). Moreover, numerous cells showed a round, condensed morphology or were detached. A very bright ITGA4-GFP-signal was localized in perinuclear regions in adherent cells. Over the time course of 20 days, a constant downregulation of transgene was observed in MSC infected with TRE-ITGA4.

Further evaluation of transgene expression was conducted by flow cytometry at day 8 and day 20 after transduction. Measurement of GFP-positive cells was performed with unstained and vital MSC. Only 4% of ITGA4-GFP-positive cells were detected for UbC-constructs (Fig. 21B, 8d and 20d), while a significant increase of positive cells up to 80% was apparent under control of TRE. Furthermore, 35% of MSC were positive for ITGA4-GFP after modification with EF1α-driven construct and 68% for CMV-driven construct (Fig. 21B, 8d). Except for UbC, a decline of ITGA4-GFP-positive MSC was noticed at day 20 after infection. No differences regarding the mean fluorescence intensity of ITGA4-GFP-positive cells were detected between UbC-, EF1α-, and CMV-constructs. Only protein expression under TRE increased fluorescence intensity significantly to reference groups at day 8 after infection (Fig. 21C, day 8). Of note, control cells (naïve MSC and Polybrene®-treated MSC) were also measured, but no GFP-positive cells were detected.

In addition to flow cytometry, protein expression was analyzed by Western Blot. Expected molecular weights were observed for cleaved and full length ITGA4+GFP (Fig. 22B; 100kDA/170kDa). Furthermore, subsequent reduction of transgene protein expression over observation period was confirmed by Western Blot (Fig. 22). In particular, a profound downregulation was observed under CMV- and TRE-control for ITGA4-GFP (Fig. 22A). Protein expression patterns were found to be approved for each promoter. Promoter-dependent magnitude of ITGA4-GFP expression was similar to previous experiments and

confirmed the rather weak protein expression under UbC and the intensified expression under the TRE-promoter (Fig. 22).

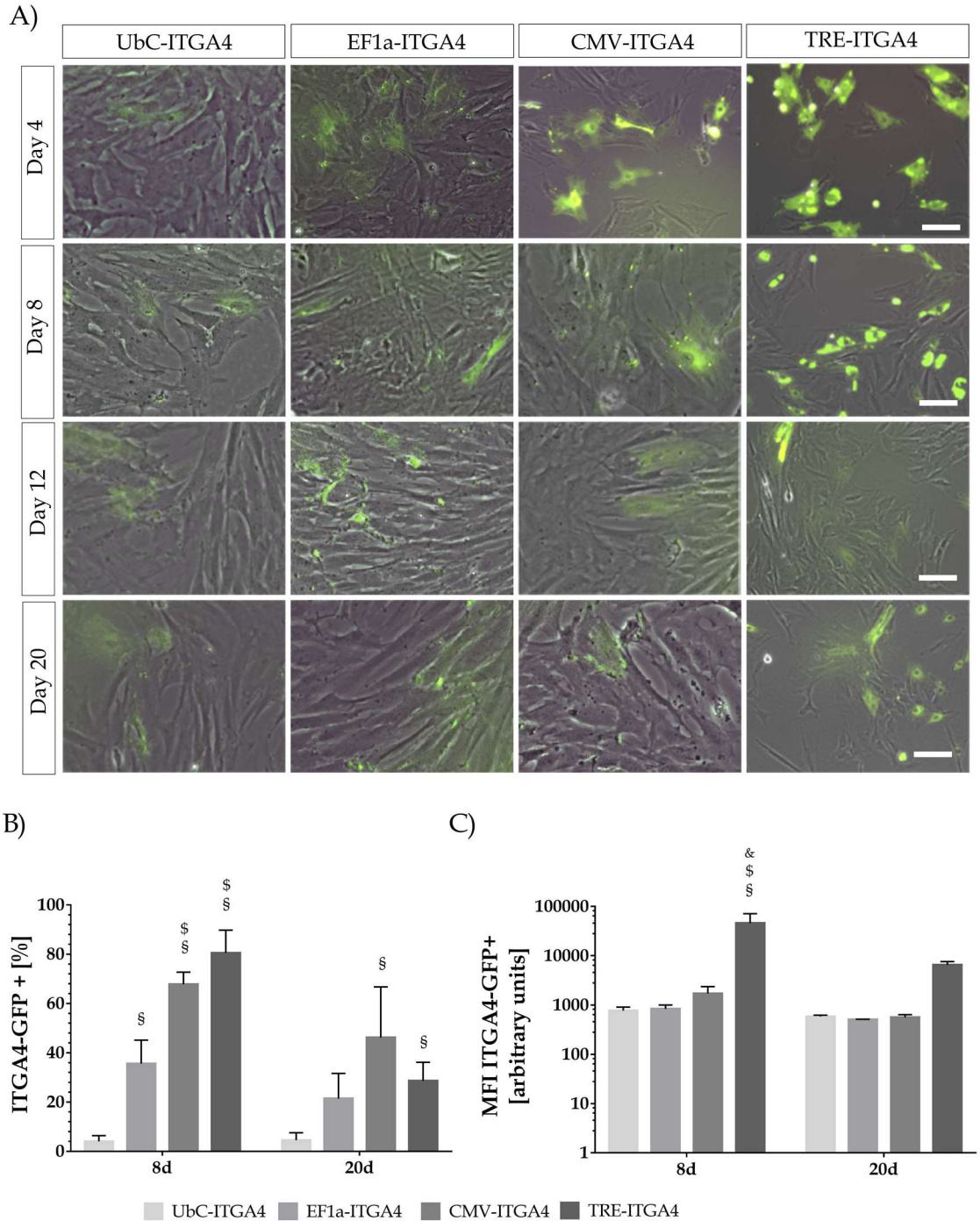


***Fig. 21 Evaluation of transgene expression of MSC infected with UbC-, EF1a-, CMV-, or TRE-ITGA4 tagged with GFP.*** *Representative fluorescence micrographs are given for day 4, 8, 12, and 20 after infection (A). Green signals were derived from expression of ITGA4-GFP fusion protein. Scale bar indicates 10µm. Flow cytometry analysis of MSC after infection with ITGA4-GFP under control of UbC-, EF1a-, CMV-, or TRE promoters. Quantitation of GFP-positive cells showed expression of the transgene (B). MFI of GFP-positive cells was also found to be influenced by promoter (C). Data are given as mean ± SD of 3 independent biological replicates (n=3). Statistical differences were calculated by two-way ANOVA with Tukey´s post hoc multiple comparison (p < 0.05, * vs. CTRL, # vs. PB-CTRL, § vs. UbC, $ vs. EF1a, & vs. CMV).*

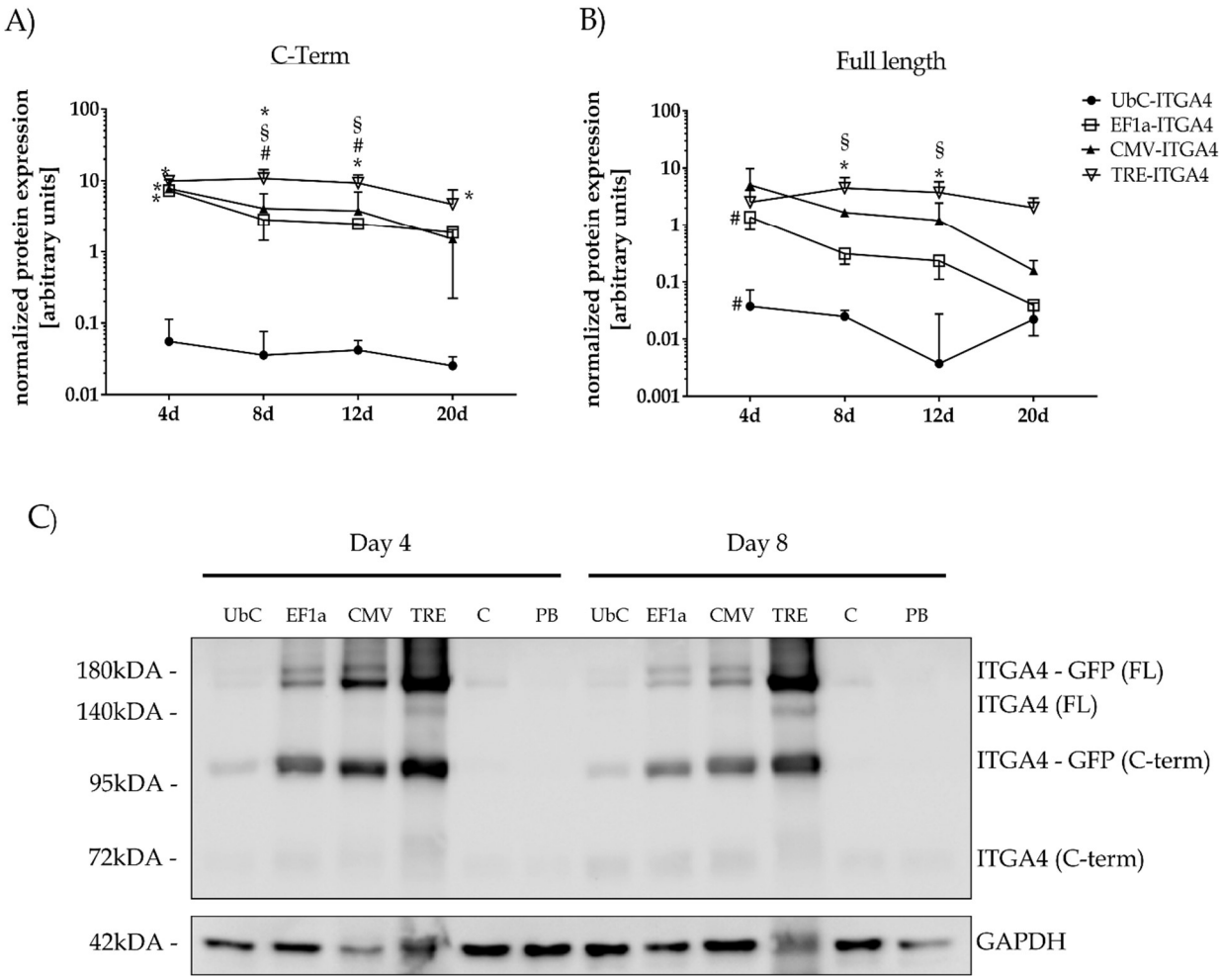


***Fig. 22 Western Blot analysis of MSC after infection with ITGA4-GFP.*** *Semiquantitative analysis of ITGA4-GFP expression was conducted for cleaved C-Terminus (A) and for full length protein (B) and normalized to GAPDH expression. Transgene expression pattern was different depending on the choice of promoter (UbC, EF1a, CMV, TRE). Data are represented as mean ± SD from 3 independent biological replicates (n=3). Statistical differences were calculated by two-way ANOVA with Tukey´s post hoc multiple comparison ($p < 0.05$, * vs. UbC-ITGA4, # vs. CMV-ITGA4, § vs. EF1a-ITGA4). A representative Western Blot is given for ITGA4-GFP samples collected at day 4 and day 8 after lentiviral infection (C). Molecular weights were visualized at 100kDa for cleaved, c-terminal ITGA4-GFP (C-term), at 170kDa for full length ITGA4-GFP (FL), and at 40kDa for GAPDH. No ITGA4-GFP was detected in native MSC (C) or Polybrene®-treated MSC (PB).*

### 4.2.2 Copy numbers

To evaluate the genomic copy number for ITGA4, gDNA samples were taken at day 8 and day 20 after infection with the lentiviral particles and analyzed by qPCR.

The results in Fig. 23 represent the copy numbers for ITGA4 normalized to GAPDH and to the Polybrene®-treated control group (PB-CTRL). Increased copy numbers were found for UbC-ITGA4, EF1α-ITGA4, CMV-ITGA4, and TRE-ITGA4 compared to native controls (CTRL) and PB-CTRL. However, significant differences were only found for CMV constructs, which led to a relative 30-fold increase compared to PB-CTRL. In contrast, relative copy numbers for UbC- construct was tripled. ITGA4 copy number were found at similar levels

after lentiviral infection with EF1a- and TRE- driven construct (Fig. 23, 12.5 for EF1a-ITGA4, 13.5 for TRE-ITGA4 at day 8). Interestingly, copy numbers decreased over the observation period, but determined promoter-dependent proportions were maintained.

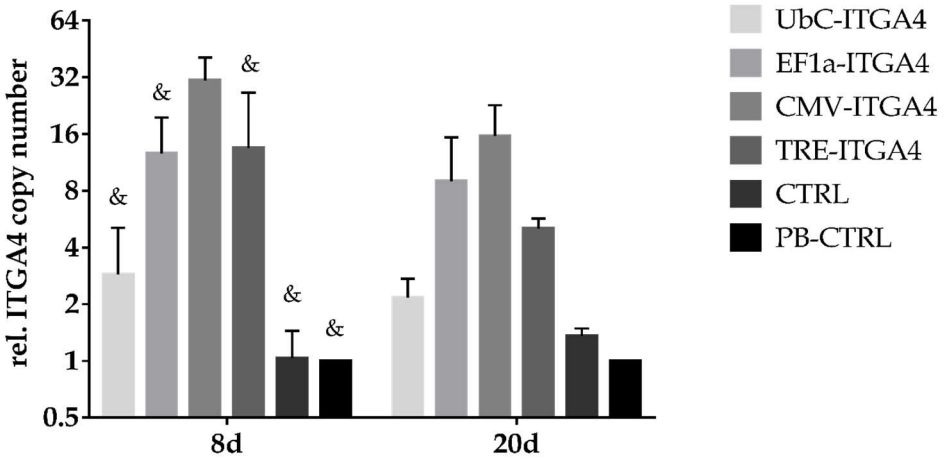


***Fig. 23 Copy number determination at day 8 and day 20 after lentiviral infection of MSC.*** *qPCR was conducted with gDNA samples of each cell line ad normalized to GAPDH and PB-CTRL. Copy numbers were massively increased after infection with EF1a-, CMV-, or TRE-driven constructs. Data are represented as mean ± SD from 3 independent biological replicates (n=3). Statistical differences were calculated by two-way ANOVA with Tukey´s post hoc multiple comparison ($p < 0.05$, & vs. CMV-ITGA4).*

### 4.2.3 Characterization of MSC overexpressing ITGA4-GFP under control of various promoters

Lentiviral transduction and overexpression of a certain transgene can impact characteristics and growth kinetics. Thus, lentivirally transduced MSC were further analyzed in terms of proliferation and viability.

#### 4.2.3.1 Growth curves and population doubling time

Proliferation of lentivirally transduced MSC was evaluated by their growth kinetic and population doubling time. After seeding, a constant increase of cell numbers was observed for all MSC lines. MSC that were transfected with TRE-ITGA4 construct showed significantly decelerated growth during the second half of the observation period (Fig. 24A). CMV-ITGA transduced MSC decreased their proliferation between day 10 and 12 after seeding. Cell numbers were significantly lower compared to Polybrene®-treated MSC and UbC-treated MSC (Fig. 24A). Growth kinetic of remaining MSC lines were similar to controls, although slightly lower in numbers.

PDT was not affected by lentiviral transduction and ranged between 1.7 to 2.1 days (Fig. 24B) except for MSC transduced with TRE-constructs. TRE-ITGA4-MSC increased their population doubling time to 9-12 days (Fig. 24B).

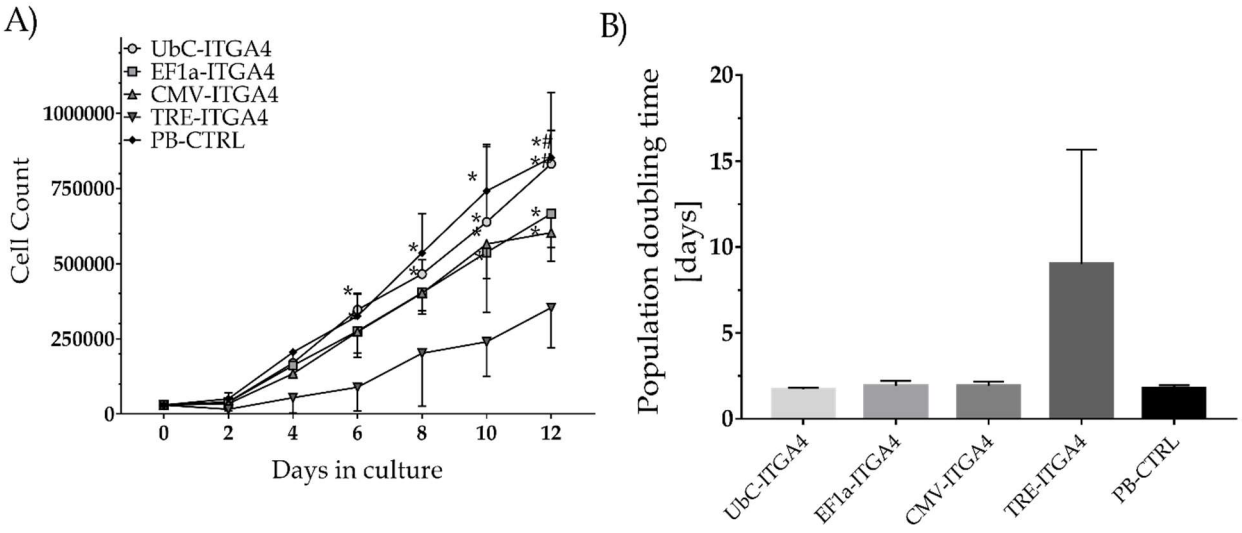


***Fig. 24 Growth characteristics of MSC overexpressing ITGA4 under the control UbC-, EF1a-, CMV-, or TRE-promoter and controls***. *Growth curves were determined after lentiviral transfection of ITGA4 (A). Population doubling times are given for ITGA4-overexpressing MSC (B). Data are represented as mean ± SD from three biological replicates (n=3). Statistics were carried out using two-way ANOVA (A and C) or one-way ANOVA (B and D) with Tukey´s post hoc multiple comparison (p < 0.05, * vs. TRE; # vs. CMV).*

#### 4.2.3.2 Cell viability

Fig. 25 shows cell viability of modified MSC and controls. Viability of CMV-ITGA-MSC was slightly affected after lentiviral transduction. This was persistent until day 8. Thereafter, these MSC lines seemed to recover and showed no longer differences to controls. Infection with TRE-ITGA4 significantly reduced viability compared to controls at day 4 and day 20 after lentiviral infection. No differences were detected between UbC-ITGA4, EF1α-ITGA4 and controls.

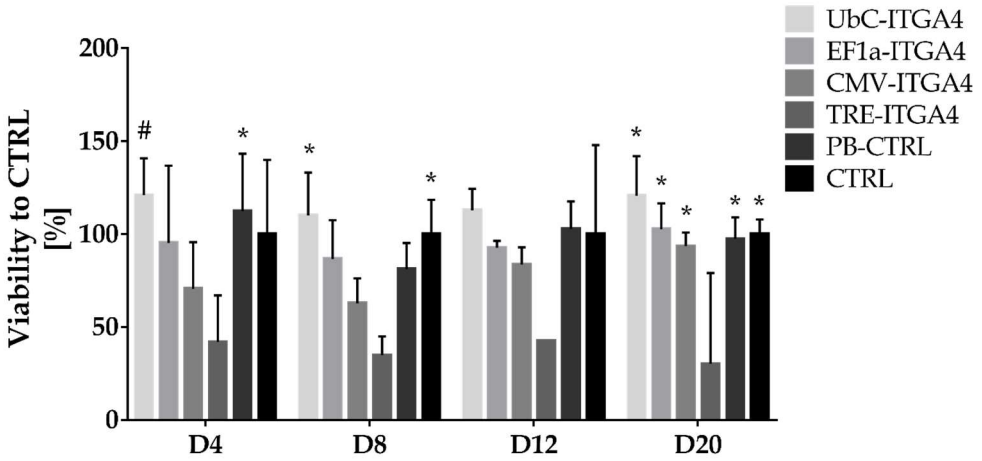


***Fig. 25 Viability of CTRL and lentivirally infected MSC.*** *Absorbance (optical density, OD) was determined after reduction of MTT and normalized to viability of CTRL. Data are represented as mean ± SD of 3 independent biological trials (n=3). Statistics were performed using two-way ANOVA with Tukey´s post hoc multiple comparison (p < 0.05, * vs. TRE, # vs. CMV).*

### 4.2.4 *In vitro* migration of EF1α-ITGA4-MSC

Assessment of lentivirally modified MSC included the evaluation of transmigratory activity. Migration of MSC infected with EF1α-ITGA4-GFP was compared against control in a FluoroBlok Boyden chamber setup (Fig. 26). No differences were observed between infected MSC and controls.

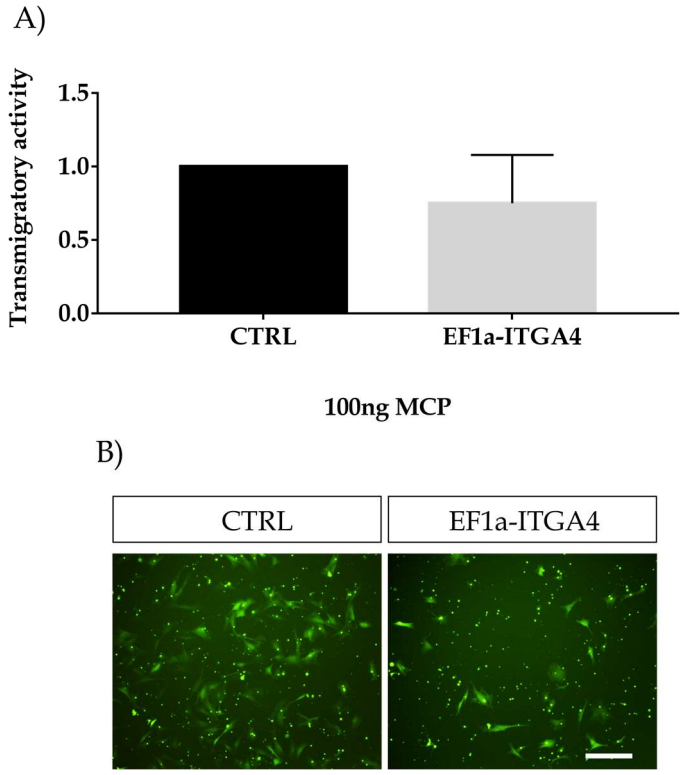


***Fig. 26 Transmigratory activity of EF1a-ITGA4-MSC and CRL-MSC.*** *CTRL-MSC and MSC overexpressing ITGA4 were seeded onto a TNFa-stimulated GPNT cells in a FluoroBlok transwell migration system (pore size of 8µm). Transmigratory activity was assessed after application of MCP1 and an overnight incubation by inversed fluorescence microcopy. (A) Transmigration activity was determined by semi-quantitative analysis and normalization to CTRL. Data are represented as mean ± SD of 3 independent biological trials (n=3). Statistics were conducted using one-way ANOVA with Tukey´s post hoc multiple comparison. (B) Representative fluorescence images, showing migrated MSC, were taken from the bottom side of the FluoroBlok transwell insert. Scale bar indicates 100µm.*

## 4.3 Enhancing homing of MSC towards cerebral ischemia

### 4.3.1 Transgene expression after lentiviral infection

Overexpression of ITGA4 and CCRR2 was achieved using lentiviral vectors generated with respective transfer plasmids. Since transduction efficiency was low for ITGA4 + tdTomato and CCR2 + tdTomato (3-8%, Fig. 27), MSC were sorted based on IRES-coupled fluorescence reporter expression (tdTomato). CTRL-MSC, transduced with tdTomato alone, showed much higher transgene expression. Nonetheless, they underwent the same sorting procedure. Fluorescence intensity of tdTomato was heterogeneous in all groups.

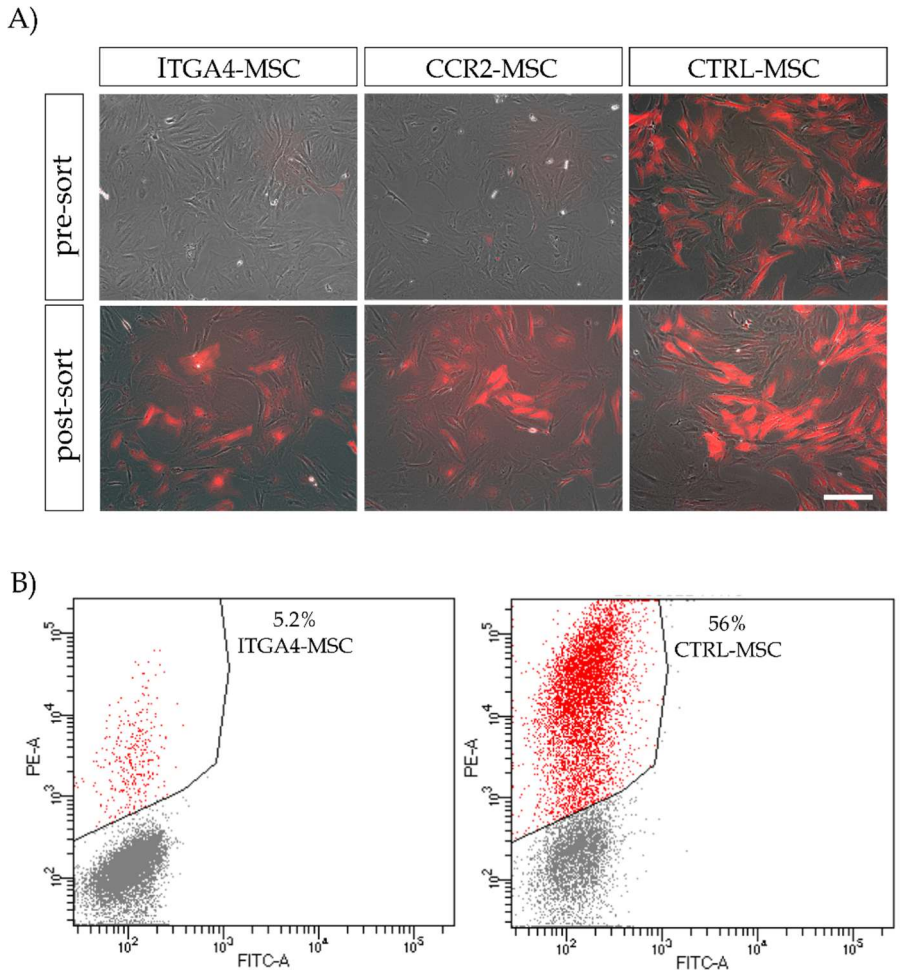


***Fig. 27 Lentiviral modification of MSC with ITGA4 +tdTomato(ITGA4-MSC), CCR2 + tdTomato (CCR2-MSC), and tdTomato alone (CTRL-MSC).*** *Fluorescence microphotographs taken 4-5d after lentiviral transduction (pre-sort) and after cell sorting (post-sort). Scale bar indicates 50µm. Cell sorting was conducted with flow cytometry based on the detection of the red-fluorescent reporter tdTomato. Representative dot blots recorded during sorting are given for ITGA4-MSC and CTRL-MSC (B).*

After sorting, MSC were analyzed by qPCR for their CCR2-, ITGA4-, and ITGB1-mRNA expression. As shown in Fig. 28, CTRL-MSC were expressing CCR2 and ITGA in inherently

low levels (0.26AU for CCR2, 0.6AU for ITGA4). Lentiviral infection and sorting led to enrichment of MSC with significantly higher mRNA-level for either CCR2 (Fig. 28A; 122.5AU for CCR2-MSC) or ITGA4 (Fig. 28B; 14.6AU for ITGA4-MSC). A constitutive expression (~2-3AU) was determined independently from infection for ITGB1 mRNA.

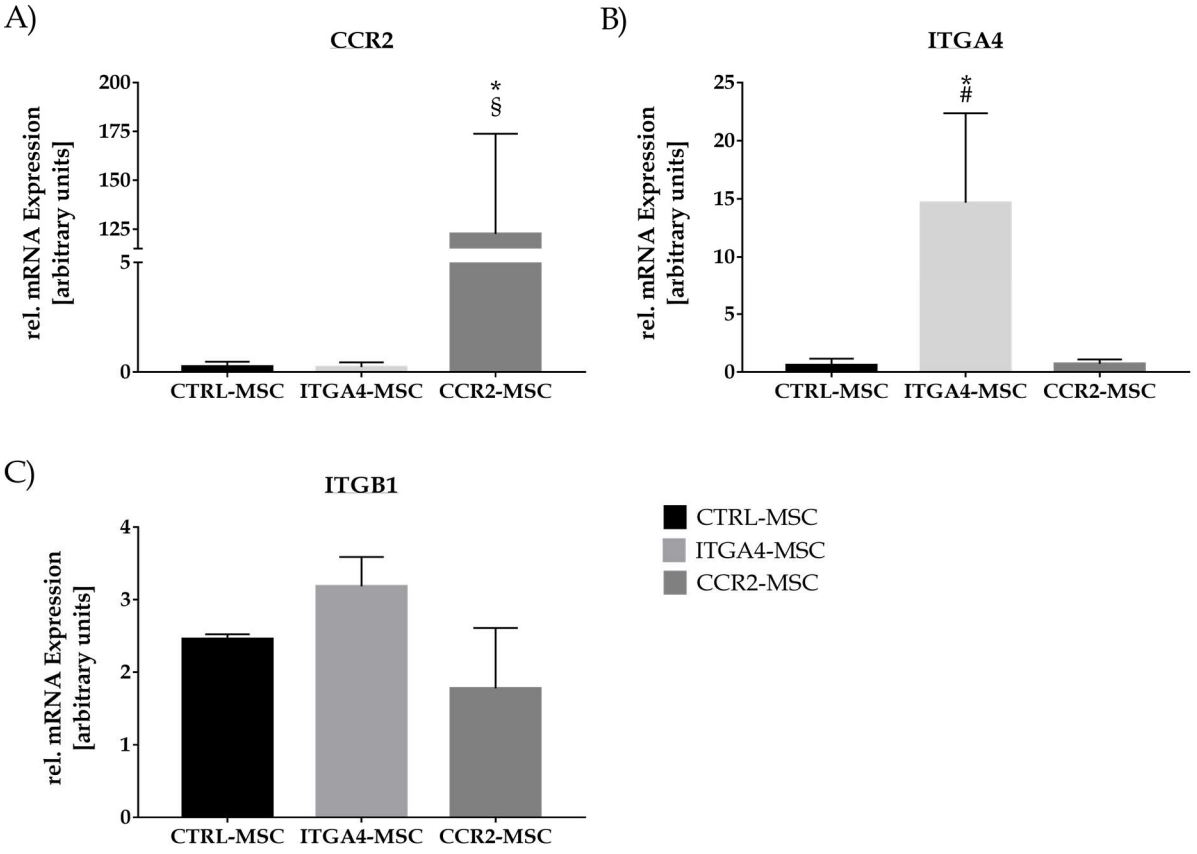


***Fig. 28 mRNA expression of CCR2 (A), ITGA4 (B) and ITGB1 (C) after lentiviral infection and sorting of MSC.*** *The diagrams show relative (transgene) mRNA expression normalized the expression of the housekeeping gene ACTB. Data are represented as mean ± SD (n=3). Statistical differences were calculated by one-way ANOVA with Tukey´s post hoc multiple comparison ($p < 0.05$, * vs. CTRL-MSC, § vs. ITGA4-MSC, # vs. CCR2-MSC).*

In order to verify correct transgene protein expression after lentiviral infection and sorting, immunofluorescence staining with specific antibodies and Western Blot were conducted.

ITGA4-MSC were positive for the desired protein (Fig. 29A). Moreover, ITGA4 was expressed throughout the cell soma and was also localized in processes. In addition, red fluorescence of tdTomato was observed by fluorescence microscopy. As confirmed by Western Blot, overexpressed ITGA4-transgene showed expected molecular weight at 140kDa and 70kDa (Fig. 29C). Respective controls, solely infected with the fluorescence reporter, showed only minor ITGA4 expression (Fig. 29A and C, CTRL-MSC).

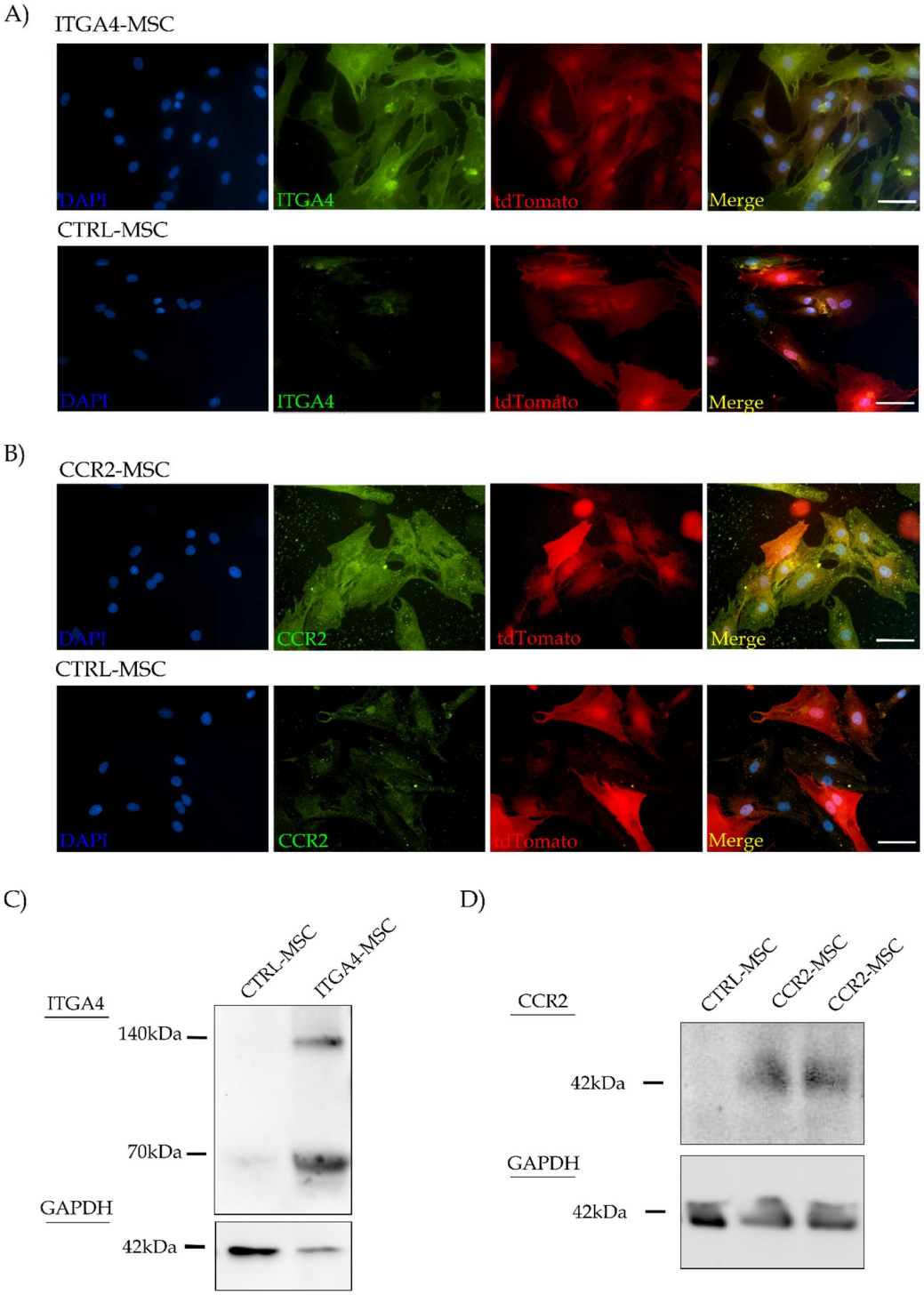


***Fig. 29 Overexpression of ITGA4 on MSC**. Representative immunofluorescence images are given for MSC transduced with ITGA4 (A) and for CTRL-MSC (B.) Expression of ITGA4 protein (green) was enhanced for ITGA4-MSC. TdTomato, serving as reporter protein, was detected by its red fluorescence. Nuclei were stained utilizing DAPI (blue). Scale bars indicate 50µm. Correct size and protein expression was also verified from lysates of CTRL-MSC and ITGA4-MSC by Western Blot (C). Protein bands for ITGA4 (140kDa and 70kDa) and for the housekeeping protein GAPDH (40kDa) were visualized with a chemiluminescence reaction.*

CCR2-MSC showed enhanced signals for CCR2 as observed after immunofluorescence staining (Fig. 29B). The membranous CCR2 receptor appeared in clusters as indicated by dotted signals distributed evenly over the cell body. Expression of tdTomato reporter was observed in parallel. In contrast, controls infected with tdTomato only showed weak

fluorescence signals for CCR2 (Fig. 29B). Furthermore, it was possible to visualize a 42kDa band from CCR2-MSC lysates by Western Blot (Fig. 29D).

### 4.3.2 Growth profiling after stable modification of MSC with ITGA4 or CCR2

MSC were evaluated by microscopic observations and growth kinetics. MSC showed a spindle-shaped morphology as already described by Pittenger et al. (Pittenger et al. 1999). Long and thin processes were observed along with a large nucleus (Fig. 30). With increasing confluency of the cell monolayer, MSC began to arrange in parallel creating a twirl-like formation. Their phenotype was not affected after lentiviral transduction and cell sorting.

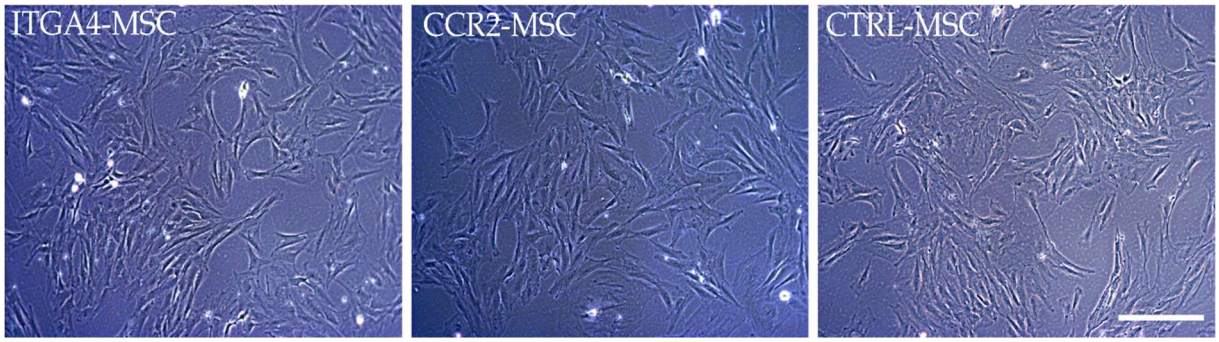


***Fig. 30 Phenotypic characterization of MSC after lentiviral modification*** *with ITGA4 (ITGA4-MSC, top left) or CCR2 (CCR2-MSC, top right) and CTRL (CTRL-MSC, bottom row) using light microscopy. All MSC exhibited spindle-shaped or fibroblast-like morphology and formation. Scale bar indicates 100µm.*

As determined by growth curves, MSC showed robust proliferation during the subconfluent stage (Fig. 31A). With increasing confluence and declining availability of space, proliferation decreased and entered a plateau between day 6 and 8 after seeding. Thus, a saturation density of 2.2 x $10^4$ cells/$cm^2$ was determined (2.3 x $10^4$ cells/$cm^2$ for ITGA4-MSC, 2.2 x $10^4$ cells/$cm^2$ for ITGA4-MSC, 2.1 x $10^4$ cells/$cm^2$ for CTRL-MSC). No significant proliferation differences were detected between the cell lines.

Population doublings were determined at passage 7. As illustrated in Fig. 31B, a steadily increase of population doubling was observed until day 8. By day 4, MSC had undergone approximately 5.5 population doublings (5,36 ± 0.47 for CTRL-MSC, 5.05 ± 0.35 for ITGA4-MSC, 6.16 ± 0.73 for CCR2-MSC). Beyond day 8, MSC showed no longer proliferation. Statistical differences were not observed between ITGA4-MSC, CCR2-MSC and controls. Furthermore, the population doubling time (PDT) was maintained in subconfluent stage between 1.9 to 2.2 days (Fig. 31C). However, growth profile of ITGA4-MSC or CCR2-MSC was not altered in comparison to CTRL-MSC and no significant differences were observed for PDT.

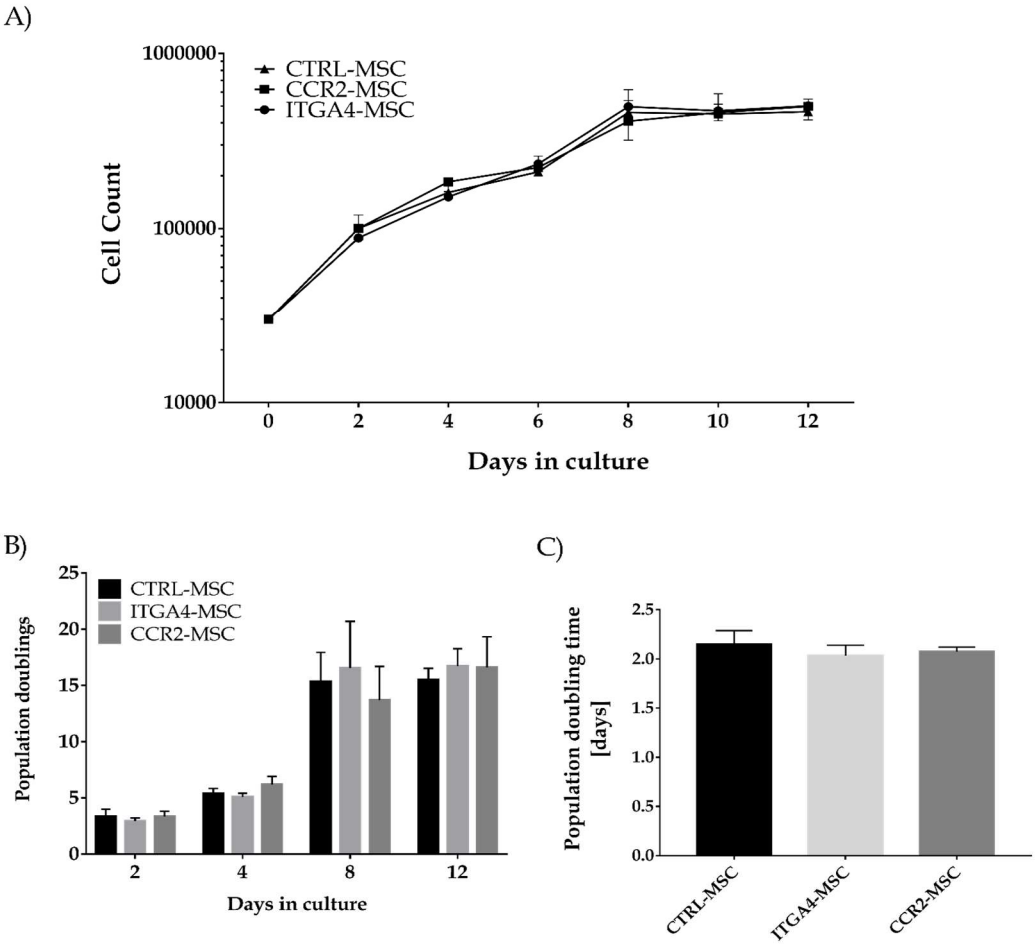


***Fig. 31 Growth characteristics of ITGA4-MSC, CCR2-MSC and CTRL-MSC*** *determined at passage 7. Growth curves (A), population doublings (B), and population doubling times (C) are given for each cell population. Date are represented as mean ± SD from at least three biological replicates (n=3). Statistics were carried out using two-way ANOVA (A, B) or one-way ANOVA (C) with Tukey´s post hoc multiple comparison.*

### 4.3.3 Maintenance of trilineage differentiation potential

Multipotency is a key feature of MSC and indicates their stemness. Thus, it had to be confirmed that MSC, used in this study, showed multipotent differentiation potential. Spontaneous differentiation during propagation of stably modified MSC and CTRLs was not observed. Therefore, MSC were subjected to culture conditions favoring either adipogenic, osteogenic or chondrogenic differentiation.

Differentiation into adipogenic phenotypes was verified by immunocytochemical detection of FABP4 (Fig. 32, top row). Adipogenesis was also accompanied with generation of lipid-rich vacuoles causing porous appearance of the cytoplasm (Fig. 32, upper row, white arrowheads). Osteocalcin indicated osteogenic differentiation of MSC (Fig. 32, middle row). Conditions favoring chondrogenic differentiation led to generation of aggrecan within 20 days (Fig. 32, bottom row). Of note, the lentivirally driven overexpression of ITGA4, CCR2 or fluorescent reporter protein did not affect the multilineage differentiation potential of MSC. Differentiation time window as well as immunoreactivity of respective lineage marker protein appeared similar as observed in controls.

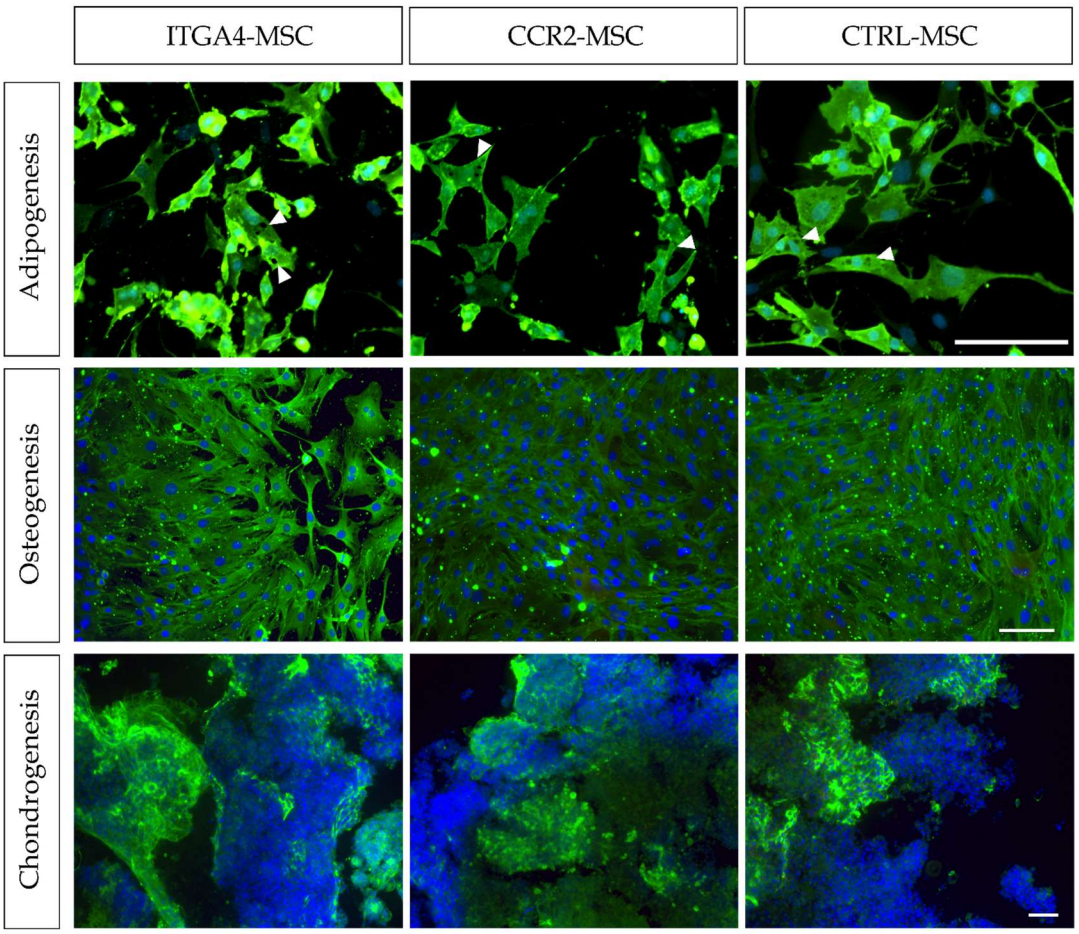


***Fig. 32 Differentiation of MSC.*** *Adipogenesis (upper row) was verified by detection of FABP4 (green channel) within 10 d after induction of adipogenesis. Arrowheads indicate hypointense areas caused by lipid vacuoles. Osteogenesis (middle row) was associated with osteocalcin appearance (green channel) within 10d. Formation of aggrecan (green channel, bottom row) proved chondrogenesis. The nuclei were visualized with DAPI stain (blue channel). Scale bars indicate 100µm.*

### 4.3.4 *In vitro* characterization of transmigration

An *in vitro* co-cultivation approach was established in a modified Boyden chamber setup to examine the transmigration capacity of MSC and the influence of ITGA4-/CCR2-overexpression. To this end, the rat brain endothelial cell line GPNT was grown to a confluent monolayer onto a collagen IV coated transwell migration chamber. ITGA4-MSC, CCR2-MSC or CTRL-MSC were added to the upper chamber and migration was evaluated towards an MCP1 gradient.

#### 4.3.4.1 Transmigratory activity across endothelial barrier

The migratory activity of CTRL-MSC and MSC overexpressing ITGA4 or CCR2 was assessed in a FluoroBlok Boyden chamber setup over an GPNT monolayer in the presence of MCP1. As illustrated in Fig. 33, migratory activity increased with augmenting MCP1 concentration in all groups. However, minor migration was observed without MCP1 addition (Fig. 33, A and B, without MCP1).

MSC overexpressing ITGA4 showed significantly increased transmigratory activity over the endothelial monolayer in the presence of 50ng and 100ng MCP as compared to CTRL-MSC (Fig. 33A and B, middle row). Furthermore, transmigratory activity was significantly enhanced in comparison to CCR2-MSC at all applied MCP1 concentrations.

In contrast, overexpression of CCR2 did not induce enhanced transmigration. Surprisingly, CCR2-MSC even showed the trend ($0.05 \leq p \leq 0.13$) for reduced transmigratory activity compared to CTRL-MSC (Fig. 33, A and B, bottom row). This observation is particularly interesting since CCR2 is the respective receptor for MCP1.

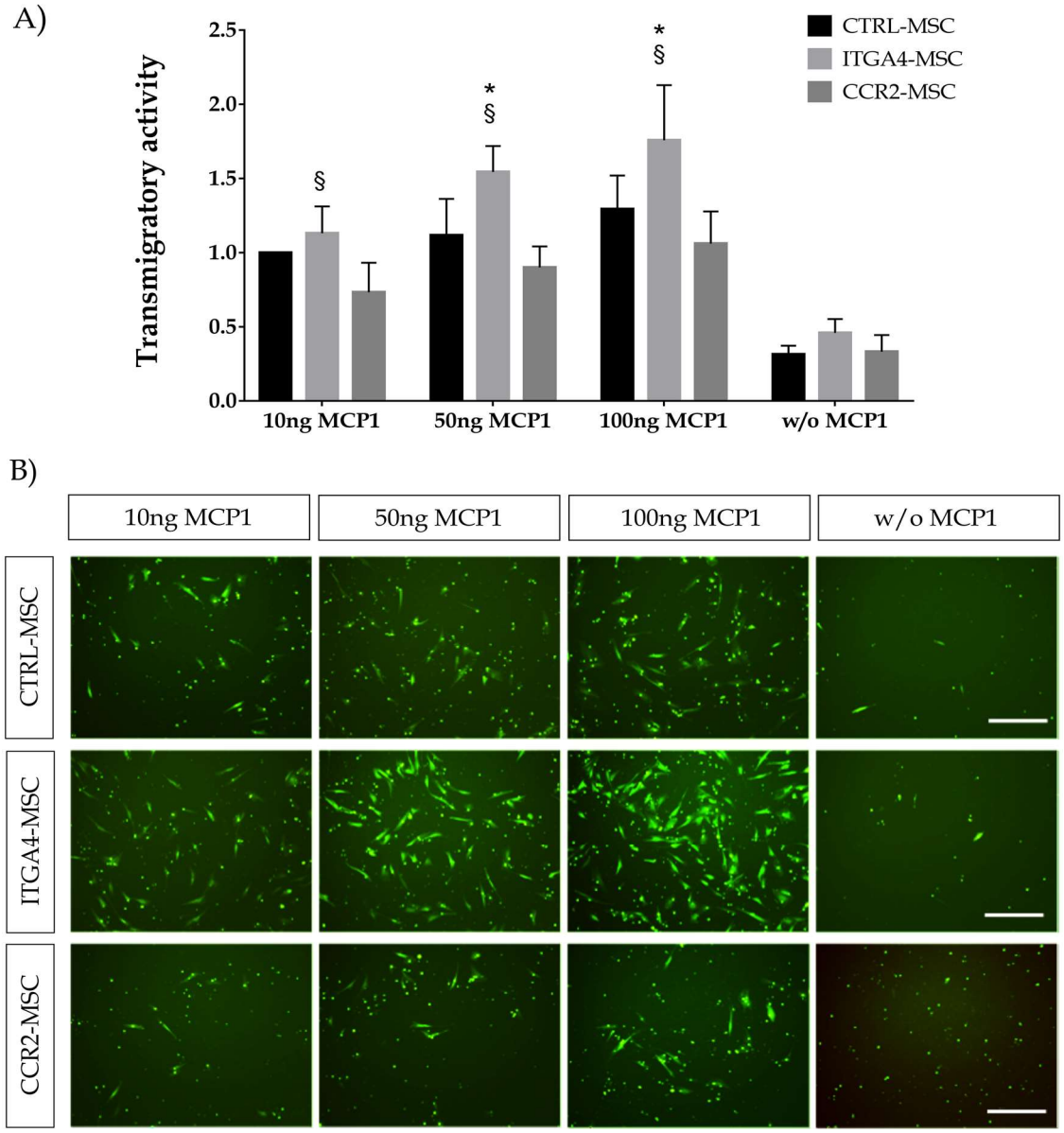


***Fig. 33 Transmigratory activity of MSC in the FluoroBlok Boyden chamber.*** *CTRLs and MSC overexpressing ITGA4 or CCR2 were seeded onto a TNFa-stimulated GPNT cells in a FluoroBlok transwell migration system with a pore size of 8µm. Transmigratory activity was assessed after application of MCP1 and overnight incubation by inversed fluorescence microcopy. (A)Transmigration activity was determined by semi-quantitative analysis and normalization to CTRL/10ng MCP1. Data are represented as mean ± SD of 6 independent biological trials (n=6). Statistical differences are calculated by Two-way ANOVA with Tukey´s post hoc multiple comparison ($p < 0.05$, * vs. CTRL, § vs. CCR2-MSC). (B) Representative fluorescence images, showing migrated MSC, were taken from the bottom side of the FluoroBlok transwell insert. Fluorescence signals through/within a pore appeared as green dots. Scale bars indicate 100µm.*

#### 4.3.4.2 Classification of migrating MSC

Further co-cultivation experiments, using the GPNT cell line in a classical Boyden chamber setup, were conducted to determine differences regarding the interaction with the endothelium between experimental groups. After confocal fluorescence imaging, MSC were calculated and categorized regarding their localization (Fig. 34). It was distinguished between non-migrated (category i-iv) and migrated (category v) MSC. The MSC-morphology was also taken into consideration. Furthermore, it was differentiated, if the MSC was completely localized within the pore or only with processes or podia (Fig. 34F-H).

Interestingly, no significant differences were found regarding the amount of non-migrated MSC, albeit numbers of ITGA4-MSC appeared increased (Fig. 35A). No differences were found between numbers of MSC located within the pore of the insert (Fig. 35A-pore; Fig. 35B category (v)a, (v)b; and (v)c). Similar to FluoroBlok experiments, significantly higher number of MSC were found for ITGA4- compared to CTRL-MSC and to CCR2-MSC (Fig. 35A and B (vi), migrated).

Detailed analysis of localization and shape of MSC are illustrated in Fig. 35B. No differences were determined between non-migrated MSC, as indicated by similar levels of obtained counts. However, amount of ITGA4-MSC appeared higher in category (i). In general, most of the non-migrated MSC were either found with a flattened phenotype above the endothelial monolayer (category ii), below the endothelial monolayer/above the mesh (category iii) or integrated within the endothelial cells (category iv). Only a few cells were present with a spherical shape, above the GPNT layer (category i). Also, analysis of cells localized within the pore revealed no statistical differences.

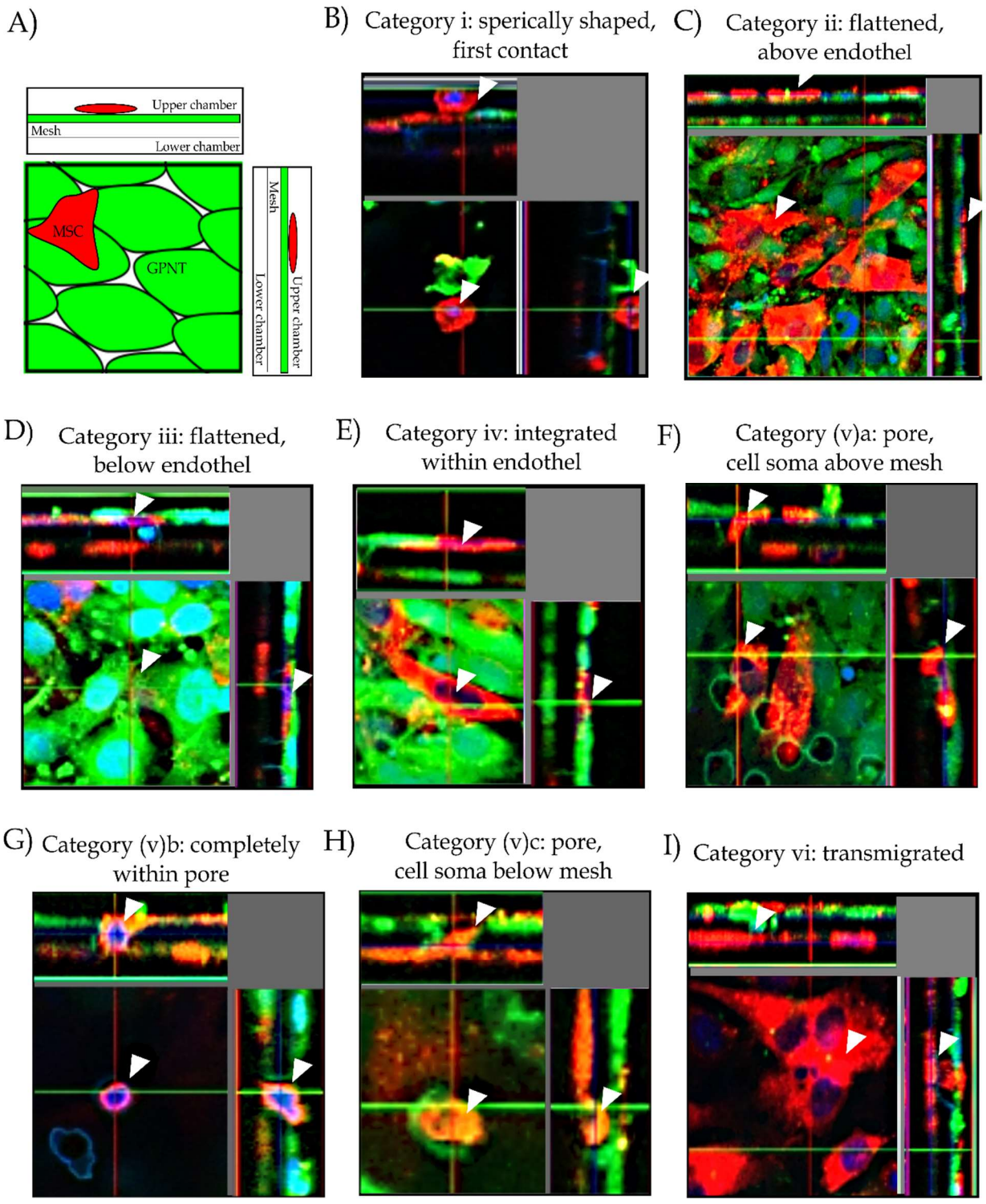


***Fig. 34 Classification of migrating MSC.*** *Confocal imaging allowed classification of MSC dependent on their localization. A schematic overview is given in (A). Vertical sections of z-stack are shown above and at the right side of chosen photograph. Representative confocal images are given for ITGA4-MSC in (B-I) and are shown in orthographical view. MSC (red) were distinguished according to their shape and position to endothelial monolayer (GPNT, green). Categories i-iv indicate MSC that did not migrate or did not complete the transmigration process. MSC localized within a mesh-pore were considered as category v. Migrated MSC were assigned to category vi. Respective MSC were are highlighted with arrow heads.*

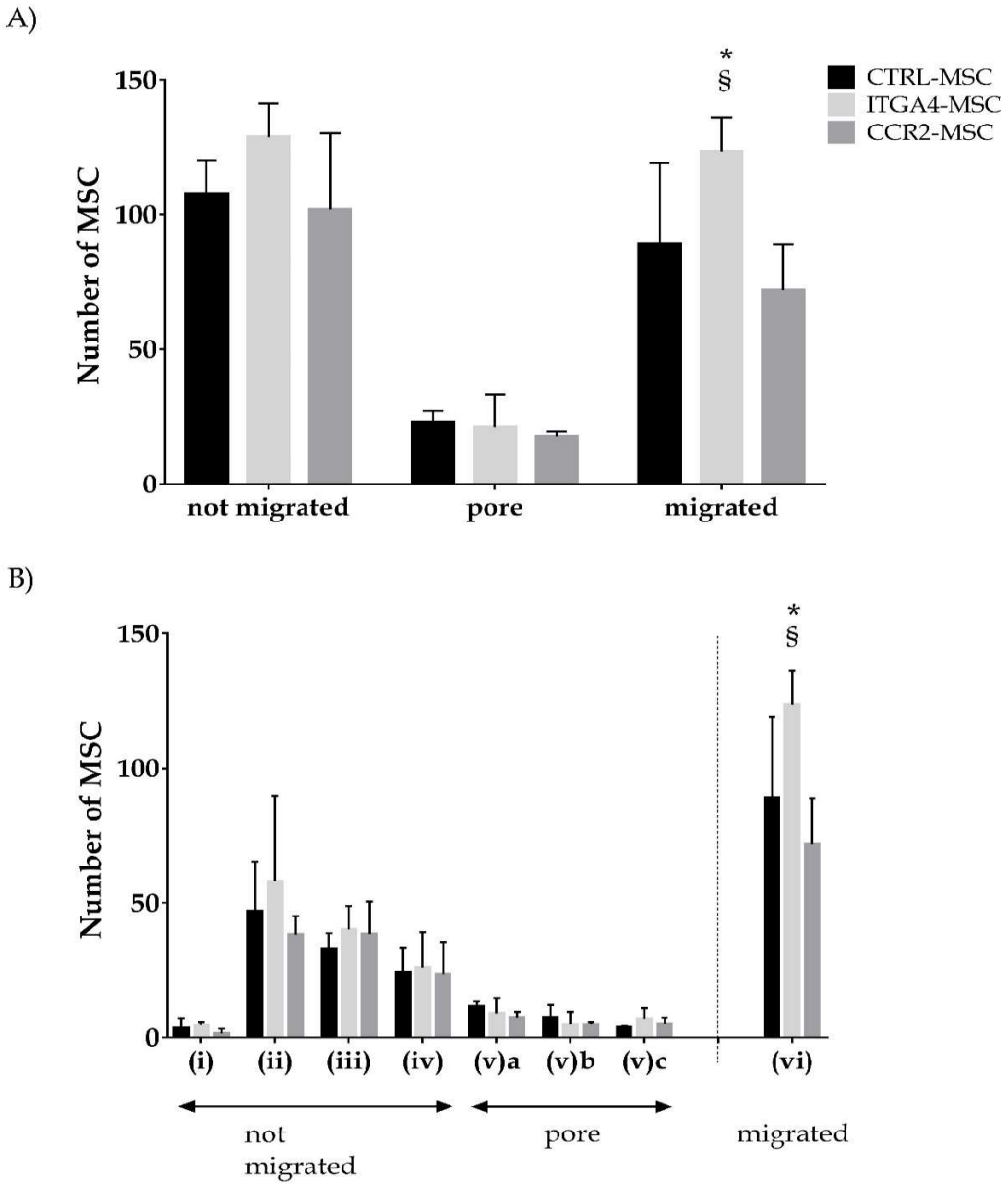


***Fig. 35 Categorization of transmigration of CTRLs and modified MSC.*** *(A) Quantification of MSC was based on their detection above the mesh (not migrated), within a pore, or below the mesh (migrated). (B) Detailed analysis after confocal fluorescence microscopy allowed exact localization and distribution in categories: (i) spherically shaped MSC, first contact; (ii) flattened MSC on endothelium, (iii) flattened MSC under endothelium, (iv) integrated in endothelial monolayer, (v) within the pore, and (vi) migrated MSC visible at bottom part of transwell mesh. Localization within the pore was further distinguished between appearance of processes in pore, cell body above mesh (v)a, cell body within pore (v)b, and appearance of processes in pore, cell body below mesh (v)c. Data are represented as mean ± SD of 3-4 independent biological replicates (n=3-4). Statistical differences were determined using two-way ANOVA with Tukey´s post hoc multiple comparison ($p < 0.05$, * vs. CTRL, § vs. CCR2).*

### 4.3.5 *In vivo* homing of modified MSC

In addition to *in vitro* migration, homing of modified and control MSC towards cerebral ischemia was evaluated by SPECT/CT imaging, gamma counting, and immunohistochemistry after intra-arterial transplantation.

#### 4.3.5.1 Mortality and evaluation of cerebral lesion

In the course of this study, 21 Wistar rats underwent a 120min transient MCAO. All animals survived this intervention. Animals received a transplantation of 0.5 million $^{111}$In-labelled MSC into the external carotid artery 24h after induction of cerebral ischemia and were investigated by SPECT/CT imaging. Two animals died during the imaging 1h after transplantation.

Localization of the lesion was verified by MRI 24h after MCAO and directly before cell transplantation. Transient occlusion of the MCA led to an infarction of the ipsilateral cortex and striatum (Fig. 36A). Only one animal was excluded due to minor cerebral lesion (Fig. 36B). Sham animals did not show any cerebral lesions (Fig. 36C).

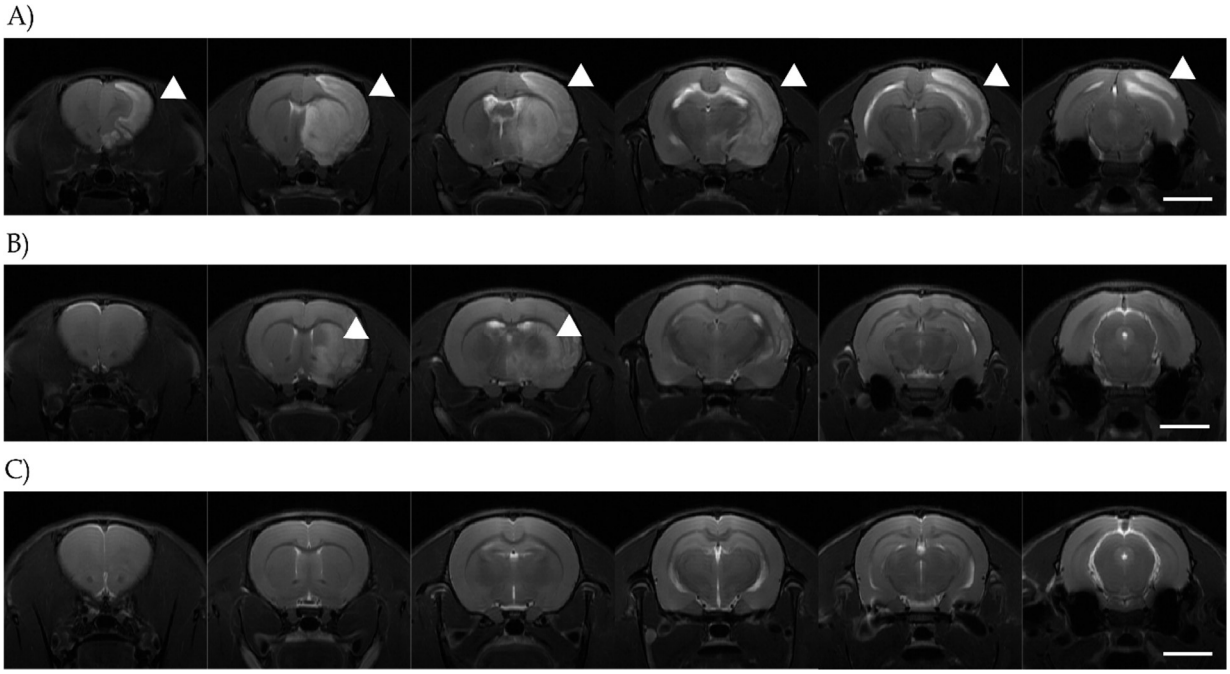


***Fig. 36 Representative MR images*** *given for a MCAO animal (A) and a sham-operated animal (C) 24h after induction of cerebral ischemia. The example for exclusion due to minor lesion is given in (B). Healthy brain tissue appears hypointense, while lesioned areas (marked with white arrowheads) and ventricles were hyperintense. Scale bars indicate10mm.*

#### 4.3.5.2 SPECT/CT-Imaging

Homing, enrichment and clearance of intra-arterially transplanted MSC was followed by SPECT/CT imaging over a time course of 48h.

MSC were labelled with $^{111}$In-oxine prior to transplantation. An average cell viability of 85% was determined after the labelling procedure. A mean $^{111}$In dose of 0.03 Bq/cell was applied and the labeling efficiency was ~65%.

A considerable amount of cells was found within the facial soft tissue and outside of the skull in most of the animals (Fig. 37A). This insufficient delivery to the brain resulted in inconsistent starting situation and varying data (table 6). This phenomenon was observed in both, SHAM and MCAO animals.

To compensate for this situation, data were normalized to baseline measurement obtained from ipsilateral hemisphere shortly after transplantation (Fig. 37B). After 24h, MCAO+CCR2-MSC showed significantly enhanced activity in the ipsilateral hemisphere compared to Sham + CTRL-MSC. Clearance of transplanted MSC was apparent from each hemishere and from the cerebellum (Fig. 37A and B), and the radioactive signal relocated to internal organs such as liver and spleen. There were no differences between experimental groups (Fig. 37A, compare 1h and 48h).

***Tab. 6 Distribution of transplanted MSC*** *in SHAM and MCAO animals determined by SPECT/CT at day 1 (1-2h post injection), day 2 (24h post injection and day 3 (48h post injection). Data are represented as percent of injected dose per cubic centimeter (%ID/cm³) and as mean ± SD from 4-5 animals per experimental group (n=4-5/group).*

| %ID/cm³ | Time | SHAM + CTRL-MSC | MCAO + CTRL-MSC | MCAO + ITGA4-MSC | MCAO + CCR2-MSC |
|---|---|---|---|---|---|
| **Contralateral** | 1h | 4.22 ± 3.6 | 1.99 ± 1.18 | 0.78 ± 0.57 | 3.25 ± 3.16 |
| **Cerebrum** | 24h | 0.42 ± 0.25 | 0.32 ± 0.16 | 0.32 ± 0.05 | 0.48 ± 0.4 |
| | 48h | 0.23 ± 0.05 | 0.24 ± 0.1 | 0.24 ± 0.05 | 0.27 ± 0.09 |
| **Ipsilateral** | 1h | 8.56 ± 7.13 | 6.96 ± 3.57 | 6.65 ± 2.11 | 13.48 ± 10.79 |
| **Cerebrum** | 24h | 0.79 ± 0.43 | 1.17 ± 0.81 | 1.01 ± 0.09 | 1.52 ± 1.05 |
| | 48h | 0.49 ± 0.21 | 0.73 ± 0.35 | 1.03 ± 0.37 | 0.8 ± 0.37 |
| **Cerebellum** | 1h | 3.46 ± 3.08 | 5.12 ± 2.1 | 1.31 ± 1.42 | 7.80 ± 7.39 |
| | 24h | 0.38 ± 0.23 | 0.64 ± 0.33 | 0.28 ± 0.05 | 0.66 ± 0.57 |
| | 48h | 0.31 ± 0.13 | 0.27 ± 0.11 | 0.23 ± 0.04 | 0.32 ± 0.15 |

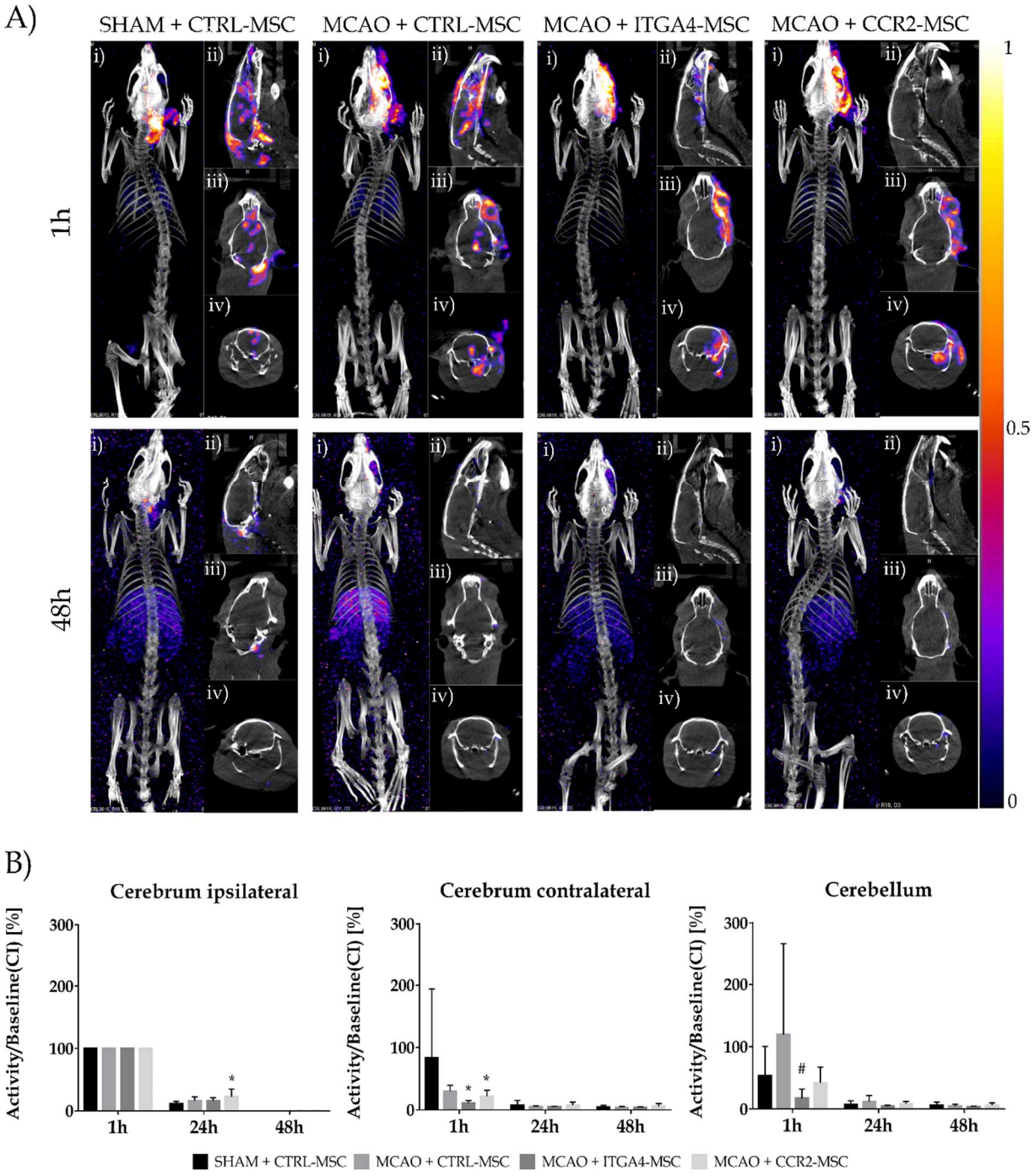


***Fig. 37 SPECT-CT-based analysis of MSC biodistribution following MCAO and intra-arterial transplantation.*** *Representative SPECT-CT images are given for SHAM-CTRL, MCAO+CTRL, MCAO+ITGA4-MSC and MCAO+CCR2-MSC 1h and 48h post administration (A). Accumulation of transplanted MSC is seen within the brain capsule and outside of the skull within the facial parts of the rat. Relocation to internal organs is visible after 48h following transplantationSPECT/CT images are given in dorsal (i), sagittal (ii), transversal (iii), and coronar orientation (iv). Semi-quantitative analysis of contralateral hemisphere, ipsilateral hemisphere and cerebellum after infusion with CTRL MSC, ITGA4-MSC or CCR2-MSC. Data are decay corrected, normed to baseline of ipsilateral cerebrum (CI) (1h) and presented as mean ± SD. Four- five animals were analyzed per group (n=4-5). Statistical significance * $p < 0.05$ vs. SHAM + CTRL, # $p < 0.05$ vs. MCAO + CTRL; in two-Way ANOVA with Tukey´s post hoc multiple comparison*

#### 4.3.5.3 Evaluation of MSC-distribution after intra-arterial transplantation

Biodistribution of modified and CTRL-MSC was evaluated after final SPECT/CT measurement following perfusion. To this end, radioactivity of internal organs was determined by gamma counting.

Strong radioactive signals were detected in liver, kidney and spleen (Fig. 38). Significant differences for liver radioactivity were found between SHAM + CTRL-MSC group versus MCAO group treated with ITGA4-MSC. Furthermore, comparison of radioactivity from spleen revealed statistically significant differences between SHAM + CTRL-MSC and all MCAO groups.

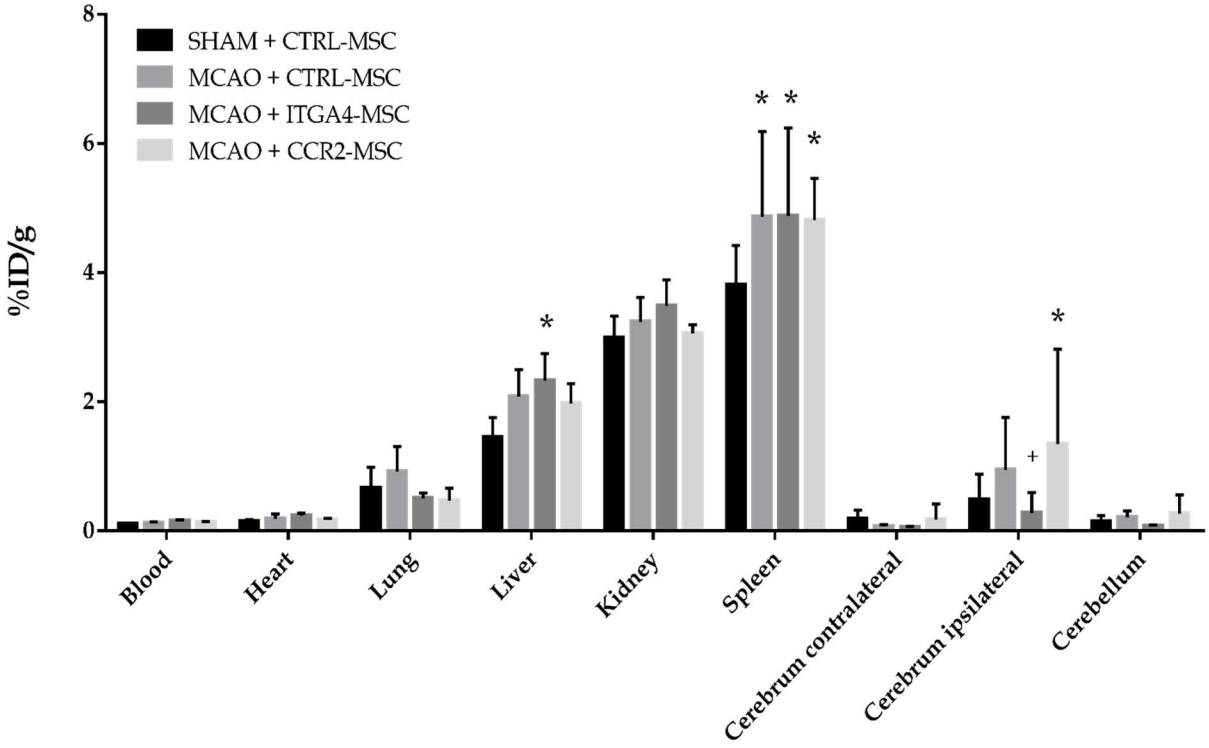


***Fig. 38 Radioactive counts represented as percent of injected dose per tissue sample weight (%ID/g)*** *are shown after injection of CTRL-MSC, ITGA4-MSC or CCR2-MSC. Each group comprised 4-5 animals (n=4-5/group). Data are represented as mean ±SD. Statistical significance was determined with two-way ANOVA with Tukey´s post hoc multiple comparison (p < 0.05; * vs. SHAM + CTRL, + vs. MCAO + CCR2-MSC).*

Gamma counting of contralateral cerebrum and cerebellum did not reveal any differences between experimental groups. Statistical differences were discovered after measurement of the ipsilateral hemisphere between SHAM + CTRL-MSC and MCAO + CCR2-MSC (Fig. 38) and between MCAO + ITGA4-MSC and MCAO + CCR2-MSC (Fig. 38).

No significant differences between experimental groups were found after evaluation of blood samples, hearts, kidney. Although not significant, smaller values were determined in

lungs obtained from MCAO animals treated with ITGA4-MSC or CCR2-MSC compared with control groups.

#### 4.3.5.4 Immunohistochemical tracking of transplanted MSC

Another important point of this study was to rediscover transplanted MSC within the brain as well as to capture their potential exit from the blood flow and entrance into the brain parenchyma. Animals showing cerebral influx after intra-arterial administration were selected for immunohistochemical evaluation.

The fluorescence reporter (GFP for CTRL-MSC, tdTomato for ITGA4- or CCR2-overexpressing cells) allowed the identification of transplanted cells within the brain tissue. Indeed, it was possible to detect a few MSC. The cells were localized in cortical and meningeal areas next to the lesion site in the ipsilateral hemisphere (Fig. 39, A and B). No MSC were detected in animals that underwent SHAM operation (Fig. 39B, SHAM+CTRL-MSC).

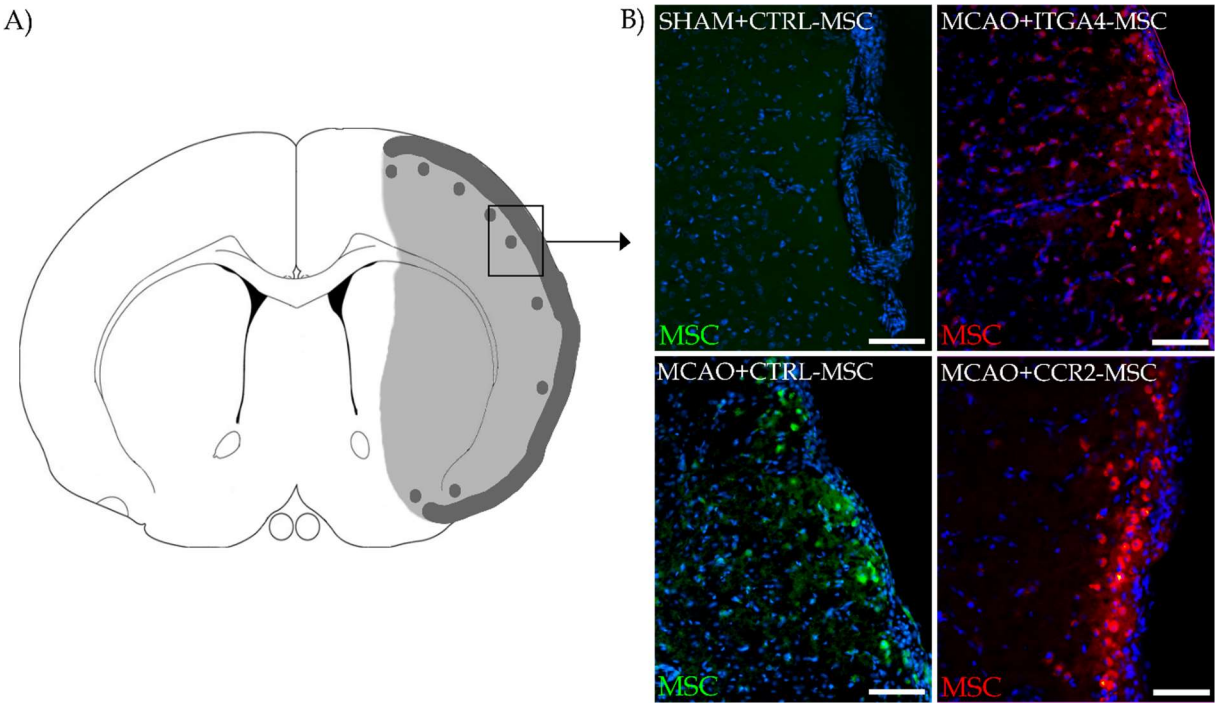


***Fig. 39 Detection of MSC based on their expression of a fluorescence reporter protein.*** *(A) Schematic drawing of coronar brain slice showing ischemic lesion (light gray area) and localization of detected MSC (dark grey areas). Picture modified after (Paxinos and Watson 2013) (B). Fluorescence images after staining against respective fluorescence reporter of transplanted MSC are shown for SHAM + CTRL-MSC (B), MCAO + CTRL-MSC (C), MCAO + ITGA4-MSC (D), and MCAO + CCR2-MSC (E). Nuclei were visualized by DAPI (blue channel). Scale bar represents 100µm.*

Lectin immunoreactivity was utilized to visualize blood vessels and macrophages. As shown in Fig. 40, MSC were found outside of blood vessels. Notably, the fluorescent signals from

reporter proteins were also co-localized with lectin-positive, cell-shaped areas (macrophages; marked with asterisk).

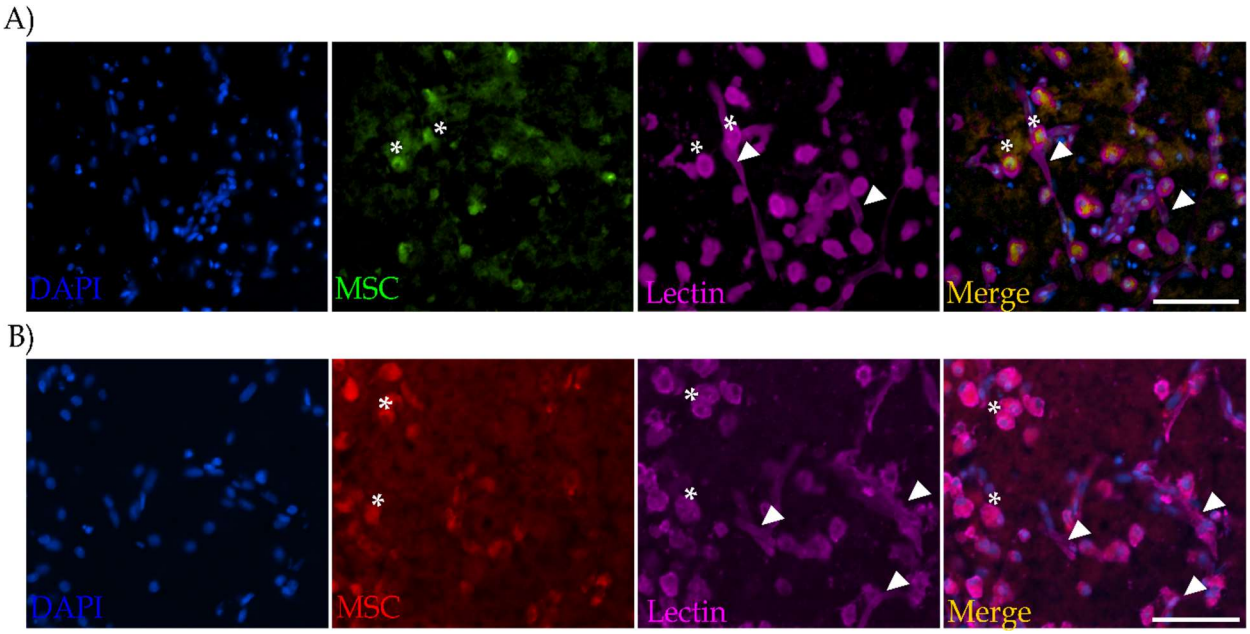


***Fig. 40 Double immunofluorescence staining against MSC reporter protein (GFP, tdTomato) and lectin.*** *Examples are given for MCAO + CTRL-MSC (A) and MCAO + CCR2-MSC (B). Pictures were taken from cortical border zone of the lesion. Examples for blood vessels are indicated by arrowheads and MSC colocalized with lectin by an asterisk. Scale bar indicates 100µm.*

Colocalization of MSC with macrophages or microglia was further evaluated by a double staining against the fluorescence reporter expressed from MSC and IBA1. In SHAM animals, no MSC reporter protein was detected and microglia showed a radial phenotype in the ipsi– and contralateral hemisphere (Fig. 41). In contrast, MSC were found in cortical/meningeal areas next to the ischemic lesion in MCAO animals as described previously. All detected MSC were also positive for IBA1. Of note, microglia presented a rounded somata within lesion- or perilesional areas (Fig. 41, A and B). Furthermore, the MSC reporter protein was apparently evenly distributed within the cell body (Fig. 41B).

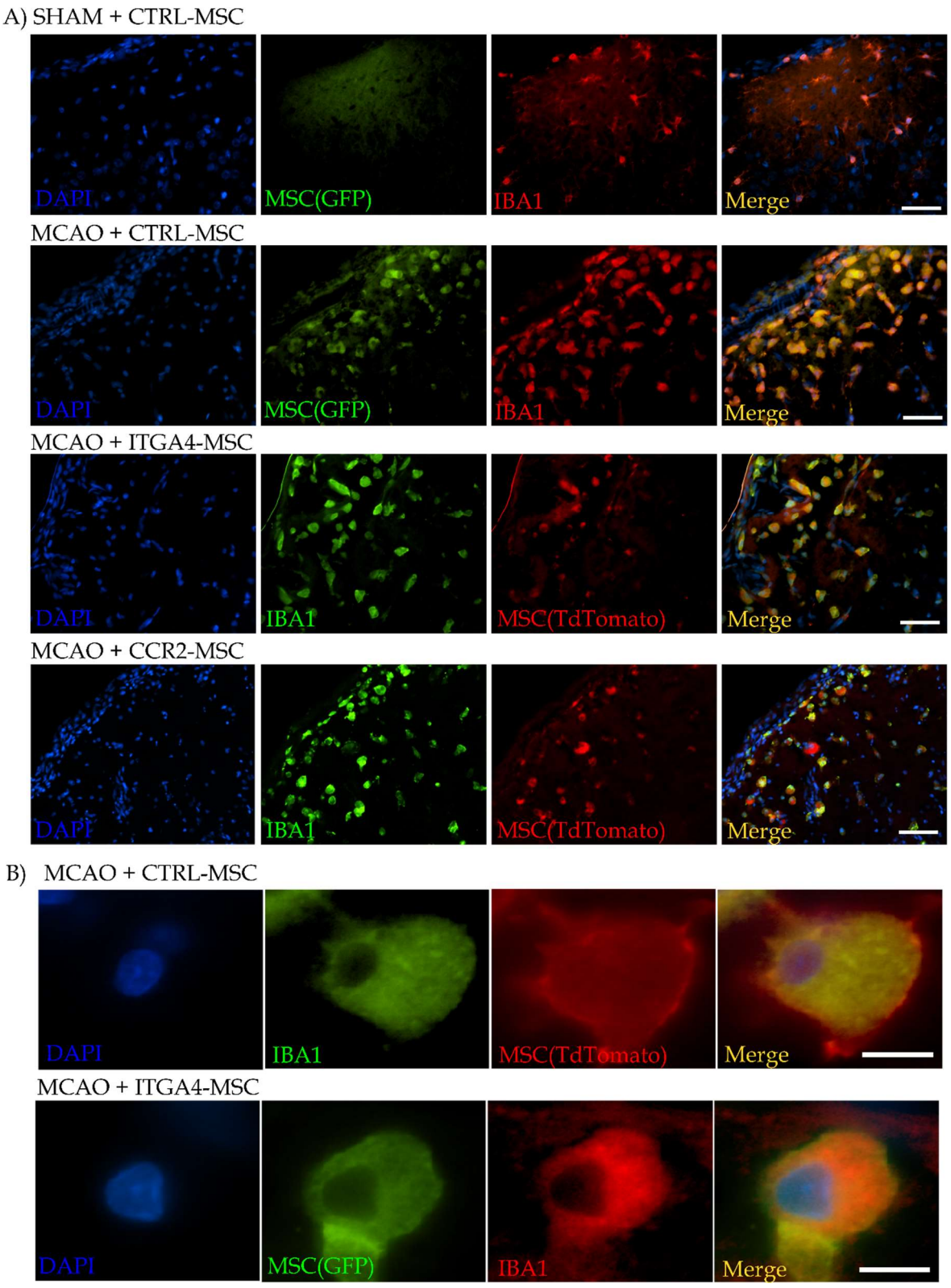


***Fig. 41 Double immunofluorescence staining against MSC reporter protein (GFP, tdTomato) and IBA1****. Examples are given for SHAM + CTRL, MCAO + CTRL, MCAO + ITGA4-MSC, and MCAO + CCR2-MSC (A). Higher magnification is shown in (B)Pictures were taken from cortical areas within the lesion. Microglia showed round somata in MCAO animals, while only radial shaped microglia were detected in SHAM animals. MSC reporter protein was colocalized with IBA-1 in all cases. Scale bar indicates 100µm(A) or 10µm (B).*

# 5 Discussion

The use of MSC for cellular therapies has emerged as a new strategy for a wide range of disorders including cerebrovascular diseases. Intra-arterial or intravenous injection facilitates minimally invasive delivery of MSC, but also requires egress from the blood flow and overcoming the endothelial barrier to reach the target area. It has been shown that less than 5% of transplanted MSC are usually rediscovered at the injury site (Kurtz 2008) what may account for constraint therapeutic success. While MSC are basically capable of endothelial (trans)migration, their surface receptor expression is not predetermined for extravasation. This fact might explain inefficient homing towards injury sites and was proven by several studies (Kumar and Ponnazhagan 2007; Kyriakou et al. 2008; Belema-Bedada et al. 2008).

Given the poor expression of homing receptors on MSC, genetic manipulation may represent a valid strategy to improve regenerative therapies. Indeed, combination of gene therapy with stem cell therapy was proven successful in experimental models of myocardial infarction (Cheng et al. 2008), osteopenic bone defects (Kumar and Ponnazhagan 2007), or cancer therapies (Hagenhoff et al. 2016). A common requirement of these studies was the improved homing of MSC towards injury site after modulation of their receptor expression. In the study by Cheng et al., MSC were modified in order to overexpress the chemokine receptor CXCR4. These CXCR4 overexpressing MSC homed more efficiently to the infarcted myocardium after intravenous delivery as compared to unmodified MSC (Cheng et al. 2008).

Besides chemokine receptors, adhesion receptors are crucially involved in migration towards lesion sites. Integrins, for example, mediate homing and cellular engraftment. They consist of an alpha and a beta-subunit. Their combination leads to a rich receptor variety (Schwartz and Ginsberg 2002). Particular the integrin receptor α4β1, or VLA4, is linked to cell-cell-interaction and ECM adhesion. Importantly, it mediates the binding to endothelium by interaction with VCAM1 (Nourshargh and Alon 2014; Ley et al. 2007). In response to inflammatory cytokines such as TNFα or IL6, the endothelium reacts with upregulation of VCAM1 (Wang et al. 2007) and thus provides the adhesion stage prior to extravasation. MSC express the integrin alpha 4-subunit only to a limited extent leading to insufficient endothelial adhesion. Its overexpression is considered to enhance MSC endothelial adhesion and, thus, homing, towards the injury.

## 5.1 mRNA as a tool for genetic engineering of MSC

The delivery of *in vitro* transcribed messenger RNA (IVT mRNA) has been suggested as an option of providing (therapeutic) proteins and peptides for cells. A huge disadvantage of mRNA based approaches was the instability and rapid degradation (Tavernier et al. 2011). This prevented the efficient translation into desired protein and mRNA-based modifications were not effective. This problem was addressed by several researchers and the development of several protocols allowed to improve the mRNA-stability. For example, the use of nucleoside-modified IVT mRNA can increase mRNA stability and translation while reducing the immuno-stimulatory activity via pattern recognition receptors (PRR) (Kariko et al. 2005). Thus, mRNA-based methods have been successfully used to modify stem cells for secretion of immunosuppressive proteins (Levy et al. 2013), to generate induced pluripotent stem cells (iPSC) or to induce cell fate conversion (Warren et al. 2010; Yoshioka et al. 2013) as well as to edit genomes by introducing programmable nucleases (Yang et al. 2013). It is therefore conceivable that mRNA-based modification can also improve MSC properties and capabilities. The evaluation and optimization of mRNA transfection for ITGA4 overexpression on MSC was the focus of this part of the study.

### 5.1.1 ITGA4 mRNA lipofection of MSC

Different techniques are available for mRNA delivery into MSC. On one hand, mRNA can be delivered by physical methods such as electroporation, microinjection, or sonoporation. On the other hand, chemical transfection methods including cationic lipofection, cationic polymers or nanoparticles are commonly used for delivery of nucleic acids. Here, MSC showed high mRNA uptake (Fig. 10) and only gradually decreased cell viability (Fig. 11, Fig. 12) after cationic lipofection.

First transfer of mRNA to cultured cells using liposome-mediated transfection was described by Malone et al. (Malone et al. 1989). Since then, various lipofection agents for mRNA have been developed and were also used for stem cell transfection. Several lipofection agents are available and choice usually depends on cell type. Transfection of GFP-IVT mRNA, for example, was very efficient in fibroblasts using Stemfect, while endothelial cells are hardly modified by this agent (Avci-Adali et al. 2014). Cationic lipofection is well tolerated by MSC while multipotency, viability and recovery is not affected (Madeira et al. 2010; Boura et al. 2013). It has been shown that IVT mRNA encoding for the immunosuppressive cytokine interleukin 10 (IL10) or P-selectin glycoprotein ligand 1 (PSGL1) was successfully delivered to mouse MSC by cationic lipofection (Levy et al. 2013).

It is widely accepted that mRNA is incorporated into liposomes and translocated to the cytoplasm via endosomal uptake (Leonhardt et al. 2014). However, for efficient IVT mRNA translation, endosomes need to be lysed and the nucleic acid released into the cytosol (Zabner et al. 1995). An endosomal lysis rate of 25-50% has been described (Leonhardt et al. 2014) indicating that at maximum only half of mRNA molecules are available for translation. Therefore, it may be speculated that partial endosomal release is a major obstacle for protein expression after IVT mRNA lipofection. Nevertheless, lipofection counts as suitable method for mRNA delivery and up to ~ 60% - 89% positive cells were observed in this and other

studies (Levy et al. 2013; Ryser et al. 2008). Alternative delivery methods (electroporation, polyethylenimine [PEI]) that may prevent the endosomal entrapment did, however, not improve ITGA4 expression (Fig. 9B). Instead, a major impact on cell vitality was observed what may have led to inferior mRNA translation in these cases.

An efficient protein expression after mRNA transfection depends on numerous factors including type and circumstances of delivery and transfection efficiency. Presence of serum or antibiotics, for example, can impact the transfection efficiency. It is recommended to allow the formation of mRNA-lipoplexes in antibiotic and serum free environment. By this strategy, the competition of mRNA with supplemental components is decreased during generation of cationic complexes. Furthermore, the presence of serum may have an influence on mRNA stability. There is evidence for a serum-mediated effect on cap dependent transfection efficiency (also see chapter 5.1.3), where ARCA-capped mRNA transcripts displayed higher translation efficiency than m7GpppG (=Cap0/Cap1) in the presence of serum (Tavernier et al. 2011; Zohra et al. 2007). This phenomenon probably occurs due to enhanced stability of ARCA IVT mRNA and is reversed when serum is removed (Tavernier et al. 2011).

### 5.1.2 Structural characteristics and stability of cellular mRNA

In this study, IVT mRNA was produced from cDNA sequences containing the open reading frame (ORF) for either ITGA4 or GFP. Primary *in vitro* transcripts were further capped and polyadenylated at the respective ends.

Processing of the primary RNA transcript is necessary for production of a functional mRNA and comprises 5′ capping, 3′ polyadenylation, and splicing in animal cells (Lodish 2002). This processing occurs in the nucleus and required for mRNA transportation into the cytoplasm. Here, it is accessible for translation. The 5′ cap is added by a dimeric capping enzyme already during transcription of the primary RNA. Three contributing steps lead to the generation of the cap structure (Fig. 42A). First, the triphosphate-group of the 5′ nucleotide is hydrolyzed to a diphosphate group. Second, a guanosine-monophosphate (GMP) is added and finally, a methylation is introduced at the guanosine base (Shuman 1995). As a result, the transcript is protected from exonuclease activity by the 5′cap, which contributes significantly to stability. Furthermore, the cap regulates nuclear export, translation and its initiation, as well as intron excision (Lewis and Izaurralde 1997; Burkard and Butler 2000; Sonenberg and Gingras 1998). The pre-mRNA is further processed by cleavage and polyadenylation at the 3′end (Bienroth et al. 1993). For this, a multimeric protein complex is formed at an AU-rich sequence near the 3′ end of the transcript, responsible for cleavage. The resulting end is then polyadenylated. The poly-A-tail protects from degradation and fulfills supplementing functions during transcription termination, nuclear export, and translation (Guhaniyogi and Brewer 2001). Finally, the introns are removed from the pre-mRNA and the exons are spliced together prior to nuclear export (Lodish 2002; Lewis and Izaurralde 1997). This generates a mature mRNA molecule, that provides the ORF for protein translation.

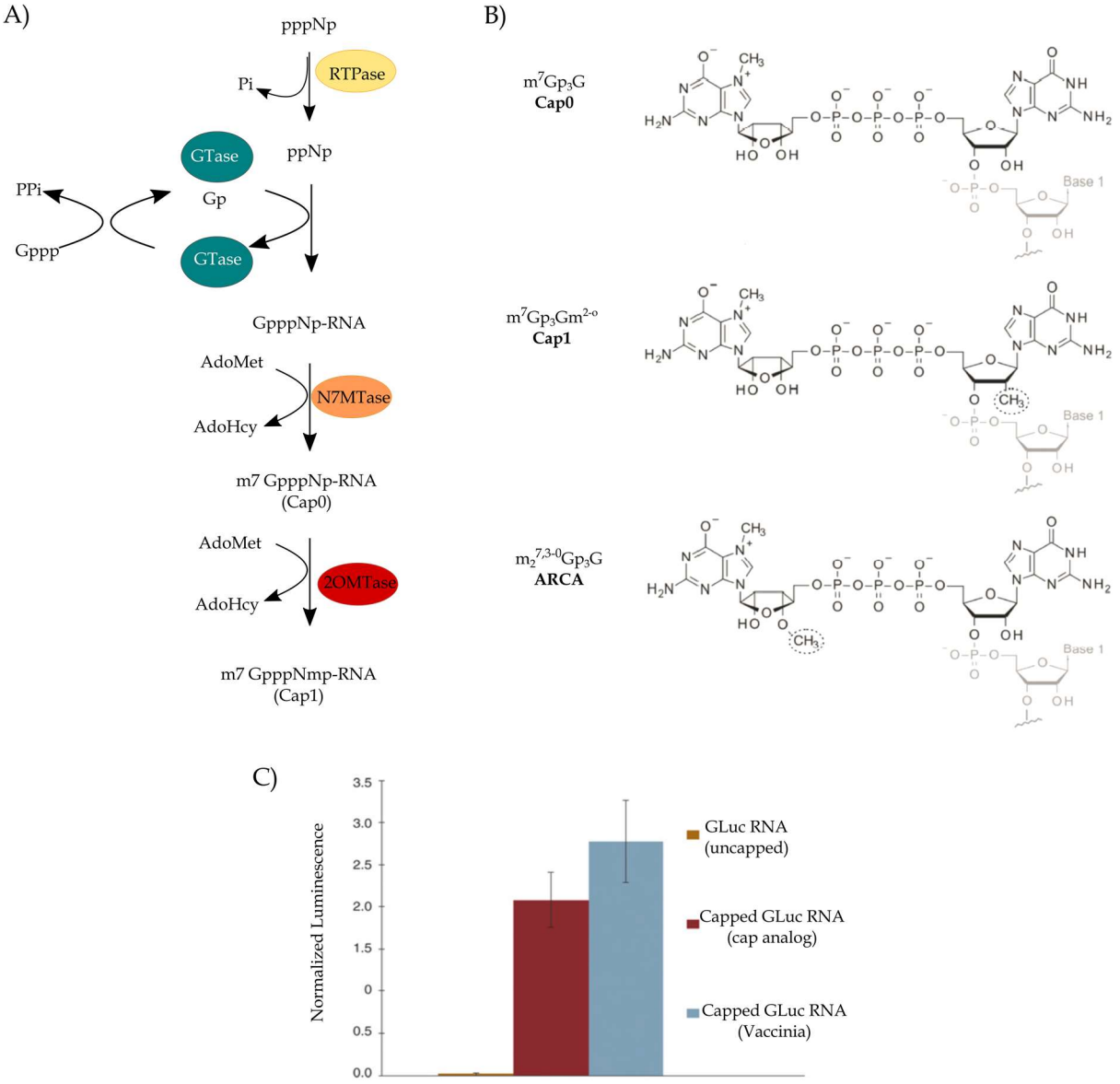


***Fig. 42 mRNA capping.*** *Capping reactions for generation of Cap0 and Cap1 are given in (A). Picture modified after Decroly et al. (2012). Structure of Cap0, Cap1, and ARCA after Grudzien-Nogalska et al. 82013) (B). Capping types are distinguished based on degree and localization of methylation. Influence of capping was shown for expression and function of luciferase in HeLa cells (Jani and Fuchs 2012) (C). Uncapped mRNA is hardly translated, while protein expression is achieved with a cap analog (=ARCA) or with vaccinia-based posttranscriptional capping (Cap0).*

Some steps of *in vivo* RNA translation, i.e. splicing and nuclear export, do not apply for IVT mRNA. Past successes suggest that splicing, although important (Nott et al. 2003), is dispensable in IVT mRNA and the ORF of the gene of interest is sufficient for obtaining functional mRNA. Thus, transcripts generated from cDNA sequences should provide an adequate basis for IVT mRNA-based modifications. However, stability and translation initiation are pivotal for the success of mRNA-based modification and can be modulated by capping. In the course of this study, capping was realized either co-transcriptionally or post-transcriptionally. An anti-reverse cap analogue (ARCA; m(2)(7,3'-)(O)GpppG) (Stepinski et al. 2001; Jemielity et al. 2003) was added into the *in vitro* transcription reaction (co-transcriptional capping). ARCA cannot be incorporated in reverse orientation because of

modifications at the C3' position of the 7-methylguanosine (m(7)G) (Fig. 42B). In a second approach, the primary mRNA molecule was capped after the *in vitro* transcription using a recombinant capping enzyme. The enzyme catalyzes the capping reaction according to the physiological reaction. This results in the generation of Cap0. By an additional methylation, Cap0 can be converted to Cap1-structure (Fig. 42, A and B).

Obtained IVT mRNA was extended enzymatically by means of recombinant poly(A)polymerase resulting in a poly(A) tail of 100 to 150 nucleotides. This is well in range of the optimal length of about 120 nucleotides (Holtkamp et al. 2006; Mockey et al. 2006), although this optimum may vary depending on target mRNA and target cells (Wahle and Keller 1992). ITGA4 mRNA levels were substantially increased for at least 12h after transfection (Fig. 10) suggesting that stabilization was not a crucial issue.

Further, substantial improvement of IVT mRNA stability and translational efficiency can be achieved by modifying its structural elements. Particularly, the incorporation of regulatory sequence elements into the 5'- and 3'-UTR may influence both, de-capping and degradation (Kuhn et al. 2012). In the present study, 5'- and 3'-UTRs were kept to a minimum (62 and 39bp, respectively), since these regions often contain destabilizing sequence elements (i.e. microRNAs and RNA-binding proteins). Of note, ITGA4-(GFP) mRNA (3+1kb) is considerably longer than GFP (about 1kb). The possibility for formation of secondary structures can increase with the length of the transcript and cause stability issues. Secondary structures are not readily accessible for translation and may influence the efficiency.

The risk for an intracellular immune response is enhanced with introduction of external nucleic acids. The mammalian cell recognizes an mRNA molecule as one of its own origin by its modifications. Lack of these modifications activates sensors of the innate immune system, type I interferons (IFNs), and proinflammatory cytokines (Quabius and Krupp 2015; Sahin et al. 2014; Kariko et al. 2011). In the consequence, the external mRNA is degraded and the cell induces (pro)inflammatory signaling pathways (Mogensen 2009). This recognition by the host defense system can be ablated by incorporation of modified nucleosides in IVT mRNA (substitution of 5-methylcytidine [5mC] for cytidine and pseudouridine [Ψ] for uridine). Activation of residual IFNs can be further suppressed by media supplementation with respective inhibitors such as the B18R protein. This treatment leads to sustained protein expression with reduced cellular toxicity (Yoshioka et al. 2013; Warren et al. 2010). Although modified nucleotides were not used in this study, cell viability was only slightly perturbed and the cells recovered swiftly after transfection (Fig. 11). This indicates that potential immunologic reactions were no major limitation.

### 5.1.3 Efficiency of ITGA4-IVT-mRNA translation

In the present study, up to 60% of ITGA4-positive cells were observed 12-24h after mRNA transfection. Interestingly, the extent of ITGA4 protein expression was dependent from the cap structure. Distinct expression of ITGA4 was possible only after substitution of co-transcriptionally added ARCA by enzymatically attached Cap0/Cap1 (Fig. 14, Fig. 15, Fig. 16). This is in contrast to the observations from mRNA based GFP transfection, where GFP expression was generally more efficient (~80%) and independent from cap structure.

Nevertheless, pronounced differences regarding extent of GFP expression on cellular level emphasized cap-dependent effect on translation (Fig. 19).

The initiation of translation is based on the dialogue between the core initiation factors and the mRNA. Binding of a functional 5'cap structure to eukaryotic initiation factor 4E (eIF4E) is a key mechanism (Jackson et al. 2010). Its interaction with the cap-structure recruits the 5'end of the mRNA to the 40S subunit of the ribosome (Topisirovic et al. 2011). Thus, eIF4E counts as the primary initiator of translation and its interaction with the 5'end can be modified by the cap structure (Cai et al. 1999). Several synthetic caps have been developed with the aim to increase translation efficiency. Among them, ARCA has gained attraction for production of synthetic mRNA. However, the translation of ARCA-ITGA4 transcripts was less effective than with Cap0/Cap1 transcripts. Since expression of GFP readily succeeded from ARCA IVT mRNA (Fig. 19), it is unlikely that a substantially impaired ARCA function accounts for the major differences between ARCA and Cap0/1 ITGA4 IVT mRNA translation. A potentially altered affinity to eIF4E is one contributing option that may have led to weaker translation efficiency of ARCA mRNA. Some synthetic caps are known to be more inhibitory than others, and therefore demonstrate a lower equilibrium binding affinity to elf4E. In this case the affinity for ARCA (10.2 ±0.3 Kas x $10^{-3}$) is somewhat lower than that for m7GpppG (12.6 ±0.3 Kas x $10^{-3}$) (Grudzien et al. 2004). This difference might not explain the great manifestation of translation differences, but it is likely that it at least contributes to it.

Another reason for lower ITGA4 translation of ARCA constructs might be related to the capping reaction. As mentioned, ARCA is added co-transcriptionally causing a direct competition with the GTP nucleoside for transcription initiation by the polymerase. However, some transcripts are initiated with the GTP nucleoside and are therefore uncapped (approximately 10-25% of the mRNA). Importantly, that proportion also remains translationally inactive due to lacking recognition by eIF4E. Nonetheless, the advantage of ARCA is that nearly all capped mRNA can be directed to translation due to correct cap orientation (Stepinski et al. 2001). In contrast, co-transcriptionally used m7GpppG cap (Cap0) of natural eukaryotic mRNA can be also incorporated in reverse orientation. Therefore, a substantial proportion (30-50%) of such IVT mRNA will not be recognized by the translational machinery. To overcome reverse incorporation, a natural m7GpppG cap structure can be added enzymatically utilizing recombinant capping enzymes (Martin et al. 1975) in a second step after the initial IVT mRNA synthesis (post-transcriptional). This way, nearly all IVT mRNA will be capped with Cap0/Cap1 in correct orientation (Jani and Fuchs 2012).

Only few studies directly compared co-transcriptionally ARCA mRNA with enzymatically m7GpppG capped mRNA. Using luciferase, a similar difference was observed between the expression of ARCA-capped and m7GpppG capped transcripts (Fig. 42C) (Jani and Fuchs 2012; Tavernier et al. 2011). Interestingly, other studies have shown that translational efficiency of ARCA-luciferase mRNA was about twice that of co-transcriptionally m7GpppG capped luciferase mRNA (Jemielity et al. 2003; Stepinski et al. 2001). This is well in range or even slightly above values that would be expected by eliminating reversely m7GpppG capped mRNA.

The mRNA transfection was more efficient for GFP in comparison with ITGA4. It is unlikely that this difference is related to the half-life of GFP as stated in other studies (Dullaers et al. 2004; Corish and Tyler-Smith 1999) that revealed an accumulation of the eGFP protein with a half-life of >24h (Corish and Tyler-Smith 1999). In this study, a monomeric GFP from copepod was used. Importantly, a destabilization domain was introduced shortening its half-life to ~1h. Literature regarding ITGA4 half-life is not available, but given the protein expression data (Fig. 14, Fig. 15, Fig. 16), a limited life span might be assumed.

A major difference between ITGA4 and GFP arises from the destination of the translated protein. While ITGA4 is ought to assemble with its partner ITGB1 and is then transported to the cell membrane, the GFP protein accumulates in the cytoplasm. During the synthesis, the proteins are bound to the endoplasmic reticulum (ER). The ER itself functions as the primary protein sorter and is connected to the secretory pathway, that transports proteins towards the cell membrane (Lodish 2002). The entrance to the secretory pathway requires the presence of respective signaling peptides (Farhan and Rabouille 2011). It should be emphasized that both the ARCA and Cap0/1 ITV ITGA4 mRNA constructs contained the full sequence of rat ITGA4 including that for the signal peptide. It may be speculated that a lack of "zip code" elements (typically in the 3'-UTR) as in the present study is less detrimental for translation of cytosolic GFP than for that of membrane bound ITGA4. Successful expression of ITGA4 from Cap0/1 ITV mRNA, however, suggests that the signal recognition pathway (SRP) pathway is sufficient. The same consideration should apply for ARCA IVT ITGA4 mRNA expression.

### 5.1.4 Processing of ITGA4 after mRNA-transfection and implications for its biological function

A considerable amount of endogenous ITGA4 was detected by flow cytometry and Western Blot (Fig. 14, Fig. 16). Both analyses consistently revealed about 20 % of native MSC to be ITGA4-positive. Data on ITGA4 in rat MSC are rare, but a previous study reported no VLA4 detection by flow cytometry (Xiao et al. 2012). Similarly, no ITGA4 was reported in mouse MSC (Chen et al. 2014) or in only 25 % of the cells at very low MFI, respectively (Ip et al. 2007). While expression was found in about 60 % of the MSC up to 24 h after Cap0/Cap1 ITGA4 mRNA transfection, this increase was much less pronounced after ARCA mRNA transfection. Of note, the mean fluorescent intensity (MFI) of transfected cells only moderately increased compared to native MSCs. Again, this increase was minimal after ARCA ITGA4 mRNA transfection.

ITGA4 expression allowed a basic evaluation of its biological processing in MSC. Of note, full length protein was observed mainly during the first hours after mRNA delivery (Fig. 16C, 140kDa + 30kDa GFP). However, the extent of cleaved ITGA4 was predominantly observed after 12h.

Post-transcriptional processing is a major part in the maturation of proteins into their functional form. Often, this includes the enzymatic modification of the amino acid chain during their transfer through the secretory pathway. Insights into processing of ITGA4 were gained from experiments using leukocytes (Teixido et al. 1992; Takada et al. 1989;

Bednarczyk et al. 1992). Its processing includes cleavage conducted by the main cellular convertases furin and the pre-protein convertase 5A (PC5A) (Bergeron et al. 2003; Bednarczyk et al. 1992). Unlike other cleavable α-integrins, the pro-α4 (150kDa) endoproteolysis occurs in the middle of its ectodomain and generates N-terminal (80kDa) and C-terminal (70kDa) products (Bergeron et al. 2003). Both fragments are held together non-covalently (Bednarczyk et al. 1992; Teixido et al. 1992). While most cleavable α-subunits are present at the cell surface only in processed forms, α4 chains may also be present as unprocessed proteins (Teixido et al. 1992). The physiological consequences of pro-α subunit processing are still not clear, as unprocessed α4β1 can bind to VCAM1 and fibronectin, what was suspected to be relevant for inside-out signaling (Bergeron et al. 2003; Teixido et al. 1992). Of note, the extent of the α4 endogenous cleavage varied considerably in five haematopoietic cell lines (22–89%) and generally correlated with their furin and PC5 mRNA expression (Teixido et al. 1992). In the present study, the vast majority (>90%, except 50-60% 4.5h after transfection) of integrin expressed after ITV mRNA transfection was detected in its processed form (Fig. 16). This clearly indicates that MSC are capable of processing ITGA4.

Beside the processing of the ITGA4 protein, the assembly with partner ITGB1 is necessary to form the VLA4 receptor. Furthermore, the assembled receptor has to be transported towards and integrated into the cell membrane. ITGB1 is constitutively expressed and consistently found in MSC at high concentrations (Kumar and Ponnazhagan 2007). In leukocytes, the ITGA4 subunit associates with ITGB1 already in the ER and prior to its maturation in Golgi apparatus (Teixido et al. 1992). The result of VLA4 assembly and its transport to the cell membrane was evaluated by LDV-FITC, that mimics the binding of a natural ligand (Chigaev et al. 2008). Particularly increased LDV binding upon ITGA4 mRNA transfection indicates that the availability of ITGB1 for VLA4 assembly was not limiting. LDV-FITC binding followed the kinetic of ITGA4 expression with a similar extent indicating specific binding. It has already been shown that the overexpression of the ITGA4 subunit led to successful heterodimerization with ITGB1. Moreover, it subsequently increased the homing towards bone in immunocompetent mice (Kumar and Ponnazhagan 2007). Supported by this, the fully functional processing of VLA4 and its integration into the cell membrane can be assumed after ITGA4 mRNA transfection.

### 5.1.5 Concluding remarks for mRNA-based modification of MSC

In this section, it was shown that mRNA based cell engineering is a suitable tool for the overexpression of adhesion receptors. Importantly, mRNA delivery using lipofection was well tolerated by MSC and did not affect cell viability. It provides a clinically compatible method for transient protein expression, when important structural elements as capping or polyadenylation are taken into account. In particular, the application of posttranscriptional capping during IVT mRNA synthesis benefits substantially the ITGA4 protein expression. Furthermore, mRNA driven ITGA4 protein expression results in processing and maturation necessary for biological functionality. Thus, ITGA4 overexpression by IVT mRNA can be considered as a valuable tool for MSC modification.

## 5.2 Lentiviral-based modification of MSC and its optimization by promoter substitution

Complex retroviruses such as lentiviruses can deliver genes to a wide range of cell types. The transgene and part of the lentiviral genes (provirus) integrate into the host genome and are transmitted to the offspring (Pfeifer et al. 2002). It was reported that particular self-inactivating human immunodeficiency virus type 1 (HIV1) derived lentiviral vectors are efficient tools for genetic manipulation (Gropp et al. 2003). The majority of the HIV genes were eliminated, retaining only the structural viral proteins and enzymes (*gag/pol*) and those for transcriptional purposes *(tat/rev*) (McGinley et al. 2011). By additional separation of the viral genes on different plasmids, the safety risk is minimal and, thus, the method is extremely attractive for gene therapy (Nowakowski et al. 2013). Importantly, they do not require complete cell divisions to transduce their target cells due to accessibility of accessory proteins that enable integration (Cooray et al. 2012; Ferry et al. 2011). This point is important considering that a subset of MSC are reported to be in a quiescent state (Conget and Minguell 1999).

The host range of a lentiviral vector can be extended by a process called pseudotyping. By this, lentiviruses are generated with glycoproteins that derived from the envelope of other viruses. The vesicular stomatitis virus glycoprotein (VSV-G) is applied commonly and was used in this study. VSV-G pseudotyped lentiviruses have been proven to be efficient for MSC transduction of different sources and species (Zhang et al. 2002; McGinley et al. 2011; Ricks et al. 2008). Lentiviral gene transfer is commonly used to ensure high transduction efficiency and stable integration of the transgene into the host genome. By testing different viral vectors for infection of rat MSC, lentiviral vectors were proven to be the most efficient (McMahon et al. 2006). Moreover, the lentiviral infection did not induce cell death in comparison with other viral vectors, such as AAV (McMahon et al. 2006).

In this study, the HIV1 derived lentiviral vector contained a posttranscriptional element of the woodchuck hepatitis virus (WPRE) and the central polypurine tract (cPPT) of the *pol* gene of HIV1 (Zufferey et al. 1999; Follenzi et al. 2000). Both elements have been reported to enhance transgene expression in various cells including stem cells (Sirven et al. 2000). HIV1-based lentiviral vectors have been shown to efficiently deliver GFP or RFP to MSC (Zhang et al. 2002) and, therefore, were considered as suitable tools for this study.

Lentiviral vectors efficiently manipulate gene expression and usually infect a high proportion of cells (Nowakowski et al. 2013). Overexpression of CXCR4-GFP on MSC utilizing lentiviral vectors was reported to achieve > 92% of positive cells (Yang et al. 2015a). Efficient transgene expression, however, strongly depends on the promoter driving the transgene. It is possible to regulate and to optimize the transgene expression for a particular cell type through this element. Constitutive and inducible promoters from eukaryotic-mammalian or viral origin can ensure a long-lasting and high level gene expression. In this part of the study, ITGA4-transgene expression by different promoters was compared after lentiviral transduction of bone marrow derived MSC.

### 5.2.1 Lentiviral modification: a matter of promoter choice?

Lentiviral overexpression of ITGA4 was analyzed under control of TRE-, UbC-, EF1α-, or CMV promoter. The TRE promoter led to a high ITGA4 expression in about ~80% of the transduced MSC, while lower numbers were observed with the other promoters (Fig. 20, Fig. 21).

Several promoters have been reported as suitable for transgene expression in MSC after lentiviral transduction. The systemic comparison of GFP expression under control of UbC-, EF1α-, CMV-, or TRE were already performed for MSC (Qin et al. 2010; Ferreira et al. 2012; Zhang et al. 2002) and revealed differences in transgene expression. This was used for the deduction of promoter-strength and promoter-dependent transgene expression within a certain cell type.

The TRE-promoter is a ligand inducible-promoter system (tet on) that allows pharmalogical control of transgene expression (Zoltick and Wilson 2001). Transgene transcription is silenced under normal conditions, but activated as soon as soon as tetracycline (doxycycline) is applied to the system. Doxycycline binds to the reverse tet repressor transactivator (rtTA). This mediates binding of rtTA to the tet-operon of the TRE-promoter what activates transgene transcription (Papadakis et al. 2004). The TRE-promoter is considered as a strong promoter that drives high transgene expression (Gossen and Bujard 1992), what was approved for MSC used in this study. Its strength is even more highlighted when considering the mid-ranged relative copy number (Fig. 23).

In contrast to the inducible TRE promoter, UbC-, EF1α- and the CMV are constitutive active promoters. The UbC- promoter is generally described as a promoter with weak activity and, thus, results in rather low to moderate transgene levels (Qin et al. 2010; Varma et al. 2011). Of note, only 10% GFP-positive cells were observed after lentiviral transduction of HSC with an UbC-driven construct (Varma et al. 2011). This is well in line with the efficiency observed for MSC in this and other studies (Qin et al. 2010). A fairly high and consistent strength is described for the EF1α promoter (Papadakis et al. 2004). It should be pointed out that the EF1α promoter used in this study was an optimized version for enhanced transgene expression by the combination of the core promoter with a viral terminal repeat sequence (Orlova et al. 2014). The CMV promoter can induce a strong transgene expression, but its strength and activity is influenced by the modified cell type (Keating et al. 1990; Muller et al. 1990; Qin et al. 2010). Lee and coworkers transduced monkey bone marrow-derived MSC with eGFP under the control of CMV or EF1α-promoter. They observed a substantial higher amount of GFP-positive MSC for CMV-driven expression as compared to EF1α (Lee et al. 2004). In contrast, it was shown for rat derived MSC that GFP expression driven by EF1α was more efficient as compared to CMV (Qin et al. 2010). This appears controversial but might be related to species differences. Weak transgene expression with the CMV-promoter was shown for rodent-derived cell lines as NIH-3T3, NRK, or HSN. Substitution of CMV with EF1a achieved a more efficient transduction and transgene expression (Ikeda et al. 2002).

In the first place, it may be presumed that magnitude of ITGA4-transgene expression correlates with promoter strength. However, control experiments by UbC-driven GFP (or tdTomato, Fig. 27) achieved a higher percentage of positive cells. After analyzing relative ITGA4 copy number, it became evident that the ITGA4-mRNA expression (Fig. 20) and the

number of GFP-positive MSC (Fig. 21B) under UbC, EF1α, and CMV rather correlated with the copy number than with presumed promoter strength. Further supported by similar MFI of positive MSC (Fig. 21C), these data suggest a comparable activity of UbC-, EF1α-, CMV-promoter.

A bottleneck for the promoter comparison in this study was the determination of an exact virus titer. Importantly, production of lentiviruses bearing different promoters for the transgene was conducted equally and in parallel by using same lentiviral backbone, same packaging system, same molar plasmid ratios during helper cell transfection, same batch of helper and target cells, and the same harvesting procedure. The presence and quality of lentiviral particles was verified by p24 protein detection. This supports the conclusion that lentiviral production was in a usable range with minimum quantity. However, the prediction of a lentiviral-mediated gene transfer is difficult even if the virus titer or multiplicity of infection (MOI) is determined and adjusted in advance. Lentiviral titers are easily affected by a number of factors including transduction conditions, inoculum volume, type and number of target cells, or exposure time (Zhang et al. 2004). In addition, the half-life of a lentiviral particle is rather short (Sakuma et al. 2010) meaning that efficiency of lentiviral modification is also time-sensitive. Furthermore, promoter-dependent variations of transgene copy number might occur even after application of analogous titers (Xia et al. 2007; Norrman et al. 2010). Therefore, the determination and adjustment of transgene copy numbers in advance might be a more reliable method for creating conditions that allow more comparable (promoter) analyses. Nonetheless, analogous handling has led to varying copy numbers depending from promoter-bearing construct. Thus, different efficiencies regarding lentiviral production or integration might be assumed for each construct. The UbC-, EF1α-, and CMV bearing expression vectors were identical except for the promoter sequences. These were differing in size (1.2kb for UbC vs. 0.493kb for EF1α vs. 0.58kb for CMV; total viral genome size 7.5-8.2kb) what may have affected the lentiviral production. It is known for AAV, that the viral genome is truncated when exceeding a crucial size (> ~5.2kb). This leads to lower titers and reduced transgene expression (Holehonnur et al. 2015). Genome size for lentiviruses are limited to 10-11kb and titers decrease with growing length (Kumar et al. 2001). Therefore, an impairment of viral production by significantly larger UbC promoter can be basically excluded. However, the promoter size or sequence may have led to disturbances for e.g. during integration or nuclear export causing differences in copy number at second instance.

The integration of the provirus into the host genome is a multistep process that includes cutting of the 3'vector end, cutting of the host genome, insertion, gap repair and ligation (Craigie 2001). Some mechanisms of the integration process are not fully understood. Recently, it was reported that the retroviral integration is rather inefficient and the generation of episomal circles is a common phenomenon (Moldt et al. 2008). These episomal circles are unable to replicate and are considered as dead-end products of viral reverse transcription (Moldt et al. 2008). Their presence can falsify the genomic copy numbers of viral genes during the first days after transduction. Importantly, transgene transcription is still possible (Wanisch and Yanez-Munoz 2009; Wu 2008) what may contribute to enhanced transgene protein levels shortly after transduction. Since episomal circles disappear after a few cell divisions, their impact is lost within a short time. The site-specific integration is also

not fully elucidated and, although under consideration, the integration sites are assumed to be random (Marini et al. 2015; Logan et al. 2002). Given the unpredictability of the integration site, it might be possible that the transgenes were either introduced at loci with high transcriptional activity or the contrary might also occur. This altogether may have contributed to different extent of transgene expression.

### 5.2.2 Promoter-dependent silencing

In this study, a time-dependent downregulation of transgene expression was observed for EF1α-, CMV-, and TRE-promoter (Fig. 20, Fig. 21). Downregulation of transgene expression was already observed in numerous cell lines and described as promoter and cell-type dependent (Wang et al. 2008; Xia et al. 2007; Liu et al. 2006). For example, inactivation was shown for GFP expression in hematopoietic stem cells, where more than 95% of the transgene were suppressed under control of CMV promoter (Xia et al. 2007).

In general, there is some major concern that the transgene expression may be inactivated in the host cell after lentiviral transduction. This gene inactivation is referred to as silencing and two mechanisms can be exercised. First, it may be possible that gene inactivation is caused by cell propagation and/or differentiation (Cherry et al. 2000; Laker et al. 1998). By this, former active gene loci are inactivated, while others get active. Since lentiviruses integrate into the host genome, this holds also true for the transgene and possibly affect its transcription rate. Second, the gene inactivation happens immediately after lentiviral transduction and integration as a defense mechanism (Xia et al. 2007). Foreign viral genes are recognized and, thus, inactivated. Silencing is mediated by methylation of the promoter sequence blocking the transgene transcription (Doerfler et al. 1989; Muiznieks and Doerfler 1994). Particularly, the CMV promoter, which is of viral origin, is affected by methylation (Prosch et al. 1995). A similar mechanism might be assumed for EF1α promoter, but with lower peculiarity.

In contrast, transgene expression under control of UbC promotor was maintained at the same level throughout the observation period. Therefore, the UbC promoter seemed not to be affected by silencing in MSC.

### 5.2.3 Promoter-dependent transgene expression: impact on cell viability

Lentivirally mediated gene transfer can impact cell viability and proliferation capacity. It became apparent that the use of strong promoters as CMV or TRE led to reduced viability after transduction. While MSC transduced with a CMV construct recovered over time, the viability was strongly affected for MSC being transduced by a TRE construct. Moreover, the significant reduction of cell viability and growth was prominent throughout the experiments.

It may be hypothesized that the strong activity of the TRE promoter and the resulting excessive transgene levels have reduced cell viability and induced cytotoxicity. Similar effects were already observed for GFP expression using strong promoters. This phenomenon can even be increased by multiple copies (Zychlinski et al. 2008). It may be further speculated that TRE promoter leads to an overload of cellular protein production and degradation

machinery impacting the physiological status of the cell. Especially, GFP-fusion proteins are known to affect cell physiology and inhibit cell growth e.g. due to defective polyubiquitination (Liu et al. 1999; Baens et al. 2006). Similar effects might account for a CMV promoter, which also drives high gene expression. Recovery of MSC being transduced with CMV constructs might be supported by promoter silencing reducing the transgene overload.

### 5.2.4 Concluding remarks for promoter-dependent lentiviral modifications

The magnitude of transgene expression can be modified by substitution of the promoter sequence. Aim of this part was to determine and to optimize lentiviral efficiency in order to achieve a high proportion of MSC overexpressing ITGA4 for proof-of-principle studies. By this, a potential sorting for positive cells could be possibly omitted. Transgene expression under control of TRE led to a high amount of positive MSC with high levels of ITGA4 expression, but impacted considerably cell viability. As seen for UbC-, EF1aα-, and CMV promoter, the number of transgene expressing cells correlated strongly with its genomic copies (CMV> EF1α>UbC). While UbC induced a stable and long-term ITGA4 expression, EF1α and CMV driven expression was affected by silencing.

Of note, a long-term expression of ITGA4 is not necessarily required to improve transmigratory behavior of MSC. Thus, the silencing effect might not play a major role in this case. Since the high number of genomic ITGA4 copies in CMV-ITGA4 MSC might affect their fitness and also bears a higher mutagenic potential, modification with this construct does not seem to be the most beneficial choice. Lentiviral modification by EF1α driven constructs might circumvent this obstacle. With 30% positive MSC, however, sorting for the positive cells would still be required and therefore would not provide substantial benefits over the cell-friendly UbC promoter. Nonetheless, transmigration of EF1α-ITGA4 overexpressing MSC was tested in a pilot experiment. Enhanced transmigration was not observed (Fig. 26). Most likely, this can be ascribed to the low percentage of modified cells and to the generation of a fusion protein, where the GFP-tag impairs the function of the receptor. Although low in efficiency, the UbC-promoter showed some distinct advantages compared to the other promoters. These include the maintenance of cell fitness and a low susceptibility for silencing. Thus, the UbC is attractive for modification of MSC

## 5.3 Overexpression of surface receptors for improved homing towards cerebral ischemia

The directed MSC targeting towards the brain is extremely challenging after minimally-invasive intravascular transplantation since the cells have to overcome several hurdles such as the endothelial barrier or the BBB (Liu et al. 2013). In addition, culture conditions as well as extended expansion periods are influencing the MSC receptor configuration (Rombouts and Ploemacher 2003). It has been shown that culture-expanded MSC dramatically decreased the expression of chemokine receptors and, thus, forfeit the responsiveness to chemotactic stimuli (Wynn et al. 2004). Similar observations apply for adhesion receptors (Kumar and Ponnazhagan 2007; Semon et al. 2010). In this study, MSC were initially expanded and then used in experiments before reaching passage 9. Their CCR2 and ITGA4 mRNA expression was limited (Fig. 28) confirming the insufficient expression of homing receptors as described elsewhere (Semon et al. 2010; Kumar and Ponnazhagan 2007; Ugarte et al. 2003; Spaeth et al. 2008; Chamberlain et al. 2007; Majumdar et al. 2003). Thus, lentiviral driven overexpression of ITGA4 and CCR2 was used to improve homing capabilities of MSC and to facilitate their CNS trafficking.

### 5.3.1 The relevance of CCR2 and ITGA4 for MSC-migration towards cerebral ischemia

The molecules ITGA4 and CCR2 play an important role after cerebral ischemia and are considered to enhance the homing behavior of MSC.

Homing and extravasation of cells from the blood flow relies on inflammatory molecules present at injury site. Cerebral ischemia triggers the release of various cytokines and chemokines mediating the process of post-infarction repair (Le Thuc et al. 2015). Among others, the chemokine MCP1 is crucially involved in these processes (Yamagami et al. 1999; An et al. 2014). It has been associated with trafficking and migration of immune cells or progenitors (Emsley et al. 2008; Abangan, JR et al. 2010) and is upregulated within a few hours after an ischemic insult. Here, elevated MCP1 levels are observed for up to 2 days (Yamagami et al. 1999). Counterpart for MCP1 is the G-protein coupled chemokine receptor CCR2, which is expressed on monocytes, T-cells and a small proportion of MSC (Yamagami et al. 1999; Wang et al. 2002a; Chamberlain et al. 2007; Spaeth et al. 2008). The MCP1/CCR2 axis might also play a role in stem cell homing towards (ischemic) lesion sites, and thus, may contribute to improved recovery of function mediated by MSC (Wang et al. 2002b; Jiang et al. 2008). As demonstrated by Guo and coworkers, CCR2-expressing MSC migrated towards MCP1 *in vitro* and in an experimental model of dilated cardiomyopathy (Guo et al. 2013a).

Next to MCP1, the adhesion molecule VCAM1 is involved in inflammation and progression of the ischemic injury after a cerebral insult (Supanc et al. 2011). It mediates the adhesion to endothelial cell and, therefore, initiates the extravasation of leukocytes (Wang et al. 2007). Prior work has shown increased VCAM1 expression within hours after cerebral ischemia (Blann et al. 1999; Justicia et al. 2006). Although its expression peaks 24h after onset, VCAM1 remains upregulated for a longer period (Justicia et al. 2006). The reinforced endothelial adhesion through VCAM1/VLA4 interaction also provides a potential mechanism to improve homing of systemically infused progenitors. For example, binding capabilities of

glial precursors to endothelium were modulated by transfection of ITGA4 and ITGB1. The resulting overexpression of VLA4 led to increased adhesion *in vitro* and *in vivo* as seen in an experimental model of brain inflammation (Gorelik et al. 2012).

Taken together, targeting the MCP1/CCR2 axis and the reinforcement of endothelial adhesion by VL4/VCAM1 might improve homing of MSC towards cerebral ischemia.

### 5.3.2 Lentiviral modification of MSC for improved homing

Lentiviral transductions with the pFN-3M or pFN-7M construct resulted in 3-8% ITGA4/CCR2-positive MSC (Fig. 27). Thus, sorting for the CCR2- or ITGA4-positive subset through gating for tdTomato expression was conducted resulting in enrichment of the desired population (Fig. 29). Transgene expression was maintained over ~2 additional passages until use in experiments

Compared to other methods, lentiviral modification induces a long-lasting protein expression. By this, the MSC modification is not restricted to a short expression time window making lentiviruses a suitable tool for proof-of-principle studies. In this part of the study, the transgene expression was put under control of an UbC promoter cloned 34-37 bp upstream of the start codon. As elucidated previously, the UbC-promoter counts as a weak promoter that causes only a tenuous transgene expression (Qin et al. 2010; Varma et al. 2011). Since other tested promoters did not yield a significant advantage, the UbC promoter was a valid choice due to its insusceptibility for silencing. Although the low efficiency can be deduced predominantly from the promoter capabilities, the design of the expression cassette might have had additional impact. The tdTomato reporter was coupled to the first transgene by an IRES-sequence. This strategy ensured the expression of two proteins from a bi-cistronic mRNA driven by a single promotor. Despite its popularity, there is a major drawback leading to an underestimation of positive cells (Chiarella et al. 2014). The expression of an IRES-dependent second gene from a bi-cistronic vector can be reduced to only 6-50% compared to the expression upstream of IRES (Mizuguchi et al. 2000). Nevertheless, it is widely applied to detect and isolate positive cells and was also successfully used in stem and progenitor cells (Chung et al. 2006; Wunderlich et al. 2006; Ye et al. 2004). Here, it was inevitable to introduce a fluorescence reporter that is not directly fused to the transgene. First, the low transduction efficiency required an option to identify and to select positive MSC. Second, it was likely that a fusion construct impairs the receptor function fundamentally as seen in Fig. 26.

Hence, purification of the positive MSC-fraction required an initial expansion followed by fluorescence activated cell sorting. Thereafter, further cultivation is needed to expand the population and to obtain a sufficient number of MSC for experiments. Lentiviral transduction and subsequent sorting was successfully applied to MSC as shown by Kallifatidis and coworkers. They observed 23% positive MSC after lentiviral transfer of a GFP-transgene (MOI 2) and enriched the positive fraction by flow cytometry (Kallifatidis et al. 2008). In contrast to their results, subsequent downregulation of transgene expression was not observed what can be associated with the promoter choice (van Damme et al. 2006). Nonetheless, the cultivation period is remarkably prolonged and additional effects by the

sorting cannot be excluded. Hydrodynamic, extensional and shear forces are applied during the sorting procedure possibly causing significant cell damage (Mollet et al. 2008). It was already described earlier that extensive and prolonged cultivation of MSC can affect their phenotype, proliferation, and protein expression profile (Baksh et al. 2007) and, thus, their stem cell properties. Of note, neither cell characteristics nor proliferation potential was significantly affected by lentiviral transduction and sorting in this study (see chapter 5.3.3). Alternative enrichment methods such as antibiotic-based selection for transduced MSC might have provided some advantage (Kallifatidis et al. 2008) but require a multi-cistronic vector. This complicates the estimation of individual transgene expression and it cannot be excluded that the antibiotic burden influences the stem cell fitness (Piccoli et al. 2008).

### 5.3.3 Characterization of modified MSC

The mesenchymal and tissue stem cell committee of the International Society for Cell Therapy (ISCT) has defined minimal criteria for human MSC. These comprise plastic adherence and proliferation in cell culture, the expression of certain surface receptors, lack of hematopoietic markers, as well as the differentiation into adipogenic, osteogenic, and chondrogenic (Dominici et al. 2006). In this study, MSC were routinely subjected to respective quality controls after lentiviral infection and sorting.

Initial expansion until passage 2 and determination of surface receptors was conducted by the manufacturer. It should be taken into account that MSC do not express a unique marker that verifies their identity (Docheva et al. 2007). MSC were positive for specific markers and cell adhesion molecules such as CD44, CD90, and CD29 (ITGB1) and low in expression for hematopoietic lineage markers (CD45, CD34, CD11b/c). This meets the ISCT-criteria indicating the mesenchymal lineage properties (Kern et al. 2006).

MSC were adherent to plastic surfaces and possessed a fibroblast-like morphology (Fig. 30). Thus, cell phenotypes were in line with ISCT criteria and with previous descriptions (Friedenstein et al. 1976; Pittenger et al. 1999; Li et al. 2015) and were not affected by lentiviral transduction or sorting.

Expansion capacity and proliferation are crucial hallmarks of MSC identity. Growth characteristics are also important for application in cell therapy and tissue engineering (Hass et al. 2011). In this study, MSC showed robust proliferation with a PDT of ~2 days (Fig. 31). For bone marrow derived MSC, a proliferation doubling time of 2 days has been described repeatedly (Baksh et al. 2007; Lu et al. 2006). Therefore, proliferation capacity of lentivirally modified MSC was in line with the common observations (Baksh et al. 2007).

Multi-lineage potential of cultured and modified MSC was assessed by adipogenic, osteogenic, and chondrogenic differentiation trials (Fig. 32). Conditions favoring the adipogenic differentiation of MSC are established by the addition of specific supplements such as indomethacine, isobutylmethylxanthine (IBMX), or hydrocortisone (Shipunova et al. 2013; Scott et al. 2011). These components activate transcription factors such as peroxisome proliferator-activated receptor gamma (PPARγ) or CCAAT/enhancer binding protein beta (C/EBPβ) (Qian et al. 2010). Osteogenesis was induced by addition of osteogenic cocktail composed of dexamethasone, ascorbate-phosphate, β-glycerolphosphate, and bone

morphogenetic protein 2 (BMP2). The osteogenic cocktail stimulated the proliferation of MSC and activated osteogenic signaling pathways (e.g. Wnt, Hedgehoc) that control the Runt-related transcription factor 2 (Runx2) (James 2013). Furthermore, it also supports the maturation of new-born osteoblasts and generation of matrix (Langenbach and Handschel 2013). Induction of chondrogenesis depends on cell density. Thus, the differentiation protocol included pelleting of MSC, maintenance of serum-free environment, and the addition of growth factors (Ullah et al. 2012). By this, the differentiation of MSC into chondrocytes was promoted as was the formation of proteoglycans (e.g. aggrecan, versican, brevican). By these protocols the multipotency of MSC was shown in this and other studies ((Shipunova et al. 2013; Langenbach and Handschel 2013). Similar differentiation patterns were observed for adipogenesis, osteogenesis, and chondrogenesis of CTRL-MSC, ITGA4-MSC, and CCR2. Hence, lentiviral infection, sorting and transgene expression did not impact the multilineage differentiation potential.

MSC used in this study fulfilled the ISCT criteria although they were not of human origin. Therefore, it was assumed that used cells are stem cells of the mesenchymal lineage and maintained their characteristics upon lentiviral modification and sorting.

### 5.3.4 (Trans)migration activity of modified MSC *in vitro*

*In vitro* migration of CTRL-MSC, ITGA4-MSC, and CCR2-MSC towards MCP1 was evaluated in a Boyden chamber setup. Migration across the endothelium was simulated by a confluent GPNT monolayer grown onto the upper site of the transwell mesh. MCP1 was applied to attract MSC to the lower transwell chamber. Contrary to expectations, CCR2 overexpression did not lead to enhanced migration towards MCP1. Instead, ITGA4-MSC showed enhanced transmigration activity compared to control and CCR2-MSC (Fig. 33).

Chemokines usually induce migration in a dose-dependent manner. Increasing chemokine concentrations are augmenting the migration until reaching a saturation threshold. Further increase of concentration will not enhance the chemotaxis. Here, experiments were conducted in the presence of MCP1 ranging between 10ng/well (12ng/mL) and 100ng/well (120ng/mL). The directed migration towards the chemokine indicates chemotaxis and excludes chemokinesis (non-specific movement of stimulated cells). One study reported increasing transwell migration up to 300ng MCP1/mL (Wang et al. 2002a). Thus, higher transmigration activity with a chemokine concentration beyond 100ng/well might be expected. In accordance, saturation was not observed in the course of the experiments and it may be assumed that concentration > 100ng/well could have further enhanced the transmigration activity.

The importance of the MCP1/CCR2 axis for stem cell migration has already been elucidated in numerous studies (Andres et al. 2011; Belema-Bedada et al. 2008). It was demonstrated that MCP1 stimulates MSC migration *in vitro* through transwell inserts with a pore size of 8µm as used in this study (Belema-Bedada et al. 2008; Boomsma and Geenen 2012; Xu et al. 2010). This is basically in accordance with the present findings regarding the chemotactic activity of CTRL-MSC. Nonetheless, this was also surprising since there was a limited CCR2 expression observed on mRNA and protein-level. Moreover, chemotaxis was specifically

induced by MCP1 as distinguishable by concentration dependent transmigratory activity (Fig. 33). This suggests that MCP1 may act though receptors other than CCR2. MCP1 can also operate through CCR4 signaling as demonstrated in cancer studies (Sun et al. 2016). Thus, it may be hypothesized that MSC responded to MCP1 via CCR4 signaling, especially since CCR4 is sufficiently expressed on MSC (Ponte et al. 2007; Chamberlain et al. 2007). Nonetheless, further evaluation would be necessary to clarify the role of MCP1/CCR4 signaling in MSC.

Successful overexpression of CCR2 might have driven the assumption that the chemokine receptor occurs in functional state. This includes the correct protein folding, availability of the binding pocket, and the integration into the downstream signaling networks. The nucleotide sequence for CCR2 was verified by sequencing after cloning. Therefore, it can be excluded that potential errors on DNA-level (e.g. mutations or open-reading frameshifts) caused protein misbehavior. Several downstream acting proteins are involved in the signal transduction upon chemokine receptor binding. It has been shown for leukocytes that the mediator FROUNT links the activated CCR2 receptor to the PI(3)K-Rac-lamellipodium-protrusion cascade and stimulates migration (Terashima et al. 2005). The necessity of CCR2-FROUNT interaction for MCP1-mediated homing has been shown for bone marrow derived MSC (Belema-Bedada et al. 2008). According to the conducted literature research, the study of Belema-Bedada and coworkers is the only one reporting the relevance of MCP1/CCR2 signaling with FROUNT in MSC. Of note, MSC showed a natural high expression of CCR2 and FROUNT (Belema-Bedada et al. 2008). This is in contrast to the present work, where CCR2 expression was determined at relatively low levels. Since the overexpression of CCR2 in this study did not lead to enhanced migration, it may be speculated that the receptor was not fully linked to the signaling cascade. Thus, it might be possible that the overexpressed receptor did not operate on a functional level and remained effectless for migration towards MCP1 gradients. In addition, it was reported that MCP1 stimulation did not necessarily result in migration, although the CCR2 receptor is expressed (Ringe et al. 2007). In fact, the number of migrating MSC was even lower than in negative controls (Ringe et al. 2007). Similarly, CCR2-overexpressing MSC appeared to migrate less efficiently compared to controls in the present study (Fig. 33). Chemokine receptors are stored within the cytoplasm and are mobilized to the cell membrane upon chemokine stimulation (Wynn et al. 2004). In the present study, the CCR2 receptor may not have been successfully transported to the cell surface. However, this does not explain the reduced migration of CCR2-MSC compared to controls. It rather implies that CCR2 overexpression disturbed the physiological behavior of MSC upon MCP1 stimulation. To conclude, the reason for reduced transmigration of CCR2-MSC awaits further clarification, but the contribution of other factors should be taken into account (Zannettino et al. 2008).

Contrasting the observations after lentiviral modification with CCR2, overexpression of ITGA4 induced enhanced transmigration towards MCP1 of MSC *in vitro*. In general, integrins are capable of establishing sudden and very stable interactions with their endothelial ligand expressed on the inner vessel wall after inflammation (Montresor et al. 2012). Conformational changes of integrin receptors are influencing their affinity, and, thus their adhesiveness (Chavakis et al. 2009). It is known from the leukocyte adhesion cascade, that chemokine signaling and integrin adhesion are indirectly linked via several signaling

pathways. During slow rolling, the cell is exposed to immobilized chemokines at the apical site of endothelial cells (Henschler et al. 2008). Binding of the chemokines to their G-protein-coupled receptors (GPCR) induces downstream signaling by activation of phospholipase C (PLC, Fig. 43A) (Chavakis et al. 2009).

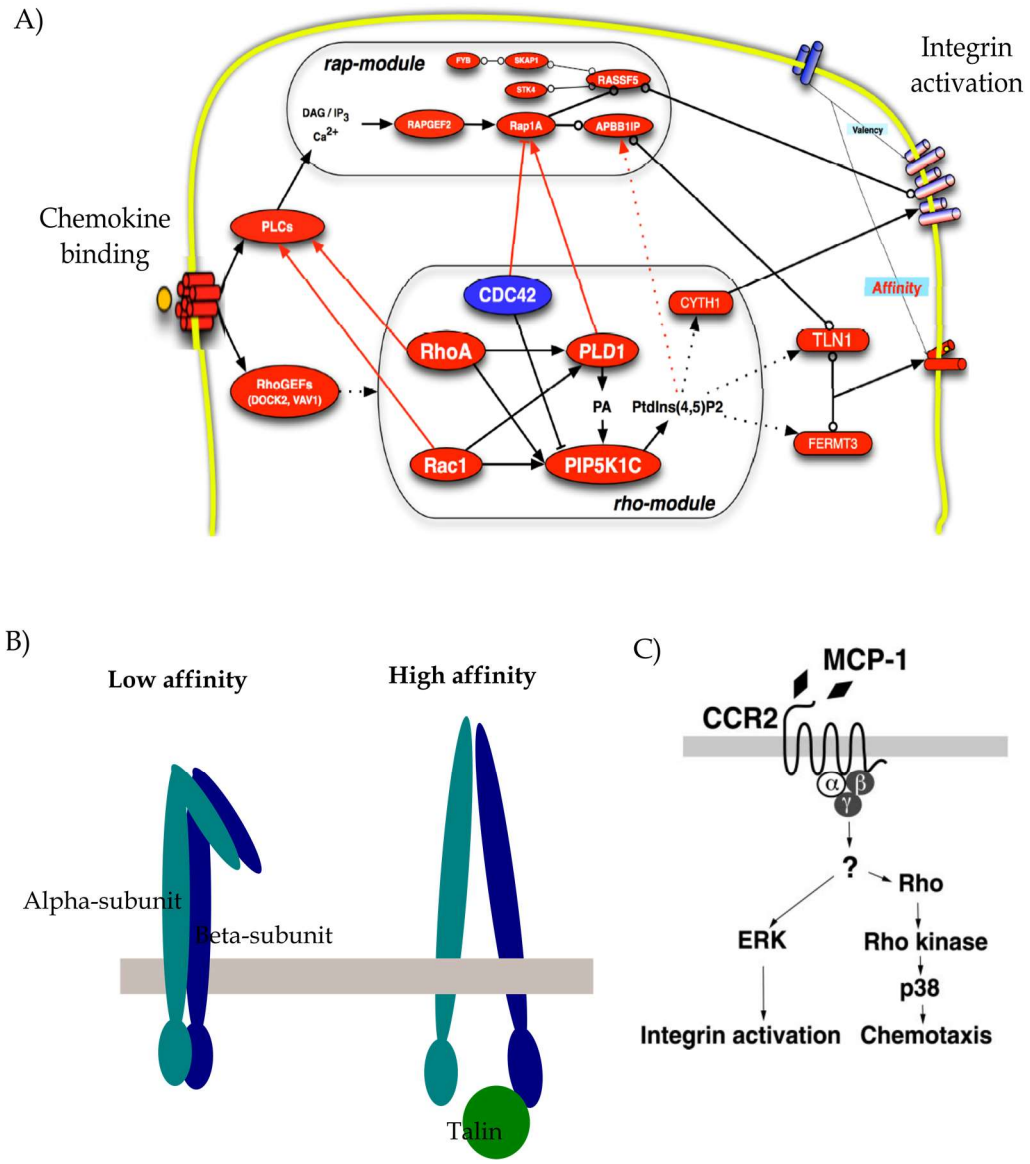


***Fig. 43 Interplay between chemokine signaling and Integrin activation.*** *Chemokines modulate integrin affinity via rap and rho modules (A). Picture modified after Montresor et al. (2012). Affinity of integrin receptors is affected by the conformation (B). Bend receptors are associated with low ligand affinity, while straightened receptors have high ligand affinity. MCP1-mediated integrin activation is dependent on ERK signaling and chemotaxis is regulated by rho (C). Original picture taken from Ashida et al. (2001).*

This results in an increase of intracellular $Ca^{2+}$-levels. $Ca^{2+}$-ions activate guanine-exchange factors (GEF) which in turn activate small GTPases, such as Rap1 or Rho a (Ley et al. 2007). One of the targets from this downstream signaling is talin1 (TLN1). TLN1 moves to the cell membrane and interacts with the β-subunit of the integrin receptor (Vestweber 2012). This

leads to a widening of the distance between cytoplasmic tails of both subunits and straitening of the integrin receptor (Fig. 43B). Therefore, the binding pocket is exposed. Blocking experiments with THP-cells have revealed the interplay between MCP1 and VLA4 (Fig. 43C) (Ashida et al. 2001). It was shown that MCP1 causes the activation of VLA4 via ERK pathway and, furthermore, induce chemotaxis via p38-MAPK. It might be concluded that overexpression of ITGA4 has provided a pool of VLA4 receptors in MSC. Given the possibility that MCP1 may act through alternative chemokine receptors, the connection was established between GPCR signaling and VLA4 activation.

The driving mechanisms of MSC migration through the endothelium remain unclear due to uncertainty of contributing key pathways. Nonetheless, enhanced VLA4 expression has increased *in vitro* migration. In leukocytes, the chemokine activated VLA4 interacts with VCAM1. Integrin-associated proteins get activated and form focal adhesion sites. These attachment sites have a signaling function. This leads to reorganization of the cytoskeleton and contributes to substrate adhesion, change in cell polarity, directed cell migration, and motility (Docheva et al. 2007). Furthermore, chemokine receptors are concentrated at the leading pol and recruit VLA4 to the guiding lamellopodium by signaling through small GTPases (Hyun et al. 2009). This mechanism can be conveyed to MSC and it seems feasible that it has mediated the enhanced *in vitro* migration after ITGA4 overexpression. However, further experiments are necessary to clearly identify the contributing molecules and mechanisms.

### 5.3.5 Interaction of MSC with endothelium *in vitro*

Overcoming the endothelial barrier is the most important step during the MSC homing process. An endothelial co-culture model was established *in vitro* to obtain a better understanding of MSC transmigration. The MSC localization was investigated by confocal fluorescence microscopy after overnight transmigratory stimulation. MSC were counted and classified according to their position to the endothelial monolayer. A profound migration across the endothelial monolayer was observed for CTRL-MSC, ITGA4-MSC, and CCR2-MSC.

MSC are capable of migration over the endothelial barrier. However, contributing steps as well as the molecular basis are only partially understood. Hitherto, it is known that endothelial activation by TNFα, VLA4/VCAM1 interaction, and GPCR signaling play a crucial role (Steingen et al. 2008; Matsushita et al. 2011; Teo et al. 2012; Schmidt et al. 2006b; Liu et al. 2013). TNFα is a proinflammatory cytokine that activates the endothelium. It stimulates the expression and presentation of chemokines and adhesion molecules including VCAM1 (Ley et al. 2007). It was observed by Teo et al. that MSC transmigration and adhesion was substantially increased upon TNFα-activation of the endothelium. Thus, the endothelial monolayer was stimulated with TNFα (100ng/mL) prior to the Boyden chamber assay in the present study.

The morphology of the transmigrating MSC can provide important information. The MSC exhibits a rounded shape during establishment of the first contact with the endothelium (Steingen et al. 2008; Teo et al. 2012). Then, the MSC starts to flatten and to integrate into the

endothelial monolayer. Of note, the amount of flattened and integrated MSC increases with progressing time and depends on the endothelial phenotype (Steingen et al. 2008). In this study, a very small proportion of MSC showed a spherical shape. Flattened morphology of MSC was also observed (Fig. 34 and Fig. 35, category ii and iii). Importantly, those categories comprised the majority of the non-migrated MSC, while integrated MSC were determined to some extent (category iv). Although the categorization was not conducted with serial observations over time, this is in line with the findings of Steingen and colleagues above described.

In addition, there are some similarities with proposed MSC transmigration by Teo et al. (Fig. 44) (Teo et al. 2012), who also initially observed a round MSC morphology. In the subsequent step, the MSC is stepwisely advancing into the endothelial monolayer (GPNT). Integration and subendothelial spreading were discovered prior to completed transmigration. Establishing of endothelial contact and subsequent activation induces cytoskeletal reorganization. Thus, flattened morphology is an expression of the structural alteration due to transmigration. Of note, differences were observed regarding cup- and gap formation (Fig. 44, B and C).

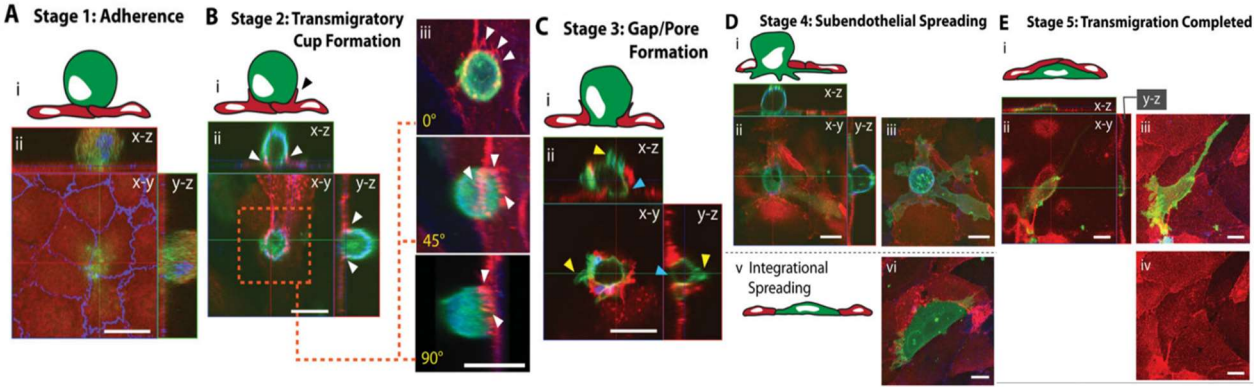


***Fig. 44 MSC transmigration over an endothelial monolayer.*** *GPNT cells were grown on cover slides and co-cultivated with MSC. Transmigration involved adherence (A), transmigratory cup formation with microvilli-like projections, gap formation associated with endothelial discontinuity (C), invasion of subendothelial space by advancincing lamellopodium (D). Temporarly integration is possible before completing transmigration (E). Picture modified after Teo et al. (2012). Scale bar indicates 20µm.*

The limited third dimension might have led to these differences since their co-cultivation was conducted on glass slides. In a Boyden chamber, a third dimension is expanded and an additional barrier is provided by the mesh. Thus, the transmigration model might be extended by migration through a pore. As observed in the present study, the MSC formed plasmic podia advancing through the GPNT monolayer into a pore (category (v)a). A completely condensed and rounded morphology was observed for MSC within the pore (category (v)b). The migration through the small pore sizes required extensive reorganization to enable the passage. A similar phenomenon might be required *in vivo* for migration through the endothelial basal membrane.

The role of integration into the endothelial monolayer is discussed controversially and seems overestimated by *in vitro* studies (Teo et al. 2012). A proportion of MSC was observed to integrate into the vascular cell layer in this and other studies (Teo et al. 2012; Steingen et al. 2008; Matsushita et al. 2011). However, extent of integration versus diapedesis varies and integration seemed to be favored in some cases (Steingen et al. 2008). It has been suggested, that the quality of the endothelial monolayer affects the mode of action (Teo et al. 2012). Physiological aspects including shear stress, integrity of the monolayer, or cell-substrate contacts are different with *in vitro* cultivation of endothelial cells. The lack of shear stress, as well as the plating on stiff substrates lead to hypercontractile phenotype. This can cause cell retraction and gap formation. Thus, integration is facilitated and transmigration occurs less pronounced (Krishnan et al. 2011). In turn, sufficiently formed monolayers support transmigration and reduce integration. Therefore, the confluency of the endothelial monolayer was grown to 100% prior to transmigration experiments. The retained physiology further supports the robust barrier function of the GPNT cell line (Teo et al. 2012). Thus, it may be assumed that integration as observed in this study occurs as a contributing event to transmigration rather than due to endothelial discontinuity.

In addition, the endothelial phenotype is a key player for transmigration and can influence the morphological appearance of MSC (Steingen et al. 2008; Segers, Vincent et al. 2006). A considerable variety derives from the endothelial diversity within the vascular tree. For instance, the amount of tight junctions differs, causes variable permeability (Dejana et al. 1995), and influences formation of plasmic podia and transmigration speed. The GPNT cell line was isolated from rat brain endothelium and immortalized by SV40 (Greenwood et al. 1996; Regina et al. 1999). This cell line was already used in *in vitro* transmigration setups similar to this study (Matsushita et al. 2011). According to Matsushita et al., a time dependent transmigration of MSC across the GPNT monolayer was observed involving spherical morphology and invasion of the subendothelial space. Furthermore, transmigration via temporarily occurring endothelial gaps was observed (Matsushita et al. 2011), what could be considered as integration. Similar morphological appearances were classified in the present study, indicating that the GPNT phenotype supports MSC transmigration.

Previous data suggest that transendothelial MSC migration is initiated similarly to that of leukocytes and hematopoetic stem cells (Ley et al. 2007). The leukocyte guidance through endothelial junction requires a strict coordination of the interaction between the endothelial monolayer and the transmigrating leukocyte (Nourshargh and Alon 2014). When the leukocyte has found an optimal spot for transmigration between endothelial cells, integrin binding to VCAM1 or ICAM1 activates signaling pathways what leads to high receptor trafficking in the endothelial cell. Interaction of integrins with their ligands prepares the endothelium for resolution of the intercellular adhesion structures. MSC and endothelium actively cooperate to enable guidance towards the subendothlelial space (Teo et al. 2012). It may be assumed that MSC-endothelial cooperation may induce similar endothelial signaling and reorganization as seen after leukocyte adhesion. An important role for MSC transmigration is attributed to interaction of VLA4 and VCAM1. In the present study, it was observed that ITGA4 overexpression led to enhanced transmigration. In addition, numbers of non-migrated ITGA4-MSC (Fig. 35, category ii) appeared increased compared to controls

or CCR2-MSC. In contrast, overexpression of CCR2 did not achieve an increased transmigratory rate. This indicates an intensified interaction of ITGA4-MSC with the endothelium prior to transmigration. Therefore, it may be concluded that increased availability of ITGA4, and thus VLA4 lead to enhanced cooperation between MSC and endothelium and transmigration. Accordingly, it was shown that ITGA4 upregulation by adenoviral transfection leads to a 10-fold increase of bone homing compared to controls (Kumar and Ponnazhagan 2007) whereas blocking of VCAM1 or VLA4 decreases transmigration significantly (Steingen et al. 2008).

### 5.3.6 Delivery and homing of MSC towards cerebral ischemia after intra-arterial transplantation

For cell therapy, efficient delivery and homing of transplanted cells to injured tissue plays a major role. Major questions are (i) how many MSC home towards cerebral ischemia and (ii) if the homing behavior can be influenced by overexpression of ITGA4 or CCR2.

In the present study, cerebral ischemia was induced by a transient MCAO using the filament model. MCAO produced an ischemic lesion affecting the striatum and cortex in the ipsilateral hemisphere (Fig. 36). This is in line with other studies that were observing ischemic lesions or similar extent using the same MCAO model (Calloni et al. 2010; Garcia et al. 1995). The advantage of this model is that an invasive craniotomy is not necessary and it avoids additional extralesional influences on cranial pressure and temperature (Chiang et al. 2011), as well as craniotomy-associated animal morbidity (Carmichael 2005). Furthermore, the filament model follows the human stroke conditions of large artery occlusion (Carmichael 2005) and allows blood flow restoration and reperfusion. With that, this method also reflects endovascular thrombectomy, where the blood flow is restored by mechanical removal of the clot (Sutherland et al. 2016). In this study, reperfusion of the MCA was allowed after 120min. This is important as a permanent occlusion of the MCA at the site of the intra-arterial administration would block the stem cell delivery to the infarcted area (Vikram 2015).

The time point of administration is a critical issue that has an impact on the outcome. MSC were administered via the ECA stump 24h after MCAO. This is comparable to other studies (Mitkari et al. 2014; Toyoshima et al. 2015), where transplantation was conducted 24h after MCAO. Numerous controversies are existing regarding the optimal time point of cell transplantation. Early stem cell transplantations are aiming to reduce the infarct size by attenuating inflammation and cell death (Toyoshima et al. 2015). In contrast, later administration (days-weeks) are intended to support recovery and regeneration (Vikram 2015). MSC are able to address both mechanisms and, thus, are applicable in a wide therapeutic time window (Leong et al. 2013). The acute phase of stroke is characterized by the release of proinflammatory and inflammatory signals, chemoattractant cues and the expression of adhesion molecules. This provides the basis for the attraction of stem cells (Borlongan et al. 2012). Furthermore, the breakdown of the blood brain barrier may facilitate the entry of stem cells into the brain parenchyma (Vikram 2015). In this study, MSC should be delivered to the cerebrum and home to the ischemic area based on the upregulation of

inflammatory key molecules within the subacute phase. Thus, the administration time point was chosen for 24h after MCAO.

In this study, $0.5x10^6$ MSC per rat were administered within a volume of 600-700µl over a period of <5min. Inappropriate infusion velocity, cell dose or infusion volume can cause complications after intra-arterial cell transplantation as shown by Cui et al (Cui et al. 2015). It is stated that higher cell doses (e.g. $1x10^6$ cells/animal) evoked a reduction in cerebral blood flow and harbor the risk for microemboli. Hence, the cell dose was decreased to $0.5x10^6$ MSC/animal to avoid adverse effects. Further decrease was not realized to ensure sufficient signal strength during SPECT imaging. It was also observed that infusion volume does not play a major role, while the infusion velocity dramatically impacts the CBF (Cui et al. 2015). Faster infusion times (~3min) does not cause severe side effects (Cui et al. 2015). Although the infusion speed was slightly longer, no adverse effects were observed in the present study.

Localization of intra-arterially administered MSC was assessed by SPECT/CT over a time course of 48h. Prior to transplantation, MSC were labelled with $^{111}$In-oxine. This isotope is a suitable radioactive tracer with a half-life radioactivity of 2.8 days. The labelling procedure is simple and highly efficient. The isotope can penetrate the cell membrane easily due to its lipophilic character. After uptake to the cytoplasm, $^{111}$In is bound to cytoplasmic proteins (Raki et al. 2013). Labelling efficiencies for MSC were reported to range between 25-90% (Bindslev et al. 2006; Gholamrezanezhad et al. 2009). This is in line with the labelling efficiency of ~50% observed in this study. Adjustment of labelling dose is a crucial parameter in order to avoid radioactivity-associated cell toxicity. It was reported that labelling with an $^{111}$In dose below 38 Bq/cell did not affect cell viability (Yoon et al. 2010). Labelling dose was ~0.03 Bq/cell and, thus, cell toxicity due to radioactivity was not an issue in this study (~85% viable cells).

A major advantage of SPECT imaging is the possibility to evaluate the accumulation of cells in the ischemic brain in relation to other organs. With the choice of tracer, it is also possible to follow the time-dependent distribution of cells after a single injection (Raki et al. 2013). It turned out that transplanted MSC were not efficiently transported to the brain rather the cells were detected in the facial soft tissue in the majority of the animals. Therefore, the homing behavior was only assessable to a lower extent. The facial accumulation can be explained with the vascular anatomy of the rat and the *modus operanti* of the transplantation (Fig. 45, A and B).

MSC were transported to the supply areas of the ICA and its branches after transplantation. A major branch of the ICA is the pterygolpalatine artery (PPA) supplying the facial parts. A considerable amount of MSC was localized outside of the skull within the soft tissue indicating unintended distribution of the cell suspension via the PPA rather than to the ischemic brain (Fig. 45B). Numerous studies tried to circumvent this scenario by the improvement of transplantation techniques including the occlusion of the PPA prior to cell administration or by the application of an ICA injection needle (Fig. 45C) (Chua et al. 2011; Zhu et al. 2011; Guo et al. 2013b). The PPA-occlusion prevents the blood- and cell shunt into the PPA, but it is difficult because of its anatomical position (Chen et al. 2008) and can have severe side effects such as secondary embolism (Guo et al. 2013b). A targeted administration

to the ICA by temporal PPA-occlusion reduces this risk and prevents a fault localization of MSC. On the other hand, the physiological situation was maintained in this study what is an important fact for potential translation to the clinics.

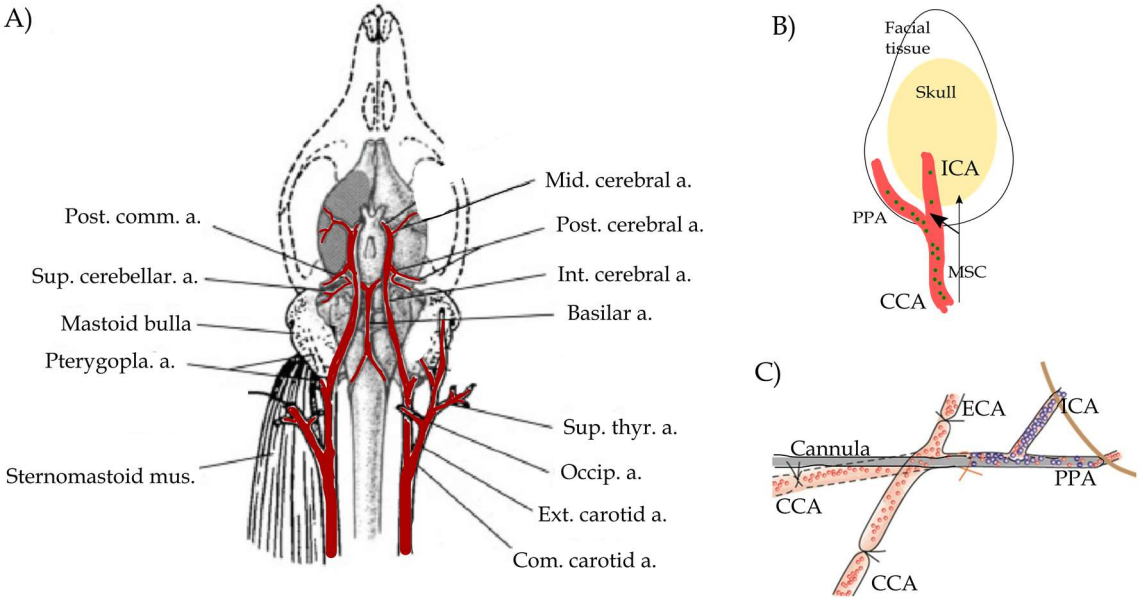


***Fig. 45 Vascular anatomy of the rat.*** *Branching of the common carotid artery (Com. Carotid a) is given in (A). Picture modified after (Longa et al. 1989). Schematic drawing of MSC distribution from internal carotid artery (ICA) toward facial parts via the pterygopalatine artery (PPA) (B). The ICA injection needle (C) has a closed end for occlusion of the PPA and a lateral opening for stem cell delivery into the ICA. Picture modified after Guo et al. (2013b)*

Biodistribution of systematically administered stem cells has already been monitored after MCAO in several studies (Tang et al. 2015; Khabbal et al. 2014; Lappalainen et al. 2008). Depending on the administration route, the biodistribution differed markedly. The stem cell entrapment in internal organs was observed after intravenous transplantation (Lappalainen et al. 2008; Tang et al. 2015). In contrast, intra-arterial infusion usually results in targeting stem cells to the ischemic hemisphere as observed by SPECT imaging (Lappalainen et al. 2008; Mitkari et al. 2013; Khabbal et al. 2014). In the follow-up, the researchers were able to obtain radioactive signals from the brain 24h after transplantation (Mitkari et al. 2013). Although the present study was conducted similarly, the cerebral targeting of MSC was a major obstacle (Fig. 37) and related to the above described errors of the model.

However, MSC could be delivered at least partly to the ischemic brain in a few animals. A retrospective analysis of these animals (1-2 animals per group, n=1-2, Fig. 47, supplements) showed that initial accumulation from brain was resolved within 24h after administration and further clearance of MSC from brain proceeded until termination of the experiment (Fig. 47, A and B; see also Fig. 37, A and B). In parallel, detection of radioactive signals from liver, spleen and guts were increasingly detected. (Fig. 47A, 48h). The clearance of bone-marrow derived MSC from the brain was reported to occur quickly after infusion (Khabbal et al. 2014). The radioactive signal of these $^{99m}$Tc-labelled MSC was reduced by 50% within 6h

(Khabbal et al. 2014). This is in line with the relocation from the brain in the present study. However, the mechanism behind the clearance is not completely resolved. It was speculated that transplanted cells become necrotic or apoptotic as indicated by TUNEL staining 3h after transplantation (Brenneman et al. 2010). Another possibility is the phagocytosis by host immune cells such as microglia. In particularly, this hold true if cells were transplanted in the acute phase of cerebral ischemia (Rosenblum et al. 2012).

Independently from the fate of transplanted MSC, the radioactive signal was primarily found in the internal organs 48h after transplantation (Fig. 37A, Fig. 38, see also Fig. 47A). Considerable high amount of radioactivity was measured in liver, kidneys and spleen. The relocation to the internal organs, as seen in Fig. 47A and Fig. 37, was already observed previously (Khabbal et al. 2014; Makinen et al. 2006; Mitkari et al. 2013; Detante et al. 2009; Vasconcelos-dos-Santos et al. 2012). The radioactivity from spleen, kidney and liver has been associated with the elimination process of administered cells (Khabbal et al. 2014; Mitkari et al. 2013; Detante et al. 2009). Nonetheless, it cannot be completely excluded that MSC at least partly home to the internal organs (Vasconcelos-dos-Santos et al. 2012).

It remained unclear whether the cells were actively homing to the brain or stuck within the vasculature (Mitkari et al. 2013). There is a possibility that cells were entrapped in small diameter vessels, being compressed due to severe brain edema after MCAO (Mitkari et al. 2013). Also the size of MSC might be taken into account for passive entrapment in cerebral micro-vessels. The average size of culture-expanded rat MSC with ~23µm (Toma et al. 2009) leads to microvascular plugging and decreased blood flow (Mitkari et al. 2014). This decreases the MSC survival rate dramatically (Mitkari et al. 2014). Furthermore, SPECT is unable to dissociate radioactive signals from surviving cells or debris from dead cells (Raki et al. 2013). Thus, it is necessary to investigate the fate of transplanted cells by histology or sophisticated high-resolution imaging techniques such as two-photon imaging. Of note, only a very small fraction of cells was found to engraft in the brain (Mitkari et al. 2013). Furthermore, it was not possible to elucidate the effect of ITGA4 or CCR2 overexpression on homing towards ischemic brain due to transplantation-related difficulties.

### 5.3.7 MSC after intra-arterial transplantation: are they really gone?

Part of the current study addressed the fate of transplanted MSC and whether they are able to enter the brain parenchyma. Since the used model had major limitations, this question could be only answered insufficiently. Speculations about the fate of transplanted cells were deduced from histology performed with animals that showed acceptable MSC delivery to the brain. Here, MSC could be localized in cortical and meningeal areas in the ischemic zone. A particular hint about destination of transplanted MSC could be derived from positive labelling with IBA1 due to colocalization with MSC reporter protein.

A cascade of immunologic processes is initiated after onset of cerebral ischemia. The ischemic insult leads to the activation of local immune cells residing within the brain and to the recruitment of leukocytes from peripheral organs (Wang et al. 2007). Macrophages and microglia play a particular role during post-ischemic injury (Patel et al. 2013). Microglia are an integral part of the resident immune cell population in the CNS (Mildner et al. 2007) and

possess a radial morphology with thin ramified processes under healthy conditions (Schwarz et al. 2012). With proinflammatory signaling during cerebral ischemia, microglia become activated and present a rounded, amoeboid phenotype (Nayak et al. 2014). Once activated, they develop macrophage-like properties including phagocytosis, cytokine production, and antigen presentation (Patel et al. 2013; Iadecola and Anrather 2011). This leads to leakage of the blood brain barrier and facilitates the entry of peripheral immune cells (Patel et al. 2013). As the first actors, microglia are ought to remove debris and dead cells (Denes et al. 2007). From that point of view, it seems likely that transplanted MSC were phagocytosed and thus cleared from the brain. That assumption is underlined by the observation that the fluorescent MSC-reporter (GFP or tdTomato) was colocalized with the macrophage marker IBA1.

The internalized particle is digested in the phagolysosome upon phagocytosis (Aderem 2003). Since the phagolysosome is a defined compartment of the cytoplasm, one could expect a spatially separated localization of the MSC-fluorescence reporter. However, this was not the case. The fluorescence protein was rather evenly distributed within the cytoplasm. Hence, other mechanisms might explain the fate of MSC. One possibility is that MSC differentiated into cells of the monocytic/macrophage lineage, and thus occur positive for IBA1. A direct differentiation of MSC into microglia is not described in the literature leaving some uncertainty about this issue.

The spleen plays an important role in stroke pathology. A reservoir of lymphocytes, macrophages, neutrophils, and NK-cells is found within the red pulp. These cells are released into the circulation upon cerebral ischemia and migrate to the brain (Seifert et al. 2012). Furthermore, it is known that those peripheral blood-borne immune cells can enter the ischemic brain by different routes. Among others, they are delivered via the branching vascular tree that enters the brain over the pia mater and the subarachnoidal space (Möller et al. 2014). The breakdown of the blood brain barrier further facilitates the ingress of (immune) cells (Wilson et al. 2010). Intravascular transplanted MSC are distributed by the blood flow. With their surface receptor expression, including overexpressed VLA4 or CCR2, they are at least partially susceptible for the leukocytic recruiting signals. Unfortunately, the literature is scarce, but at least one publication described the localization of MSC in the peri-infarct regions 24h after transplantation (Vasconcelos-dos-Santos et al. 2012). In this study, MSC were rediscovered within the cortical infarct border. Thus, it might be possible that they enter the brain by the meninges covering the ischemic area as observed for leukocytes (Möller et al. 2014).

### 5.3.8 Concluding remarks for improved homing after ITGA4- and CCR2 overexpression

In this part of the study, it was shown that lentiviral transduction of homing receptors and sorting did not affect MSC characteristics. Furthermore, ITGA4 overexpression increased *in vitro* transmigration towards MCP1 what could be correlated with enhanced cooperation with the endothelium. In contrast, the overexpression of CCR2 impaired the *in vitro* transmigration.

Modified MSC were further transplanted intra-arterially after transient MCAO in rats. The transplantation method was fraught with problems making it difficult to assess the homing

behavior of MSC. Nevertheless, SPECT/CT imaging revealed a relocalization of transplanted cells towards the internal organs (liver and spleen) indicating rejection and clearance.

Histology from selected animals showed evidence for MSC within the cortical infarct zone. Their immunoreactivity for IBA1 points towards differentiation into macrophage/microglia/monocyte phenotype or their phagocytosis. However, in both cases the egress from the blood vessel and the entrance into the brain parenchyma is likely and might be supported by the blood brain barrier breakdown. The role of ITGA4- or CCR2 overexpression on MSC could not be clarified for homing towards cerebral ischemia.

# 6 Conclusions and outlook

The potential of genetically modified MSC is already well documented for numerous diseases (Levy et al. 2013; Ryser et al. 2008; Kumar and Ponnazhagan 2007). Although the benefit of genetically "improved" MSC is reasonable, there are only limited studies available addressing cerebrovascular disorders. In this particular field genetically optimizations have the capacity to bridge over MSC-shortcomings in homing and, thus, enhance their therapeutic effect. Essential point of this study was to genetically modify MSC and, by that, to enhance their homing behavior towards cerebral ischemia.

On the basis of comparative analyses on molecular and cellular level, it was possible to identify key aspects that drive successful surface receptor modification on MSC by mRNA and lentiviruses. Modalities of genetic modification were exercised with the example of ITGA4-overexpression. In the first part of this study, the goal was to engineer MSC with ITGA4 by mRNA transfection (objective I). mRNA based modifications were successfully applied for transient receptor overexpression of MSC. It was possible to achieve ITGA4-specific processing, maturation, and assembly with ITGB1 to a functional VLA4 receptor. Lipofection induced only a partial and transient decrease of cell viability. Furthermore, the maximal extent of protein expression was observed 12-24h after transfection. This provides a time window that is suitable for potential transplantation preparation. Importantly, the ITGA4 protein expression is maintained over several hours and, thus, the MSC is allowed to be efficiently targeted to intended the lesion site. Furthermore, it turned out that capping as an important structural element has a major impact on extent of protein expression. Particularly, the preparation of physiologically capped mRNA (Cap0, Cap1) was shown to foster efficient protein translation. This was associated with the structural characteristics of the mRNA and with the translation machinery. Importantly, MSC multipotency potential is not affected by mRNA transfection. In summary, mRNA based gene transfer is a powerful, efficient and non-toxic approach for transient protein expression in MSC. It can be concluded that mRNA based modification is eligible and can be considered as a useful tool for clinical grade cell-based therapeutics

Lentiviruses are a widely used tools to drive the overexpression of certain proteins on stem cells. The protein expression is thereby associated with promoter strength. A second aim of this study was the evaluation of long-term ITGA4 expression and its optimization by promoter substitution (objective II). All tested promoters induced long-term expression. Although very efficient, stronger promoters crucially affected cell viability and were susceptible for silencing. While lentiviral expression was well tolerated with UbC- and EF1α-bearing constructs, they are also less efficient. Efficiency and tolerance were associated with promoter strength. The UbC-promoter is considered suitable for protein overexpression in MSC since cell characteristics were not affected. It was also less prone to silencing. The population of positive cells can be enriched by flow cytometric sorting without affection of important MSC characteristics. To conclude, lentiviruses are very powerful vectors for long-term genetic modification and this study underlines the importance of promoter choice for the overexpression of surface receptors on MSC.

Both, mRNA and lentiviral-based modification are efficient tools to mediate gene transfer for hard to transfect cell types and difficult transgenes (Dullaers et al. 2004; Boissel et al. 2012). A summarizing overview for both techniques is given in table 7.

*Tab. 7 Comparison of lentiviral and mRNA based modification of MSC*

| Parameter | Lentiviral-based modification | mRNA-based modification |
|---|---|---|
| **Efficiency** | 5 – 80% promoter/copy/transgene-dependent | 50-85% cap/transgene dependent |
| **mRNA-expression/level** | Moderate-high and sustained, but promoter dependent | Very high, but timely limited |
| **Duration of protein expression** | Long-term (days, weeks) promoter-dependent | Transient, up to 24h |
| **Functionality of overexpressed ITGA4 protein** | Given by enhanced transmigration *in vitro* | Given by enhanced LDV-FITC binding |
| **Biological safety** | Safety level 2 required | Safety level 1 sufficient |
| **Workload** | Sophisticated cloning, lentiviral production, time intensive | Simple DNA-template, fast production and read out possible, cost-intensive |
| **Transplantation safety** | Risk of mutagenesis | Considered as clinically safe |
| **Application** | Experimental proof-of-principle applications favored, increased mutagenic risk by repetition | Experimental and most likely clinically applications, repetitions are possible |
| **Phenotype, viability, proliferation** | Maintained (except for TRE driven constructs) | Maintained, transient impact of transfection |
| **Multipotency** | Unaffected; Maintenance of adipogenic, osteogenic, and chondrogenic potential | Unaffected; Maintenance of adipogenic, osteogenic, and chondrogenic potential |

MSC have attracted considerable attention for the development of cell-based therapies for stroke. It was overserved in preclinical studies, that homing and migration towards the brain is very limited after intravascular transplantation of MSC. Proinflammatory molecules that are upregulated after cerebral ischemia can attract MSC if they are susceptible for these signals. Thus, the overexpression of ITGA4 and CCR2 on MSC was intended to increase their homing towards cerebral ischemia (objectives III and IV).

By the overexpression of CCR2, MSC ought to enhance their responsiveness to the chemokine MCP1 what is released from the ischemic lesion (objective III). Although the receptor was successfully expressed after lentiviral modification and sorting, it did not enhance the *in vitro* migration towards MCP1. It was assumed that CCR2 overexpression had an impact on the physiological behavior that even decreased migration *in vitro*. In contrast, ITGA4-overexpression enhanced the *in vitro* migration. The generation of a fully functional

VLA4 receptor was driven by ITGA4 overexpression and most likely its sufficient integration into various signaling pathways enhanced the migration towards MCP1. It can further be concluded, that MSC (trans)migration is based on the interaction with the endothelium, which is strengthened after ITGA4 overexpression (objective IV).

While the *in vitro* data were promising, the evaluation of *in vivo* homing towards cerebral ischemia remains open. The circumstances during intra-arterial transplantation led to accumulation in facial soft tissue instead in the brain. Thus, the MSC homing and extravasation after overexpression of CCR2 or ITGA4 could not be analyzed properly (objective III and IV). In general, MSC relocated to internal organs independent from successful delivery to the brain or modification. This was considered as part of their elimination process. In a few examples, it was possible to target the MSC to the brain. There, they departed the blood vessel and entered the brain parenchyma but were then probably attacked by the immune system.

Albeit the obtained data confirmed the eligibility of transient and long-term genetic modification and further highlighted the promising role of ITGA4 to enhance MSC homing, a few points remained open. These need to be elucidated in future research and particularly address the homing behavior *in vivo*. In a first instance, the intra-arterial infusion technique has to be optimized in order to avoid accumulation of MSC outside of the skull. Then, biodistribution and pathotropism assessment of modified MSC is possible and expose if receptor overexpression indeed enhances the cerebral homing. In a second instance, the detailed mechanism of cerebral pathotropism need to be clarified for MSC. This requires more specialized *in vitro* tests such as the evaluation of endothelial adhesion in flow chamber setup. Here, the application of additional parameters as shear stress allow the molecular assessment of endothelial interaction, and, furthermore, enhance the predictability of *in vivo* extravasation behavior. On the other hand, sophisticated imaging techniques such as two-photon imaging allow the specific determination of MSC homing and extravasation in the brain as well as the influence of receptor overexpression. In a final instance, the functional evaluation of mRNA-modified MSC in an animal model of stroke to assess applicability and effectivity of the approach.

# 7 References


Abangan RS, JR, Williams CR, Mehrotra M, Duncan JD, Larue AC (2010) MCP1 directs trafficking of hematopoietic stem cell-derived fibroblast precursors in solid tumor. Am J Pathol 176(4):1914–1926. doi: 10.2353/ajpath.2010.080839

Aderem A (2003) Phagocytosis and the inflammatory response. J Infect Dis 187 Suppl 2:S340-5. doi: 10.1086/374747

Aggarwal S, Pittenger MF (2005) Human mesenchymal stem cells modulate allogeneic immune cell responses. Blood 105(4):1815–1822. doi: 10.1182/blood-2004-04-1559

Aldridge V, Garg A, Davies N, Bartlett DC, Youster J, Beard H, Kavanagh DP, Kalia N, Frampton J, Lalor PF, Newsome PN (2012) Human mesenchymal stem cells are recruited to injured liver in a beta1-integrin and CD44 dependent manner. Hepatology 56(3):1063–1073. doi: 10.1002/hep.25716

Amiri F, Jahanian-Najafabadi A, Roudkenar MH (2015) In vitro augmentation of mesenchymal stem cells viability in stressful microenvironments: In vitro augmentation of mesenchymal stem cells viability. Cell Stress Chaperones 20(2):237–251. doi: 10.1007/s12192-014-0560-1

An C, Shi Y, Li P, Hu X, Gan Y, Stetler RA, Leak RK, Gao Y, Sun B-L, Zheng P, Chen J (2014) Molecular dialogs between the ischemic brain and the peripheral immune system: dualistic roles in injury and repair. Prog Neurobiol 115:6–24. doi: 10.1016/j.pneurobio.2013.12.002

Andres RH, Choi R, Pendharkar AV, Gaeta X, Wang N, Nathan JK, Chua JY, Lee SW, Palmer TD, Steinberg GK, Guzman R (2011) The CCR2/CCL2 interaction mediates the transendothelial recruitment of intravascularly delivered neural stem cells to the ischemic brain. Stroke 42(10):2923–2931. doi: 10.1161/STROKEAHA.110.606368

Ansboro S, Greiser U, Barry F, Murphy M (2012) Strategies for improved targeting of therapeutic cells: implications for tissue repair. Eur Cell Mater 23:310-8; discussion 318-9

Armando S, Quoyer J, Lukashova V, Maiga A, Percherancier Y, Heveker N, Pin J-P, Prezeau L, Bouvier M (2014) The chemokine CXC4 and CC2 receptors form homo- and heterooligomers that can engage their signaling G-protein effectors and betaarrestin. FASEB J 28(10):4509–4523. doi: 10.1096/fj.13-242446

Ashida N, Arai H, Yamasaki M, Kita T (2001) Distinct signaling pathways for MCP-1-dependent integrin activation and chemotaxis. J Biol Chem 276(19):16555–16560. doi: 10.1074/jbc.M009068200

Augello A, Kurth TB, Bari C de (2010) Mesenchymal stem cells: a perspective from in vitro cultures to in vivo migration and niches. Eur Cell Mater 20:121–133

Avci-Adali M, Behring A, Keller T, Krajewski S, Schlensak C, Wendel HP (2014) Optimized conditions for successful transfection of human endothelial cells with in vitro synthesized and modified mRNA for induction of protein expression. J Biol Eng 8(1):8. doi: 10.1186/1754-1611-8-8

Baek SJ, Kang SK, Ra JC (2011) In vitro migration capacity of human adipose tissue-derived mesenchymal stem cells reflects their expression of receptors for chemokines and growth factors. Exp Mol Med 43(10):596–603. doi: 10.3858/emm.2011.43.10.069

Baens M, Noels H, Broeckx V, Hagens S, Fevery S, Billiau AD, Vankelecom H, Marynen P (2006) The dark side of EGFP: defective polyubiquitination. PLoS One 1:e54. doi: 10.1371/journal.pone.0000054

Baksh D, Song L, Tuan RS (2004) Adult mesenchymal stem cells: characterization, differentiation, and application in cell and gene therapy. J Cell Mol Med 8(3):301–316

Baksh D, Yao R, Tuan RS (2007) Comparison of proliferative and multilineage differentiation potential of human mesenchymal stem cells derived from umbilical cord and bone marrow. Stem Cells 25(6):1384–1392. doi: 10.1634/stemcells.2006-0709

Barry FP, Murphy JM (2004) Mesenchymal stem cells: clinical applications and biological characterization. Int J Biochem Cell Biol 36(4):568–584. doi: 10.1016/j.biocel.2003.11.001

Bartholomew A, Patil S, Mackay A, Nelson M, Buyaner D, Hardy WB, Mosca JD, Sturgeon C, Siatskas M, Mahmud N, Ferrer K, Deans R, Moseley A, Hoffman R, Devine SM (2001) Baboon mesenchymal stem cells can be genetically modified to secrete human erythropoietin in vivo. Hum Gene Ther 12(12):1527–1541. doi: 10.1089/10430340152480258

Becker A de, van Hummelen P, Bakkus M, Vande Broek I, Wever J de, Waele M de, van Riet I (2007) Migration of culture-expanded human mesenchymal stem cells through bone marrow endothelium is regulated by matrix metalloproteinase-2 and tissue inhibitor of metalloproteinase-3. Haematologica 92(4):440–449

Becker A de, van Riet I (2016) Homing and migration of mesenchymal stromal cells: How to improve the efficacy of cell therapy? World J Stem Cells 8(3):73–87. doi: 10.4252/wjsc.v8.i3.73

Bednarczyk JL, Szabo MC, McIntyre BW (1992) Post-translational processing of the leukocyte integrin alpha 4 beta 1. J Biol Chem 267(35):25274–25281

Belema-Bedada F, Uchida S, Martire A, Kostin S, Braun T (2008) Efficient homing of multipotent adult mesenchymal stem cells depends on FROUNT-mediated clustering of CCR2. Cell Stem Cell 2(6):566–575. doi: 10.1016/j.stem.2008.03.003

Bergeron E, Basak A, Decroly E, Seidah NG (2003) Processing of alpha4 integrin by the proprotein convertases: histidine at position P6 regulates cleavage. Biochem J 373(Pt 2):475–484. doi: 10.1042/BJ20021630

Bienroth S, Keller W, Wahle E (1993) Assembly of a processive messenger RNA polyadenylation complex. EMBO J 12(2):585–594

Bindslev L, Haack-Sorensen M, Bisgaard K, Kragh L, Mortensen S, Hesse B, Kjaer A, Kastrup J (2006) Labelling of human mesenchymal stem cells with indium-111 for SPECT imaging: effect on cell proliferation and differentiation. Eur J Nucl Med Mol Imaging 33(10):1171–1177. doi: 10.1007/s00259-006-0093-7

Bing W, Pang X, Qu Q, Bai X, Yang W, Bi Y, Bi X (2016) Simvastatin improves the homing of BMSCs via the PI3K/AKT/miR-9 pathway. J Cell Mol Med 20(5):949–961. doi: 10.1111/jcmm.12795

Blann A, Kumar P, Krupinski J, McCollum C, Beevers DG, Lip GY (1999) Soluble intercelluar adhesion molecule-1, E-selectin, vascular cell adhesion molecule-1 and von Willebrand factor in stroke. Blood Coagul Fibrinolysis 10(5):277–284

Bliss TM, Andres RH, Steinberg GK (2010) Optimizing the success of cell transplantation therapy for stroke. Neurobiol Dis 37(2):275–283. doi: 10.1016/j.nbd.2009.10.003

Bobis S, Jarocha D, Majka M (2006) Mesenchymal stem cells: characteristics and clinical applications. Folia Histochem Cytobiol 44(4):215–230

Boiret N, Rapatel C, Veyrat-Masson R, Guillouard L, Guerin J-J, Pigeon P, Descamps S, Boisgard S, Berger MG (2005) Characterization of nonexpanded mesenchymal progenitor cells from normal adult human bone marrow. Exp Hematol 33(2):219–225. doi: 10.1016/j.exphem.2004.11.001

Boissel L, Betancur M, Lu W, Wels WS, Marino T, van Etten RA, Klingemann H (2012) Comparison of mRNA and lentiviral based transfection of natural killer cells with chimeric antigen receptors recognizing lymphoid antigens. Leuk Lymphoma 53(5):958–965. doi: 10.3109/10428194.2011.634048

Boomsma RA, Geenen DL (2012) Mesenchymal stem cells secrete multiple cytokines that promote angiogenesis and have contrasting effects on chemotaxis and apoptosis. PLoS One 7(4):e35685. doi: 10.1371/journal.pone.0035685

Borlongan CV, Glover LE, Sanberg PR, Hess DC (2012) Permeating the blood brain barrier and abrogating the inflammation in stroke: implications for stroke therapy. Curr Pharm Des 18(25):3670–3676

Borlongan CV, Glover LE, Tajiri N, Kaneko Y, Freeman TB (2011) The great migration of bone marrow-derived stem cells toward the ischemic brain: therapeutic implications for stroke and other neurological disorders. Prog Neurobiol 95(2):213–228. doi: 10.1016/j.pneurobio.2011.08.005

Boura JS, Santos FD, Gimble JM, Cardoso CMP, Madeira C, Cabral JMS, Silva CLd (2013) Direct head-to-head comparison of cationic liposome-mediated gene delivery to mesenchymal stem/stromal cells of different human sources: a comprehensive study. Hum Gene Ther Methods 24(1):38–48. doi: 10.1089/hgtb.2012.185

Brenneman M, Sharma S, Harting M, Strong R, Cox CS, JR, Aronowski J, Grotta JC, Savitz SI (2010) Autologous bone marrow mononuclear cells enhance recovery after acute ischemic stroke in young and middle-aged rats. J Cereb Blood Flow Metab 30(1):140–149. doi: 10.1038/jcbfm.2009.198

Bronckaers A, Hilkens P, Martens W, Gervois P, Ratajczak J, Struys T, Lambrichts I (2014) Mesenchymal stem/stromal cells as a pharmacological and therapeutic approach to accelerate angiogenesis. Pharmacol Ther 143(2):181–196. doi: 10.1016/j.pharmthera.2014.02.013

Bruder SP, Jaiswal N, Haynesworth SE (1997) Growth kinetics, self-renewal, and the osteogenic potential of purified human mesenchymal stem cells during extensive subcultivation and following cryopreservation. J Cell Biochem 64(2):278–294

Burkard KT, Butler JS (2000) A nuclear 3'-5' exonuclease involved in mRNA degradation interacts with Poly(A) polymerase and the hnRNA protein Npl3p. Mol Cell Biol 20(2):604–616

Cai A, Jankowska-Anyszka M, Centers A, Chlebicka L, Stepinski J, Stolarski R, Darzynkiewicz E, Rhoads RE (1999) Quantitative assessment of mRNA cap analogues as inhibitors of in vitro translation. Biochemistry 38(26):8538–8547. doi: 10.1021/bi9830213

Calloni RL, Winkler BC, Ricci G, Poletto MG, Homero WM, Serafini EP, Corleta OC (2010) Transient middle cerebral artery occlusion in rats as an experimental model of brain ischemia. Acta Cir Bras 25(5):428–433

Cao J, Wang L, Du Z-j, Liu P, Zhang Y-b, Sui J-f, Liu Y-p, Lei D-l (2013) Recruitment of exogenous mesenchymal stem cells in mandibular distraction osteogenesis by the

stromal cell-derived factor-1/chemokine receptor-4 pathway in rats. Br J Oral Maxillofac Surg 51(8):937–941. doi: 10.1016/j.bjoms.2013.05.003

Caplan AI (1994) The mesengenic process. Clin Plast Surg 21(3):429–435

Caplan AI, Bruder SP (2001) Mesenchymal stem cells: building blocks for molecular medicine in the 21st century. Trends Mol Med 7(6):259–264

Caplan AI, Correa D (2011) The MSC: an injury drugstore. Cell Stem Cell 9(1):11–15. doi: 10.1016/j.stem.2011.06.008

Caplan AI, Dennis JE (2006) Mesenchymal stem cells as trophic mediators. J Cell Biochem 98(5):1076–1084. doi: 10.1002/jcb.20886

Carmeliet P, Jain RK (2011) Molecular mechanisms and clinical applications of angiogenesis. Nature 473(7347):298–307. doi: 10.1038/nature10144

Carmichael ST (2005) Rodent models of focal stroke: size, mechanism, and purpose. NeuroRx 2(3):396–409. doi: 10.1602/neurorx.2.3.396

Carvalho MM, Teixeira FG, Reis RL, Sousa N, Salgado AJ (2011) Mesenchymal stem cells in the umbilical cord: phenotypic characterization, secretome and applications in central nervous system regenerative medicine. Curr Stem Cell Res Ther 6(3):221–228

Chamberlain G, Fox JM, Ashton BA, Middleton J (2007) Concise review: mesenchymal stem cells: their phenotype, differentiation capacity, immunological features, and potential for homing. Stem Cells 25(11):2739–2749. doi: 10.1634/stemcells.2007-0197

Chamberlain G, Smith H, Rainger GE, Middleton J (2011) Mesenchymal stem cells exhibit firm adhesion, crawling, spreading and transmigration across aortic endothelial cells: effects of chemokines and shear. PLoS One 6(9):e25663. doi: 10.1371/journal.pone.0025663

Chavakis E, Choi EY, Chavakis T (2009) Novel aspects in the regulation of the leukocyte adhesion cascade. Thromb Haemost 102(2):191–197. doi: 10.1160/TH08-12-0844

Chen J, Li Y, Katakowski M, Chen X, Wang L, Lu D, Lu M, Gautam SC, Chopp M (2003a) Intravenous bone marrow stromal cell therapy reduces apoptosis and promotes endogenous cell proliferation after stroke in female rat. J Neurosci Res 73(6):778–786. doi: 10.1002/jnr.10691

Chen J, Zhang ZG, Li Y, Wang L, Xu YX, Gautam SC, Lu M, Zhu Z, Chopp M (2003b) Intravenous administration of human bone marrow stromal cells induces angiogenesis in the ischemic boundary zone after stroke in rats. Circ Res 92(6):692–699. doi: 10.1161/01.RES.0000063425.51108.8D

Chen Q, Shou P, Zhang L, Xu C, Zheng C, Han Y, Li W, Huang Y, Zhang X, Shao C, Roberts AI, Rabson AB, Ren G, Zhang Y, Wang Y, Denhardt DT, Shi Y (2014) An osteopontin-integrin interaction plays a critical role in directing adipogenesis and osteogenesis by mesenchymal stem cells. Stem Cells 32(2):327–337. doi: 10.1002/stem.1567

Chen W, Li M, Cheng H, Yan Z, Cao J, Pan B, Sang W, Wu Q, Zeng L, Li Z, Xu K (2013) Overexpression of the mesenchymal stem cell Cxcr4 gene in irradiated mice increases the homing capacity of these cells. Cell Biochem Biophys 67(3):1181–1191. doi: 10.1007/s12013-013-9632-6

Chen Y, Ito A, Takai K, Saito N (2008) Blocking pterygopalatine arterial blood flow decreases infarct volume variability in a mouse model of intraluminal suture middle cerebral artery occlusion. J Neurosci Methods 174(1):18–24. doi: 10.1016/j.jneumeth.2008.06.021

Cheng Z, Ou L, Zhou X, Li F, Jia X, Zhang Y, Liu X, Li Y, Ward CA, Melo LG, Kong D (2008) Targeted migration of mesenchymal stem cells modified with CXCR4 gene to infarcted myocardium improves cardiac performance. Mol Ther 16(3):571–579. doi: 10.1038/sj.mt.6300374

Cherry SR, Biniszkiewicz D, van Parijs L, Baltimore D, Jaenisch R (2000) Retroviral expression in embryonic stem cells and hematopoietic stem cells. Mol Cell Biol 20(20):7419–7426

Chiang T, Messing RO, Chou W-H (2011) Mouse model of middle cerebral artery occlusion. J Vis Exp(48). doi: 10.3791/2761

Chiarella E, Carra G, Scicchitano S, Codispoti B, Mega T, Lupia M, Pelaggi D, Marafioti MG, Aloisio A, Giordano M, Nappo G, Spoleti CB, Grillone T, Giovannone ED, Spina R, Bernaudo F, Moore MAS, Bond HM, Mesuraca M, Morrone G (2014) UMG Lenti: novel lentiviral vectors for efficient transgene- and reporter gene expression in human early hematopoietic progenitors. PLoS One 9(12):e114795. doi: 10.1371/journal.pone.0114795

Chigaev A, Waller A, Amit O, Sklar LA (2008) Galphas-coupled receptor signaling actively down-regulates alpha4beta1-integrin affinity: a possible mechanism for cell de-adhesion. BMC Immunol 9:26. doi: 10.1186/1471-2172-9-26

Chopp M, Zhang ZG, Jiang Q (2007) Neurogenesis, angiogenesis, and MRI indices of functional recovery from stroke. Stroke 38(2 Suppl):827–831. doi: 10.1161/01.STR.0000250235.80253.e9

Chua JY, Pendharkar AV, Wang N, Choi R, Andres RH, Gaeta X, Zhang J, Moseley ME, Guzman R (2011) Intra-arterial injection of neural stem cells using a microneedle technique does not cause microembolic strokes. J Cereb Blood Flow Metab 31(5):1263–1271. doi: 10.1038/jcbfm.2010.213

Chung KY, Morrone G, Schuringa JJ, Plasilova M, Shieh J-H, Zhang Y, Zhou P, Moore MAS (2006) Enforced expression of NUP98-HOXA9 in human CD34(+) cells enhances stem cell proliferation. Cancer Res 66(24):11781–11791. doi: 10.1158/0008-5472.CAN-06-0706

Conget PA, Minguell JJ (1999) Phenotypical and functional properties of human bone marrow mesenchymal progenitor cells. J Cell Physiol 181(1):67–73. doi: 10.1002/(SICI)1097-4652(199910)181:1<67:AID-JCP7>3.0.CO;2-C

Cooray S, Howe SJ, Thrasher AJ (2012) Retrovirus and lentivirus vector design and methods of cell conditioning. Methods Enzymol 507:29–57. doi: 10.1016/B978-0-12-386509-0.00003-X

Corish P, Tyler-Smith C (1999) Attenuation of green fluorescent protein half-life in mammalian cells. Protein Eng 12(12):1035–1040

Craigie R (2001) HIV integrase, a brief overview from chemistry to therapeutics. J Biol Chem 276(26):23213–23216. doi: 10.1074/jbc.R100027200

Cselenyak A, Pankotai E, Horvath EM, Kiss L, Lacza Z (2010) Mesenchymal stem cells rescue cardiomyoblasts from cell death in an in vitro ischemia model via direct cell-to-cell connections. BMC Cell Biol 11:29. doi: 10.1186/1471-2121-11-29

Cui L, Kerkela E, Bakreen A, Nitzsche F, Andrzejewska A, Nowakowski A, Janowski M, Walczak P, Boltze J, Lukomska B, Jolkkonen J (2015) The cerebral embolism evoked by intra-arterial delivery of allogeneic bone marrow mesenchymal stem cells in rats is related to cell dose and infusion velocity. Stem Cell Res Ther 6:11. doi: 10.1186/scrt544

Decroly E, Ferron F, Lescar J, Canard B (2012) Conventional and unconventional mechanisms for capping viral mRNA. Nat Rev Microbiol 10(1):51–65. doi: 10.1038/nrmicro2675

Dejana E, Corada M, Lampugnani MG (1995) Endothelial cell-to-cell junctions. FASEB J 9(10):910–918

Denes A, Vidyasagar R, Feng J, Narvainen J, McColl BW, Kauppinen RA, Allan SM (2007) Proliferating resident microglia after focal cerebral ischaemia in mice. J Cereb Blood Flow Metab 27(12):1941–1953. doi: 10.1038/sj.jcbfm.9600495

Detante O, Moisan A, Dimastromatteo J, Richard M-J, Riou L, Grillon E, Barbier E, Desruet M-D, Fraipont F de, Segebarth C, Jaillard A, Hommel M, Ghezzi C, Remy C (2009) Intravenous administration of 99mTc-HMPAO-labeled human mesenchymal stem cells after stroke: in vivo imaging and biodistribution. Cell Transplant 18(12):1369–1379. doi: 10.3727/096368909X474230

Devine SM (2002) Mesenchymal stem cells: will they have a role in the clinic? J Cell Biochem Suppl 38:73–79

Ding D-C, Lin C-H, Shyu W-C, Lin S-Z (2013) Neural stem cells and stroke. Cell Transplant 22(4):619–630. doi: 10.3727/096368912X655091

Docheva D, Popov C, Mutschler W, Schieker M (2007) Human mesenchymal stem cells in contact with their environment: surface characteristics and the integrin system. J Cell Mol Med 11(1):21–38. doi: 10.1111/j.1582-4934.2007.00001.x

Doerfler W, Hoeveler A, Weisshaar B, Dobrzanski P, Knebel D, Langner KD, Achten S, Muller U (1989) Promoter inactivation or inhibition by sequence-specific methylation and mechanisms of reactivation. Cell Biophys 15(1-2):21–27

Dominici M, Le Blanc K, Mueller I, Slaper-Cortenbach I, Marini FC, Krause D, Deans R, Keating A, Prockop DJ, Horwitz EM (2006) Minimal criteria for defining multipotent mesenchymal stromal cells. The International Society for Cellular Therapy position statement. Cytotherapy 8(4):315–317. doi: 10.1080/14653240600855905

D'souza N, Rossignoli F, Golinelli G, Grisendi G, Spano C, Candini O, Osturu S, Catani F, Paolucci P, Horwitz EM, Dominici M (2015) Mesenchymal stem/stromal cells as a delivery platform in cell and gene therapies. BMC Med 13:186. doi: 10.1186/s12916-015-0426-0

Dullaers M, Breckpot K, van Meirvenne S, Bonehill A, Tuyaerts S, Michiels A, Straetman L, Heirman C, Greef C de, van der Bruggen P, Thielemans K (2004) Side-by-side comparison of lentivirally transduced and mRNA-electroporated dendritic cells: implications for cancer immunotherapy protocols. Mol Ther 10(4):768–779. doi: 10.1016/j.ymthe.2004.07.017

Eckert MA, Vu Q, Xie K, Yu J, Liao W, Cramer SC, Zhao W (2013) Evidence for high translational potential of mesenchymal stromal cell therapy to improve recovery from ischemic stroke. J Cereb Blood Flow Metab 33(9):1322–1334. doi: 10.1038/jcbfm.2013.91

Emsley HCA, Smith CJ, Tyrrell PJ, Hopkins SJ (2008) Inflammation in acute ischemic stroke and its relevance to stroke critical care. Neurocrit Care 9(1):125–138. doi: 10.1007/s12028-007-9035-x

Endres M, Dirnagl U, Moskowitz MA (2009) The ischemic cascade and mediators of ischemic injury. Handb Clin Neurol 92:31–41. doi: 10.1016/S0072-9752(08)01902-7

Everaert BR, Bergwerf I, Vocht N de, Ponsaerts P, Van Der Linden, Annemie, Timmermans J-P, Vrints CJ (2012) Multimodal in vivo imaging reveals limited allograft survival, intrapulmonary cell trapping and minimal evidence for ischemia-directed BMSC homing. BMC Biotechnol 12:93. doi: 10.1186/1472-6750-12-93

Ezquer FE, Ezquer ME, Vicencio JM, Calligaris SD (2016) Two complementary strategies to improve cell engraftment in mesenchymal stem cell-based therapy: increasing transplanted cell resistance and increasing tissue receptivity. Cell Adh Migr:0. doi: 10.1080/19336918.2016.1197480

Farhan H, Rabouille C (2011) Signalling to and from the secretory pathway. J Cell Sci 124(Pt 2):171–180. doi: 10.1242/jcs.076455

Ferreira E, Potier E, Vaudin P, Oudina K, Bensidhoum M, Logeart-Avramoglou D, Mir LM, Petite H (2012) Sustained and promoter dependent bone morphogenetic protein expression by rat mesenchymal stem cells after BMP-2 transgene electrotransfer. Eur Cell Mater 24:18–28

Ferry N, Pichard V, Sebastien Bony DA, Nguyen TH (2011) Retroviral vector-mediated gene therapy for metabolic diseases: an update. Curr Pharm Des 17(24):2516–2527

Fischer UM, Harting MT, Jimenez F, Monzon-Posadas WO, Xue H, Savitz SI, Laine GA, Cox CS, JR (2009) Pulmonary passage is a major obstacle for intravenous stem cell delivery: the pulmonary first-pass effect. Stem Cells Dev 18(5):683–692. doi: 10.1089/scd.2008.0253

Follenzi A, Ailles LE, Bakovic S, Geuna M, Naldini L (2000) Gene transfer by lentiviral vectors is limited by nuclear translocation and rescued by HIV-1 pol sequences. Nat Genet 25(2):217–222. doi: 10.1038/76095

Francois S, Mouiseddine M, Allenet-Lepage B, Voswinkel J, Douay L, Benderitter M, Chapel A (2013) Human mesenchymal stem cells provide protection against radiation-induced liver injury by antioxidative process, vasculature protection, hepatocyte differentiation, and trophic effects. Biomed Res Int 2013:151679. doi: 10.1155/2013/151679

Friedenstein AJ, Gorskaja JF, Kulagina NN (1976) Fibroblast precursors in normal and irradiated mouse hematopoietic organs. Exp Hematol 4(5):267–274

Garcia JH, Liu KF, Ho KL (1995) Neuronal necrosis after middle cerebral artery occlusion in Wistar rats progresses at different time intervals in the caudoputamen and the cortex. Stroke 26(4):636-42; discussion 643

George PM, Steinberg GK (2015) Novel Stroke Therapeutics: Unraveling Stroke Pathophysiology and Its Impact on Clinical Treatments. Neuron 87(2):297–309. doi: 10.1016/j.neuron.2015.05.041

Gholamrezanezhad A, Mirpour S, Ardekani JM, Bagheri M, Alimoghadam K, Yarmand S, Malekzadeh R (2009) Cytotoxicity of 111In-oxine on mesenchymal stem cells: a time-dependent adverse effect. Nucl Med Commun 30(3):210–216. doi: 10.1097/MNM.0b013e328318b328

Gorelik M, Orukari I, Wang J, Galpoththawela S, Kim H, Levy M, Gilad AA, Bar-Shir A, Kerr DA, Levchenko A, Bulte JWM, Walczak P (2012) Use of MR cell tracking to evaluate targeting of glial precursor cells to inflammatory tissue by exploiting the very late antigen-4 docking receptor. Radiology 265(1):175–185. doi: 10.1148/radiol.12112212

Gossen M, Bujard H (1992) Tight control of gene expression in mammalian cells by tetracycline-responsive promoters. Proc Natl Acad Sci U S A 89(12):5547–5551

Greenwood J, Pryce G, Devine L, Male DK, dos Santos WL, Calder VL, Adamson P (1996) SV40 large T immortalised cell lines of the rat blood-brain and blood-retinal barriers retain their phenotypic and immunological characteristics. J Neuroimmunol 71(1-2):51–63

Grinnemo KH, Mansson A, Dellgren G, Klingberg D, Wardell E, Drvota V, Tammik C, Holgersson J, Ringden O, Sylven C, Le Blanc K (2004) Xenoreactivity and engraftment of

human mesenchymal stem cells transplanted into infarcted rat myocardium. J Thorac Cardiovasc Surg 127(5):1293–1300. doi: 10.1016/j.jtcvs.2003.07.037

Gropp M, Itsykson P, Singer O, Ben-Hur T, Reinhartz E, Galun E, Reubinoff BE (2003) Stable genetic modification of human embryonic stem cells by lentiviral vectors. Mol Ther 7(2):281–287

Grudzien E, Stepinski J, Jankowska-Anyszka M, Stolarski R, Darzynkiewicz E, Rhoads RE (2004) Novel cap analogs for in vitro synthesis of mRNAs with high translational efficiency. RNA 10(9):1479–1487. doi: 10.1261/rna.7380904

Grudzien-Nogalska E, Kowalska J, Su W, Kuhn AN, Slepenkov SV, Darzynkiewicz E, Sahin U, Jemielity J, Rhoads RE (2013) Synthetic mRNAs with superior translation and stability properties. Methods Mol Biol 969:55–72. doi: 10.1007/978-1-62703-260-5_4

Guhaniyogi J, Brewer G (2001) Regulation of mRNA stability in mammalian cells. Gene 265(1-2):11–23

Guo J, Zhang H, Xiao J, Wu J, Ye Y, Li Z, Zou Y, Li X (2013a) Monocyte chemotactic protein-1 promotes the myocardial homing of mesenchymal stem cells in dilated cardiomyopathy. Int J Mol Sci 14(4):8164–8178. doi: 10.3390/ijms14048164

Guo L, Ge J, Wang S, Zhou Y, Wang X, Wu Y (2013b) A novel method for efficient delivery of stem cells to the ischemic brain. Stem Cell Res Ther 4(5):116. doi: 10.1186/scrt327

Gutierrez-Fernandez M, Rodriguez-Frutos B, Ramos-Cejudo J, Teresa Vallejo-Cremades M, Fuentes B, Cerdan S, Diez-Tejedor E (2013) Effects of intravenous administration of allogenic bone marrow- and adipose tissue-derived mesenchymal stem cells on functional recovery and brain repair markers in experimental ischemic stroke. Stem Cell Res Ther 4(1):11. doi: 10.1186/scrt159

Guzman R, Bliss TM, Los Angeles A de, Moseley ME, Palmer TD, Steinberg GK (2008) Neural progenitor cells transplanted into the uninjured brain undergo targeted migration after stroke onset. J Neurosci Res 86(4):873–882. doi: 10.1002/jnr.21542

Hagenhoff A, Bruns CJ, Zhao Y, Luttichau I von, Niess H, Spitzweg C, Nelson PJ (2016) Harnessing mesenchymal stem cell homing as an anticancer therapy. Expert Opin Biol Ther:1–14. doi: 10.1080/14712598.2016.1196179

Hass R, Kasper C, Bohm S, Jacobs R (2011) Different populations and sources of human mesenchymal stem cells (MSC): A comparison of adult and neonatal tissue-derived MSC. Cell Commun Signal 9:12. doi: 10.1186/1478-811X-9-12

Haynesworth SE, Goshima J, Goldberg VM, Caplan AI (1992) Characterization of cells with osteogenic potential from human marrow. Bone 13(1):81–88

Henschler R, Deak E, Seifried E (2008) Homing of Mesenchymal Stem Cells. Transfus Med Hemother 35(4):306–312. doi: 10.1159/000143110

Herzmann N, Salamon A, Fiedler T, Peters K (2016) Analysis of migration rate and chemotaxis of human adipose-derived mesenchymal stem cells in response to LPS and LTA in vitro. Exp Cell Res 342(2):95–103. doi: 10.1016/j.yexcr.2016.03.016

Hodgkinson CP, Gomez JA, Mirotsou M, Dzau VJ (2010) Genetic engineering of mesenchymal stem cells and its application in human disease therapy. Hum Gene Ther 21(11):1513–1526. doi: 10.1089/hum.2010.165

Holehonnur R, Lella SK, Ho AD, Luong JA, Ploski JE (2015) The production of viral vectors designed to express large and difficult to express transgenes within neurons. Mol Brain 8:12. doi: 10.1186/s13041-015-0100-7

Holtkamp S, Kreiter S, Selmi A, Simon P, Koslowski M, Huber C, Tureci O, Sahin U (2006) Modification of antigen-encoding RNA increases stability, translational efficacy, and T-cell stimulatory capacity of dendritic cells. Blood 108(13):4009–4017. doi: 10.1182/blood-2006-04-015024

Honmou O, Onodera R, Sasaki M, Waxman SG, Kocsis JD (2012) Mesenchymal stem cells: therapeutic outlook for stroke. Trends Mol Med 18(5):292–297. doi: 10.1016/j.molmed.2012.02.003

Hyun Y-M, Chung H-L, McGrath JL, Waugh RE, Kim M (2009) Activated integrin VLA-4 localizes to the lamellipodia and mediates T cell migration on VCAM-1. J Immunol 183(1):359–369. doi: 10.4049/jimmunol.0803388

Iadecola C, Anrather J (2011) The immunology of stroke: from mechanisms to translation. Nat Med 17(7):796–808. doi: 10.1038/nm.2399

Ikeda Y, Collins MKL, Radcliffe PA, Mitrophanous KA, Takeuchi Y (2002) Gene transduction efficiency in cells of different species by HIV and EIAV vectors. Gene Ther 9(14):932–938. doi: 10.1038/sj.gt.3301708

Ip JE, Wu Y, Huang J, Zhang L, Pratt RE, Dzau VJ (2007) Mesenchymal stem cells use integrin beta1 not CXC chemokine receptor 4 for myocardial migration and engraftment. Mol Biol Cell 18(8):2873–2882. doi: 10.1091/mbc.E07-02-0166

Jackson RJ, Hellen CUT, Pestova TV (2010) The mechanism of eukaryotic translation initiation and principles of its regulation. Nat Rev Mol Cell Biol 11(2):113–127. doi: 10.1038/nrm2838

James AW (2013) Review of Signaling Pathways Governing MSC Osteogenic and Adipogenic Differentiation. Scientifica (Cairo) 2013:684736. doi: 10.1155/2013/684736

Jani B, Fuchs R (2012) In vitro transcription and capping of Gaussia luciferase mRNA followed by HeLa cell transfection. J Vis Exp(61). doi: 10.3791/3702

Jemielity J, Fowler T, Zuberek J, Stepinski J, Lewdorowicz M, Niedzwiecka A, Stolarski R, Darzynkiewicz E, Rhoads RE (2003) Novel "anti-reverse" cap analogs with superior translational properties. RNA 9(9):1108–1122

Jiang L, Newman M, Saporta S, Chen N, Sanberg CD, Sanberg PR, Willing AE (2008) MIP-1alpha and MCP-1 Induce Migration of Human Umbilical Cord Blood Cells in Models of Stroke. Curr Neurovasc Res 5(2):118–124

Jin K, Minami M, Lan JQ, Mao XO, Batteur S, Simon RP, Greenberg DA (2001) Neurogenesis in dentate subgranular zone and rostral subventricular zone after focal cerebral ischemia in the rat. Proc Natl Acad Sci U S A 98(8):4710–4715. doi: 10.1073/pnas.081011098

Jin Z, Pan X, Zhou K, Bi H, Wang L, Yu L, Wang Q (2015) Biological effects and mechanisms of action of mesenchymal stem cell therapy in chronic obstructive pulmonary disease. J Int Med Res 43(3):303–310. doi: 10.1177/0300060514568733

Justicia C, Martin A, Rojas S, Gironella M, Cervera A, Panes J, Chamorro A, Planas AM (2006) Anti-VCAM-1 antibodies did not protect against ischemic damage either in rats or in mice. J Cereb Blood Flow Metab 26(3):421–432. doi: 10.1038/sj.jcbfm.9600198

Kallifatidis G, Beckermann BM, Groth A, Schubert M, Apel A, Khamidjanov A, Ryschich E, Wenger T, Wagner W, Diehlmann A, Saffrich R, Krause U, Eckstein V, Mattern J, Chai M, Schutz G, Ho AD, Gebhard MM, Buchler MW, Friess H, Buchler P, Herr I (2008) Improved lentiviral transduction of human mesenchymal stem cells for therapeutic intervention in pancreatic cancer. Cancer Gene Ther 15(4):231–240. doi: 10.1038/sj.cgt.7701097

Kang SK, Shin IS, Ko MS, Jo JY, Ra JC (2012) Journey of mesenchymal stem cells for homing: strategies to enhance efficacy and safety of stem cell therapy. Stem Cells Int 2012:342968. doi: 10.1155/2012/342968

Kariko K, Buckstein M, Ni H, Weissman D (2005) Suppression of RNA recognition by Toll-like receptors: the impact of nucleoside modification and the evolutionary origin of RNA. Immunity 23(2):165–175. doi: 10.1016/j.immuni.2005.06.008

Kariko K, Muramatsu H, Ludwig J, Weissman D (2011) Generating the optimal mRNA for therapy: HPLC purification eliminates immune activation and improves translation of nucleoside-modified, protein-encoding mRNA. Nucleic Acids Res 39(21):e142. doi: 10.1093/nar/gkr695

Karp JM, Teo, GS (2009) Mesenchymal stem cell homing: the devil is in the details. Cell Stem Cell 4(3):206–216. doi: 10.1016/j.stem.2009.02.001

Kavanagh DP, Robinson J, Kalia N (2014) Mesenchymal Stem Cell Priming: Fine-tuning Adhesion and Function. Stem Cell Rev. doi: 10.1007/s12015-014-9510-7

Kean TJ, Lin P, Caplan AI, Dennis JE (2013) MSCs: Delivery Routes and Engraftment, Cell-Targeting Strategies, and Immune Modulation. Stem Cells Int 2013:732742. doi: 10.1155/2013/732742

Keating A (2012) Mesenchymal stromal cells: new directions. Cell Stem Cell 10(6):709–716. doi: 10.1016/j.stem.2012.05.015

Keating A, Horsfall W, Hawley RG, Toneguzzo F (1990) Effect of different promoters on expression of genes introduced into hematopoietic and marrow stromal cells by electroporation. Exp Hematol 18(2):99–102

Kemp K, Hares K, Mallam E, Heesom KJ, Scolding N, Wilkins A (2010) Mesenchymal stem cell-secreted superoxide dismutase promotes cerebellar neuronal survival. J Neurochem 114(6):1569–1580. doi: 10.1111/j.1471-4159.2009.06553.x

Kerkela E, Hakkarainen T, Makela T, Raki M, Kambur O, Kilpinen L, Nikkila J, Lehtonen S, Ritamo I, Pernu R, Pietila M, Takalo R, Juvonen T, Bergström K, Kalso E, Valmu L, Laitinen S, Lehenkari P, Nystedt J (2013) Transient proteolytic modification of mesenchymal stromal cells increases lung clearance rate and targeting to injured tissue. Stem Cells Transl Med 2(7):510–520. doi: 10.5966/sctm.2012-0187

Kern S, Eichler H, Stoeve J, Kluter H, Bieback K (2006) Comparative analysis of mesenchymal stem cells from bone marrow, umbilical cord blood, or adipose tissue. Stem Cells 24(5):1294–1301. doi: 10.1634/stemcells.2005-0342

Khabbal J, Kerkela E, Mitkari B, Raki M, Nystedt J, Mikkonen V, Bergström K, Laitinen S, Korhonen M, Jolkkonen J (2014) Differential Clearance of Rat and Human Bone Marrow-Derived Mesenchymal Stem Cells from the Brain After Intra-arterial Infusion in Rats. Cell Transplant. doi: 10.3727/096368914X679336

Khaldoyanidi S (2008) Directing stem cell homing. Cell Stem Cell 2(3):198–200. doi: 10.1016/j.stem.2008.02.012

Knight S, Collins M, Takeuchi Y (2013) Insertional mutagenesis by retroviral vectors: current concepts and methods of analysis. Curr Gene Ther 13(3):211–227

Koizumi J (1986) Experimental studies of ischemic brain edema. I. A new experimental model of cerebral embolism in rats in which recirculation can be introduced in the ischemic area. Jpn J Stroke(8):1–8

Korbling M, Estrov Z, Champlin R (2003) Adult stem cells and tissue repair. Bone Marrow Transplant 32 Suppl 1:S23-4. doi: 10.1038/sj.bmt.1703939

Krishnan R, Klumpers DD, Park CY, Rajendran K, Trepat X, van Bezu J, van Hinsbergh, Victor W M, Carman CV, Brain JD, Fredberg JJ, Butler JP, van Nieuw Amerongen, Geerten P (2011) Substrate stiffening promotes endothelial monolayer disruption through enhanced physical forces. Am J Physiol Cell Physiol 300(1):C146-54. doi: 10.1152/ajpcell.00195.2010

Kuhn AN, Beibetaert T, Simon P, Vallazza B, Buck J, Davies BP, Tureci O, Sahin U (2012) mRNA as a versatile tool for exogenous protein expression. Curr Gene Ther 12(5):347–361

Kumar M, Keller B, Makalou N, Sutton RE (2001) Systematic determination of the packaging limit of lentiviral vectors. Hum Gene Ther 12(15):1893–1905. doi: 10.1089/104303401753153947

Kumar S, Chanda D, Ponnazhagan S (2008) Therapeutic potential of genetically modified mesenchymal stem cells. Gene Ther 15(10):711–715. doi: 10.1038/gt.2008.35

Kumar S, Ponnazhagan S (2007) Bone homing of mesenchymal stem cells by ectopic alpha 4 integrin expression. FASEB J 21(14):3917–3927. doi: 10.1096/fj.07-8275com

Kurtz A (2008) Mesenchymal stem cell delivery routes and fate. Int J Stem Cells 1(1):1–7

Kyriakou C, Rabin N, Pizzey A, Nathwani A, Yong K (2008) Factors that influence short-term homing of human bone marrow-derived mesenchymal stem cells in a xenogeneic animal model. Haematologica 93(10):1457–1465. doi: 10.3324/haematol.12553

Laitinen A, Lampinen M, Liedtke S, Kilpinen L, Kerkela E, Sarkanen J-R, Heinonen T, Kogler G, Laitinen S (2016) The effects of culture conditions on the functionality of efficiently obtained mesenchymal stromal cells from human cord blood. Cytotherapy 18(3):423–437. doi: 10.1016/j.jcyt.2015.11.014

Laker C, Meyer J, Schopen A, Friel J, Heberlein C, Ostertag W, Stocking C (1998) Host cis-mediated extinction of a retrovirus permissive for expression in embryonal stem cells during differentiation. J Virol 72(1):339–348

Langenbach F, Handschel J (2013) Effects of dexamethasone, ascorbic acid and beta-glycerophosphate on the osteogenic differentiation of stem cells in vitro. Stem Cell Res Ther 4(5):117. doi: 10.1186/scrt328

Lappalainen RS, Narkilahti S, Huhtala T, Liimatainen T, Suuronen T, Narvanen A, Suuronen R, Hovatta O, Jolkkonen J (2008) The SPECT imaging shows the accumulation of neural progenitor cells into internal organs after systemic administration in middle cerebral artery occlusion rats. Neurosci Lett 440(3):246–250. doi: 10.1016/j.neulet.2008.05.090

Le Thuc O, Blondeau N, Nahon J-L, Rovere C (2015) The complex contribution of chemokines to neuroinflammation: switching from beneficial to detrimental effects. Ann N Y Acad Sci 1351:127–140. doi: 10.1111/nyas.12855

Lee CI, Kohn DB, Ekert JE, Tarantal AF (2004) Morphological analysis and lentiviral transduction of fetal monkey bone marrow-derived mesenchymal stem cells. Mol Ther 9(1):112–123

Lee T (2010) Host tissue response in stem cell therapy. World J Stem Cells 2(4):61–66. doi: 10.4252/wjsc.v2.i4.61

Leite C, Silva NT, Mendes S, Ribeiro A, Faria JP de, Lourenco T, dos Santos F, Andrade PZ, Cardoso CMP, Vieira M, Paiva A, da Silva CL, Cabral JMS, Relvas JB, Graos M (2014)

Differentiation of human umbilical cord matrix mesenchymal stem cells into neural-like progenitor cells and maturation into an oligodendroglial-like lineage. PLoS One 9(10):e111059. doi: 10.1371/journal.pone.0111059

Leong WK, Lewis MD, Koblar SA (2013) Concise review: Preclinical studies on human cell-based therapy in rodent ischemic stroke models: where are we now after a decade? Stem Cells 31(6):1040–1043. doi: 10.1002/stem.1348

Leonhardt C, Schwake G, Stogbauer TR, Rappl S, Kuhr J-T, Ligon TS, Radler JO (2014) Single-cell mRNA transfection studies: delivery, kinetics and statistics by numbers. Nanomedicine 10(4):679–688. doi: 10.1016/j.nano.2013.11.008

Levy O, Zhao W, Mortensen LJ, Leblanc S, Tsang K, Fu M, Phillips JA, Sagar V, Anandakumaran P, Ngai J, Cui CH, Eimon P, Angel M, Lin CP, Yanik MF, Karp JM (2013) mRNA-engineered mesenchymal stem cells for targeted delivery of interleukin-10 to sites of inflammation. Blood 122(14):e23-32. doi: 10.1182/blood-2013-04-495119

Lewis JD, Izaurralde E (1997) The role of the cap structure in RNA processing and nuclear export. Eur J Biochem 247(2):461–469

Ley K, Laudanna C, Cybulsky MI, Nourshargh S (2007) Getting to the site of inflammation: the leukocyte adhesion cascade updated. Nat Rev Immunol 7(9):678–689. doi: 10.1038/nri2156

Li C-y, Wu X-y, Tong J-b, Yang X-x, Zhao J-l, Zheng Q-f, Zhao G-b, Ma Z-j (2015) Comparative analysis of human mesenchymal stem cells from bone marrow and adipose tissue under xeno-free conditions for cell therapy. Stem Cell Res Ther 6:55. doi: 10.1186/s13287-015-0066-5

Li N, Sarojini H, An J, Wang E (2010) Prosaposin in the secretome of marrow stroma-derived neural progenitor cells protects neural cells from apoptotic death. J Neurochem 112(6):1527–1538. doi: 10.1111/j.1471-4159.2009.06565.x

Li Y, Chen J, Chen XG, Wang L, Gautam SC, Xu YX, Katakowski M, Zhang LJ, Lu M, Janakiraman N, Chopp M (2002) Human marrow stromal cell therapy for stroke in rat: neurotrophins and functional recovery. Neurology 59(4):514–523

Liang C-M, Weng S-J, Tsai T-H, Li I-H, Lu P-H, Ma K-H, Tai M-C, Chen J-T, Cheng C-Y, Huang Y-S (2014) Neurotrophic and neuroprotective potential of human limbus-derived mesenchymal stromal cells. Cytotherapy 16(10):1371–1383. doi: 10.1016/j.jcyt.2014.05.015

Lin H (2002) The stem-cell niche theory: lessons from flies. Nat Rev Genet 3(12):931–940. doi: 10.1038/nrg952

Lin M-N, Shang D-S, Sun W, Li B, Xu X, Fang W-G, Zhao W-D, Cao L, Chen Y-H (2013) Involvement of PI3K and ROCK signaling pathways in migration of bone marrow-derived mesenchymal stem cells through human brain microvascular endothelial cell monolayers. Brain Res 1513:1–8. doi: 10.1016/j.brainres.2013.03.035

Liu HS, Jan MS, Chou CK, Chen PH, Ke NJ (1999) Is green fluorescent protein toxic to the living cells? Biochem Biophys Res Commun 260(3):712–717. doi: 10.1006/bbrc.1999.0954

Liu JW, Pernod G, Dunoyer-Geindre S, Fish RJ, Yang H, Bounameaux H, Kruithof EKO (2006) Promoter dependence of transgene expression by lentivirus-transduced human blood-derived endothelial progenitor cells. Stem Cells 24(1):199–208. doi: 10.1634/stemcells.2004-0364

Liu L, Eckert MA, Riazifar H, Kang D-K, Agalliu D, Zhao W (2013) From blood to the brain: can systemically transplanted mesenchymal stem cells cross the blood-brain barrier? Stem Cells Int 2013:435093. doi: 10.1155/2013/435093

Lodish H (2002) Molecular cell biology, 4. ed., [Nachdr.]. Media connected. Freeman, New York, NY

Logan AC, Lutzko C, Kohn DB (2002) Advances in lentiviral vector design for gene-modification of hematopoietic stem cells. Curr Opin Biotechnol 13(5):429–436

Longa EZ, Weinstein PR, Carlson S, Cummins R (1989) Reversible middle cerebral artery occlusion without craniectomy in rats. Stroke 20(1):84–91

Lu L-L, Liu Y-J, Yang S-G, Zhao Q-J, Wang X, Gong W, Han Z-B, Xu Z-S, Lu Y-X, Liu D, Chen Z-Z, Han Z-C (2006) Isolation and characterization of human umbilical cord mesenchymal stem cells with hematopoiesis-supportive function and other potentials. Haematologica 91(8):1017–1026

Lundberg J, Sodersten E, Sundstrom E, Le Blanc K, Andersson T, Hermanson O, Holmin S (2012) Targeted intra-arterial transplantation of stem cells to the injured CNS is more effective than intravenous administration: engraftment is dependent on cell type and adhesion molecule expression. Cell Transplant 21(1):333–343. doi: 10.3727/096368911X576036

Madeira C, Mendes RD, Ribeiro SC, Boura JS, Aires-Barros MR, da Silva CL, Cabral JMS (2010) Nonviral gene delivery to mesenchymal stem cells using cationic liposomes for gene and cell therapy. J Biomed Biotechnol 2010:735349. doi: 10.1155/2010/735349

Madrigal M, Rao KS, Riordan NH (2014) A review of therapeutic effects of mesenchymal stem cell secretions and induction of secretory modification by different culture methods. J Transl Med 12:260. doi: 10.1186/s12967-014-0260-8

Maijenburg MW, van der Schoot, C Ellen, Voermans C (2012) Mesenchymal stromal cell migration: possibilities to improve cellular therapy. Stem Cells Dev 21(1):19–29. doi: 10.1089/scd.2011.0270

Majore I, Moretti P, Stahl F, Hass R, Kasper C (2011) Growth and differentiation properties of mesenchymal stromal cell populations derived from whole human umbilical cord. Stem Cell Rev 7(1):17–31. doi: 10.1007/s12015-010-9165-y

Majumdar MK, Keane-Moore M, Buyaner D, Hardy WB, Moorman MA, McIntosh KR, Mosca JD (2003) Characterization and functionality of cell surface molecules on human mesenchymal stem cells. J Biomed Sci 10(2):228–241

Makinen S, Kekarainen T, Nystedt J, Liimatainen T, Huhtala T, Narvanen A, Laine J, Jolkkonen J (2006) Human umbilical cord blood cells do not improve sensorimotor or cognitive outcome following transient middle cerebral artery occlusion in rats. Brain Res 1123(1):207–215. doi: 10.1016/j.brainres.2006.09.056

Malone RW, Felgner PL, Verma IM (1989) Cationic liposome-mediated RNA transfection. Proc Natl Acad Sci U S A 86(16):6077–6081

Maltman DJ, Hardy SA, Przyborski SA (2011) Role of mesenchymal stem cells in neurogenesis and nervous system repair. Neurochem Int 59(3):347–356. doi: 10.1016/j.neuint.2011.06.008

Manochantr S, Tantrawatpan C, Kheolamai P, U-pratya Y, Supokawej A, Issaragrisil S (2010) Isolation, characterization and neural differentiation potential of amnion derived mesenchymal stem cells. J Med Assoc Thai 93 Suppl 7:S183-91

Marini B, Kertesz-Farkas A, Ali H, Lucic B, Lisek K, Manganaro L, Pongor S, Luzzati R, Recchia A, Mavilio F, Giacca M, Lusic M (2015) Nuclear architecture dictates HIV-1 integration site selection. Nature 521(7551):227–231. doi: 10.1038/nature14226

Marquez-Curtis LA, Gul-Uludag H, Xu P, Chen J, Janowska-Wieczorek A (2013) CXCR4 transfection of cord blood mesenchymal stromal cells with the use of cationic liposome enhances their migration toward stromal cell-derived factor-1. Cytotherapy 15(7):840–849. doi: 10.1016/j.jcyt.2013.02.009

Marquez-Curtis LA, Janowska-Wieczorek A (2013) Enhancing the migration ability of mesenchymal stromal cells by targeting the SDF-1/CXCR4 axis. Biomed Res Int 2013:561098. doi: 10.1155/2013/561098

Martin SA, Paoletti E, Moss B (1975) Purification of mRNA guanylyltransferase and mRNA (guanine-7-) methyltransferase from vaccinia virions. J Biol Chem 250(24):9322–9329

Mastri M, Lin H, Lee T (2014) Enhancing the efficacy of mesenchymal stem cell therapy. World J Stem Cells 6(2):82–93. doi: 10.4252/wjsc.v6.i2.82

Mathews S, Lakshmi Rao K, Suma Prasad K, Kanakavalli MK, Govardhana Reddy A, Avinash Raj T, Thangaraj K, Pande G (2015) Propagation of pure fetal and maternal mesenchymal stromal cells from terminal chorionic villi of human term placenta. Sci Rep 5:10054. doi: 10.1038/srep10054

Matsushita T, Kibayashi T, Katayama T, Yamashita Y, Suzuki S, Kawamata J, Honmou O, Minami M, Shimohama S (2011) Mesenchymal stem cells transmigrate across brain microvascular endothelial cell monolayers through transiently formed inter-endothelial gaps. Neurosci Lett 502(1):41–45. doi: 10.1016/j.neulet.2011.07.021

McGinley L, McMahon J, Strappe P, Barry F, Murphy M, O'Toole D, O'Brien T (2011) Lentiviral vector mediated modification of mesenchymal stem cells & enhanced survival in an in vitro model of ischaemia. Stem Cell Res Ther 2(2):12. doi: 10.1186/scrt53

McMahon J, Conroy S, Lyons M, Greiser U, O'shea C, Strappe P, Howard L, Murphy M, Barry F, O'Brien T (2006) Gene transfer into rat mesenchymal stem cells: a comparative study of viral and nonviral vectors. Stem Cells Dev 15(1):87–96. doi: 10.1089/scd.2006.15.87

Mezey E, Chandross KJ (2000) Bone marrow: a possible alternative source of cells in the adult nervous system. Eur J Pharmacol 405(1-3):297–302

Mildner A, Schmidt H, Nitsche M, Merkler D, Hanisch U-K, Mack M, Heikenwalder M, Bruck W, Priller J, Prinz M (2007) Microglia in the adult brain arise from Ly-6ChiCCR2+ monocytes only under defined host conditions. Nat Neurosci 10(12):1544–1553. doi: 10.1038/nn2015

Mitkari B, Kerkela E, Nystedt J, Korhonen M, Mikkonen V, Huhtala T, Jolkkonen J (2013) Intra-arterial infusion of human bone marrow-derived mesenchymal stem cells results in transient localization in the brain after cerebral ischemia in rats. Exp Neurol 239:158–162. doi: 10.1016/j.expneurol.2012.09.018

Mitkari B, Nitzsche F, Kerkela E, Kuptsova K, Huttunen J, Nystedt J, Korhonen M, Jolkkonen J (2014) Human bone marrow mesenchymal stem/stromal cells produce efficient localization in the brain and enhanced angiogenesis after intra-arterial delivery in rats with cerebral ischemia, but this is not translated to behavioral recovery. Behav Brain Res 259:50–59. doi: 10.1016/j.bbr.2013.10.030

Mitsiades CS, Mitsiades N, Poulaki V, Schlossman R, Akiyama M, Chauhan D, Hideshima T, Treon SP, Munshi NC, Richardson PG, Anderson KC (2002) Activation of NF-kappaB and upregulation of intracellular anti-apoptotic proteins via the IGF-1/Akt signaling in human multiple myeloma cells: therapeutic implications. Oncogene 21(37):5673–5683. doi: 10.1038/sj.onc.1205664

Mizuguchi H, Xu Z, Ishii-Watabe A, Uchida E, Hayakawa T (2000) IRES-dependent second gene expression is significantly lower than cap-dependent first gene expression in a bicistronic vector. Mol Ther 1(4):376–382. doi: 10.1006/mthe.2000.0050

Mockey M, Goncalves C, Dupuy FP, Lemoine FM, Pichon C, Midoux P (2006) mRNA transfection of dendritic cells: synergistic effect of ARCA mRNA capping with Poly(A) chains in cis and in trans for a high protein expression level. Biochem Biophys Res Commun 340(4):1062–1068. doi: 10.1016/j.bbrc.2005.12.105

Mogensen TH (2009) Pathogen recognition and inflammatory signaling in innate immune defenses. Clin Microbiol Rev 22(2):240-73, Table of Contents. doi: 10.1128/CMR.00046-08

Moldt B, Staunstrup NH, Jakobsen M, Yanez-Munoz RJ, Mikkelsen JG (2008) Genomic insertion of lentiviral DNA circles directed by the yeast Flp recombinase. BMC Biotechnol 8:60. doi: 10.1186/1472-6750-8-60

Möller K, Boltze J, Pösel C, Seeger J, Stahl T, Wagner D-C (2014) Sterile inflammation after permanent distal MCA occlusion in hypertensive rats. J Cereb Blood Flow Metab 34(2):307–315. doi: 10.1038/jcbfm.2013.199

Mollet M, Godoy-Silva R, Berdugo C, Chalmers JJ (2008) Computer simulations of the energy dissipation rate in a fluorescence-activated cell sorter: Implications to cells. Biotechnol Bioeng 100(2):260–272. doi: 10.1002/bit.21762

Montresor A, Toffali L, Constantin G, Laudanna C (2012) Chemokines and the signaling modules regulating integrin affinity. Front Immunol 3:127. doi: 10.3389/fimmu.2012.00127

Muiznieks I, Doerfler W (1994) The impact of 5'-CG-3' methylation on the activity of different eukaryotic promoters: a comparative study. FEBS Lett 344(2-3):251–254

Muller SR, Sullivan PD, Clegg DO, Feinstein SC (1990) Efficient transfection and expression of heterologous genes in PC12 cells. DNA Cell Biol 9(3):221–229. doi: 10.1089/dna.1990.9.221

Muller WA (2009) Mechanisms of transendothelial migration of leukocytes. Circ Res 105(3):223–230. doi: 10.1161/CIRCRESAHA.109.200717

Muller WA (2011) Mechanisms of leukocyte transendothelial migration. Annu Rev Pathol 6:323–344. doi: 10.1146/annurev-pathol-011110-130224

Murphy MB, Moncivais K, Caplan AI (2013) Mesenchymal stem cells: environmentally responsive therapeutics for regenerative medicine. Exp Mol Med 45:e54. doi: 10.1038/emm.2013.94

Nayak D, Roth TL, McGavern DB (2014) Microglia development and function. Annu Rev Immunol 32:367–402. doi: 10.1146/annurev-immunol-032713-120240

Norrman K, Fischer Y, Bonnamy B, Wolfhagen Sand F, Ravassard P, Semb H (2010) Quantitative comparison of constitutive promoters in human ES cells. PLoS One 5(8):e12413. doi: 10.1371/journal.pone.0012413

Nott A, Meislin SH, Moore MJ (2003) A quantitative analysis of intron effects on mammalian gene expression. RNA 9(5):607–617

Nourshargh S, Alon R (2014) Leukocyte migration into inflamed tissues. Immunity 41(5):694–707. doi: 10.1016/j.immuni.2014.10.008

Nowakowski A, Andrzejewska A, Janowski M, Walczak P, Lukomska B (2013) Genetic engineering of stem cells for enhanced therapy. Acta Neurobiol Exp (Wars) 73(1):1–18

Orlova NA, Kovnir SV, Hodak JA, Vorobiev II, Gabibov AG, Skryabin KG (2014) Improved elongation factor-1 alpha-based vectors for stable high-level expression of heterologous proteins in Chinese hamster ovary cells. BMC Biotechnol 14:56. doi: 10.1186/1472-6750-14-56

Papadakis ED, Nicklin SA, Baker AH, White SJ (2004) Promoters and control elements: designing expression cassettes for gene therapy. Curr Gene Ther 4(1):89–113

Park HW, Chang JW, Yang YS, Oh W, Hwang JH, Kim DG, Paek SH (2015a) The Effect of Donor-Dependent Administration of Human Umbilical Cord Blood-Derived Mesenchymal Stem Cells following Focal Cerebral Ischemia in Rats. Exp Neurobiol 24(4):358–365. doi: 10.5607/en.2015.24.4.358

Park JS, Suryaprakash S, Lao Y-H, Leong KW (2015b) Engineering mesenchymal stem cells for regenerative medicine and drug delivery. Methods 84:3–16. doi: 10.1016/j.ymeth.2015.03.002

Patel AR, Ritzel R, McCullough LD, Liu F (2013) Microglia and ischemic stroke: a double-edged sword. Int J Physiol Pathophysiol Pharmacol 5(2):73–90

Paul G, Li J-Y, Brundin P (2002) Stem cells: hype or hope? Drug Discov Today 7(5):295–302

Paxinos G, Watson C (2013) The Rat Brain in Stereotaxic Coordinates: Hard Cover Edition, 7th ed. Elsevier Science, Burlington

Penn MS, Mangi AA (2008) Genetic enhancement of stem cell engraftment, survival, and efficacy. Circ Res 102(12):1471–1482. doi: 10.1161/CIRCRESAHA.108.175174

Pessina A, Gribaldo L (2006) The key role of adult stem cells: therapeutic perspectives. Curr Med Res Opin 22(11):2287–2300. doi: 10.1185/030079906X148517

Pevsner-Fischer M, Levin S, Zipori D (2011) The origins of mesenchymal stromal cell heterogeneity. Stem Cell Rev 7(3):560–568. doi: 10.1007/s12015-011-9229-7

Pfeifer A, Ikawa M, Dayn Y, Verma IM (2002) Transgenesis by lentiviral vectors: lack of gene silencing in mammalian embryonic stem cells and preimplantation embryos. Proc Natl Acad Sci U S A 99(4):2140–2145. doi: 10.1073/pnas.251682798

Phinney DG, Prockop DJ (2007) Concise review: mesenchymal stem/multipotent stromal cells: the state of transdifferentiation and modes of tissue repair--current views. Stem Cells 25(11):2896–2902. doi: 10.1634/stemcells.2007-0637

Piccoli C, Scrima R, Ripoli M, Di Ianni M, Del Papa B, D'Aprile A, Quarato G, Martelli MP, Servillo G, Ligas C, Boffoli D, Tabilio A, Capitanio N (2008) Transformation by retroviral vectors of bone marrow-derived mesenchymal cells induces mitochondria-dependent cAMP-sensitive reactive oxygen species production. Stem Cells 26(11):2843–2854. doi: 10.1634/stemcells.2007-0885

Pittenger MF, Mackay A, Beck SC, Jaiswal RK, Douglas R, Mosca JD, Moorman MA, Simonetti DW, Craig S, Marshak DR (1999) Multilineage potential of adult human mesenchymal stem cells. Science 284(5411):143–147

Pittenger MF, Martin BJ (2004) Mesenchymal stem cells and their potential as cardiac therapeutics. Circ Res 95(1):9–20. doi: 10.1161/01.RES.0000135902.99383.6f

Ponte AL, Marais E, Gallay N, Langonne A, Delorme B, Herault O, Charbord P, Domenech J (2007) The in vitro migration capacity of human bone marrow mesenchymal stem cells: comparison of chemokine and growth factor chemotactic activities. Stem Cells 25(7):1737–1745. doi: 10.1634/stemcells.2007-0054

Poulsom R, Alison MR, Forbes SJ, Wright NA (2002) Adult stem cell plasticity. J Pathol 197(4):441–456. doi: 10.1002/path.1176

Prosch S, Staak K, Stein J, Liebenthal C, Stamminger T, Volk HD, Kruger DH (1995) Stimulation of the human cytomegalovirus IE enhancer/promoter in HL-60 cells by TNFalpha is mediated via induction of NF-kappaB. Virology 208(1):197–206. doi: 10.1006/viro.1995.1143

Qian S-W, Li X, Zhang Y-Y, Huang H-Y, Liu Y, Sun X, Tang Q-Q (2010) Characterization of adipocyte differentiation from human mesenchymal stem cells in bone marrow. BMC Dev Biol 10:47. doi: 10.1186/1471-213X-10-47

Qin HH, Filippi C, Sun S, Lehec S, Dhawan A, Hughes RD (2015) Hypoxic preconditioning potentiates the trophic effects of mesenchymal stem cells on co-cultured human primary hepatocytes. Stem Cell Res Ther 6:237. doi: 10.1186/s13287-015-0218-7

Qin JY, Zhang L, Clift KL, Hulur I, Xiang AP, Ren B-Z, Lahn BT (2010) Systematic comparison of constitutive promoters and the doxycycline-inducible promoter. PLoS One 5(5):e10611. doi: 10.1371/journal.pone.0010611

Qiu X-C, Jin H, Zhang R-Y, Ding Y, Zeng X, Lai B-Q, Ling E-A, Wu J-L, Zeng Y-S (2015) Donor mesenchymal stem cell-derived neural-like cells transdifferentiate into myelin-forming cells and promote axon regeneration in rat spinal cord transection. Stem Cell Res Ther 6:105. doi: 10.1186/s13287-015-0100-7

Quabius ES, Krupp G (2015) Synthetic mRNAs for manipulating cellular phenotypes: an overview. N Biotechnol 32(1):229–235. doi: 10.1016/j.nbt.2014.04.008

Raki M, Bergström K, Jolkkonen J (2013) In Vivo Biodistribution Studies and Cell Tracking in Stroke Using SPECT Imaging. In: Jolkkonen J, Walczak P (eds) Cell-Based Therapies in Stroke. Springer Vienna, Vienna, pp 137–149

Regina A, Romero IA, Greenwood J, Adamson P, Bourre JM, Couraud PO, Roux F (1999) Dexamethasone regulation of P-glycoprotein activity in an immortalized rat brain endothelial cell line, GPNT. J Neurochem 73(5):1954–1963

Ricks DM, Kutner R, Zhang X-Y, Welsh DA, Reiser J (2008) Optimized lentiviral transduction of mouse bone marrow-derived mesenchymal stem cells. Stem Cells Dev 17(3):441–450. doi: 10.1089/scd.2007.0194

Ringe J, Strassburg S, Neumann K, Endres M, Notter M, Burmester G-R, Kaps C, Sittinger M (2007) Towards in situ tissue repair: human mesenchymal stem cells express chemokine receptors CXCR1, CXCR2 and CCR2, and migrate upon stimulation with CXCL8 but not CCL2. J Cell Biochem 101(1):135–146. doi: 10.1002/jcb.21172

Rombouts WJC, Ploemacher RE (2003) Primary murine MSC show highly efficient homing to the bone marrow but lose homing ability following culture. Leukemia 17(1):160–170. doi: 10.1038/sj.leu.2402763

Rosenblum S, Wang N, Smith TN, Pendharkar AV, Chua JY, Birk H, Guzman R (2012) Timing of intra-arterial neural stem cell transplantation after hypoxia-ischemia influences cell engraftment, survival, and differentiation. Stroke 43(6):1624–1631. doi: 10.1161/STROKEAHA.111.637884

Ryser MF, Ugarte F, Thieme S, Bornhäuser M, Roesen-Wolff A, Brenner S (2008) mRNA transfection of CXCR4-GFP fusion--simply generated by PCR-results in efficient migration of primary human mesenchymal stem cells. Tissue Eng Part C Methods 14(3):179–184. doi: 10.1089/ten.tec.2007.0359

Sahin U, Kariko K, Tureci O (2014) mRNA-based therapeutics--developing a new class of drugs. Nat Rev Drug Discov 13(10):759–780. doi: 10.1038/nrd4278

Sakuma T, Ravin SS de, Tonne JM, Thatava T, Ohmine S, Takeuchi Y, Malech HL, Ikeda Y (2010) Characterization of retroviral and lentiviral vectors pseudotyped with xenotropic murine leukemia virus-related virus envelope glycoprotein. Hum Gene Ther 21(12):1665–1673. doi: 10.1089/hum.2010.063

Salem HK, Thiemermann C (2010) Mesenchymal stromal cells: current understanding and clinical status. Stem Cells 28(3):585–596. doi: 10.1002/stem.269

Sawitza I, Kordes C, Gotze S, Herebian D, Haussinger D (2015) Bile acids induce hepatic differentiation of mesenchymal stem cells. Sci Rep 5:13320. doi: 10.1038/srep13320

Schmidt A, Ladage D, Schinkothe T, Klausmann U, Ulrichs C, Klinz F-J, Brixius K, Arnhold S, Desai B, Mehlhorn U, Schwinger, Robert H G, Staib P, Addicks K, Bloch W (2006a) Basic fibroblast growth factor controls migration in human mesenchymal stem cells. Stem Cells 24(7):1750–1758. doi: 10.1634/stemcells.2005-0191

Schmidt A, Ladage D, Steingen C, Brixius K, Schinkothe T, Klinz F-J, Schwinger, Robert H G, Mehlhorn U, Bloch W (2006b) Mesenchymal stem cells transmigrate over the endothelial barrier. Eur J Cell Biol 85(11):1179–1188. doi: 10.1016/j.ejcb.2006.05.015

Schwartz MA, Ginsberg MH (2002) Networks and crosstalk: integrin signalling spreads. Nat Cell Biol 4(4):E65-8. doi: 10.1038/ncb0402-e65

Schwarz JM, Sholar PW, Bilbo SD (2012) Sex differences in microglial colonization of the developing rat brain. J Neurochem 120(6):948–963. doi: 10.1111/j.1471-4159.2011.07630.x

Scott MA, Nguyen VT, Levi B, James AW (2011) Current methods of adipogenic differentiation of mesenchymal stem cells. Stem Cells Dev 20(10):1793–1804. doi: 10.1089/scd.2011.0040

Segers, Vincent F M, van Riet I, Andries LJ, Lemmens K, Demolder MJ, De Becker, Ann J M L, Kockx MM, De Keulenaer, Gilles W (2006) Mesenchymal stem cell adhesion to cardiac microvascular endothelium: activators and mechanisms. Am J Physiol Heart Circ Physiol 290(4):H1370-7. doi: 10.1152/ajpheart.00523.2005

Seifert HA, Hall AA, Chapman CB, Collier LA, Willing AE, Pennypacker KR (2012) A transient decrease in spleen size following stroke corresponds to splenocyte release into systemic circulation. J Neuroimmune Pharmacol 7(4):1017–1024. doi: 10.1007/s11481-012-9406-8

Semon JA, Nagy LH, Llamas CB, Tucker HA, Lee RH, Prockop DJ (2010) Integrin expression and integrin-mediated adhesion in vitro of human multipotent stromal cells (MSCs) to endothelial cells from various blood vessels. Cell Tissue Res 341(1):147–158. doi: 10.1007/s00441-010-0994-4

Shen LH, Li Y, Chen J, Zacharek A, Gao Q, Kapke A, Lu M, Raginski K, Vanguri P, Smith A, Chopp M (2007) Therapeutic benefit of bone marrow stromal cells administered 1 month after stroke. J Cereb Blood Flow Metab 27(1):6–13. doi: 10.1038/sj.jcbfm.9600311

Shipunova IN, Petinati NA, Drize NI (2013) Effect of hydrocortisone on multipotent human mesenchymal stromal cells. Bull Exp Biol Med 155(1):159–163

Shuman S (1995) Capping enzyme in eukaryotic mRNA synthesis. Prog Nucleic Acid Res Mol Biol 50:101–129

Sirven A, Pflumio F, Zennou V, Titeux M, Vainchenker W, Coulombel L, Dubart-Kupperschmitt A, Charneau P (2000) The human immunodeficiency virus type-1 central

DNA flap is a crucial determinant for lentiviral vector nuclear import and gene transduction of human hematopoietic stem cells. Blood 96(13):4103–4110

Smith SM, Wunder MB, Norris DA, Shellman YG (2011) A simple protocol for using a LDH-based cytotoxicity assay to assess the effects of death and growth inhibition at the same time. PLoS One 6(11):e26908. doi: 10.1371/journal.pone.0026908

Sohni A, Verfaillie CM (2013) Mesenchymal Stem Cells Migration Homing and Tracking. Stem Cells Int 2013:130763. doi: 10.1155/2013/130763

Sonenberg N, Gingras AC (1998) The mRNA 5' cap-binding protein eIF4E and control of cell growth. Curr Opin Cell Biol 10(2):268–275

Sordi V (2009) Mesenchymal stem cell homing capacity. Transplantation 87(9 Suppl):S42-5. doi: 10.1097/TP.0b013e3181a28533

Spaeth E, Klopp A, Dembinski JL, Andreeff M, Marini FC (2008) Inflammation and tumor microenvironments: defining the migratory itinerary of mesenchymal stem cells. Gene Ther 15(10):730–738. doi: 10.1038/gt.2008.39

Spradling A, Drummond-Barbosa D, Kai T (2001) Stem cells find their niche. Nature 414(6859):98–104. doi: 10.1038/35102160

Steingen C, Brenig F, Baumgartner L, Schmidt J, Schmidt A, Bloch W (2008) Characterization of key mechanisms in transmigration and invasion of mesenchymal stem cells. J Mol Cell Cardiol 44(6):1072–1084. doi: 10.1016/j.yjmcc.2008.03.010

Stepinski J, Waddell C, Stolarski R, Darzynkiewicz E, Rhoads RE (2001) Synthesis and properties of mRNAs containing the novel "anti-reverse" cap analogs 7-methyl(3'-O-methyl)GpppG and 7-methyl (3'-deoxy)GpppG. RNA 7(10):1486–1495

Sun W, Li W-J, Wei F-Q, Wong T-S, Lei W-B, Zhu X-L, Li J, Wen W-P (2016) Blockade of MCP-1/CCR4 signaling-induced recruitment of activated regulatory cells evokes an antitumor immune response in head and neck squamous cell carcinoma. Oncotarget. doi: 10.18632/oncotarget.9265

Supanc V, Biloglav Z, Kes VB, Demarin V (2011) Role of cell adhesion molecules in acute ischemic stroke. Ann Saudi Med 31(4):365–370. doi: 10.4103/0256-4947.83217

Sutherland BA, Neuhaus AA, Couch Y, Balami JS, DeLuca GC, Hadley G, Harris SL, Grey AN, Buchan AM (2016) The transient intraluminal filament middle cerebral artery occlusion model as a model of endovascular thrombectomy in stroke. J Cereb Blood Flow Metab 36(2):363–369. doi: 10.1177/0271678X15606722

Takada Y, Elices MJ, Crouse C, Hemler ME (1989) The primary structure of the alpha 4 subunit of VLA-4: homology to other integrins and a possible cell-cell adhesion function. EMBO J 8(5):1361–1368

Takeda YS, Xu Q (2015) Neuronal Differentiation of Human Mesenchymal Stem Cells Using Exosomes Derived from Differentiating Neuronal Cells. PLoS One 10(8):e0135111. doi: 10.1371/journal.pone.0135111

Tang Y, Zhang C, Wang J, Lin X, Zhang L, Yang Y, Wang Y, Zhang Z, Bulte JWM, Yang G-Y (2015) MRI/SPECT/Fluorescent Tri-Modal Probe for Evaluating the Homing and Therapeutic Efficacy of Transplanted Mesenchymal Stem Cells in a Rat Ischemic Stroke Model. Adv Funct Mater 25(7):1024–1034. doi: 10.1002/adfm.201402930

Tate CC, Fonck C, McGrogan M, Case CC (2010) Human mesenchymal stromal cells and their derivative, SB623 cells, rescue neural cells via trophic support following in vitro ischemia. Cell Transplant 19(8):973–984. doi: 10.3727/096368910X494885

Tavernier G, Andries O, Demeester J, Sanders NN, Smedt SC de, Rejman J (2011) mRNA as gene therapeutic: how to control protein expression. J Control Release 150(3):238–247. doi: 10.1016/j.jconrel.2010.10.020

Teixido J, Parker CM, Kassner PD, Hemler ME (1992) Functional and structural analysis of VLA-4 integrin alpha 4 subunit cleavage. J Biol Chem 267(3):1786–1791

Teo, GSL, Ankrum JA, Martinelli R, Boetto SE, Simms K, Sciuto TE, Dvorak AM, Karp JM, Carman CV (2012) Mesenchymal stem cells transmigrate between and directly through tumor necrosis factor-alpha-activated endothelial cells via both leukocyte-like and novel mechanisms. Stem Cells 30(11):2472–2486. doi: 10.1002/stem.1198

Terashima Y, Onai N, Murai M, Enomoto M, Poonpiriya V, Hamada T, Motomura K, Suwa M, Ezaki T, Haga T, Kanegasaki S, Matsushima K (2005) Pivotal function for cytoplasmic protein FROUNT in CCR2-mediated monocyte chemotaxis. Nat Immunol 6(8):827–835. doi: 10.1038/ni1222

Tolar J, Le Blanc K, Keating A, Blazar BR (2010) Concise review: hitting the right spot with mesenchymal stromal cells. Stem Cells 28(8):1446–1455. doi: 10.1002/stem.459

Toma C, Wagner WR, Bowry S, Schwartz A, Villanueva F (2009) Fate of culture-expanded mesenchymal stem cells in the microvasculature: in vivo observations of cell kinetics. Circ Res 104(3):398–402. doi: 10.1161/CIRCRESAHA.108.187724

Topisirovic I, Svitkin YV, Sonenberg N, Shatkin AJ (2011) Cap and cap-binding proteins in the control of gene expression. Wiley Interdiscip Rev RNA 2(2):277–298. doi: 10.1002/wrna.52

Toyoshima A, Yasuhara T, Kameda M, Morimoto J, Takeuchi H, Wang F, Sasaki T, Sasada S, Shinko A, Wakamori T, Okazaki M, Kondo A, Agari T, Borlongan CV, Date I (2015) Intra-Arterial Transplantation of Allogeneic Mesenchymal Stem Cells Mounts Neuroprotective Effects in a Transient Ischemic Stroke Model in Rats: Analyses of Therapeutic Time Window and Its Mechanisms. PLoS One 10(6):e0127302. doi: 10.1371/journal.pone.0127302

Ugarte DA de, Alfonso Z, Zuk PA, Elbarbary A, Zhu M, Ashjian P, Benhaim P, Hedrick MH, Fraser JK (2003) Differential expression of stem cell mobilization-associated molecules on multi-lineage cells from adipose tissue and bone marrow. Immunol Lett 89(2-3):267–270

Ullah M, Hamouda H, Stich S, Sittinger M, Ringe J (2012) A reliable protocol for the isolation of viable, chondrogenically differentiated human mesenchymal stem cells from high-density pellet cultures. Biores Open Access 1(6):297–305. doi: 10.1089/biores.2012.0279

van Damme A, Thorrez L, Ma L, Vandenburgh H, Eyckmans J, Dell'Accio F, Bari C de, Luyten F, Lillicrap D, Collen D, VandenDriessche T, Chuah MKL (2006) Efficient lentiviral transduction and improved engraftment of human bone marrow mesenchymal cells. Stem Cells 24(4):896–907. doi: 10.1634/stemcells.2003-0106

Van Tendeloo, Viggo F I, Ponsaerts P, Berneman ZN (2007) mRNA-based gene transfer as a tool for gene and cell therapy. Curr Opin Mol Ther 9(5):423–431

van Velthoven C, Sheldon RA, Kavelaars A, Derugin N, Vexler ZS, Willemen, Hanneke L D M, Maas M, Heijnen CJ, Ferriero DM (2013) Mesenchymal stem cell transplantation attenuates brain injury after neonatal stroke. Stroke 44(5):1426–1432. doi: 10.1161/STROKEAHA.111.000326

Varma N, Janic B, Ali M, Iskander A, Arbab A (2011) Lentiviral Based Gene Transduction and Promoter Studies in Human Hematopoietic Stem Cells (hHSCs). J Stem Cells Regen Med 7(1):41–53

Vasconcelos-dos-Santos A, Rosado-de-Castro PH, Lopes de Souza, Sergio Augusto, da Costa Silva, Juliana, Ramos AB, Rodriguez de Freitas, Gabriel, Barbosa da Fonseca, Lea Mirian, Gutfilen B, Mendez-Otero R (2012) Intravenous and intra-arterial administration of bone marrow mononuclear cells after focal cerebral ischemia: Is there a difference in biodistribution and efficacy? Stem Cell Res 9(1):1–8. doi: 10.1016/j.scr.2012.02.002

Veerbeek JM, van Wegen E, van Peppen R, van der Wees, Philip Jan, Hendriks E, Rietberg M, Kwakkel G (2014) What is the evidence for physical therapy poststroke? A systematic review and meta-analysis. PLoS One 9(2):e87987. doi: 10.1371/journal.pone.0087987

Vestweber D (2012) Novel insights into leukocyte extravasation. Curr Opin Hematol 19(3):212–217. doi: 10.1097/MOH.0b013e3283523e78

Vikram J (2015) Intra-arterial Approaches to Stem Cell Therapy for Ischemic Stroke. In: Hess DC (ed) Cell therapy for brain injury. Springer, Cham, pp 65–89

Voulgari-Kokota A, Fairless R, Karamita M, Kyrargyri V, Tseveleki V, Evangelidou M, Delorme B, Charbord P, Diem R, Probert L (2012) Mesenchymal stem cells protect CNS neurons against glutamate excitotoxicity by inhibiting glutamate receptor expression and function. Exp Neurol 236(1):161–170. doi: 10.1016/j.expneurol.2012.04.011

Wagers AJ, Weissman IL (2004) Plasticity of adult stem cells. Cell 116(5):639–648

Wagner W, Ho AD (2007) Mesenchymal stem cell preparations--comparing apples and oranges. Stem Cell Rev 3(4):239–248. doi: 10.1007/s12015-007-9001-1

Wahle E, Keller W (1992) The biochemistry of 3'-end cleavage and polyadenylation of messenger RNA precursors. Annu Rev Biochem 61:419–440. doi: 10.1146/annurev.bi.61.070192.002223

Walczak P, Zhang J, Gilad AA, Kedziorek DA, Ruiz-Cabello J, Young RG, Pittenger MF, van Zijl, Peter C M, Huang J, Bulte JWM (2008) Dual-modality monitoring of targeted intraarterial delivery of mesenchymal stem cells after transient ischemia. Stroke 39(5):1569–1574. doi: 10.1161/STROKEAHA.107.502047

Wang L, Li Y, Chen J, Gautam SC, Zhang Z, Lu M, Chopp M (2002a) Ischemic cerebral tissue and MCP-1 enhance rat bone marrow stromal cell migration in interface culture. Exp Hematol 30(7):831–836

Wang L, Li Y, Chen X, Chen J, Gautam SC, Xu Y, Chopp M (2002b) MCP-1, MIP-1, IL-8 and ischemic cerebral tissue enhance human bone marrow stromal cell migration in interface culture. Hematology 7(2):113–117. doi: 10.1080/10245330290028588

Wang Q, Tang XN, Yenari MA (2007) The inflammatory response in stroke. J Neuroimmunol 184(1-2):53–68. doi: 10.1016/j.jneuroim.2006.11.014

Wang R, Liang J, Jiang H, Qin L-J, Yang H-T (2008) Promoter-dependent EGFP expression during embryonic stem cell propagation and differentiation. Stem Cells Dev 17(2):279–289. doi: 10.1089/scd.2007.0084

Wanisch K, Yanez-Munoz RJ (2009) Integration-deficient lentiviral vectors: a slow coming of age. Mol Ther 17(8):1316–1332. doi: 10.1038/mt.2009.122

Warren L, Manos PD, Ahfeldt T, Loh Y-H, Li H, Lau F, Ebina W, Mandal PK, Smith ZD, Meissner A, Daley GQ, Brack AS, Collins JJ, Cowan C, Schlaeger TM, Rossi DJ (2010) Highly efficient reprogramming to pluripotency and directed differentiation of human cells with synthetic modified mRNA. Cell Stem Cell 7(5):618–630. doi: 10.1016/j.stem.2010.08.012

Wei H, Li Z, Hu S, Chen X, Cong X (2010) Apoptosis of mesenchymal stem cells induced by hydrogen peroxide concerns both endoplasmic reticulum stress and mitochondrial death pathway through regulation of caspases, p38 and JNK. J Cell Biochem 111(4):967–978. doi: 10.1002/jcb.22785

Wilkins A, Kemp K, Ginty M, Hares K, Mallam E, Scolding N (2009) Human bone marrow-derived mesenchymal stem cells secrete brain-derived neurotrophic factor which promotes neuronal survival in vitro. Stem Cell Res 3(1):63–70. doi: 10.1016/j.scr.2009.02.006

Wilson EH, Weninger W, Hunter CA (2010) Trafficking of immune cells in the central nervous system. J Clin Invest 120(5):1368–1379. doi: 10.1172/JCI41911

Wolff JA, Malone RW, Williams P, Chong W, Acsadi G, Jani A, Felgner PL (1990) Direct gene transfer into mouse muscle in vivo. Science 247(4949 Pt 1):1465–1468

Wu Y (2008) The second chance story of HIV-1 DNA: Unintegrated? Not a problem! Retrovirology 5:61. doi: 10.1186/1742-4690-5-61

Wunderlich M, Krejci O, Wei J, Mulloy JC (2006) Human CD34+ cells expressing the inv(16) fusion protein exhibit a myelomonocytic phenotype with greatly enhanced proliferative ability. Blood 108(5):1690–1697. doi: 10.1182/blood-2005-12-012773

Wynn RF, Hart CA, Corradi-Perini C, O'Neill L, Evans CA, Wraith JE, Fairbairn LJ, Bellantuono I (2004) A small proportion of mesenchymal stem cells strongly expresses functionally active CXCR4 receptor capable of promoting migration to bone marrow. Blood 104(9):2643–2645. doi: 10.1182/blood-2004-02-0526

Xia X, Zhang Y, Zieth CR, Zhang S-C (2007) Transgenes delivered by lentiviral vector are suppressed in human embryonic stem cells in a promoter-dependent manner. Stem Cells Dev 16(1):167–176. doi: 10.1089/scd.2006.0057

Xiao Q, Wang S-k, Tian H, Xin L, Zou Z-g, Hu Y-l, Chang C-m, Wang X-y, Yin Q-s, Zhang X-h, Wang L-y (2012) TNF-alpha increases bone marrow mesenchymal stem cell migration to ischemic tissues. Cell Biochem Biophys 62(3):409–414. doi: 10.1007/s12013-011-9317-y

Xu F, Shi J, Yu B, Ni W, Wu X, Gu Z (2010) Chemokines mediate mesenchymal stem cell migration toward gliomas in vitro. Oncol Rep 23(6):1561–1567

Yamagami S, Tamura M, Hayashi M, Endo N, Tanabe H, Katsuura Y, Komoriya K (1999) Differential production of MCP-1 and cytokine-induced neutrophil chemoattractant in the ischemic brain after transient focal ischemia in rats. J Leukoc Biol 65(6):744–749

Yan T, Venkat P, Ye X, Chopp M, Zacharek A, Ning R, Cui Y, Roberts C, Kuzmin-Nichols N, Sanberg CD, Chen J (2014) HUCBCs increase angiopoietin 1 and induce neurorestorative effects after stroke in T1DM rats. CNS Neurosci Ther 20(10):935–944. doi: 10.1111/cns.12307

Yang H, Wang H, Shivalila CS, Cheng AW, Shi L, Jaenisch R (2013) One-step generation of mice carrying reporter and conditional alleles by CRISPR/Cas-mediated genome engineering. Cell 154(6):1370–1379. doi: 10.1016/j.cell.2013.08.022

Yang J-X, Zhang N, Wang H-W, Gao P, Yang Q-P, Wen Q-P (2015a) CXCR4 receptor overexpression in mesenchymal stem cells facilitates treatment of acute lung injury in rats. J Biol Chem 290(4):1994–2006. doi: 10.1074/jbc.M114.605063

Yang Z, Cai X, Xu A, Xu F, Liang Q (2015b) Bone marrow stromal cell transplantation through tail vein injection promotes angiogenesis and vascular endothelial growth factor expression in cerebral infarct area in rats. Cytotherapy 17(9):1200–1212. doi: 10.1016/j.jcyt.2015.06.005

Ye Q, Shieh J-H, Morrone G, Moore MAS (2004) Expression of constitutively active Notch4 (Int-3) modulates myeloid proliferation and differentiation and promotes expansion of hematopoietic progenitors. Leukemia 18(4):777–787. doi: 10.1038/sj.leu.2403291

Yoon J-K, Park B-N, Shim W-Y, Shin JY, Lee G, Ahn YH (2010) In vivo tracking of 111In-labeled bone marrow mesenchymal stem cells in acute brain trauma model. Nucl Med Biol 37(3):381–388. doi: 10.1016/j.nucmedbio.2009.12.001

Yoshioka N, Gros E, Li H-R, Kumar S, Deacon DC, Maron C, Muotri AR, Chi NC, Fu X-D, Yu BD, Dowdy SF (2013) Efficient generation of human iPSCs by a synthetic self-replicative RNA. Cell Stem Cell 13(2):246–254. doi: 10.1016/j.stem.2013.06.001

Zabner J, Fasbender AJ, Moninger T, Poellinger KA, Welsh MJ (1995) Cellular and molecular barriers to gene transfer by a cationic lipid. J Biol Chem 270(32):18997–19007

Zacharek A, Chen J, Cui X, Li A, Li Y, Roberts C, Feng Y, Gao Q, Chopp M (2007) Angiopoietin1/Tie2 and VEGF/Flk1 induced by MSC treatment amplifies angiogenesis and vascular stabilization after stroke. J Cereb Blood Flow Metab 27(10):1684–1691. doi: 10.1038/sj.jcbfm.9600475

Zannettino ACW, Psaltis PJ, Gronthos S (2008) Home is where the heart is: via the FROUNT. Cell Stem Cell 2(6):513–514. doi: 10.1016/j.stem.2008.05.012

Zhang B, Metharom P, Jullie H, Ellem KAO, Cleghorn G, West MJ, Wei MQ (2004) The significance of controlled conditions in lentiviral vector titration and in the use of multiplicity of infection (MOI) for predicting gene transfer events. Genet Vaccines Ther 2(1):6. doi: 10.1186/1479-0556-2-6

Zhang J, Huang X, Wang H, Liu X, Zhang T, Wang Y, Hu D (2015) The challenges and promises of allogeneic mesenchymal stem cells for use as a cell-based therapy. Stem Cell Res Ther 6:234. doi: 10.1186/s13287-015-0240-9

Zhang X-Y, La Russa VF, Bao L, Kolls J, Schwarzenberger P, Reiser J (2002) Lentiviral vectors for sustained transgene expression in human bone marrow-derived stromal cells. Mol Ther 5(5 Pt 1):555–565. doi: 10.1006/mthe.2002.0585

Zhu JM, Zhao YY, Chen SD, Zhang WH, Lou L, Jin X (2011) Functional recovery after transplantation of neural stem cells modified by brain-derived neurotrophic factor in rats with cerebral ischaemia. J Int Med Res 39(2):488–498

Zohra FT, Chowdhury EH, Tada S, Hoshiba T, Akaike T (2007) Effective delivery with enhanced translational activity synergistically accelerates mRNA-based transfection. Biochem Biophys Res Commun 358(1):373–378. doi: 10.1016/j.bbrc.2007.04.059

Zoltick PW, Wilson JM (2001) Regulated gene expression in gene therapy. Ann N Y Acad Sci 953:53–63

Zufferey R, Donello JE, Trono D, Hope TJ (1999) Woodchuck hepatitis virus posttranscriptional regulatory element enhances expression of transgenes delivered by retroviral vectors. J Virol 73(4):2886–2892

Zychlinski D, Schambach A, Modlich U, Maetzig T, Meyer J, Grassman E, Mishra A, Baum C (2008) Physiological promoters reduce the genotoxic risk of integrating gene vectors. Mol Ther 16(4):718–725. doi: 10.1038/mt.2008

# 8 Supplements

A)

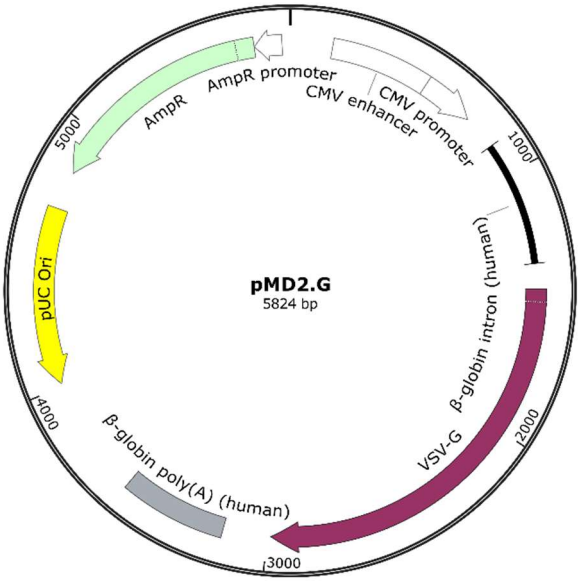


B)

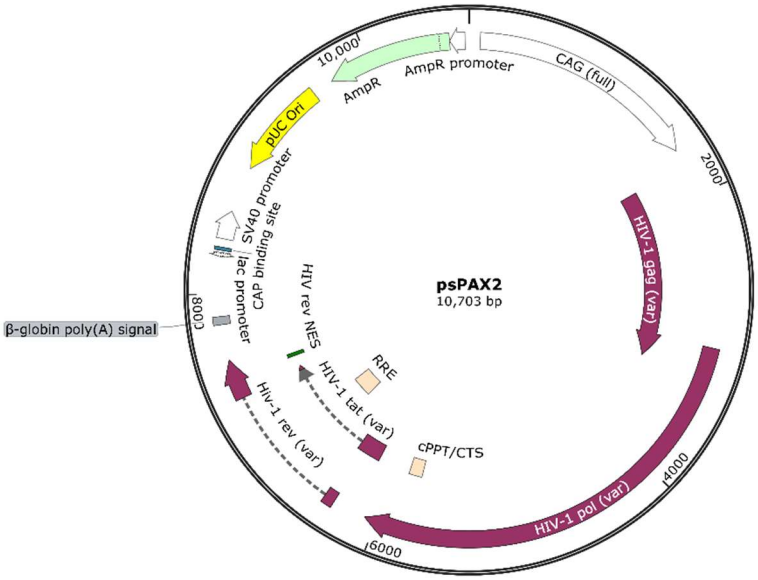

C)

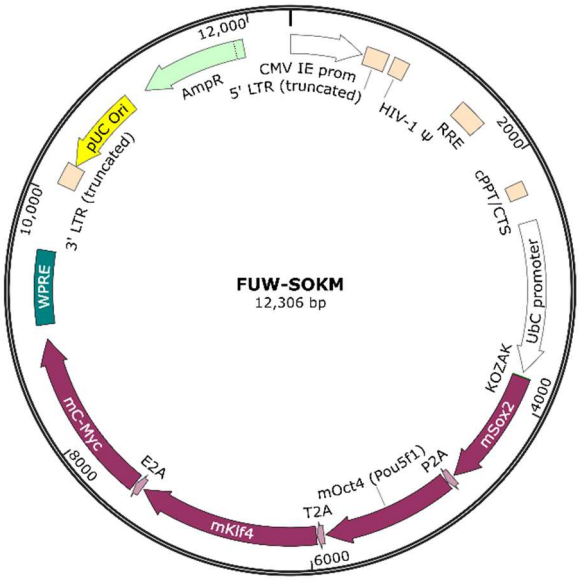
FUW-SOKM
12,306 bp
12,000
CMV IE prom
5' LTR (truncated)
HIV-1 Ψ
RRE
2000
cPPT/CTS
UbC promoter
KOZAK
4000
mSox2
P2A
mOct4 (Pou5f1)
T2A
mKlf4
6000
E2A
mC-Myc
8000
WPRE
10,000
3' LTR (truncated)
pUC Ori
AmpR

D)

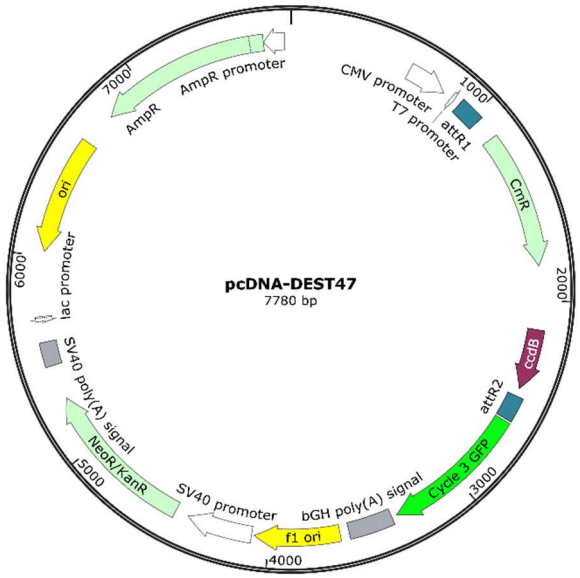
pcDNA-DEST47
7780 bp
7000
AmpR
AmpR promoter
CMV promoter
T7 promoter
1000
attR1
CmR
2000
ccdB
attR2
Cycle 3 GFP
3000
bGH poly(A) signal
f1 ori
4000
SV40 promoter
NeoR/KanR
5000
SV40 poly(A) signal
lac promoter
6000
ori

E)

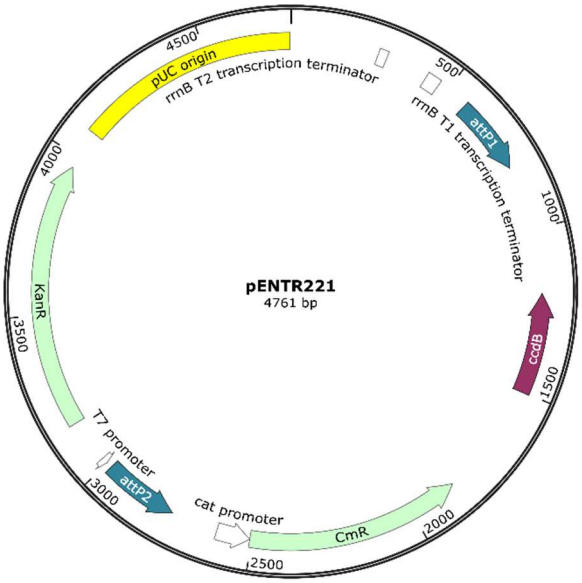
pENTR221
4761 bp
4500
pUC origin
rrnB T2 transcription terminator
500
rrnB T1 transcription terminator
attP1
1000
ccdB
1500
CmR
2000
cat promoter
2500
attP2
3000
T7 promoter
3500
KanR
4000

F)

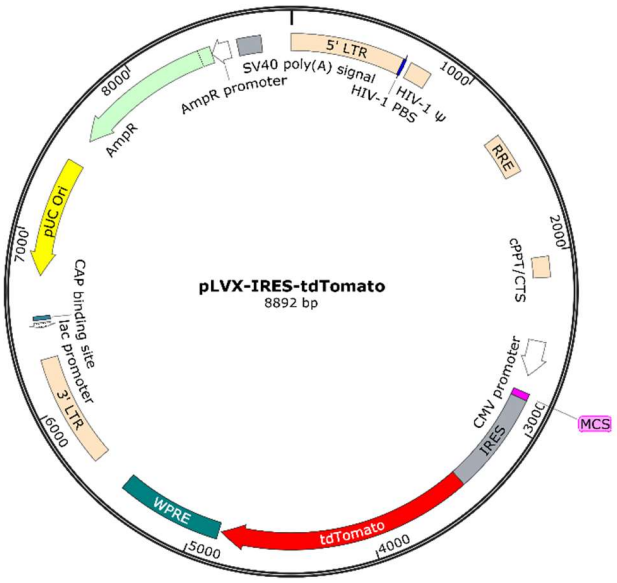
pLVX-IRES-tdTomato
8892 bp
5' LTR
SV40 poly(A) signal
HIV-1 PBS
HIV-1 ψ
RRE
cPPT/CTS
CMV promoter
MCS
IRES
tdTomato
WPRE
3' LTR
lac promoter
CAP binding site
pUC Ori
AmpR
AmpR promoter
1000
2000
3000
4000
5000
6000
7000
8000

G)

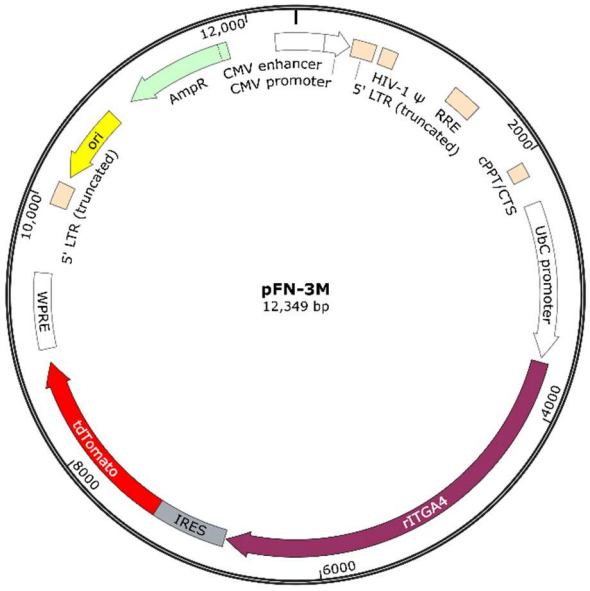
pFN-3M
12,349 bp
CMV enhancer
CMV promoter
AmpR
HIV-1 ψ
5' LTR (truncated)
RRE
cPPT/CTS
UbC promoter
rTTGA4
IRES
tdTomato
WPRE
5' LTR (truncated)
ori
2000
4000
6000
8000
10,000
12,000

H)

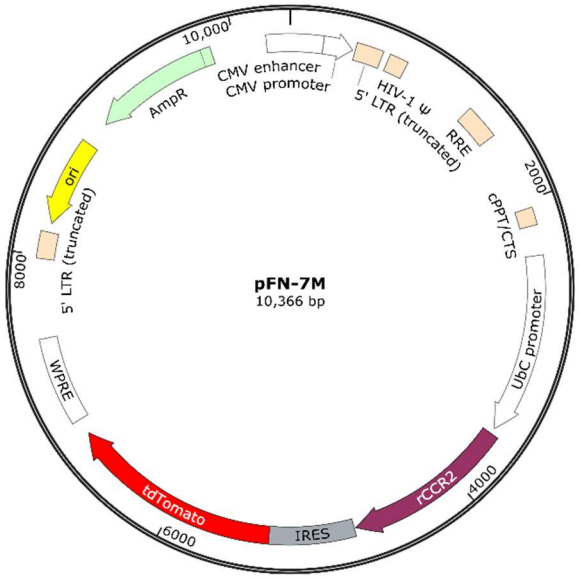
pFN-7M
10,366 bp
CMV enhancer
CMV promoter
AmpR
HIV-1 ψ
5' LTR (truncated)
RRE
cPPT/CTS
UbC promoter
rCCR2
IRES
tdTomato
WPRE
5' LTR (truncated)
ori
2000
4000
6000
8000
10,000

I)

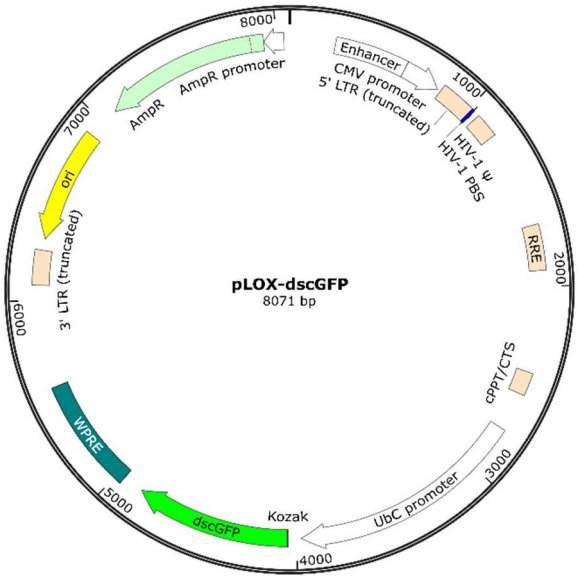
pLOX-dscGFP
8071 bp
8000
Enhancer
CMV promoter
5' LTR (truncated)
1000
HIV-1 ψ
HIV-1 PBS
RRE
2000
cPPT/CTS
3000
UbC promoter
Kozak
4000
dscGFP
5000
WPRE
6000
3' LTR (truncated)
ori
7000
AmpR
AmpR promoter

J)

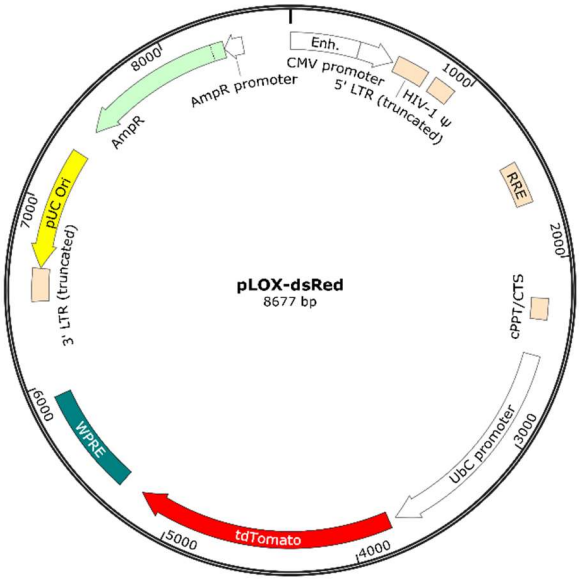
pLOX-dsRed
8677 bp
8000
Enh.
CMV promoter
5' LTR (truncated)
1000
HIV-1 ψ
RRE
2000
cPPT/CTS
3000
UbC promoter
4000
tdTomato
5000
WPRE
6000
3' LTR (truncated)
pUC Ori
7000
AmpR
AmpR promoter

K)

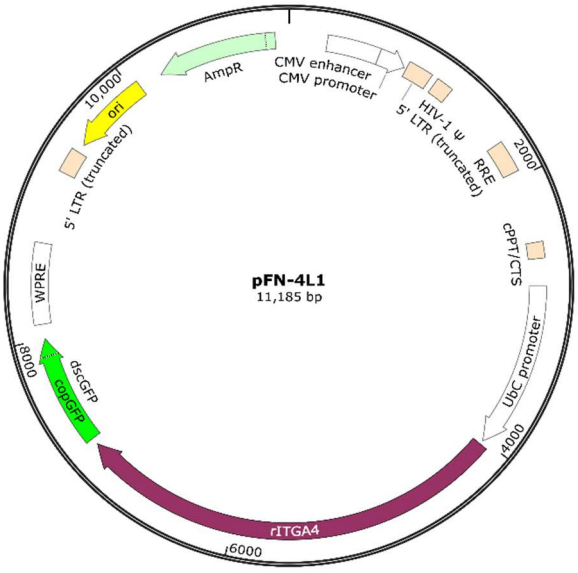
pFN-4L1
11,185 bp
AmpR
CMV enhancer
CMV promoter
5' LTR (truncated)
HIV-1 ψ
RRE
2000
cPPT/CTS
UbC promoter
4000
rITGA4
6000
dscGFP
copGFP
8000
WPRE
5' LTR (truncated)
ori
10,000

L)

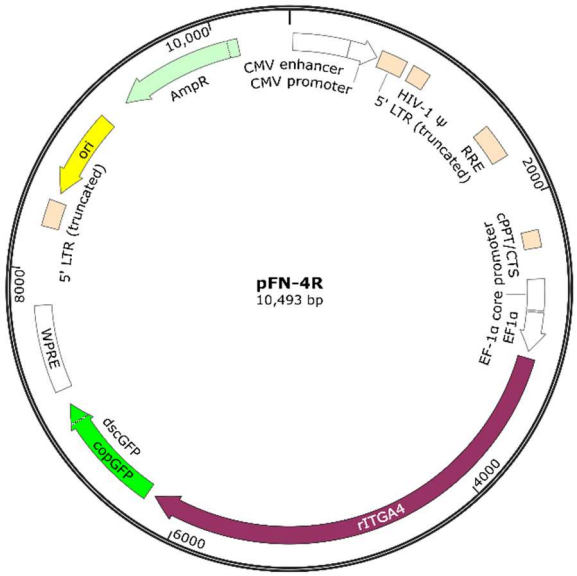
pFN-4R
10,493 bp
10,000
CMV enhancer
CMV promoter
AmpR
HIV-1 ψ
5' LTR (truncated)
RRE
2000
cPPT/CTS
EF-1α core promoter
EF1α
4000
rtTGA4
6000
dscGFP
copGFP
WPRE
8000
5' LTR (truncated)
ori

M)

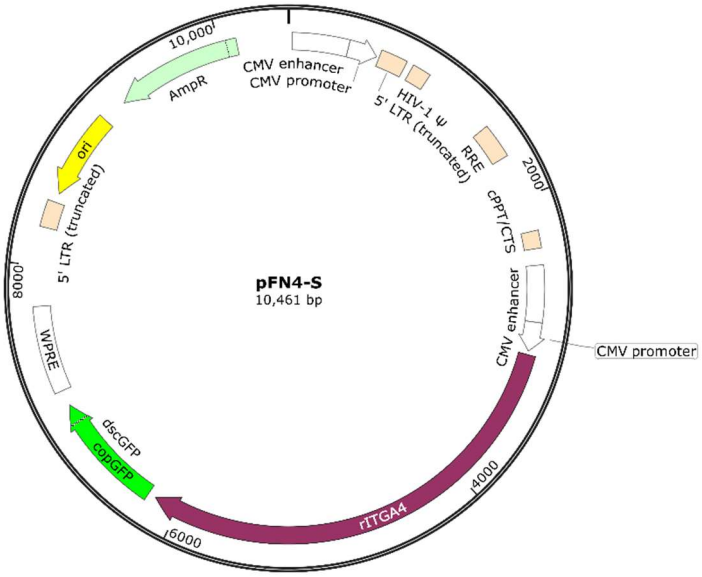
pFN4-S
10,461 bp
10,000
CMV enhancer
CMV promoter
AmpR
HIV-1 ψ
5' LTR (truncated)
RRE
2000
cPPT/CTS
CMV enhancer
CMV promoter
4000
rtTGA4
6000
dscGFP
copGFP
WPRE
8000
5' LTR (truncated)
ori

N)

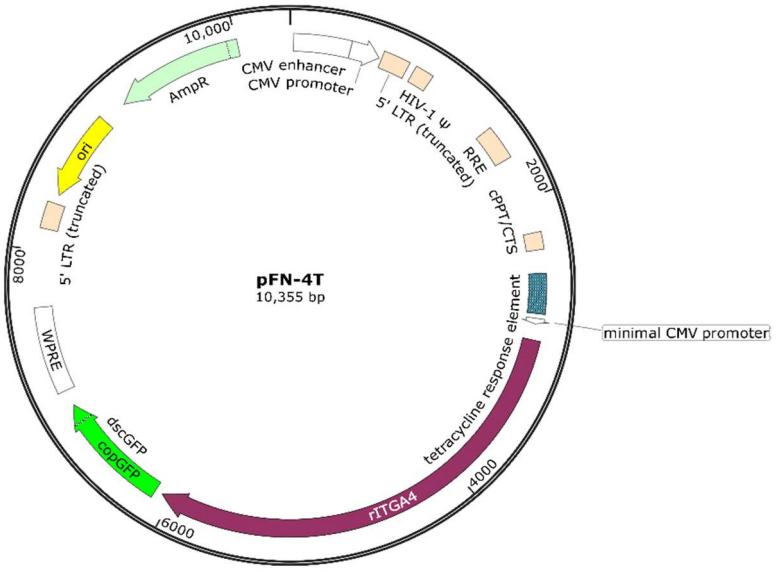
pFN-4T
10,355 bp
10,000
CMV enhancer
CMV promoter
AmpR
HIV-1 ψ
5' LTR (truncated)
RRE
2000
cPPT/CTS
minimal CMV promoter
tetracycline response element
4000
rtTGA4
6000
dscGFP
copGFP
WPRE
8000
5' LTR (truncated)
ori

O)

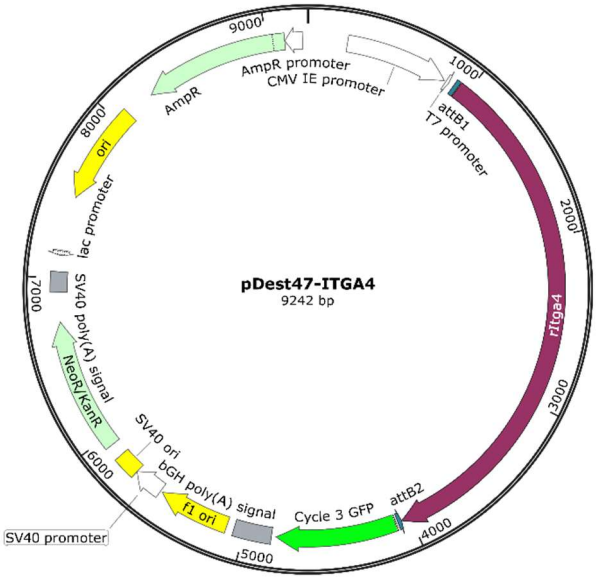
pDest47-ITGA4
9242 bp
AmpR promoter
CMV IE promoter
attB1
T7 promoter
rITGA4
attB2
Cycle 3 GFP
f1 ori
bGH poly(A) signal
SV40 ori
NeoR/KanR
SV40 poly(A) signal
lac promoter
ori
AmpR
SV40 promoter
1000
2000
3000
4000
5000
6000
7000
8000
9000

P)

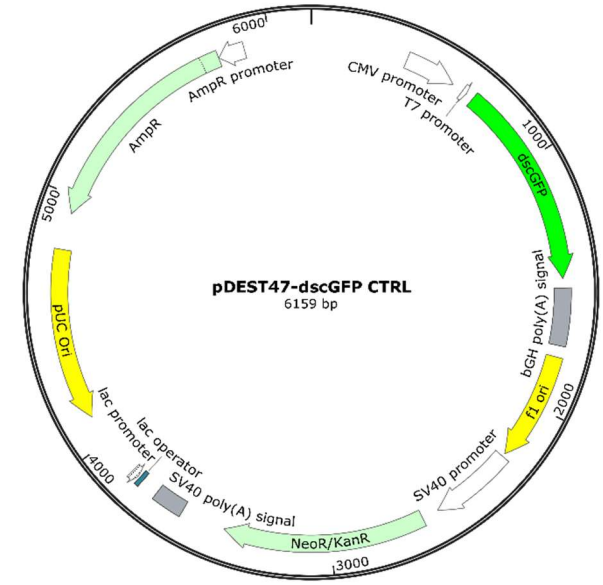
pDEST47-dscGFP CTRL
6159 bp
AmpR promoter
CMV promoter
T7 promoter
dscGFP
bGH poly(A) signal
f1 ori
SV40 promoter
SV40 poly(A) signal
NeoR/KanR
lac operator
lac promoter
pUC Ori
AmpR
1000
2000
3000
4000
5000
6000

Q)

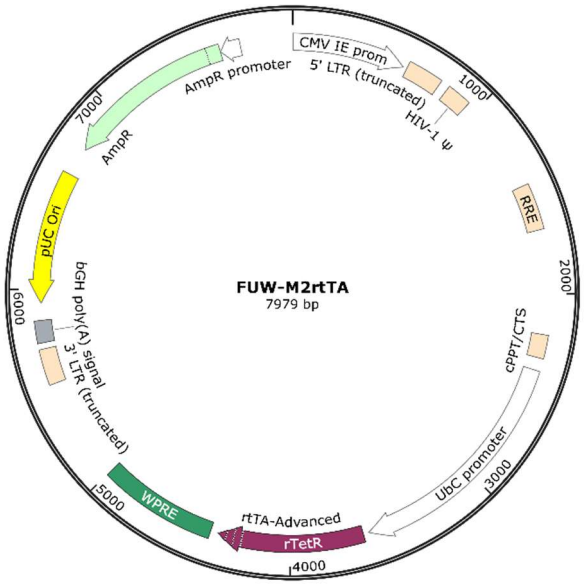
FUW-M2rtTA
7979 bp
CMV IE prom
5' LTR (truncated)
HIV-1 Ψ
RRE
cPPT/CTS
UbC promoter
rtTA-Advanced
rTetR
WPRE
3' LTR (truncated)
bGH poly(A) signal
pUC Ori
AmpR promoter
AmpR
1000
2000
3000
4000
5000
6000
7000

R)

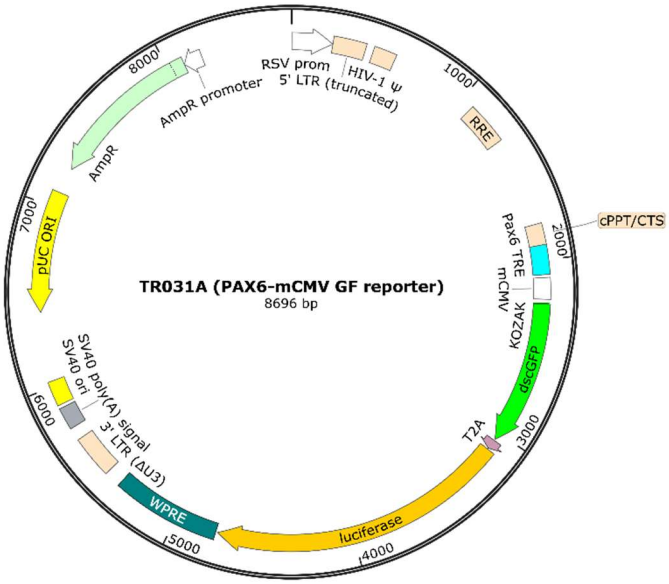


***Fig. 46 Plasmid maps*** *of pMD2G (A), psPAX2 (B), FUW-SOKM (C), pcDNA-DEST47 (D), pENTR221 (E), pLVX-IRES-tdTomato (F), pFN-3M (G), pFN-7M (H), pLOX-dscGFP (I), pLOX-dsRed (J), pFN-4L1 (K), pFN-4R (L), pFN-4S (M), pFN-4T (N), pDest47-ITGA4 (O), pDEST47-dscGFP CTRL (P), FUW-M2rtTA (Q), and TRO31A (R)*

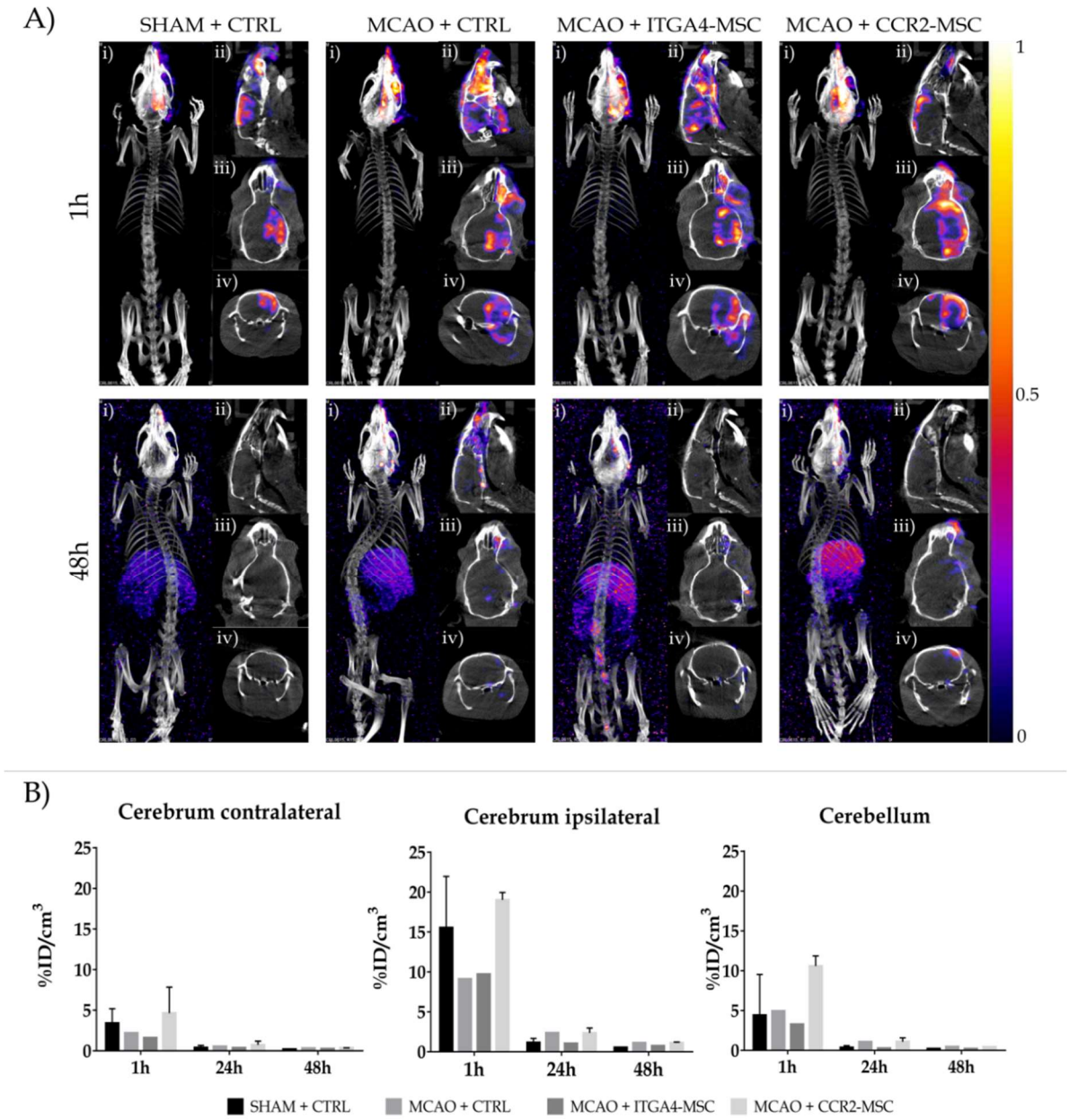


***Fig. 47 SPECT-CT images and analysis of selected animals with cerebral influx of transplanted cells.*** *(A) Color-coded radioactive signals show accumulation of CTRL and modified MSC at day 1 (1-2h post administration, upper row) and day 3 (48h post administration, bottom row). SPECT/CT images are shown in dorsal (i), sagittal (ii), transversal (iii), and coronar orientation (iv). (B) Analysis of contra- and ipsilateral hemisphere, as well as cerebellum underlined inconsistent influx and clearance from brain. Data are decay corrected and if possible given as mean ± SD from 1-2 animals per group (n=1-2).*

## Acknowledgements

Many people have contributed in numerous way to the successful accomplishment of this work. I would like to acknowledge them in this section, even though this is only in a very small way.

First and foremost, I would like to thank Prof. Dr. Dr. Johannes Boltze for providing me the opportunity to work on this topic within an excellent environment with many inspiring people and researchers. I am very grateful for his support, comments and suggestions that were very essential for the accomplishment of the thesis.

I would like to express my deep gratitude to Prof. Dr. Jukka Jolkkonen who constantly helped me during my research work. His mentorship guided me through all complications and helped me to overcome many challenges, which I am grateful for.

My special thanks to PD Dr. Alexander Deten for making it possible to improve my scientific skills and for providing me the independence to pursue my ideas. I would like to express my thanks for generously sharing his time and knowledge, and for being an inspiration to me.

Several parts of my work required the expertise of scientists in many different fields and were done in fruitful collaborations. Therefore, I am eternally grateful to the Charles River Research Laboratories in Kuopio, Finland. Also, I would like to thank all members of the MEMS-IRBI consortium for their scientific support and for the lively discussions.

Further, I would like to express my sincere thanks to Ina Bosse for her technical expertise and for standing by me during long lab hours. She has become a real friend. I also would like to acknowledge all colleagues of the Department for Cell therapy, Fraunhofer Institute of Cell Therapy and Immunology and the Stroke Research Unit at the University of Eastern Finland, Kuopio. It has been a pleasure to work with them. Also, a special thanks goes to my fellow sufferers.

Keeping up motivation and occasional distraction from every-day lab routine are inevitable to survive a PhD. Thus, I would like to thank my dear friends, Claudia and Julia, for having an open ear. A thousand thanks deserves Marcus for being a strong shoulder to lean on. I do not know what I would have done without you! I hope, I can give this all back to you!

Of course, my greatest gratitude, affection, and love belong to my parents, the ones that are and will be there for me, no matter where I am and what my choices are. Thank you for supporting, for encouraging, for suffering, for cheering with me and above all for making me a fighter. To you I owe everything I am and my achievements.

## Statement of authorship

I hereby certify that this dissertation is the result of my own work. No other person's work has been used without due acknowledgement. This dissertation has not been submitted in the same or similar form to other institutions.

Furthermore, I hereby declare that I am familiar with the doctorate regulations of the MINT sections (computer sciences/engineering, and sciences) University of Lübeck (version of April 18th, 2016) and that I fully respect these regulations.

## Selbständigkeitserklärung

Hiermit erkläre ich, dass ich die vorliegende Dissertation eigenständig und ohne fremde Hilfe angefertigt habe. Arbeiten Dritter wurden entsprechend zitiert. Diese Dissertation wurde bisher in dieser oder ähnlicher Form noch bei keiner anderen Institution eingereicht.

Weiterhin erkläre ich hiermit, dass mir die Promotionsordnung der Universität Lübeck der Sektion Informatik/Technik und Naturwissenschaften (mit Stand vom 18. April 2016) bekannt ist und dass ich diese in vollem Umfang anerkenne.

Leipzig, den

## Curriculum vitae

**Franziska Nitzsche, M.Sc.**

## List of publications

Boltze J, **Nitzsche F**, Jolkkonen J, Nitzsche B, Wagner DC. Concise review: increasing the validity of cerebrovascular disease models for translational stem cell research. Review, Submitted

**Nitzsche F**, Bluemel S, Muehlenbruch L, MEMS–IRBI consortium, Deten A. Overexpression of ITGA4 on MSC induced by mRNA transfection. Original research article, Submitted

**Nitzsche F**, Müller C, Lukomska B, Jolkkonen J, Deten A, Boltze J. The MSC adhesion cascade- insights into homing and transendothelial migration. Review. Ready for submission

Cui LL, Kerkelä E, Bakreen A, **Nitzsche F**, Andrzejewska A, Nowakowski A, Janowski M, Walczak P, Boltze J, Lukomska B, Jolkkonen J. The cerebral embolism evoked by intra-arterial delivery of allogeneic bone marrow mesenchymal stem cells in rats is related to cell dose and infusion velocity. Stem Cell Res Ther. 2015 Jan 27;6:11. PMID: 25971703
*Impact Factor: 3.4*

Kuptsova K, Kvist E, **Nitzsche F**, Jolkkonen J. Combined enriched environment ÷atipamezole treatment transiently improves sensory functions in stroke rats independent from neurogenesis and angiogenesis. Rom J Morphol Embryol. 2015;56(1):41-7.PMID:25826486
*Impact-Factor: 0.7*

Boltze J, Lukomska B, Jolkkonen J; **MEMS–IRBI consortium (Nitzsche F)**. Mesenchymal stromal cells in stroke: improvement of motor recovery or functional compensation? J Cereb Blood Flow Metab. 2014 Aug;34(8):1420-1. PMID: 24849662
*Impact Factor: 5.4*

Mitkari B, **Nitzsche F**, Kerkelä E, Kuptsova K, Huttunen J, Nystedt J, Korhonen M, Jolkkonen J. Human bone marrow mesenchymal stem/stromal cells produce efficient localization in the brain and enhanced angiogenesis after intra-arterial delivery in rats with cerebral ischemia, but this is not translated to behavioral recovery. Behav Brain Res. 2014 Feb 1;259:50-9. PMID: 24177208
Shared 1st authorship,
*Impact Factor: 3.0*

Kranz A, Wagner DC, Kamprad M, Scholz M, Schmidt UR, **Nitzsche F**, Aberman Z, Emmrich F, Riegelsberger UM, Boltze J. Transplantation of placenta-derived mesenchymal stromal cells upon experimental stroke in rats. Brain Res. 2010 Feb 22;1315:128-36.PMID:20004649
*Impact-Factor: 2.8*